

VIRAL AND CELLULAR DETERMINANTS OF REOVIRUS-INDUCED NF- κ B ACTIVATION
AND APOPTOSIS

By

Mark William Hansberger

Dissertation

Submitted to the Faculty of the
Graduate School of Vanderbilt University

in partial fulfillment of the requirements

for the degree of

DOCTOR OF PHILOSOPHY

in

Microbiology and Immunology

December, 2006

Nashville, Tennessee

Approved:

Terence S. Dermody

Dean W. Ballard

Christopher Aiken

Bruce D. Carter

Sebastian Joyce

Dedicated to My Parents
Thomas and Shirley Hansberger

ACKNOWLEDGEMENTS

I have had the privilege of meeting so many unique and wonderful people during the course of my life. Each and every one of those people had an influence on the choices I made and the direction my decisions took me. I could not have made it this far without the support of so many people. I would like to especially thank the following for making it possible for me to have the opportunity to train in such a great environment provided by Vanderbilt University:

- My parents for the infinite amount of guidance and support that they have provided me. You mean the world to me and I hope I make you feel as proud as you have made me feel loved.
- My brother for being my best friend and always being there to listen.
- Scott Lyons for his eternal friendship and for teaching me how valuable life is. I hope to be half the person you were.
- Jackie Campbell for being one of my favorite people. Without you, I never would have made it this far.
- The entire Campbell family. You welcomed me into your family with open arms and I'll never forget that.
- Terry Dermody for being a great mentor and friend during my time at Vanderbilt. I will always be grateful to you for the training and counseling you gave me and the fun times we had.
- Past and present members of the Dermody lab. I've enjoyed the friendship and the atmosphere in which you all have contributed. I especially would like to thank Craig

Forrest for getting me started in the lab and Pranav Danthi for sharing so many laughs with me.

- Greg Wilson for sharing his space with me and putting up with my nonsense for so many years. Thanks for being a good friend Greg.
- My dissertation committee, Sebastian Joyce, Dean Ballard, Chris Aiken, and Bruce Carter for insightful advice and critical review of my science.
- My undergraduate mentor, Dr. Karen Coats for starting me on the path to science.
- My softball and poker buddies for all the great times and unforgettable laughs.
- Thank you to the Division of Pediatric Infectious Disease, the Department of Microbiology and Immunology, the Department of Pathology, and the Lamb Center for Pediatric Research for educational and financial support.

TABLE OF CONTENTS

	Page
DEDICATION	ii
ACKNOWLEDGEMENTS	iii
LIST OF TABLES	viii
LIST OF FIGURES	ix
LIST OF ABBREVIATIONS	xi
Chapter	Page
I. BACKGROUND AND LITERATURE REVIEW	1
Overview of virus-induced apoptosis	1
Reovirus structure and replication	2
Reovirus pathogenesis and disease	6
Genetics of reovirus-induced apoptosis	7
Apoptosis induced by reovirus requires activation of NF- κ B	10
Significance of the Research	13
II. JAM-A-INDEPENDENT, ANTIBODY-MEDIATED UPTAKE OF REOVIRUS INTO CELLS LEADS TO APOPTOSIS	14
Introduction	14
<i>Results</i>	16
A JAM-A truncation mutant lacking the cytoplasmic tail is expressed at the cell surface	16
Reovirus induces equivalent levels of apoptosis in CHO cells that express JAM-A and JAM-A Δ CT	16
Antibody-mediated uptake of reovirus into Fc receptor-expressing cells leads to infection and apoptosis	18
Viral disassembly is required for apoptosis-induced by Fc-mediated uptake of reovirus	21
Fc receptor-dependent infection abolishes σ 1-related differences in the apoptosis-inducing capacity of reovirus	23
Differences in apoptosis induction following Fc receptor-dependent infection of T1L x T3D reassortant viruses are linked to the M2 gene segment	25
Reovirus mutant tsA279 is inefficient in apoptosis induction	27

Discussion.....	30
III. IKKα AND IKKγ ARE REQUIRED FOR REOVIRUS-INDUCED NF-κB ACTIVATION AND APOPTOSIS	36
Introduction	36
<i>Results</i>	37
Reovirus infection results in the biphasic activation of NF- κ B/Rel DNA- binding proteins	37
Reovirus infection leads to the selective degradation of I κ B α	41
IKK α and IKK γ are required for reovirus-induced NF- κ B activation.....	41
IKK α and IKK γ are required for reovirus-induced apoptosis	49
Discussion.....	51
IV. ORGAN-SPECIFIC ROLES FOR TRANSCRIPTION FACTOR NF-κB REOVIRUS INDUCED APOPTOSIS AND DISEASE.....	55
Introduction	55
<i>Results</i>	56
Reovirus activates NF- κ B in vivo.....	56
Reovirus-induced activation of NF- κ B in the murine CNS and heart is dependent on p50	58
NF- κ B subunit p50 is not required for efficient reovirus replication or dissemination in the murine host.....	60
NF- κ B subunit p50 is required for efficient induction of apoptosis in the CNS following reovirus infection	60
Absence of NF- κ B subunit p50 leads to enhanced pathology and massive apoptosis in the murine heart following reovirus infection	64
IFN- β is induced in the heart of wild-type mice following reovirus infection	70
IFN- β treatment of p50-null mice attenuates reovirus-induced myocarditis	70
Discussion.....	73
V. IFN-β INHIBITS REOVIRUS-INDUCED APOPTOSIS BY REDUCING REOVIRUS REPLICATION IN CARDIAC MYOCYTES	78
Introduction	78
<i>Results</i>	79
Reovirus infection of primary cardiac myocytes	79
Reovirus growth in primary cardiac myocytes.....	80
Reovirus-induced caspase 3/7 activity of primary cardiac myocytes.....	83
Reovirus induces caspase 3/7 activity in cardiac myocytes lacking the IFN- α / β receptor	83
Discussion.....	87

VI. SUMMARY AND FUTURE DIRECTIONS.....	90
VII. DETAILED METHODS OF PROCEDURE.....	96
Appendix	
A. JAM-A-INDEPENDENT, ANTIBODY-MEDIATED UPTAKE OF REOVIRUS INTO CELLS LEADS TO APOPTOSIS	109
B. I κ B KINASE SUBUNITS α AND γ ARE REQUIRED FOR ACTIVATION OF NF- κ B AND INDUCTION OF APOPTOSIS BY MAMMALIAN REOVIRUS.....	120
C. ORGAN-SPECIFIC ROLES FOR TRANSCRIPTION FACTOR NF- κ B IN REOVIRUS-INDUCED APOPTOSIS AND DISEASE.....	152
REFERENCES	163

LIST OF TABLES

Table	Page
1. Apoptosis induction by T1L x T3D reassortant viruses in CHO-B1 cells.....	28

LIST OF FIGURES

Figure	Page
1. The reovirus virion.....	3
2. Entry of reovirus into cells.....	5
3. Reovirus-induced apoptosis.....	8
4. NF- κ B activation in response to reovirus.....	12
5. Stable expression of JAM-A and JAM- Δ ACT in CHO cells.....	17
6. Infection and apoptosis of JAM-A- and JAM- Δ ACT-expressing CHO cells.....	19
7. Infection and apoptosis of HeLa cells and CHO-B1 cells in the presence of mAb 9BG5.....	22
8. Effect of inhibitors of viral replication on apoptosis induced by reovirus.....	24
9. Apoptosis induction in CHO-B1 cells following Fc-mediated infection by T1L and T3SA-.....	26
10. Apoptosis induced by μ 1 temperature-sensitive mutant tsA279.64.....	29
11. Biphasic activation of NF- κ B/Rel proteins in reovirus-infected cells.....	39
12. Processing of p100 to p52 during reovirus infection.....	40
13. Reovirus infection leads to degradation of I κ B α but not I κ B β or I κ B ϵ	42
14. Involvement of IKKs in reovirus-induced NF- κ B activation.....	44
15. IKK α and IKK γ are required for reovirus-induced activation of NF- κ B.....	46
16. Cells deficient in IKK subunits are permissive for reovirus infection and growth.....	47
17. Reovirus-induced activation of NF- κ B in NIK-deficient cells.....	48
18. IKK α and IKK γ are required for reovirus-induced apoptosis.....	50
19. NF- κ B activation following reovirus infection of HLL mice.....	57

20.	Reovirus-induced NF- κ B gel-shift activity following infection of p50 +/+ and p50 -/- mice	59
21.	Growth of reovirus in p50 +/+ and p50 -/- mice	61
22.	Inflammation, reovirus protein expression, TUNEL staining, and immunohistochemical detection of activated caspase-3 in the brain of reovirus-infected p50 +/+ and p50 -/- mice	62
23.	Quantitation of TUNEL staining in cortex and hippocampus, basal ganglia and diencephalon, and brain stem of reovirus-infected p50 +/+ and p50 -/- mice	65
24.	Heart pathology following reovirus infection of p50 +/+ and p50 -/- mice.....	67
25.	Inflammation, reovirus protein expression, TUNEL staining, and immunohistochemical detection of activated caspase 3 in the heart of reovirus-infected p50 +/+ and p50 -/- mice.....	69
26.	Levels of IFN- β mRNA in brain and heart of p50 +/+ and p50 -/- mice.....	71
27.	Reovirus replication and apoptosis in infected p50 -/- mice following treatment with IFN- β	72
28.	Reovirus infection in PCMCs	81
29.	Reovirus growth in PCMCs	82
30.	IFN diminishes apoptosis in PCMCs following reovirus infection	84
31.	Reovirus growth in PCMCs lacking the IFN- α/β receptor.....	85
32.	Reovirus induces apoptosis in PCMCs lacking the IFN- α/β receptor.....	86

LIST OF ABBREVIATIONS

AC	Ammonium chloride
AO	Acridine Orange
CNS	Central nervous system
CHO	Chinese hamster ovary cells
CAR	Coxsackievirus and adenovirus receptor
DNA	Deoxyribonucleic acid
dsRNA	Double-stranded ribonucleic acid
EMSA	Electrophoretic mobility shift assay
FFU	Fluorescent focus unit
GAPDH	Glyceraldehyde-3-phosphate dehydrogenase
H	Hours
H&E	Hemotoxylin and Eosin
HLL	HIV long-terminal repeat luciferase
HTLV	Human T-cell lymphotropic virus
IFN	Interferon
I κ B	Inhibitor of κ B
IKK	I κ B kinase
IL	Interleukin
IPS	Interferon promoter stimulator
IRF	Interferon regulatory factor
ISG	Interferon stimulated gene
ISVP	Infectious subvirion particles

HIV	Human immunodeficiency virus
JAK	Janus-associated kinase
JAM	Junctional adhesion molecule
L	L929
mAb	Monoclonal antibody
MEF	Murine embryo fibroblasts
Min	Minute
MDCK	Madin-Darby canine kidney
MOI	Multiplicity of infection
mRNA	Message ribonucleic acid
NF- κ B	Nuclear factor- κ B
NGS	Normal goat serum
NIK	NF- κ B inducing kinase
PAGE	Polyacrylamide gel electrophoresis
PBS	Phosphate-buffered saline
PCFC	Primary cardiac fibroblast culture
PCMC	Primary cardiac myocyte culture
PCR	Polymerase chain reaction
PFU	Plaque forming units
PKR	RNA-dependent protein kinase
PSL	Photostimulus luminescence
RNA	Ribonucleic acid
SA	Sialic acid

SDS	Sodium dodecyl sulphate
SEC	Seconds
STAT	Signal transducer and activator of transcription
T1	Type 1
T2	Type 2
T3	Type 3
TNF	Tumor Necrosis Factor
TUNEL	Terminal dUTP nick-end labeling
UV	Ultraviolet
Wt	Wild-type

CHAPTER I

BACKGROUND AND LITERATURE REVIEW

Overview of virus-induced apoptosis

Processes by which viruses injure and kill host cells are essential determinants of viral pathogenesis. Apoptosis is a genetically programmed form of cell death that plays an important regulatory role in many biological processes such as organ development, cellular homeostasis, and immunity. Apoptosis can be triggered by a variety of environmental stimuli and results in numerous morphological and biochemical changes including cell shrinkage, vacuolization, membrane blebbing, condensation of nuclear chromatin, and cleavage of chromosomal DNA into oligonucleosome-length fragments (3, 126, 167, 218). Membrane-bound fragments of apoptotic cells are efficiently removed by phagocytes without inducing an inflammatory response.

Many viruses are capable of inducing apoptosis of infected cells (126, 140, 153, 167, 188). In some cases, apoptosis triggered by virus infection may serve as a component of host defense to limit viral replication or spread (162). This defense mechanism is mediated either directly by self-destruction of host cells prior to completion of the viral replication cycle or indirectly through immune recognition of infected cells by cytotoxic T lymphocytes (126, 167). In other instances apoptosis may enhance viral infection by facilitating viral dissemination or allowing the virus to evade host inflammatory responses (37, 126, 188). For some viruses, cellular factors operant during apoptosis may function to increase the production of viral progeny (140, 167). The biochemical pathways activated by most viruses to induce apoptosis are largely unknown.

This thesis was focused on mechanisms used by mammalian reoviruses to induce apoptosis. Reoviruses are highly tractable models for studies of viral replication and pathogenesis. Apoptosis is the principal means of cell killing employed by some reovirus strains and therefore may influence viral virulence (40, 125, 128, 145, 199). My research was directed toward identifying components of the cellular signaling apparatus required for reovirus-induced apoptosis and determining the effector mechanisms that elicit the apoptotic response during reovirus infection. Identifying and understanding the cellular components of the virus-induced apoptotic signaling machinery will help understand disease mechanisms and identify new targets for therapeutic intervention.

Reovirus structure and replication

Mammalian reoviruses are nonenveloped viruses that contain a genome of 10 discrete segments of double-stranded (ds) RNA (reviewed in Nibert and Schiff (122)). These viruses are the prototype members of the *Orthoreovirus* genus of the *Reoviridae* family. Reoviruses exhibit a broad host range infecting most mammalian species, including humans (reviewed in Tyler (195)). Reoviruses were named respiratory enteric orphan viruses on the basis of their repeated isolation from the respiratory and enteric tracts of children with no obvious clinical symptoms of illness (157). Disease associated with reovirus infection is unusual and restricted to the very young. There are three reovirus serotypes, which can be differentiated on the basis of hemagglutination profiles and neutralization assays (149). A major mechanism of cell killing by reovirus is the genetically programmed cell death pathway that leads to apoptosis.

Reoviruses particles are approximately 85 nm in diameter and formed by eight structural proteins arranged in two concentric protein shells (or capsids) with icosahedral symmetry (42, 52) (Fig. 1). The T=1 inner capsid surrounds the centrally condensed 10

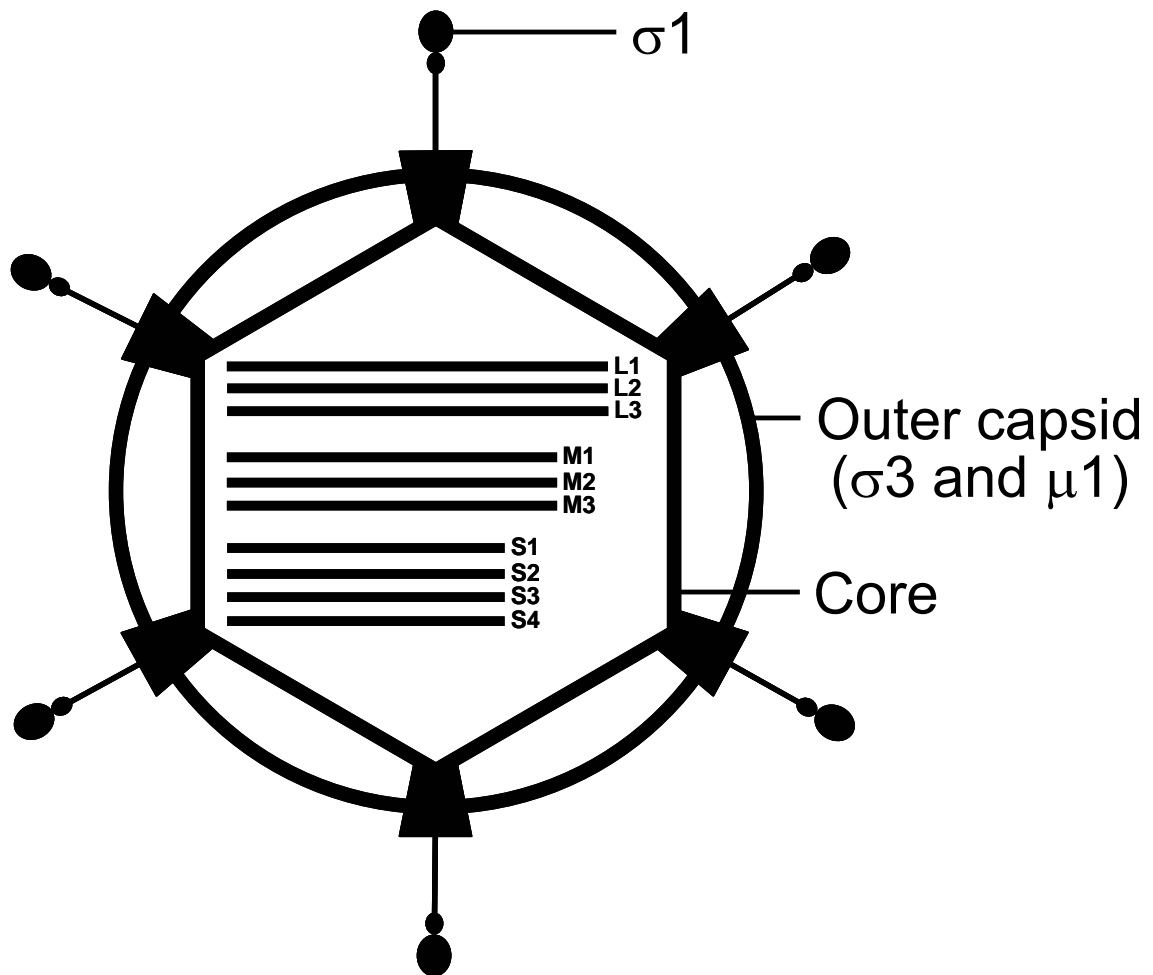


Figure 1. The reovirus virion. The reovirus virion contains two concentric protein shells termed the outer capsid and core. The core contains 10 dsRNA gene segments that are classified by size as large (L), medium (M), or small (S). The viral attachment protein, σ_1 , is depicted as a ball and stick model protruding from the outer capsid. Viral proteins σ_3 and μ_1 form the outer capsid and serve as substrates for endocytic proteases.

dsRNA gene segments and, together with the genomic RNA, forms the tightly packed viral core. It is assembled from two major proteins, $\lambda 1$ and $\sigma 2$ (120 and 150 copies each, respectively) (42, 142), and minor core proteins $\mu 2$ (~20 copies) and $\lambda 3$ (~12 copies) (43). The T=13 (left-handed) outer capsid is constructed from complexes of proteins $\sigma 3$ and $\mu 1$ present in 600 copies each. A core spike, formed by pentamers of the $\lambda 2$ protein (60 copies), projects from the inner capsid through the outer capsid at the 12 axes of five-fold symmetry (142). Partially inserted within a turret-like opening of the $\lambda 2$ pentamer is the delicate, fiber-like trimeric attachment protein, $\sigma 1$ (36 copies) (29, 58).

The reovirus replication cycle is entirely cytoplasmic (reviewed in Nibert and Schiff (122)). Reovirus virions are capable of binding to cell-surface carbohydrate (11), and junctional adhesion molecule-A (JAM-A) (11). Following viral attachment, reovirus virions enter cells by receptor-mediated endocytosis (6, 20, 155, 183), in which $\beta 1$ integrins mediate internalization (102). Within an endocytic compartment, the viral outer capsid is removed to generate infectious subvirion particles (ISVPs) (Fig. 2). During virion-to-ISVP disassembly, $\sigma 3$ is degraded and lost from virions, $\sigma 1$ undergoes a conformational change, and $\mu 1$ is cleaved to form particle-associated fragments δ and ϕ . Removal of $\sigma 3$ exposes hydrophobic domains in $\mu 1$ that facilitate interactions of ISVPs with endosomal membranes (26, 27), leading to delivery of core particles into the cytoplasm and concomitant activation of the viral transcriptase (122). Transcription of the viral genome occurs within the core, and nascent mRNAs are released through turret-like openings at the viral vertices. Viral mRNAs are used as template for viral protein synthesis and replication of viral genomic dsRNA (90, 161). Particles containing dsRNA segments are termed replication particles. These particles are transcriptionally active and yield additional viral mRNAs resulting in an amplification of

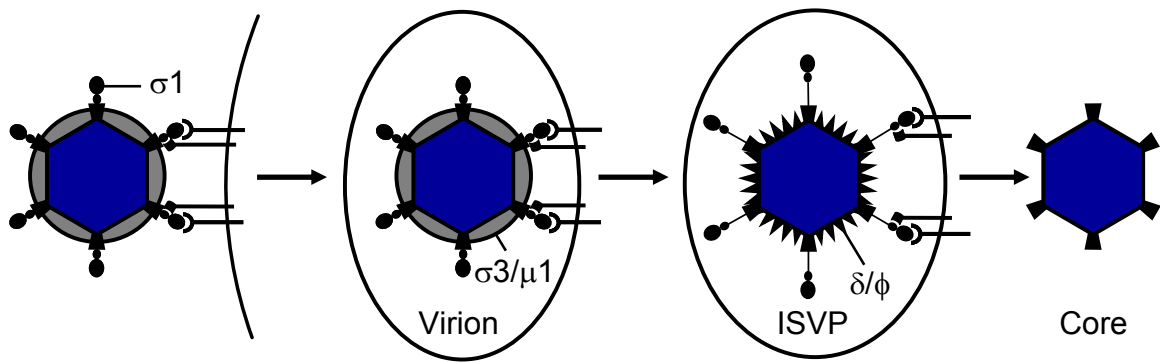


Figure 2. Entry of reovirus into cells. Following attachment to cell-surface receptors, reovirus virions enter cells by receptor-mediated endocytosis. Within an endocytic compartment, the viral outer capsid undergoes acid-dependent proteolysis resulting in generation of ISVPs. Steps in viral entry are completed by interaction of ISVPs with endosomal membranes, leading to delivery of transcriptionally active core particles into the cytoplasm.

viral protein synthesis (81, 117). Following addition of viral outer-capsid proteins to the replication particles, progeny virions are assembled and exit the cell.

Reovirus pathogenesis and diseases

The pathogenesis of reovirus infection has been studied most extensively using newborn mice, in which serotype-specific patterns of disease have been identified (reviewed in Virgin et al. (207)). The best characterized of these models is reovirus pathogenesis in the murine central nervous system (CNS). The segmented nature of the reovirus genome has allowed the determination of the genetic basis for complex viral phenotypes by analysis of reassortant viruses containing mixtures of gene segments derived from parental strains that exhibit a biological polymorphism of interest. Using this strategy, strain-specific differences in the pathogenesis of reovirus CNS infections have been genetically mapped (50, 211). This work has provided important insights into mechanisms of reovirus tropism and virulence.

Following oral inoculation of newborn mice, reovirus is internalized by intestinal M cells (216) and undergoes primary replication in lymphoid tissue of Peyer's patches (83, 118, 154). Virus then invades the CNS, yet strains of different serotypes use different routes of dissemination and manifest distinct pathologic consequences. Serotype 1 (T1) reovirus spreads to the CNS hematogenously and infects ependymal cells (197, 211), resulting in hydrocephalus (210). In contrast, serotype 3 (T3) reovirus spreads to the CNS through nerves and infects neurons (118, 197, 211), causing lethal encephalitis (187, 210). Analysis of reassortant viruses obtained by coinfecting cells with prototype strains T1 Lang (T1L) and T3 Dearing (T3D) demonstrated that the pathways of viral spread in the host (197) and tropism for neural tissues (50, 211) segregate with the viral S1 gene, which encodes the viral

attachment protein, $\sigma 1$ (89, 209). These studies suggest that $\sigma 1$ determines the CNS cell types that serve as hosts for reovirus infection.

Reovirus infection causes pathology and physiologic dysfunction in a wide range of organs and tissues, including the hepatobiliary system, the myocardium, lungs, and endocrine tissues (207). Of these, myocarditis (174) has become a particularly well-established experimental model of reovirus-induced disease. Myocarditis caused by reovirus infection is unusual in comparison to other viral etiologies of myocarditis in that the pathogenesis is not immune mediated. Instead, reovirus cytopathicity is a direct cause of myocyte injury, which results from a complex interplay of the interferon (4, 124, 175) and apoptosis pathways (44). Efficiency of viral RNA synthesis is a key factor in determining the extent of myocardial injury. Accordingly, viral gene segments encoding proteins involved in viral transcription and genome replication play important roles in determining strain-specific differences in the capacity of reovirus to induce myocarditis (171, 172, 175).

Genetics of reovirus-induced apoptosis

Reovirus induces the biochemical and morphological characteristics of apoptosis both in cultured cells (40, 145, 199) and in the murine CNS (125, 128) and heart (44, 128). Insights into mechanisms by which reovirus induces apoptosis have emerged from studies using strains T1L and T3D, which differ in the capacity to induce apoptosis in a variety of cell types (Fig. 3). Reovirus strain T3D induces apoptosis much more efficiently than T1L in murine L929 (L) cells (199), Madin-Darby canine kidney (MDCK) cells (145), and HeLa cells (38). These differences have been analyzed genetically using T1L x T3D reassortant viruses and indicate that the S1 gene is the principal determinant of differences in the

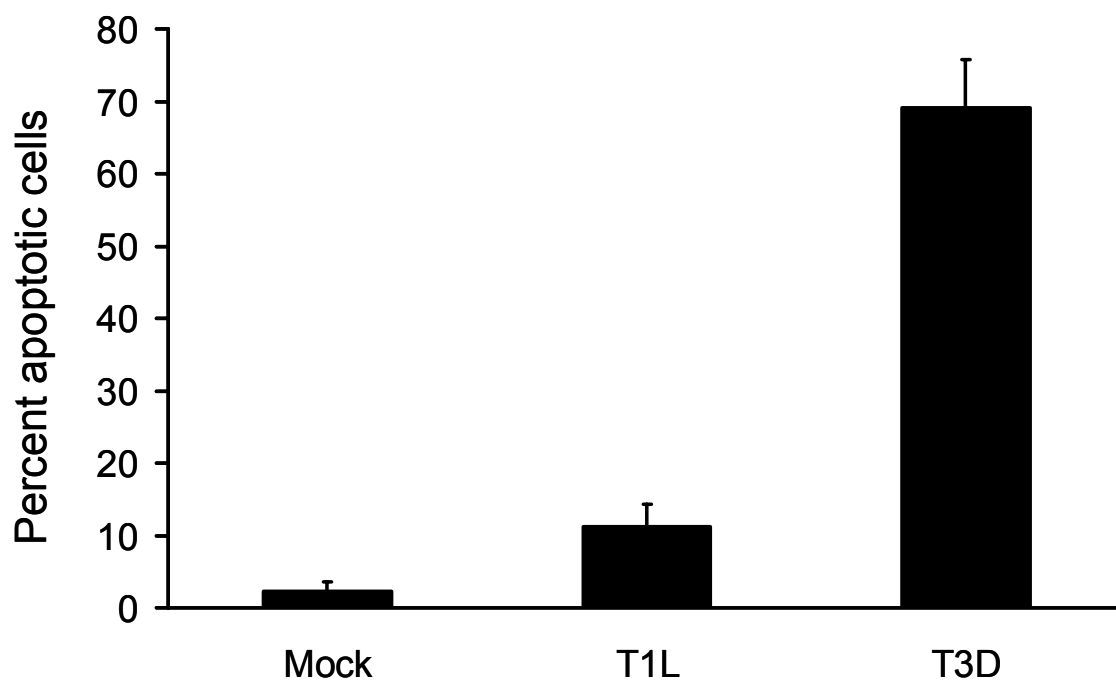


Figure 3. Reovirus-induced apoptosis. HeLa cells were adsorbed with either gel saline (mock), T1L, or T3D at an MOI of 100 PFU/cell and incubated at 37°C for 48 h in medium. Cells were harvested, stained with acridine orange (AO), and scored for apoptosis using morphological criteria. The results are expressed as the mean percentage of cells undergoing apoptosis for three independent experiments. Error bars indicate standard deviations.

capacity of T1L and T3D to induce apoptosis (38, 145, 199). However, a smaller, independent contribution is made by the M2 gene segment.

The S1 gene is bicistronic and encodes the nonstructural protein $\sigma 1s$, along with the attachment protein $\sigma 1$ (55, 75, 158). The role of $\sigma 1s$ in reovirus-induced apoptosis was tested using strains T3C84 and T3C84-MA, which vary in the expression of $\sigma 1s$. Results from these experiments showed that expression of $\sigma 1s$ is not required for apoptosis induction (146), indicating that the $\sigma 1$ protein is the S1 gene product responsible for mediating the strain-specific differences in apoptosis by reovirus.

The M2 gene encodes outer-capsid protein $\mu 1$ (112, 120), a 76-kDa amino-terminal myristylated protein (123). The $\mu 1$ protein is proteolytically cleaved within the endocytic pathway (5, 20), and these cleavage fragments are proposed to interact with endosomal membranes to deliver viral cores into the cytoplasm (70, 71, 101). The exact role of the $\mu 1$ protein in apoptosis is unknown, but it may contribute to apoptosis induction by directly interacting with intracytoplasmic sensors of viral infection resulting in proapoptotic signaling.

In addition to receptor binding steps being an important determinant of apoptosis induction by reovirus, viral replication steps following attachment are also required to induce signals that lead to apoptosis. Inhibitors of viral disassembly abolish the capacity of virions, but not ISVPs, to induce apoptosis (39). However, inhibitors of RNA synthesis, particles devoid of dsRNA, and temperature-sensitive (ts) viral mutants arrested at defined steps in reovirus replication have no effect on apoptosis induction (39). Taken together, these results suggest that reovirus disassembly resulting in ISVP formation, but not viral transcription or subsequent steps in viral replication, is required to induce apoptosis.

Apoptosis induced by reovirus requires activation of NF- κ B

A critical component of the intracellular signal transduction apparatus that leads to apoptosis following reovirus infection is nuclear factor- κ B (NF- κ B) (40). NF- κ B is a transcription factor family that plays important roles in cell growth and survival. The prototypical form of NF- κ B consists of two subunits, p50 and RelA (RelA) (7). NF- κ B is retained in the cytoplasm in a nonactivated state by the I κ B family of inhibitor proteins. Following signal-dependent phosphorylation on two amino-terminal serine residues, I κ B is ubiquitinated and targeted for degradation via the proteasome (7, 132). NF- κ B is released from I κ B, which exposes a nuclear localization signal on NF- κ B and results in its translocation to the nucleus (17). Agonists that stimulate a transient pattern of NF- κ B activity, such as TNF- α , promote the selective degradation of I κ B α (16). In contrast, agents that elicit a prolonged NF- κ B response, including bacterial lipopolysaccharide and IL-1, are associated with degradation of both I κ B α and I κ B β (189). There exist two cytokine-inducible I κ B kinases (IKKs), termed IKK α and IKK β , that phosphorylate I κ B α and I κ B β at the appropriate regulatory serines (104, 203). IKK α and IKK β are components of a large (~500-900 kDa), multisubunit complex that contains a regulatory subunit called IKK γ (51, 115, 151, 223, 226). The IKK catalytic subunits are activated following stimulation with several NF- κ B-inducing agonists, including TNF- α and IL-1 (51, 115, 226).

Two principal signaling pathways are known to activate NF- κ B via the IKK complex. The classical NF- κ B pathway is stimulated in response to cytokines, LPS, dsRNA, and most negative-stranded RNA viruses. This pathway is dependent on IKK β and IKK γ for phosphorylation and subsequent degradation of I κ B α and nuclear translocation of the p50 and RelA (RelA) subunits of NF- κ B (21, 92, 156, 184, 194, 223). The alternative pathway is

dependent on the activation of NF- κ B-inducing kinase (NIK), which in turn leads to phosphorylation of IKK α (220). Activated IKK α phosphorylates the I κ B-like molecule, p100, which is processed to form the NF- κ B subunit, p52 (163). The p52 subunit binds to RelB, translocates to the nucleus, and activates NF- κ B-dependent gene expression (179). The alternative pathway of IKK activation is thought to operate independently of both IKK β and IKK γ (47).

NF- κ B activation can either potentiate (1, 62, 82) or inhibit apoptosis (15, 100, 202) depending on the nature of the NF- κ B agonist. Many RNA viruses are capable of activating NF- κ B, including dengue virus (77), influenza virus (131), reovirus (40), respiratory syncytial virus (108), and Sindbis virus (94). Interestingly, activation of NF- κ B is required for the induction of apoptosis by some viruses, including dengue virus (105), reovirus (40), and Sindbis virus (94).

Reovirus activates NF- κ B in cell culture beginning at 2-4 h post-infection and reaches maximal levels of activation at 6-8 h post-infection (Fig. 4) (40). Electrophoretic mobility shift assays using antibodies specific for p50 and RelA identified both of these subunits in the NF- κ B complexes activated during reovirus infection. Cells devoid of either p50 or RelA do not activate NF- κ B following reovirus infection (40), providing further evidence that these NF- κ B subunits are in the complexes activated by reovirus. Three lines of evidence suggest that NF- κ B activation is required by reovirus to induce apoptosis (40). First, treatment of HeLa cells with a proteasome inhibitor blocks NF- κ B activation following reovirus infection and substantially diminishes reovirus-induced apoptosis. Second, transient expression of a dominant-negative form of I κ B that constitutively represses NF- κ B activation significantly reduces levels of apoptosis induced by reovirus. Third, and most convincingly,

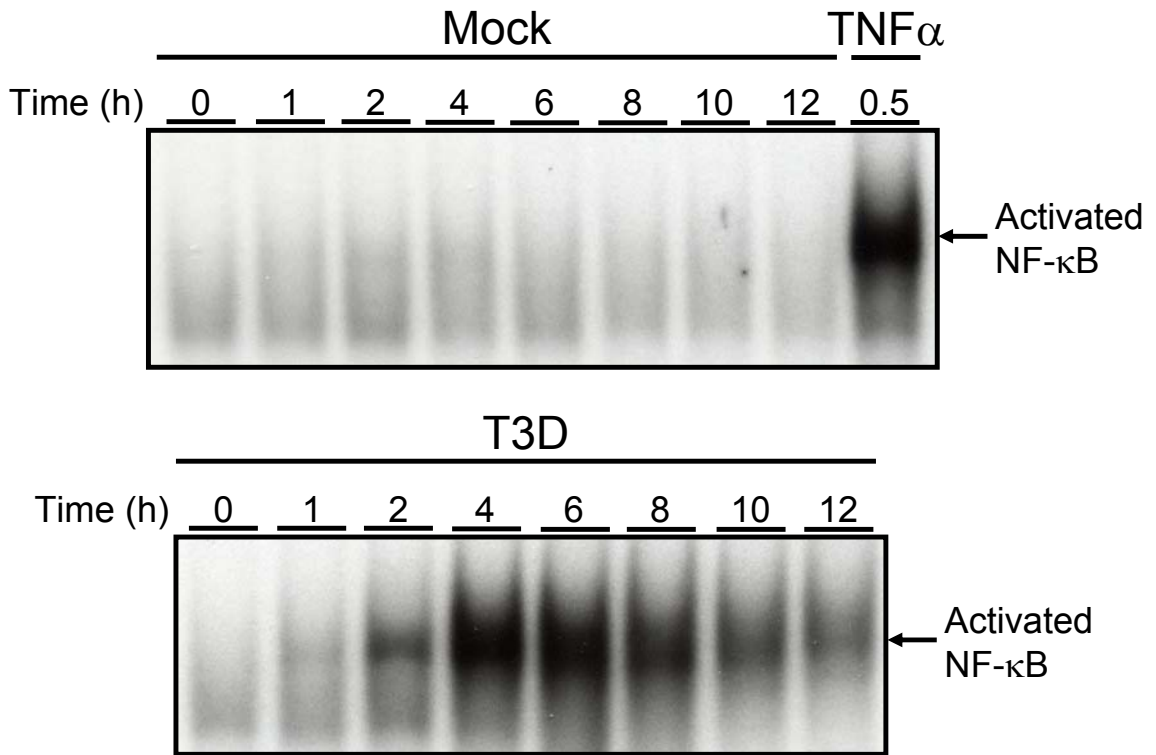


Figure 4. NF- κ B activation in response to reovirus. Nuclear extracts were prepared from uninfected HeLa cells (0 h), mock-infected cells (Mock), or cells infected with T3D at an MOI of 100 PFU/cell for the times shown. Cells also were treated with 20 ng/ml of TNF α for 30 min as a positive control. Extracts were incubated with a radiolabeled NF- κ B consensus oligonucleotide, and resulting protein-oligonucleotide complexes were resolved by acrylamide gel electrophoresis, dried, and exposed to film. NF- κ B-containing complexes are indicated.

apoptosis by reovirus is substantially diminished in mouse embryo fibroblasts lacking either of the NF- κ B subunits p50 or RelA. These findings indicate that NF- κ B plays an essential role in the mechanism by which reovirus induces apoptosis of host cells.

Significance of the research

Many viruses are capable of inducing apoptotic cell death. However, mechanisms of virus-induced apoptosis are not well understood. The main objective of this thesis research is to understand mechanisms by which reovirus activates NF- κ B and induces apoptosis. I describe four main findings that help elucidate these mechanisms. First, reovirus can induce apoptosis in cells lacking JAM-A using a mechanism dependent on the μ 1 protein. Second, IKK α and IKK γ are required for reovirus-induced NF- κ B activation and apoptosis indicating that reovirus activates a novel NF- κ B pathway resulting in cell death. Third, NF- κ B functions in a proapoptotic manner in the brain while playing an antiapoptotic function in the heart of mice infected with reovirus. Fourth, IFN- β inhibits reovirus-induced apoptosis by reducing reovirus replication in cardiac myocytes. Understanding mechanisms of NF- κ B activation may result in the development of novel pharmacologic methods to combat disease caused by pathological activation of NF- κ B. Moreover, data from this research will generate new knowledge about how viruses activate NF- κ B and induce apoptosis. Such knowledge may foster development of new antiviral therapeutics that mediate apoptosis blockade.

CHAPTER II

JAM-A-INDEPENDENT, ANTIBODY-MEDIATED UPTAKE OF REOVIRUS INTO CELLS LEADS TO APOPTOSIS

Introduction

Reovirus infection is initiated by the attachment of virions to cell-surface receptors via the $\sigma 1$ protein (89, 209). The $\sigma 1$ protein engages both JAM-A (11, 24, 57, 137) and cell-surface carbohydrate (2, 49, 133, 134) to initiate viral entry. Anti-JAM-A mAb J10.4, which inhibits reovirus binding to JAM-A, also blocks reovirus-induced apoptosis (11), indicating that JAM-A binding is essential for initiating the apoptotic process. The JAM-A cytoplasmic tail is approximately 45 amino acids in length, contains 13 potential phosphorylation sites, and interacts with several PDZ domain-containing proteins, suggesting a role in ligand-induced cell signaling (14, 54). Inhibition of binding to sialic acid by treatment with neuraminidase also diminishes the apoptotic response elicited by reovirus (38). Thus, binding to both JAM-A and sialic acid is required for maximum levels of apoptosis following reovirus infection.

In addition to receptor binding, post-attachment events are required for the induction of apoptosis by reovirus (39). Inhibition of viral disassembly using ammonium chloride, a weak base that increases vacuolar pH (110) or E64, an inhibitor of cysteine proteases such as those contained in the endocytic compartment (9), abolishes reovirus-induced apoptosis. On the other hand, interference with steps in viral replication subsequent to ISVP formation and membrane penetration using ribavirin, an inhibitor of RNA synthesis (139), does not perturb apoptosis induced by reovirus (39). Thus, in addition to sialic acid- and JAM-A-mediated attachment of reovirus to cells, replication steps during or

after viral disassembly that occur before the cytoplasmically delivered core becomes transcriptionally active, also contribute to reovirus-induced apoptosis.

In keeping with studies of inhibitors of viral receptor binding, analysis of T1L x T3D reassortant viruses indicates that the σ 1-encoding S1 gene is the primary genetic determinant of differences in the capacity of these strains to induce apoptosis in numerous cell types (145, 199, 200). The μ 1-encoding M2 gene also has been implicated in the apoptotic response induced by reovirus (199, 200). Since the μ 1 protein functions in virus-induced endosomal membrane penetration following disassembly but prior to viral RNA synthesis (93, 121, 127), the deleterious effects of reovirus disassembly inhibitors on apoptosis induction suggest a functional link between the M2 gene segment and differences in the efficiency of apoptosis exhibited by different reovirus strains (145, 199, 200).

In this study, we determined whether reovirus is capable of inducing apoptosis independent of JAM-A and sialic acid binding. We found that antibody-mediated uptake of reovirus into JAM-A-negative, Fc-receptor-expressing cells results in productive infection and leads to apoptosis in a σ 1-independent fashion. Moreover, apoptosis induced following this uptake pathway also is dependent on viral disassembly. Analysis of reassortant viruses and an M2 mutant virus demonstrates that the μ 1 protein influences the strength of proapoptotic signaling following reovirus infection. These data suggest that signaling induced as a result of σ 1 interactions with JAM-A and sialic acid are not necessary for apoptosis induced by reovirus and that the μ 1 protein is the viral factor that stimulates the cellular apoptotic machinery.

Results

A JAM-A truncation mutant lacking the cytoplasmic tail is expressed at the cell surface

To determine whether the cytoplasmic tail of JAM-A contributes to reovirus-induced apoptosis by evoking proapoptotic signaling events, chinese hamster ovary (CHO) cells were stably transfected with empty vector or vector encoding full-length JAM-A or a C-terminally truncated form of JAM-A that lacks the cytoplasmic tail (JAM-A Δ CT). CHO cells were selected since they are poorly permissive to reovirus infection (57); yields of reovirus following infection of CHO cells are 100- to 1000- fold lower in the absence of ectopic expression of JAM-A {Forrest, 2003 #4656; Campbell, 2005 #5059}. Whole-cell extracts from stably expressing cells were analyzed for expression of JAM-A by immunoblotting (Fig. 5A). While no JAM-A-specific band was detected in the vector-transfected cells, both full-length JAM-A and the faster migrating JAM-A Δ CT proteins were expressed to high levels in the cell lines tested. The surface expression of both JAM-A and JAM-A Δ CT was assessed by flow cytometry using JAM-A-specific mAb J10.4 (Fig. 5B). Both wild-type and mutant JAM-A proteins displayed approximately equivalent surface expression, suggesting that removal of the C-terminal domain of JAM-A does not prevent transport of JAM-A to the cell surface. These stably transfected cells are therefore suitable for analysis of infection and apoptosis induction by reovirus.

Reovirus induces equivalent levels of apoptosis in CHO cells that express JAM-A and JAM-A Δ CT

To determine whether CHO cells stably expressing JAM-A Δ CT can support reovirus infection, cells were adsorbed with reovirus strain T3D at an MOI of 10 PFU per cell, and viral infectivity was assessed by using indirect immunofluorescence (Fig. 6A). CHO cells

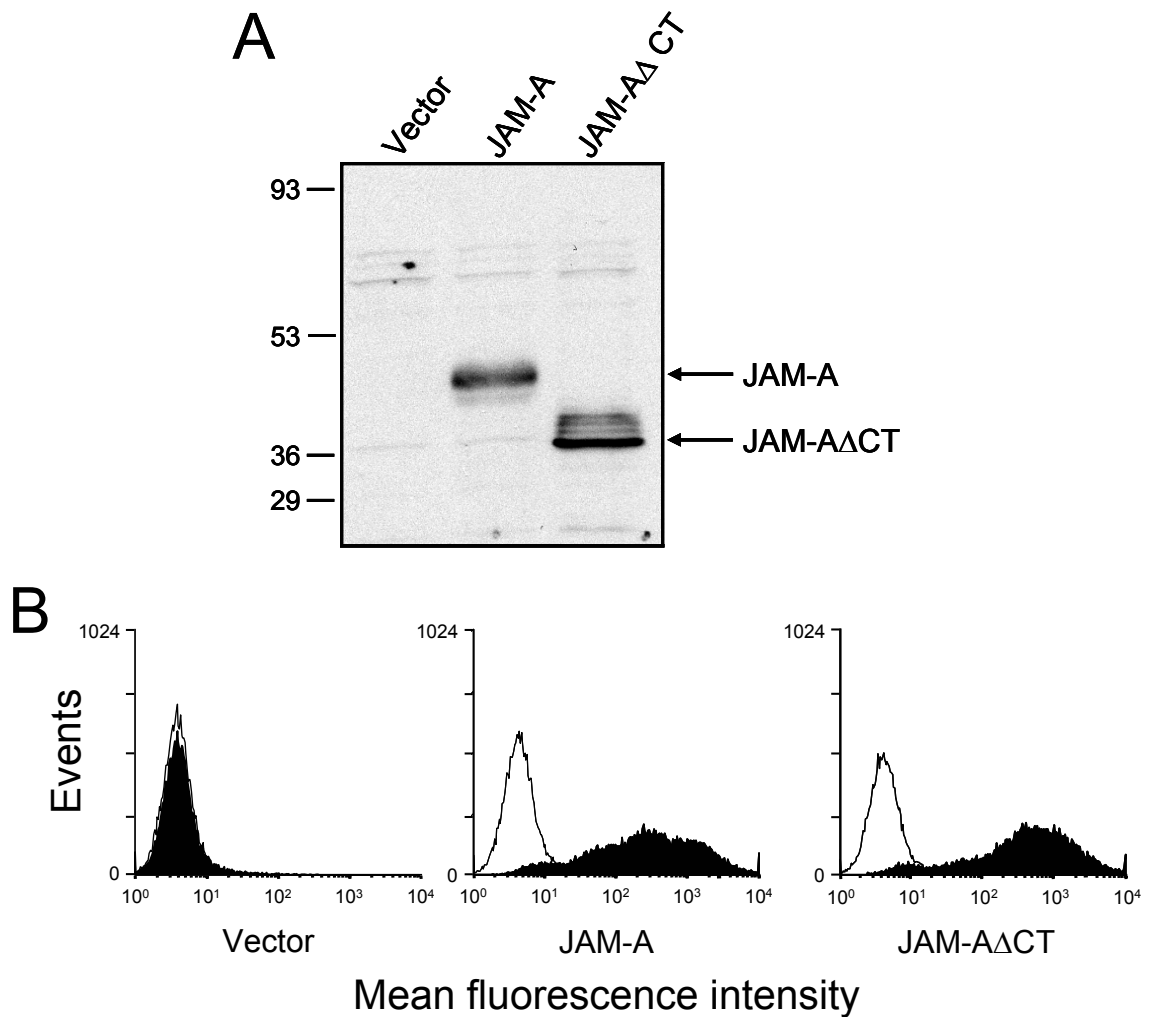


Figure 5. Stable expression of JAM-A and JAM- $\Delta\Delta$ CT in CHO cells. (A) Whole-cell lysates (1×10^5 cell equivalents) were prepared from CHO cells stably transfected with empty vector, JAM-A, or JAM- $\Delta\Delta$ CT, resolved by SDS-PAGE, transferred to nitrocellulose, and immunoblotted using anti-JAM-A mAb J10.4. The positions of full-length JAM-A and truncated JAM- $\Delta\Delta$ CT are shown on the right. The positions of molecular weight standards (in kilodaltons) are shown on the top. (B) Stably transfected CHO cells (1×10^6) were incubated with either anti-JAM mAb J10.4 (filled histograms) or an isotype-matched control mAb (open histograms) at $10 \mu\text{g/ml}$, followed by incubation with PE-labeled anti-mouse Ig secondary antibody. The results are presented as mean fluorescence intensity.

transfected with either empty vector or those engineered to stably express full-length JAM-A were used as controls. In contrast to vector-transfected cells, cells expressing either JAM-A or JAM-A Δ CT were equivalently capable of supporting infection by T3D. These data indicate that although JAM-A expression is required for efficient infection of CHO cells, the JAM-A cytoplasmic tail is dispensable.

To determine whether the JAM-A cytoplasmic tail is required for apoptosis, stably transfected CHO cell lines were adsorbed with T3D at an MOI of 100 PFU per cell, and apoptosis was assessed by using AO staining (Fig. 6B). None of the cell lines tested showed significant apoptosis following mock infection (< 5%). T3D infection of vector-transfected cells induced levels of apoptosis equivalent to those following mock infection of cells. In contrast, T3D infection of either the JAM-A- or JAM-A Δ CT-expressing cell lines induced an equivalent percentage of cells to undergo apoptosis (~ 22%). Therefore, analogous to our findings in the infectivity assays, the cytoplasmic tail of JAM-A is not required for reovirus-induced apoptosis.

Antibody-mediated uptake of reovirus into Fc receptor-expressing cells leads to infection and apoptosis

To determine whether the requirement for JAM-A during reovirus infection and apoptosis can be bypassed, we utilized antibody-mediated infection of Fc receptor-expressing CHO (CHO-B1) cells. These cells stably express the B1 isoform of the mouse Fc receptor II (80). Therefore, in the absence of JAM-A, these cells should allow internalization of antibody-reovirus complexes into cells via Fc receptors, resulting in efficient infection of normally non-permissive cells. For these experiments, T3D virions were incubated with increasing concentrations of σ 1-specific, neutralizing mAb 9BG5 (23) prior to infection of CHO-B1 cells. HeLa cells were used in parallel to confirm the neutralizing efficacy of mAb

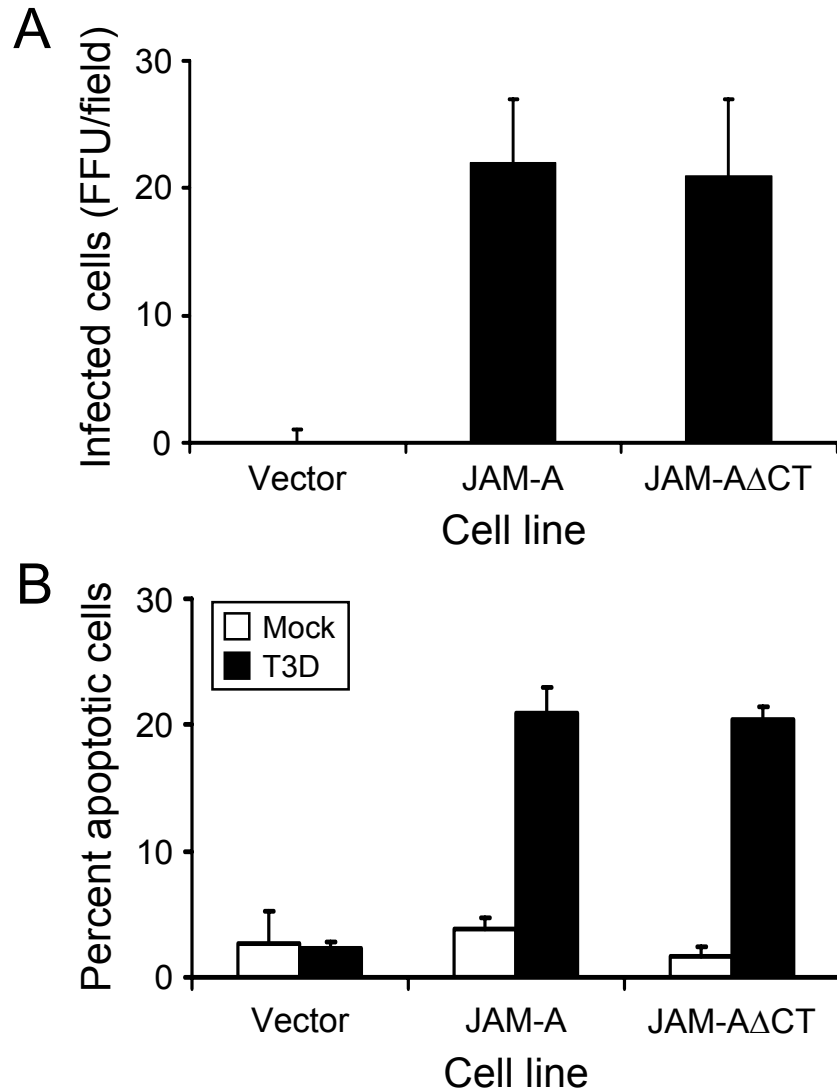


Figure 6. Infection and apoptosis of JAM-A- and JAM-A Δ CT-expressing CHO cells. (A) Cells were adsorbed with T3D at an MOI of 10 PFU/cell. After incubation at 37°C for 18 h, cells were fixed using methanol. Infected cells were visualized by immunostaining with polyclonal rabbit anti-reovirus sera, followed by incubation with Alexa546-labeled anti-rabbit IgG. Reovirus-infected cells were quantified by counting fluorescent cells. The results are presented as mean fluorescent focus units (FFU)/field. Error bars indicate standard deviations. (B) Cells were adsorbed with either PBS (mock) or T3D at an MOI of 100 PFU/cell. Cells were harvested at 48 h after infection and stained with AO. The results are expressed as the mean percentage of cells undergoing apoptosis for three independent experiments. Error bars indicate standard deviations.

9BG5 at the concentrations tested. For each cell line, the number of infected cells was assessed 18 h post-infection by indirect immunofluorescence. As anticipated, the efficiency of reovirus infection of HeLa cells decreased in proportion to antibody concentration with little infection detected in the presence of 2.5 μg per ml of 9BG5 (Fig. 7A). We conclude that 9BG5 interferes with $\sigma 1$ -JAM-A interactions, which are critical for reovirus infection of HeLa cells. In contrast, the efficiency of infection of CHO-B1 cells by T3D increased in proportion to 9BG5 concentration, with maximal infection observed in the presence of a completely neutralizing concentration of 9BG5, 2.5 μg per ml (Fig. 7A). These findings demonstrate that reovirus infection can be established in a JAM-A-independent manner if an alternative high-affinity binding moiety is provided. These data corroborate a previous report of antibody-mediated enhancement of reovirus infection of a murine macrophage-like cell line (22).

To determine whether infection initiated in a JAM-A-independent manner also triggers apoptosis, the capacity of reovirus-9BG5 complexes to induce apoptotic cell death of both HeLa cells and CHO-B1 cells was assessed by using AO staining (Fig. 7B). Approximately 35% of HeLa cells showed apoptotic nuclei at 48 h post-infection in the absence of antibody treatment of virions. Consistent with the decrease in the capacity of reovirus to infect HeLa cells in the presence of 9BG5, the percentage of cells undergoing apoptosis also decreased with increasing 9BG5 concentrations. However, in the absence of 9BG5, T3D induced minimal apoptosis in CHO-B1 cells in comparison to mock-infected cells. In concordance with the infectivity data, the percentage of apoptotic CHO-B1 cells increased with increasing concentrations of 9BG5, with maximal apoptosis seen following pretreatment with 2.5 μg per ml mAb ($\sim 25\%$). These findings demonstrate that reovirus infection initiated in the absence of JAM-A binding also leads to apoptosis. Therefore $\sigma 1$ -

JAM-A interactions or signaling pathways induced as a consequence of these interactions are dispensable for apoptosis induction by reovirus.

To exclude the possibility that binding of mAb to Fc receptor contributes to apoptosis induction, we tested whether incubation of reovirus with irrelevant anti-Myc mAb 9E10 was capable of inducing apoptosis (Fig. 7C). While incubation of T3D with two different mAbs directed against the reovirus outer-capsid, 7F4 (λ 2) and 9BG5 (σ 1), induced 21% and 22% apoptosis, respectively following infection of CHO-B1 cells, incubation of T3D with mAb 9E10 failed to induce apoptosis at levels over mock-infected cells. These findings suggest that only antibodies directed against reovirus outer-capsid proteins allow virus attachment to CHO-B1 cells and subsequent induction of apoptosis. To exclude the involvement of signaling induced as a result of Fc receptor crosslinking due to binding of reovirus-antibody complexes, Fc receptors were crosslinked using 2.4G2 (a rat anti-Fc receptor mAb) and an IgM antibody directed against rat IgG. This treatment did not induce apoptosis in CHO-B1 cells in comparison to mock-treated cells. As an additional control for the effect of crosslinking Fc receptors, T1L core particles, which lack outer-capsid proteins σ 1, σ 3, and μ 1, were incubated with mAb 7F4 and added to CHO-B1 cells. Neither untreated cores nor 7F4-core complexes induced apoptosis of these cells. These data suggest that apoptosis does not result from proapoptotic signaling induced as a consequence of Fc-receptor crosslinking but requires binding of reovirus particles containing outer-capsid proteins.

Viral disassembly is required for apoptosis-induced by Fc-mediated uptake of reovirus

To determine whether viral disassembly in cellular endosomes is required for apoptosis following Fc-mediated delivery of reovirus, CHO-B1 cells were treated with AC prior to infection by mAb-treated T3D virions. Treatment of cells with 20 mM AC, a

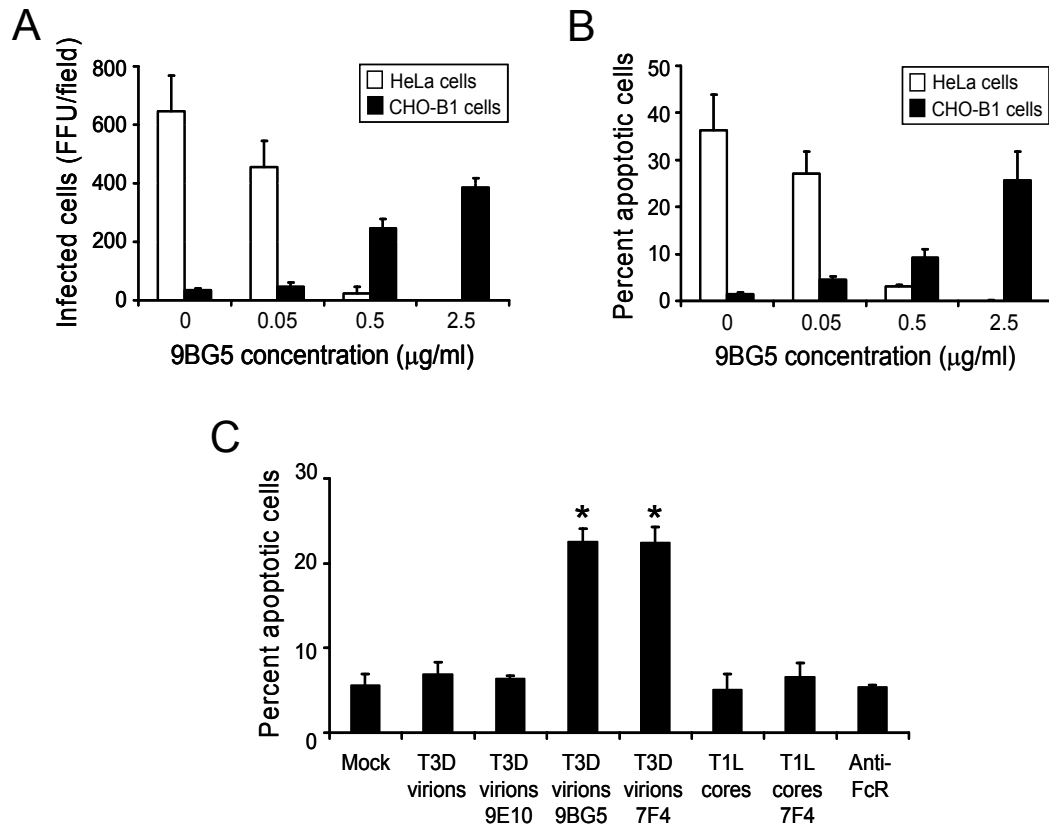


Figure 7. Infection and apoptosis of HeLa cells and CHO-B1 cells in the presence of mAb 9BG5. (A) Reovirus particles were incubated overnight with the indicated concentration of mAb 9BG5 and adsorbed to either HeLa cells or CHO-B1 cells at an MOI of 100 PFU/cell. After incubation at 37°C for 18 h, cells were fixed using methanol. Infected cells were visualized by immunostaining with polyclonal rabbit anti-reovirus sera, followed by Alexa546-labeled anti-rabbit IgG. Reovirus-infected cells were quantified by counting fluorescent cells. The results are presented as mean fluorescent focus units (FFU)/field. Error bars indicate standard deviations. (B) HeLa cells or CHO-B1 cells were adsorbed with 100 PFU/cell of either virus or virus-antibody complex and harvested at 48 h after infection and stained with AO. (C) CHO-B1 cells were mock-infected, infected with T3D virions with or without 2.5 µg per ml of Myc-specific mAb 9E10 (antibody control), σ 1-specific mAb 9BG5, or λ 2-specific mAb 7F4 at an MOI of 100 PFU/cell, or infected with T1L core particles with or without 2.5 µg per ml of mAb 7F4 at an MOI of 10^4 particles/cell. CHO-B1 cells also were incubated with 1 µg/ml anti-Fc receptor rat IgG mAb 2.4G2, followed by incubation with 5 µg/ml of IgM specific for rat IgG (anti-FcR). Cells were harvested at 48 h after infection and stained with AO. The results are expressed as the mean percentage of cells undergoing apoptosis for three independent experiments. Error bars indicate standard deviations. *, $P < 0.05$ as determined by Student's t test in comparison to T3D incubated with control mAb 9E10.

concentration sufficient to block reovirus disassembly (183, 213), abolished the capacity of T3D to induce apoptosis (Fig. 8A). Thus, acid-dependent proteolytic disassembly is required for apoptosis induction by this uptake mechanism. To determine whether the apoptosis-inhibitory effect of AC is due to blockade of viral RNA synthesis, we tested ribavirin, an inhibitor of viral RNA synthesis (139), for the capacity to diminish apoptosis. In keeping with our previously published results (39), apoptosis induced by reovirus infection via Fc-mediated uptake was unaffected by ribavirin (Fig. 8A). To corroborate these results, we tested the apoptosis inducing capacity of UV-inactivated reovirus virions, which are incapable of establishing productive infection (166). We found that UV- inactivated reovirus is capable of inducing apoptosis following Fc receptor-mediated uptake of a high MOI of virus (Fig. 8B). These findings are consistent with our previously published observations (199). Collectively, these results demonstrate that steps in reovirus replication cycle that occur after attachment but before transcription are required for virus-induced apoptosis, regardless of the type of receptor used to initiate infection (39). In addition, these results suggest that death signaling during reovirus infection may occur independently of receptor engagement.

Fc receptor-dependent infection abolishes σ 1-related differences in the apoptosis-inducing capacity of reovirus

Differences in the capacity of some reovirus strains to induce apoptosis are linked to differences in affinity for sialic acid (38). To determine whether reovirus strains that are incapable of binding to sialic acid can induce apoptosis when infection is initiated via Fc-dependent uptake, strains T1L and T3SA-, neither of which is capable of binding to sialic acid (10, 28, 49), were incubated with σ 1-specific antibodies and adsorbed to CHO-B1 cells. Incubation of T1L virions with type 1 σ 1-specific mAb 5C6 (206) and incubation of T3SA-

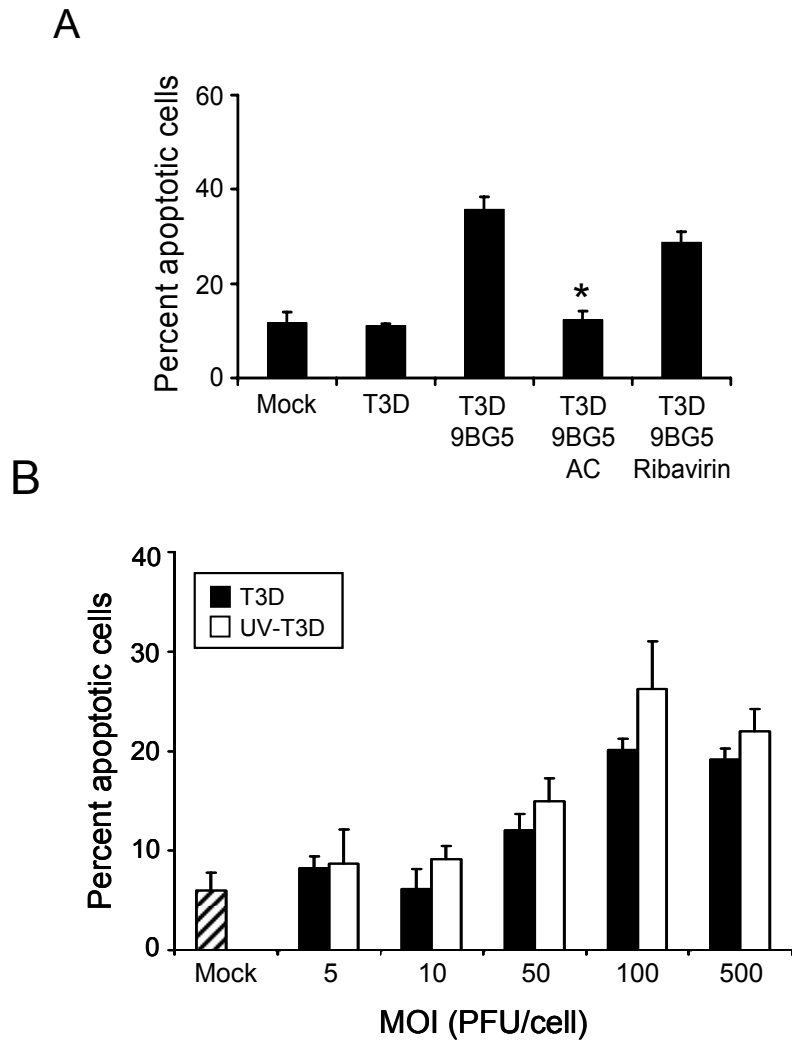


Figure 8. Effect of inhibitors of viral replication on apoptosis induced by reovirus. T3D alone or preincubated with 2.5 $\mu\text{g/ml}$ of mAb 9BG5 was adsorbed to CHO-B1 cells at an MOI of 500 PFU/cell. After incubation at 37°C for 48 h in untreated medium or medium containing either 20 mM AC or 200 μM ribavirin, cells were stained with AO. The results are expressed as the mean percentage of cells undergoing apoptosis for three independent experiments. Error bars indicate standard deviations. *, $P < 0.05$ as determined by Student's t test in comparison to T3D incubated with mAb 9BG5.

virions with type 3 σ 1-specific 9BG5 (23) resulted in significantly higher levels of apoptosis in CHO-B1 cells in comparison to levels observed following infection with T1L and T3SA-virions in the absence of antibody treatment (Fig. 9). The percentage of cells undergoing apoptosis following antibody-mediated infection of non-sialic-acid-binding reovirus strains was at least equal to that observed following infection with T3D. Therefore, σ 1-related differences in apoptosis efficiency are overcome when infection is initiated via Fc-mediated uptake. These results make it unlikely that the σ 1 protein is the viral effector of apoptosis induction.

Differences in apoptosis induction following Fc receptor-dependent infection of T1L x T3D reassortant viruses are linked to the M2 gene segment

We have demonstrated previously that the viral S1 and M2 gene segments segregate with differences in the apoptosis-inducing capacity of T1L and T3D (145, 199). To ascertain whether any strain-specific differences exist when the effect of the S1 gene segment is circumvented by Fc receptor-dependent uptake, CHO-B1 cells were adsorbed with T1L x T3D reassortant viruses after incubation with σ 1-specific antibodies. Type 1 and type 3 strains were incubated with σ 1-specific mAbs 5C6 and 9BG5, respectively, prior to infection. Each of the reassortant viruses tested produced an approximately similar number of infected cells as judged by indirect immunofluorescence (data not shown), suggesting equivalent efficiency of antibody-mediated uptake and infection. The percentage of cells undergoing apoptosis as a result of antibody-mediated infection of cells was assessed at 48 h after infection. The reassortant viruses were ranked from highest to lowest by apoptosis-inducing capacity (Table 1). Although the reassortants did not cluster distinctly into two groups with high and low apoptotic potential, six of the seven strains with the highest levels of apoptosis had an M2 gene segment derived from T3D. Conversely, seven of the eight strains with the

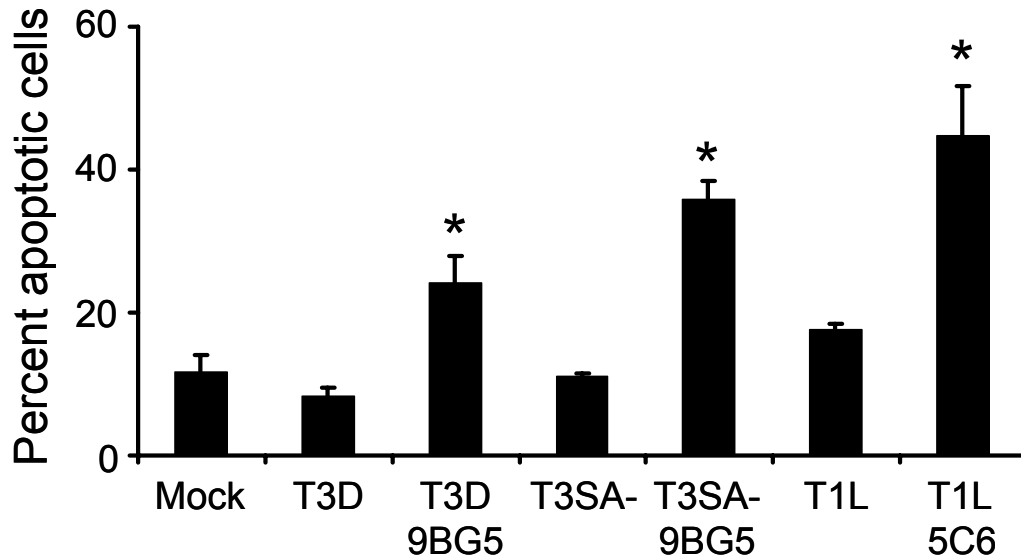


Figure 9. Apoptosis induction in CHO-B1 cells following Fc-mediated infection by T1L and T3SA-. Cells were adsorbed with T3D, T3SA-, or T1L with or without 2.5 μ g per ml of mAb 9BG5 (for type 3 strains) or mAb 5C6 (for T1L) at an MOI of 100 PFU/cell. Following infection at 37°C for 48 h, cells were harvested and stained with AO. The results are expressed as the mean percentage of cells undergoing apoptosis for three independent experiments. Error bars indicate standard deviations.

lowest levels of apoptosis had an M2 gene segment derived from T1L. Analysis of the data using the Mann-Whitney test showed that only the M2 gene segregated at a statistically significant level with the capacity of these strains to induce apoptosis ($P = 0.02$). There was not a statistically significant association between apoptosis and the S1 gene ($P = 0.28$), which is the primary apoptosis determinant following infection of JAM-A-expressing cells, when infection was initiated in an Fc-dependent fashion (38, 145, 199, 200). These data suggest that the M2-encoding $\mu 1$ protein, which functions in penetration of cell membranes (93, 121, 127), is the primary viral determinant of strain-specific differences in apoptosis induction following infection by Fc-mediated uptake.

Reovirus mutant tsA279 is inefficient in apoptosis induction

To determine whether a mutant virus with a defective $\mu 1$ protein is altered in the capacity to trigger apoptosis, we used reovirus strain tsA279.64, which contains a temperature-sensitive mutation that maps to the M2 gene segment (67). This virus was derived from a coinfection of T1L and tsA279, which contains temperature-sensitive mutations in both the M2 and L2 gene segments. The tsA279.64 virus contains the mutant M2 gene segment but not the mutant L2 gene segment, thus facilitating analysis of the contribution of the M2 gene segment to apoptosis induction. When assembled at non-permissive temperature, virions containing the mutant M2 gene segment cannot penetrate membranes due to a misfolded $\mu 1$ protein (67). To examine whether $\mu 1$ -mediated membrane penetration is required for apoptosis induction, HeLa cells were adsorbed with increasing MOIs of tsA279.64 virions assembled under permissive and non-permissive conditions. The percentage of cells with apoptotic nuclei were assessed by using AO staining 48 h after infection at non-permissive temperature (Fig. 10). At all MOIs tested, particles assembled at

Table 1. Apoptosis induction by T1L x T3D reassortant viruses in CHO-B1 cells

Virus strain	Origin of gene segments ^a										% Apoptosis ^b
	L1	L2	L3	M1	M2	M3	S1	S2	S3	S4	
EB138	D	L	L	D	D	L	D	D	L	L	80.52
KC150	D	L	L	L	D	L	D	D	L	D	62.86
EB97	D	D	L	D	D	D	D	D	D	L	52.31
EB68	L	D	L	L	D	L	L	L	D	D	41.29
1HA.3	L	L	L	L	L	L	D	L	L	L	40.63
EB144	L	L	L	L	D	D	L	L	D	L	38.27
KC9	D	D	L	D	D	D	L	D	D	D	35.06
EB98	L	D	L	L	L	L	L	D	L	D	32.62
EB121	D	D	L	D	L	D	L	D	D	D	28.94
EB120	D	D	D	L	L	D	D	D	L	L	26.69
G16	L	L	L	D	L	L	L	D	L	L	24.46
G2	L	D	L	L	L	L	D	L	L	L	23.14
EB143	D	L	L	L	L	L	D	L	L	L	23.04
EB145	D	D	D	D	D	L	L	D	D	D	16.28
EB113	L	L	L	D	L	L	L	L	D	L	14.54

^a Parental origin of each gene segment: L, gene segment derived from T1L; D, gene segment derived from T3D.

^b CHO-B1 cells (2×10^5) were adsorbed with virus strains at an MOI of 100 PFU per cell. After 1 h, the inoculum was removed, fresh medium was added, and cells were incubated at 37°C for 48 h and stained with AO to assess apoptosis. Shown are the mean percentage of cells undergoing apoptosis for three independent experiments. The M2 gene was the only gene associated with the efficiency of apoptosis as determined by using the non-parametric Mann-Whitney test, without adjusting for multiple comparisons ($P = 0.02$).

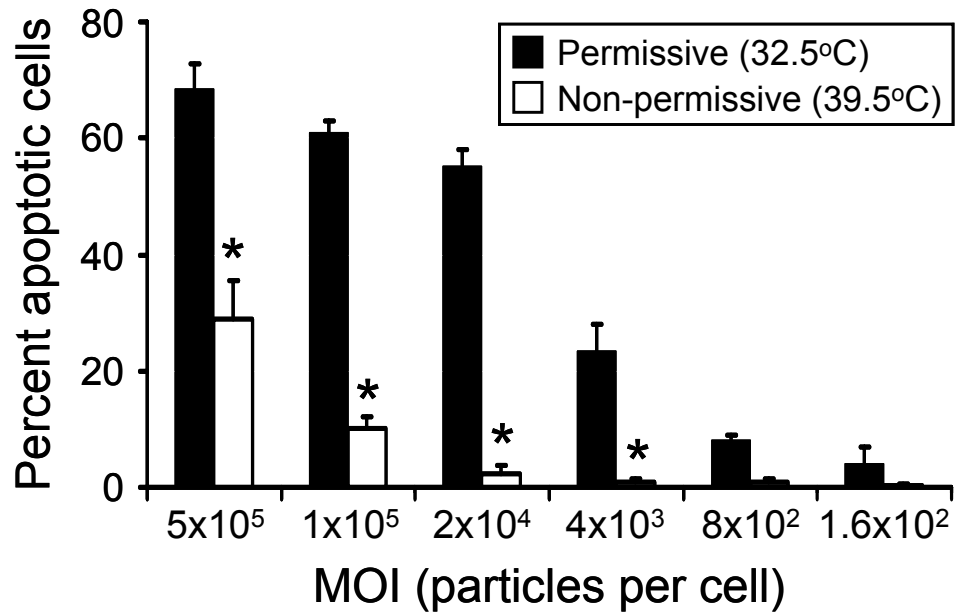


Figure 10. Apoptosis induced by $\mu 1$ temperature-sensitive mutant tsA279.64. HeLa cells were adsorbed with tsA279.64 grown at permissive or non-permissive temperatures at the MOIs shown. Following infection at 37°C for 48 h, cells were harvested and stained with AO. The results are expressed as the mean percentage of cells undergoing apoptosis for three independent experiments. Error bars indicate standard deviations. *, $P < 0.05$ as determined by Student's t test in comparison to virions grown at permissive temperature at an equivalent MOI.viations.

non-permissive temperature induced less apoptosis than particles assembled at permissive temperature. These data demonstrate that virions containing a $\mu 1$ protein that is inefficient in membrane penetration are less potent inducers of apoptosis, which further highlights a key role for the $\mu 1$ protein in apoptosis induction.

Discussion

We have previously shown that binding of reovirus to JAM-A and sialic acid is required for efficient induction of apoptosis (11, 38). In addition, we have reported that viral disassembly in cellular endosomes is also necessary for apoptosis induction by reovirus (39). However, since receptor binding is prerequisite for virus disassembly, these findings do not resolve the question of whether reovirus attachment and disassembly provide two distinct signals, both of which are required for apoptosis induction, or whether the viral disassembly events are sufficient for proapoptotic signaling. To address this question, we uncoupled reovirus attachment to JAM-A and sialic acid from viral disassembly by providing an alternative means of viral entry. We report here that antibody-mediated uptake of reovirus into Fc receptor-expressing CHO cells independent of binding to JAM-A and sialic acid leads to productive infection (22) and apoptosis. Furthermore, we demonstrate that antibody-directed binding of reovirus to Fc receptors expressed on CHO cells is not sufficient for reovirus-induced apoptosis. Analogous to JAM-A- and sialic acid-dependent infection, viral replication steps during or after disassembly in endosomes but prior to RNA synthesis also are required for reovirus-induced apoptosis when infection is initiated by Fc-mediated uptake. Analysis of apoptosis induction by T1L x T3D reassortant viruses following Fc-mediated uptake showed that differences in the efficiency of apoptosis exhibited by type 1 and type 3 strains segregates with the $\mu 1$ -encoding M2 gene segment. Neither core particles

that lack the $\mu 1$ protein and are therefore incapable of penetrating endosomal membranes, nor the thermosensitive M2 mutant virus tsA279, which contains a misfolded, penetration-defective $\mu 1$ protein, can efficiently induce apoptosis. These findings suggest that reovirus membrane-penetration protein $\mu 1$ induces proapoptotic signaling events during or after endosomal membrane penetration.

Our reassortant analysis indicated that only the viral M2 gene segment segregated statistically significantly with the capacity to induce apoptosis. Although the apoptosis-inducing capacities of T3D M2 containing reassortants were generally higher than those of T1L M2 containing viruses, the percentage of cells undergoing apoptosis formed a continuum rather than two distinct clusters. We think that since apoptosis is induced during or after membrane penetration mediated by the $\mu 1$ protein, steps in the viral replication cycle preceding these $\mu 1$ events, such as viral attachment, internalization and disassembly, also are likely to affect the magnitude of apoptosis. Thus, viral genes that affect these steps also might influence the apoptotic response. Minor strain-specific effects of other viral gene segments may also explain why we observe that Fc-mediated uptake of T1L induces significantly greater apoptosis than T3D (Fig. 5 and parents in Table 1, Student's t test, $p < 0.05$). Since we did not find any linkage between the S1 gene and apoptotic potential, we do not think that the differences in the efficiencies of the two $\sigma 1$ antibodies utilized for this analysis contribute to these results. An alternative explanation to account for the unusually high and low apoptosis inducing capacities of the reassortants may be the presence of mutations in their M2 gene that alter the capacity of the virus to induce apoptosis. Thus, although multiple reovirus genes contribute to the capacity of reovirus to induce apoptosis, based on our statistical analysis of reassortant viruses as well as analysis of an M2 ts mutant, we conclude that the M2 gene product $\mu 1$ is the primary mediator.

In addition to the findings described in this chapter, three independent lines of evidence support a crucial role for $\mu 1$ in reovirus-induced apoptosis. First, differences in apoptosis efficiency displayed by strains T1L and T3D are linked to the $\mu 1$ -encoding M2 gene (145, 199, 200). Second, studies with pharmacologic inhibitors of reovirus replication place the apoptosis-inducing events subsequent to viral disassembly but prior to RNA synthesis (39), which coincides with $\mu 1$ -mediated membrane penetration (26, 93, 121, 127). Third, transient transfection of a plasmid encoding T3D $\mu 1$ is sufficient to induce apoptosis in CHO cells (36). Interestingly, although plasmid-mediated expression of $\mu 1$ neither mimics normal delivery of $\mu 1$ via endosomal rupture during viral membrane penetration, nor de novo expression of $\mu 1$ in infected cells (since $\mu 1$ is always found associated with its protector protein $\sigma 3$ (168, 169, 190), it leads to the same consequence.

It is not known how the viral disassembly events culminating in $\mu 1$ -mediated membrane penetration elicit proapoptotic signaling. We envision two possibilities. First, endosomal disruption by $\mu 1$ may lead to release of hydrolytic enzymes such as cathepsins, which in turn damage mitochondria and stimulate death signaling (46, 64, 144). Interestingly, mitochondrial injury has been reported as early as 4 h following reovirus adsorption, suggesting the involvement of an early viral replication event (85, 86). It is also possible that release of these enzymes causes apoptosis via their action on death regulators such as Bid (182). Of note, Bid cleavage has been observed during reovirus infection and has been hypothesized to play a role in apoptosis induction (85). Second, fragments of $\mu 1$ produced during proteolytic viral disassembly are known to gain access to the cytoplasm (27). These fragments may activate other cellular sensors of viral infection or directly injure mitochondria to induce apoptosis. Concordantly, the $\mu 1$ protein localizes to mitochondria during infection or when expressed from plasmids in transfected cells, suggesting a post-

endosomal site of action. Interestingly, a 30-residue C-terminal fragment of $\mu 1$ is sufficient to localize to mitochondria and induce apoptosis in transfected cells (36).

Although our findings point to $\mu 1$ as a key viral regulator of proapoptotic signaling, this work does not explain the previously established unequivocal association between the S1-encoded $\sigma 1$ protein and the efficiency of apoptosis induction by reovirus (145, 199, 200). Strains encoding a $\sigma 1$ protein capable of binding to JAM-A and sialic acid are the most potent inducers of apoptosis (38). We did not observe efficient infection of CHO-B1 cells in the absence of mAb pretreatment at the MOIs used. Therefore, we think that these cells do not express sufficient quantities of sialic acid or JAM-A on the cell surface to effect productive infection. Thus, infection of these cells appears to be dependent only on the presence of a high-affinity receptor such as the Fc receptor. Since the efficiency of antibody-mediated uptake and delivery of both sialic-acid-binding and non-sialic-acid-binding strains of reovirus via Fc receptors is essentially equivalent in CHO-B1 cells, $\sigma 1$ -related differences are negated. An alternative explanation for our findings is that antibody-mediated attachment of virions to Fc receptors stimulates a signaling cascade in cells that mimics signaling induced as a consequence of $\sigma 1$ binding to JAM-A and sialic acid and that Fc receptor-mediated signaling acts in concert with the viral disassembly events to elicit apoptosis. However, given the marked differences in functional properties displayed by JAM-A and Fc receptors, this explanation seems less likely. Therefore, our current and previous results suggest that the linkage of $\sigma 1$ to apoptosis efficiency is not related to $\sigma 1$ -mediated stimulation of the cellular proapoptotic machinery, but rather the capacity of $\sigma 1$ to efficiently deliver virions into endosomes for disassembly. We hypothesize that as opposed to viral infection, which requires penetration by just one infectious virion, efficient apoptosis induction by reovirus requires endosomal penetration by multiple virions. Since sialic acid

allows more avid binding of virions to cells (10), we think that this entry route may deliver virions more efficiently into endosomal compartments for uncoating and subsequent membrane penetration, leading to higher levels of apoptosis (38).

This study highlights a new role for the viral membrane-penetration protein $\mu 1$ in apoptosis induction. Other viruses such as coronavirus, Sindbis virus, and vaccinia virus also have been reported to require post-attachment cell entry events in endosomes to induce apoptosis (78, 98, 138). However, the viral determinants of apoptosis by these viruses are unknown. Interestingly, entry of Sindbis virus into endosomes induces apoptosis through activation of sphingomyelinases and release of the proapoptotic second messenger, ceramide (76). Although we anticipate that interactions between the enveloped Sindbis virus with endosomes differ from those with $\mu 1$, it is possible that ceramide plays a role in reovirus-induced apoptosis. Collectively, these studies point to cellular endosomes as sites from which proapoptotic signaling events are initiated and imply a conserved mechanism by which host cells detect the presence of invading pathogens. Pathogen detection during the entry phase may allow host cells to more efficiently limit the spread of infection by initiating a suicidal response. Alternatively, induction of apoptosis by a virus early in its replication cycle may prevent the development of an inflammatory response, thereby allowing the virus to better evade host defenses.

A fascinating similarity exists between the properties of reovirus protein $\mu 1$ and several toxins elaborated by bacteria and viruses. Analogous to the capacity of $\mu 1$ to mediate membrane permeabilization (26, 71, 101, 192), α toxin of *Staphylococcus aureus*, lysteriolysin O of *Listeria monocytogenes*, and killer toxins (K1 and K2) of the yeast L-A virus, also can form pores in host cell membranes (107, 191, 212, 215). Interestingly, each of these toxins also has the capacity to induce apoptotic cell death (143, 212). Our ongoing

studies are focused on understanding the precise mechanism by which $\mu 1$ induces apoptosis during reovirus infection. Through these studies we hope to gain broader insight into events at the pathogen-host interface that evoke death signaling and cause disease.

CHAPTER III

I κ B KINASE SUBUNITS α AND γ ARE REQUIRED FOR ACTIVATION OF NF- κ B AND INDUCTION OF APOPTOSIS BY MAMMALIAN REOVIRUS

Introduction

Transcription factor NF- κ B plays an important regulatory role in apoptosis evoked by reovirus in cultured cells (40) and in vivo (128). Inducible members of the NF- κ B family are sequestered in the cytoplasm by inhibitory I κ B proteins, including I κ B α , I κ B β , I κ B ϵ , and p100/NF- κ B2 (8, 69, 176, 204, 214). In response to a wide variety of NF- κ B inducers, I κ B proteins are phosphorylated at specific serine residues, earmarking these molecules for destruction by the ubiquitin-proteasome pathway (21, 30, 69, 132, 194, 214).

Phosphorylation of I κ B proteins is mediated by cytokine-inducible I κ B kinases (IKKs) IKK α and IKK β (104, 203), which can form higher order complexes containing a regulatory subunit called IKK γ /Nemo (51, 115, 151, 223, 226). A primary function of IKK β is to modulate the inhibitory interaction of I κ B α with the prototypical form of NF- κ B containing p50/RelA dimers (48, 51, 115, 141, 177). This regulatory circuit, termed the classical pathway of NF- κ B activation, is strictly dependent on the presence of IKK γ /Nemo (156, 160, 223). In contrast, IKK α functions in an alternative IKK γ -independent pathway of NF- κ B activation that leads to proteolytic processing of p100 and production of a fully functional p52 Rel subunit (35, 163, 179). Unlike the classical, IKK β -directed pathway of NF- κ B activation, the alternative pathway involving IKK α is dependent on prior phosphorylation of this IKK by NF- κ B-inducing kinase (NIK) (95, 163, 221).

To better understand the mechanism of NF- κ B activation by reovirus, I conducted experiments to define the NF- κ B/Rel, I κ B, and IKK proteins that are under reovirus control. These studies revealed that NF- κ B/Rel proteins are mobilized to the nuclear compartment with biphasic kinetics following reovirus infection. Reovirus-induced activation of NF- κ B/Rel proteins is accompanied by selective degradation of I κ B α , suggesting a role for IKK β . However, subsequent studies with IKK subunit-deficient cells clearly demonstrate that IKK α rather than IKK β plays an essential role in the mechanism by which reovirus activates NF- κ B and downstream apoptotic genes. I also assembled evidence indicating that the reovirus/IKK α axis is intact in cells lacking NIK, an upstream activator of IKK α , but not in cells lacking the IKK β regulatory subunit IKK γ /Nemo. Taken together, these data suggest that reovirus activates the IKK α pathway of the NF- κ B signaling apparatus downstream of NIK, perhaps via direct interactions with the regulatory subunit IKK γ /Nemo.

Results

Reovirus infection results in the biphasic activation of NF- κ B/Rel DNA-binding proteins

In prior studies, we found that reovirus activates the functional expression of p50/RelA complexes, suggesting the involvement of classical NF- κ B signaling (40). However, it remained unclear whether NF- κ B/Rel proteins linked to the alternative pathway of the NF- κ B pathway are activated during reovirus infection. To more completely define the composition of NF- κ B complexes activated by reovirus, we used nuclear extracts from reovirus-infected HeLa cells and Rel-specific antibodies to monitor the composition of DNA-binding complexes formed in EMSAs. NF- κ B/Rel DNA-binding activity was readily

detected over background levels (mock treatment) within 2 hours after infection with reovirus strain T3D (Fig. 11A), which potently induces apoptosis in cultured cells (40, 145, 199) and the murine CNS (125). Peak levels of NF- κ B/Rel DNA-binding activity were observed at 4-8 h post-infection. Supershift analysis of extracts obtained at 4, 6, and 8 h post-infection revealed the presence of DNA/protein complexes containing p50 and RelA, but neither p52 nor RelB (Fig. 11B), suggesting preferential usage of the classical versus alternative NF- κ B pathway by reovirus. Complexes containing c-Rel were apparent in supershift assays only after 8 h of infection (Fig. 11B). Thus, reovirus induces a biphasic pattern of NF- κ B/Rel activation featuring the initial nuclear translocation of complexes consisting of p50 and RelA, followed by those containing p50, RelA, and c-Rel. Given that the cellular gene encoding c-Rel contains functional NF- κ B binding sites (63), this expression pattern may reflect de novo synthesis of c-Rel rather than its mobilization from a latent cytoplasmic pool.

These initial experiments conducted over an 8 h timecourse provided no evidence for the capacity of reovirus to stimulate the nuclear expression of p52, a signature Rel protein involved in the alternative pathway of NF- κ B signaling. To further investigate whether reovirus interfaces with the alternative NF- κ B pathway, we extended the timecourse of T3D infection to 24 h and monitored extracts for processing of p100 to p52 (163). Levels of p100 were significantly reduced between 16 and 24 h post-infection (Fig. 12). Consistent with a precursor/product relationship, diminution in p100 protein levels were accompanied by a significant increase in the steady-state levels of p52 (Fig. 12, panels A and C). Taken together with the NF- κ B/Rel profiling data shown in Fig. 11B, this finding suggests that reovirus engages not only the classical pathway of NF- κ B signaling but also the alternative pathway, albeit at much later times of infection.

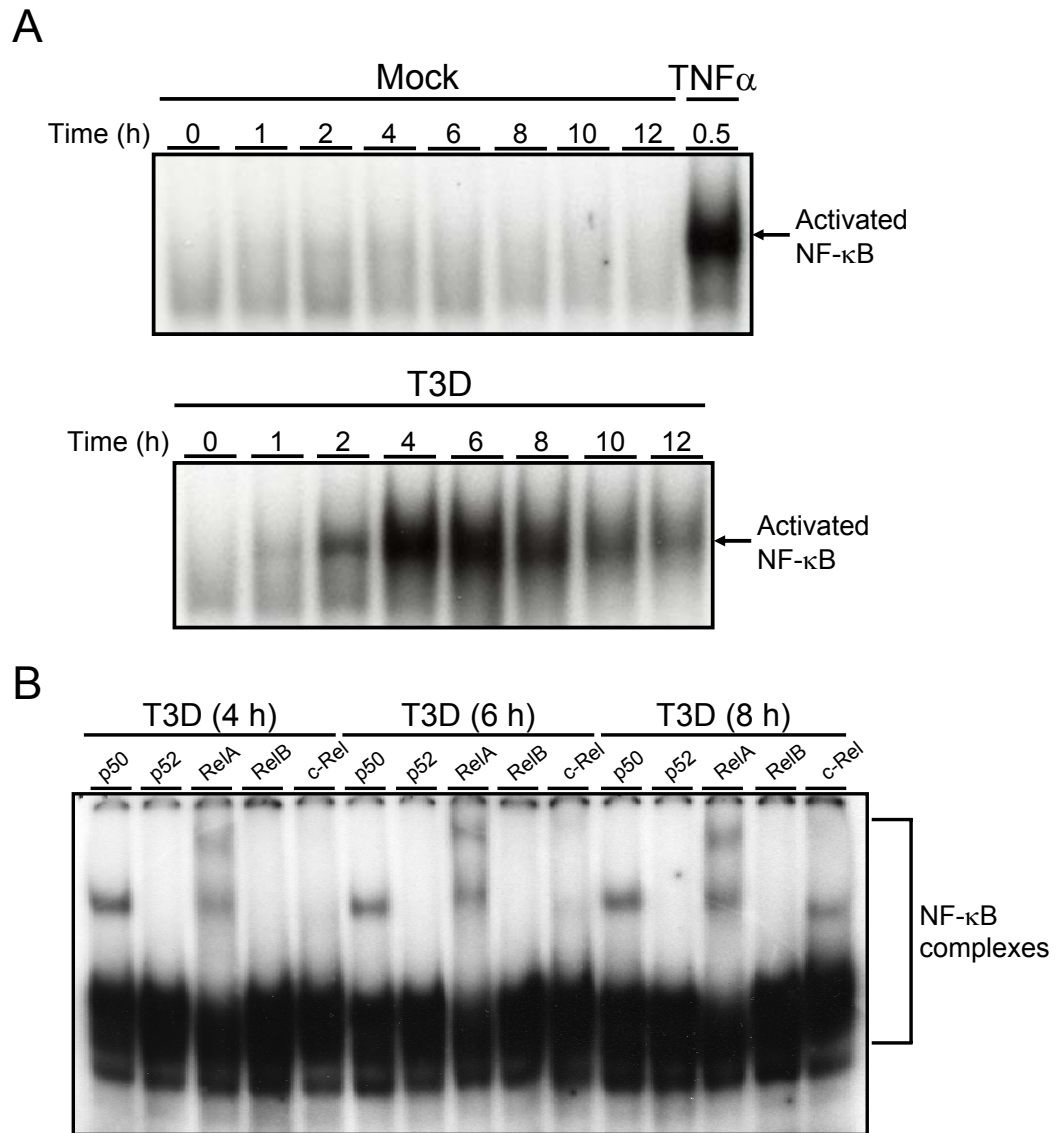


Figure 11. Biphasic activation of NF- κ B/Rel proteins in reovirus-infected cells. (A) Nuclear extracts were prepared from uninfected HeLa cells (0 h), mock-infected cells (Mock), or cells infected with T3D at an MOI of 100 PFU/cell for the times shown. Cells also were treated with 20 ng/ml of TNF α for 30 min as a positive control. Extracts were incubated with a radiolabeled NF- κ B consensus oligonucleotide, and resulting protein-oligonucleotide complexes were resolved by acrylamide gel electrophoresis, dried, and exposed to film. (B) Nuclear extracts prepared at 4, 6, and 8 h post infection were incubated with antisera specific for p50, p52, RelA, RelB, or c-Rel prior to the addition of a radiolabeled NF- κ B consensus oligonucleotide. NF- κ B-containing complexes are indicated.

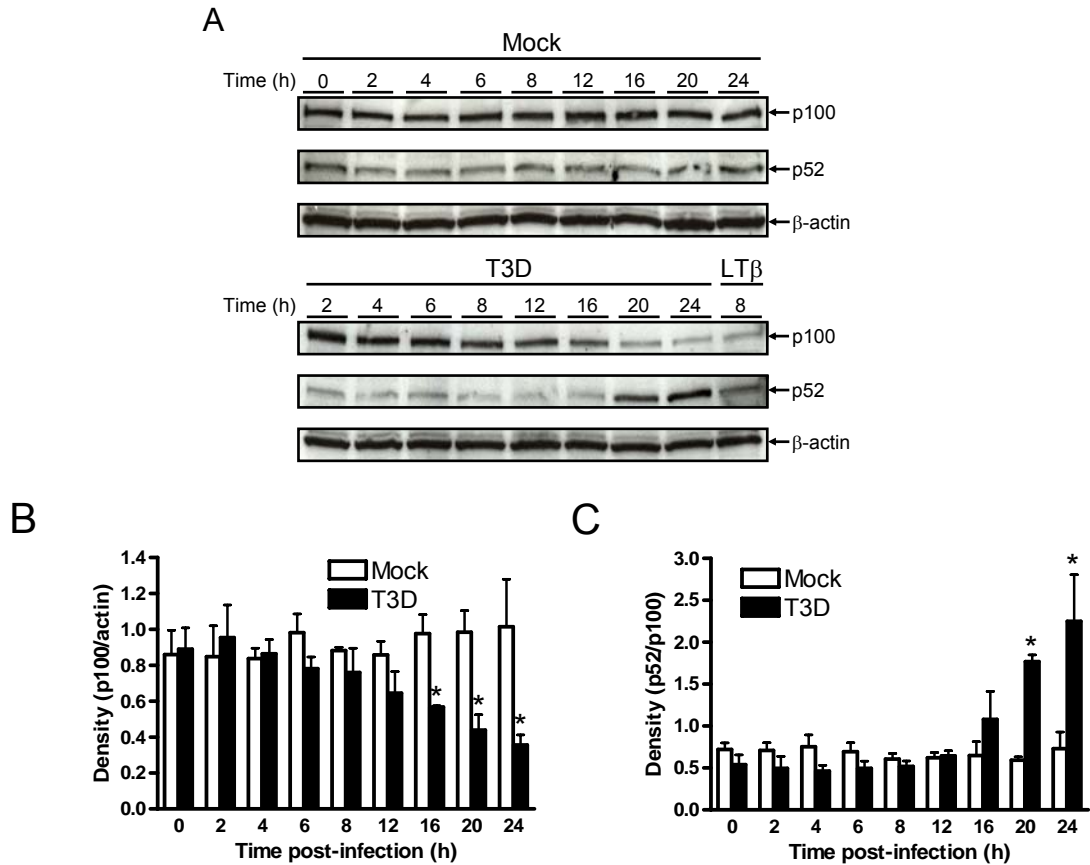


Figure 12. Processing of p100 to p52 during reovirus infection. (A) Whole-cell extracts were prepared from uninfected HeLa cells (0 h), mock-infected cells (Mock), or cells infected with reovirus T3D at an MOI of 100 PFU/cell for the times shown. Cells also were treated with 2 μ g/ml of an agonistic lymphotoxin- β receptor antiserum for 8 h as a positive control. Extracts were resolved by SDS-PAGE, transferred to nitrocellulose membranes, and immunoblotted by using an antiserum specific for p100/p52. Band intensity was quantified by using the Image J program. The results are presented as the mean ratio of (B) p100/actin or (C) p52/p100 for three independent experiments. Error bars indicate standard deviations. *, $P < 0.05$ as determined by Student's t test in comparison to untreated cells (0 h).

Reovirus infection leads to the selective degradation of I κ B α

Activation of the classical NF- κ B pathway by physiologic agonists is primarily dependent on degradation of I κ B α (reviewed in (19, 59, 66)), an inhibitor that sequesters p50/RelA complexes in the cytoplasmic compartment (8). We have previously shown that degradation-resistant forms of I κ B α attenuate reovirus-induced apoptosis, which is critically dependent on NF- κ B activation (40). However, mammalian cells express other labile inhibitors that are structurally similar to I κ B α , such as I κ B β (96) and I κ B ϵ (214). Indeed, prior studies suggest a potential role for signal-dependent degradation of I κ B β (189) and I κ B ϵ (214) in the inducible nuclear entry of c-Rel. To determine whether any of these inhibitors is under reovirus control, we monitored their levels in T3D-infected cells in immunoblotting studies using I κ B-specific antibodies. The cellular pool of I κ B α was significantly reduced within 4 h after infection with T3D (Fig. 13, A and B). In contrast, levels of I κ B β and I κ B ϵ were maintained under the same stimulatory conditions over the entire 8 h timecourse (Fig. 13, C-F). We conclude that I κ B α is a primary cellular target of reovirus, which is fully consistent with its capacity to stimulate nuclear translocation of NF- κ B p50/RelA.

IKK α and IKK γ are required for reovirus-induced NF- κ B activation

We next investigated the mechanism by which reovirus destabilizes I κ B proteins. Cytokine-induced degradation of NF- κ B inhibitors is dependent on their phosphorylation at specific serine residues by IKKs such as IKK α and IKK β (21, 51, 226). These structurally-related enzymes can interact and form higher-order complexes with other cellular proteins (reviewed in (59, 66)). Integration of the regulatory protein IKK γ /Nemo into such complexes

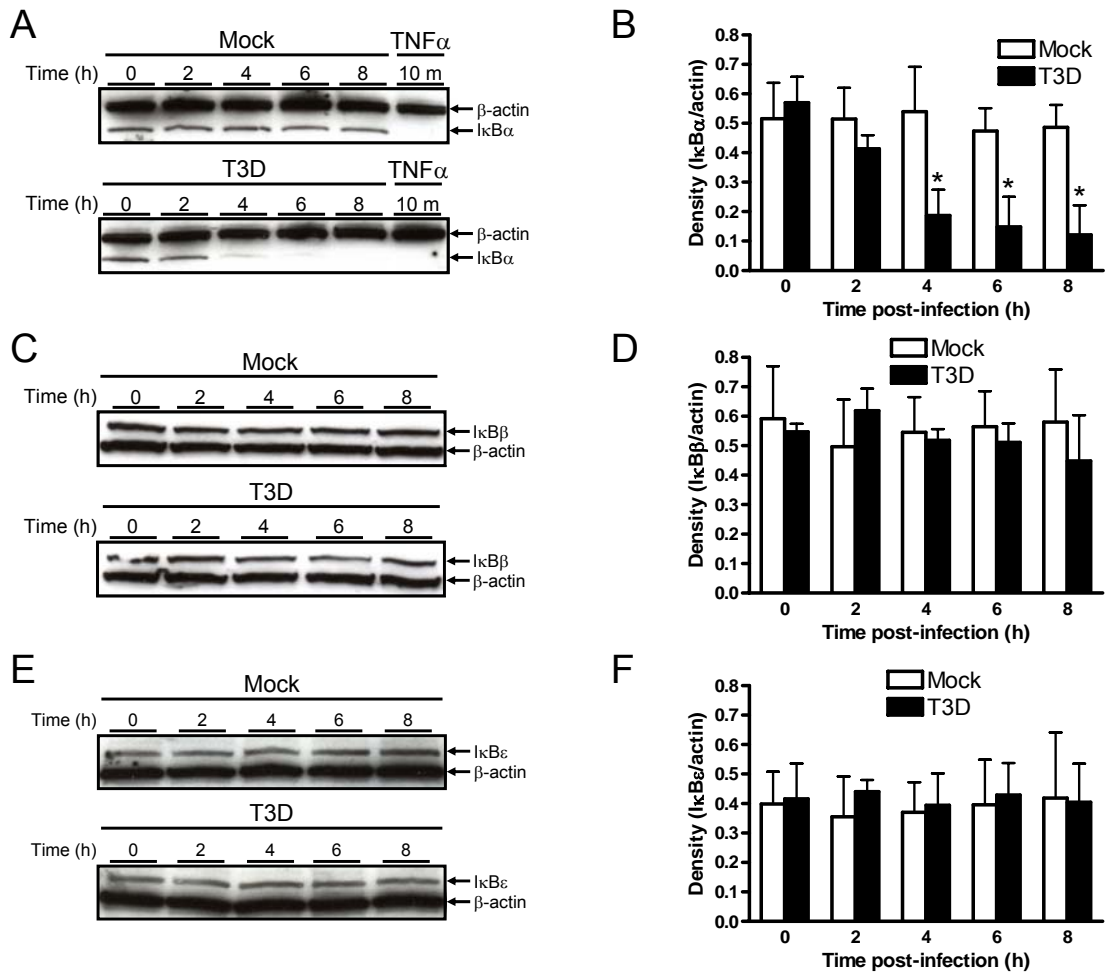


Figure 13. Reovirus infection leads to degradation of IκBα but not IκBβ or IκBε. Cytoplasmic extracts were prepared from uninfected HeLa cells (0 h), mock-infected cells (Mock), or cells infected with reovirus T3D at an MOI of 100 PFU/cell for the times shown. Cells also were treated with 20 ng/ml of TNFα for 10 min as a positive control. Extracts were resolved by SDS-PAGE, transferred to nitrocellulose membranes, and immunoblotted by using antisera specific for (A) IκBα, (C) IκBβ, or (E) IκBε. An actin-specific antiserum was used to detect levels of actin as a loading control. Band intensity corresponding to levels of (B) IκBα, (D) IκBβ, and (F) IκBε was quantified by using the Image J program. The results are presented as the mean ratio of IκB/actin for three independent experiments. Error bars indicate standard deviations. *, $P < 0.05$ as determined by Student's t test in comparison to untreated cells (0 h).

is required for the activation of IKK β (156, 160, 223) but not IKK α (35, 47, 163). The most well-characterized substrate of IKK β is I κ B α (73, 115), whereas IKK α catalyzes phosphorylation of p100/NF- κ B2 (163, 221).

To determine whether either IKK α or IKK β is required for reovirus-induced activation of NF- κ B, cellular IKK complexes were immunopurified from HeLa cells either before or after infection with T3D and monitored for their capacity to phosphorylate I κ B α in vitro. In keeping with the kinetics of I κ B α degradation (Fig. 13A) and NF- κ B activation (Fig. 11A), I κ B kinase activity exceeding basal levels in uninfected cells was readily detected within 4 h after exposure to T3D and sustained for at least an additional 4 h (Fig. 14A). These data suggest that IKKs are critically involved in the mechanism by which reovirus diminishes the cellular pool of I κ B α (Fig. 13A).

To determine whether IKK activation is required for the nuclear translocation of NF- κ B by reovirus, cells were treated with escalating doses of the IKK inhibitor BAY 65-1942 prior to infection with T3D. Importantly, BAY 65-1942 inhibits IKK β more efficiently than IKK α (227). As demonstrated in EMSAs, treatment of cells with BAY 65-1942 suppressed NF- κ B signaling induced by reovirus (Fig. 14, B and C), although incompletely, perhaps reflecting incomplete blockade of IKK α . Immunoblotting studies of nuclear extracts from the same panel of infected cells indicated that BAY 65-1943 had a profound inhibitory effect on reovirus-induced nuclear translocation of RelA (Figs. 14, D and E), which is primarily under the control of IKK β . These pharmacological data suggest that reovirus activates NF- κ B via a mechanism involving either IKK α , IKK β , or both of these IKKs.

To identify the IKK subunits responsible for NF- κ B activation by reovirus, NF- κ B DNA-binding activity was assessed in murine embryo fibroblasts (MEFs) deficient for

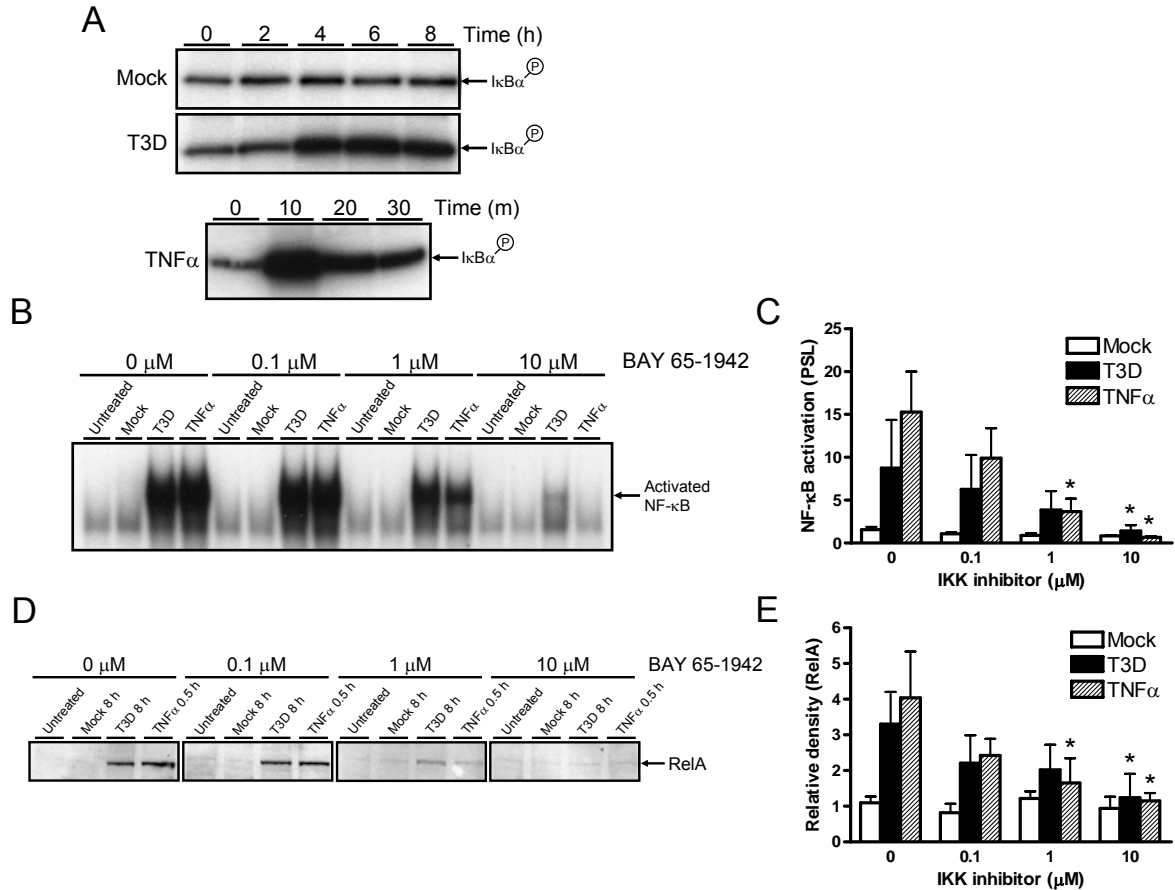


Figure 14. Involvement of IKKs in reovirus-induced NF-κB activation. (A) Whole-cell extracts were prepared from uninfected HeLa cells (0 h), mock-infected cells (Mock), or cells infected with reovirus T3D at an MOI of 100 PFU/cell for the times shown. Cells also were treated with 20 ng/ml of TNFα for the times shown as a positive control. The IKK complex was immunoprecipitated by using an IKKγ-specific antiserum prior to incubation with a GST-IκBα substrate in the presence of [γ - 32 P]ATP. Kinase reactions were resolved by SDS-PAGE, transferred to nitrocellulose, and visualized by autoradiography. (B) HeLa cells were pretreated with IKK inhibitor BAY 65-1942 for 1 h at the concentrations shown and uninfected (Untreated), mock-infected (Mock), or infected with reovirus T3D at an MOI of 100 PFU/cell for the times shown. Nuclear extracts were incubated with a radiolabeled NF-κB consensus oligonucleotide, and resulting protein-oligonucleotide complexes were resolved by acrylamide gel electrophoresis, dried, and exposed to film. (C) Band intensity was quantified by determining PSL units relative to uninfected cells for four independent experiments. Error bars indicate standard deviations. *, $P < 0.05$ as determined by Student's t test in comparison to untreated cells (0 μM). (D) Nuclear extracts from the experiment shown in panel B were resolved by SDS-PAGE, transferred to nitrocellulose, and immunoblotted by using a RelA-specific antiserum. (E) Band intensity was quantified relative to uninfected cells by using the Image J program. The results are presented as the mean RelA band intensity for three independent experiments. Error bars indicate standard deviations. *, $P < 0.05$ as determined by Student's t test in comparison to untreated cells (0 μM).

IKK α , IKK β , or the IKK β regulatory subunit IKK γ /Nemo. In initial experiments, EMSAs were conducted with nuclear extracts from wild-type MEFs following infection with T3D for 8 h, which corresponds to peak levels of NF- κ B DNA-binding activity (Fig. 11A). Reovirus induced NF- κ B DNA binding activity to levels comparable to or exceeding those observed in control experiments with wild-type MEFs treated with the cytokine TNF α (Fig. 15A), a potent agonist of IKK. Similar results were obtained with nuclear extracts from reovirus-infected MEFs lacking IKK β (Fig. 15A). However, the capacity of reovirus to activate NF- κ B was completely disrupted in MEFs lacking IKK α (Fig. 15A), indicating preferential usage of this IKK relative to IKK β . MEFs lacking the regulatory subunit IKK γ /Nemo (Fig. 15A) also were incapable of reovirus-mediated NF- κ B signaling. Immunoblotting studies of nuclear extracts from the same panel of infected cells confirmed these results (Fig. 15C). Nuclear translocation of RelA was detected in wild-type MEFs and IKK β -deficient MEFs, but not in MEFs lacking IKK α or IKK γ . Differences in reovirus-mediated signal transduction in IKK-deficient MEFs could not be attributed to differences in viral infection or growth (Fig. 16). Thus, these findings suggest that IKK α and IKK γ are required for reovirus-induced NF- κ B activation.

NIK is capable of phosphorylating and activating IKK α in response to some agonists of the alternative NF- κ B pathway, such as lymphotoxin β (95, 109). To determine whether NIK is required for NF- κ B activation in response to reovirus, NIK-deficient MEFs were used to probe for NF- κ B induction by EMSA and immunoblotting in response to reovirus T3D infection (Fig. 17). Reovirus infection resulted in NF- κ B activation in both wild-type and NIK-deficient MEFs, indicating that NIK is dispensable for reovirus-induced NF- κ B activation. Taken together, these data confirm a requirement for endogenous IKK in the

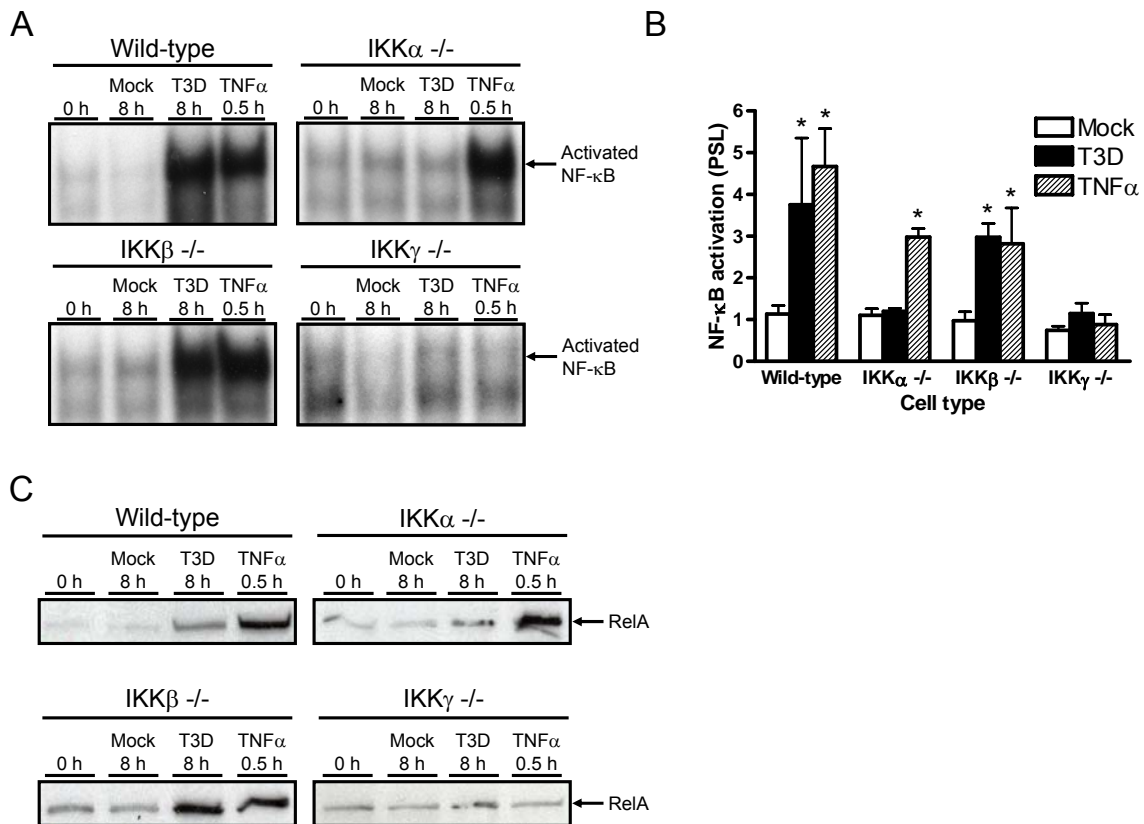


Figure 15. IKK α and IKK γ are required for reovirus-induced activation of NF- κ B. (A) Wild-type MEFs or MEFs deficient in IKK α , IKK β , or IKK γ were uninfected (0 h), mock-infected (Mock), infected with reovirus T3D at an MOI of 100 PFU/cell for 8 h, or treated with 20 ng/ml of TNF α for 1 h. Nuclear extracts were incubated with a radiolabeled NF- κ B consensus oligonucleotide. Resulting protein-oligonucleotide complexes were resolved by acrylamide gel electrophoresis, dried, and exposed to film. NF- κ B-containing complexes are indicated. (B) Band intensity was quantified by determining PSL units relative to uninfected cells for three independent experiments. Error bars indicate standard deviations. *, $P < 0.05$ as determined by Student's t test in comparison to mock-treated cells (0 h). (C) Nuclear extracts from the experiment shown in panel A were resolved by SDS-PAGE, transferred to nitrocellulose, and immunoblotted by using a RelA-specific antiserum.

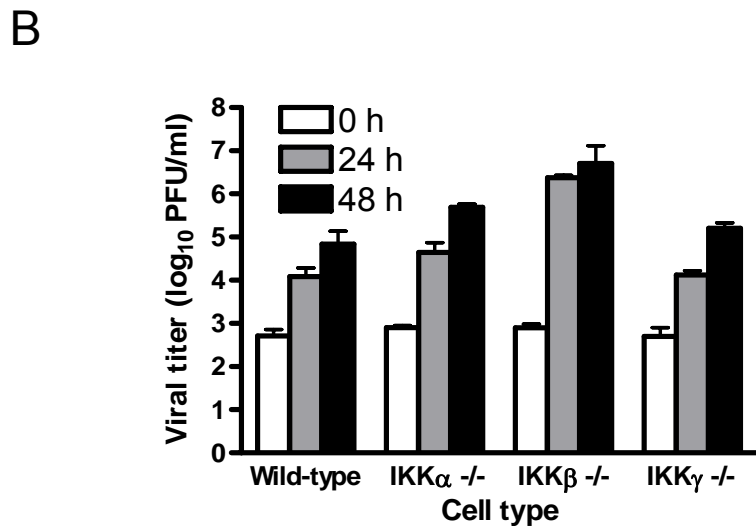
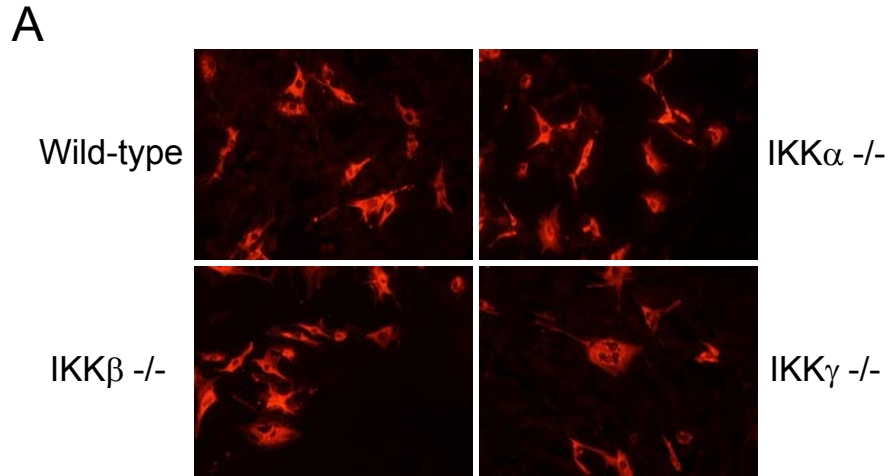


Figure 16. Cells deficient in IKK subunits are permissive for reovirus infection and growth. (A) Wild-type MEFs or MEFs deficient in IKK α , IKK β , or IKK γ were infected with T3D at an MOI of 1000 PFU/cell. After 24 h incubation, cells were fixed and incubated with reovirus-specific antiserum. Infected cells were identified by using indirect immunofluorescence. (B) Cells and medium were infected with reovirus T3D at an MOI of 1 PFU/cell and incubated for the times shown. Cells and medium were frozen and thawed twice, and viral titers were determined by plaque assay. The results are expressed as the mean viral titers for three independent experiments. Error bars indicate standard deviations.

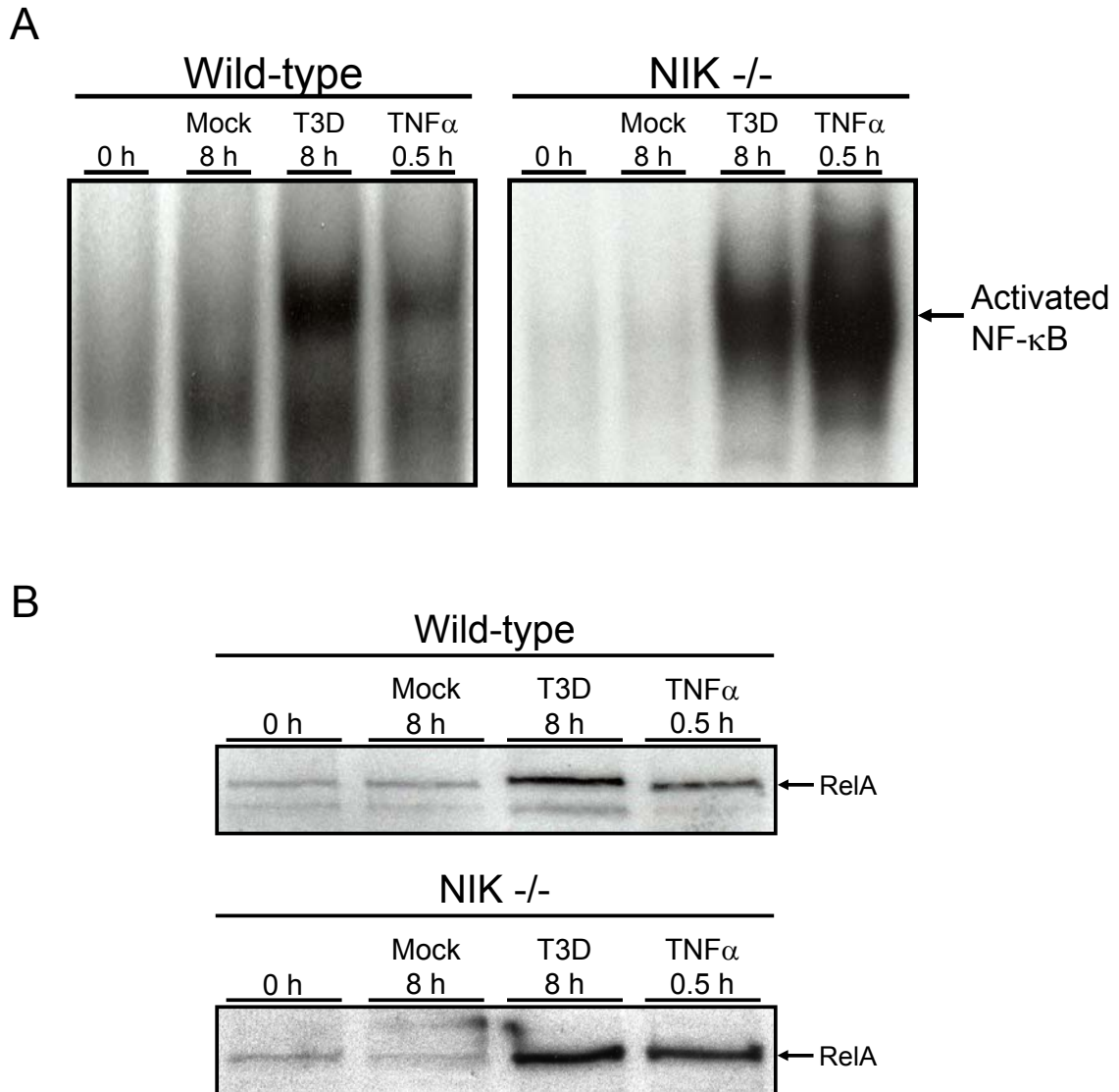


Figure 17. Reovirus-induced activation of NF- κ B in NIK-deficient cells. (A) Wild-type MEFs or NIK-deficient MEFs were uninfected (0 h), mock-infected (Mock), infected with reovirus T3D at an MOI of 1000 PFU/cell for 8 h, or treated with 20 ng/ml of TNF α for 30 min. Nuclear extracts were incubated with a radiolabeled NF- κ B consensus oligonucleotide. Resulting protein-oligonucleotide complexes were resolved by acrylamide gel electrophoresis, dried, and exposed to film. NF- κ B-containing complexes are indicated. (B) Nuclear extracts from the experiment shown in panel A were resolved by SDS-PAGE, transferred to nitrocellulose, and immunoblotted by using a RelA-specific antiserum.

mechanism by which reovirus activates NF- κ B and strongly suggest that this virus selectively utilizes the IKK α arm of the NF- κ B signaling pathway. Surprisingly, IKK γ /Nemo, which is known to regulate IKK β rather than IKK α , is also required for NF- κ B activation by reovirus, but NIK is dispensable.

IKK α and IKK γ are required for reovirus-induced apoptosis

Since IKK α and IKK γ are required for NF- κ B activation following reovirus infection (Fig. 15), we examined whether IKK stimulation by reovirus leads to apoptotic cell death. IKK-deficient MEFs were infected with reovirus T3D, and apoptosis was assessed by quantitation of caspase 3/7 activity (Fig. 18A). Levels of activated caspase 3/7 following infection of wild-type and IKK β -deficient MEFs were substantially greater than those following infection of MEFs deficient in either IKK α or IKK γ . To corroborate these results, we tested wild-type and IKK-null MEFs for viability following infection with T3D (Fig. 18B). In comparison to wild-type and IKK β -deficient MEFs, a significantly greater percentage of IKK α - and IKK γ -deficient MEFs remained viable during a time course of reovirus infection.

To determine whether NIK is required for apoptosis induction following reovirus infection, NIK-deficient MEFs were infected with reovirus T3D, and apoptosis was assessed by quantification of caspase 3/7 activity (Fig. 18C). Levels of caspase 3/7 activity in MEFs deficient in NIK were equivalent to those in wild-type cells following infection with T3D. In parallel with these results, we observed no significant difference in the viability of wild-type and NIK-deficient MEFs following T3D infection (Fig. 18D). Together, these functional data with IKK- and NIK-deficient MEFs strongly correlate with the capacity of reovirus to modulate I κ B α and NF- κ B during infection (Figs. 11-16). Our findings suggest that IKK α

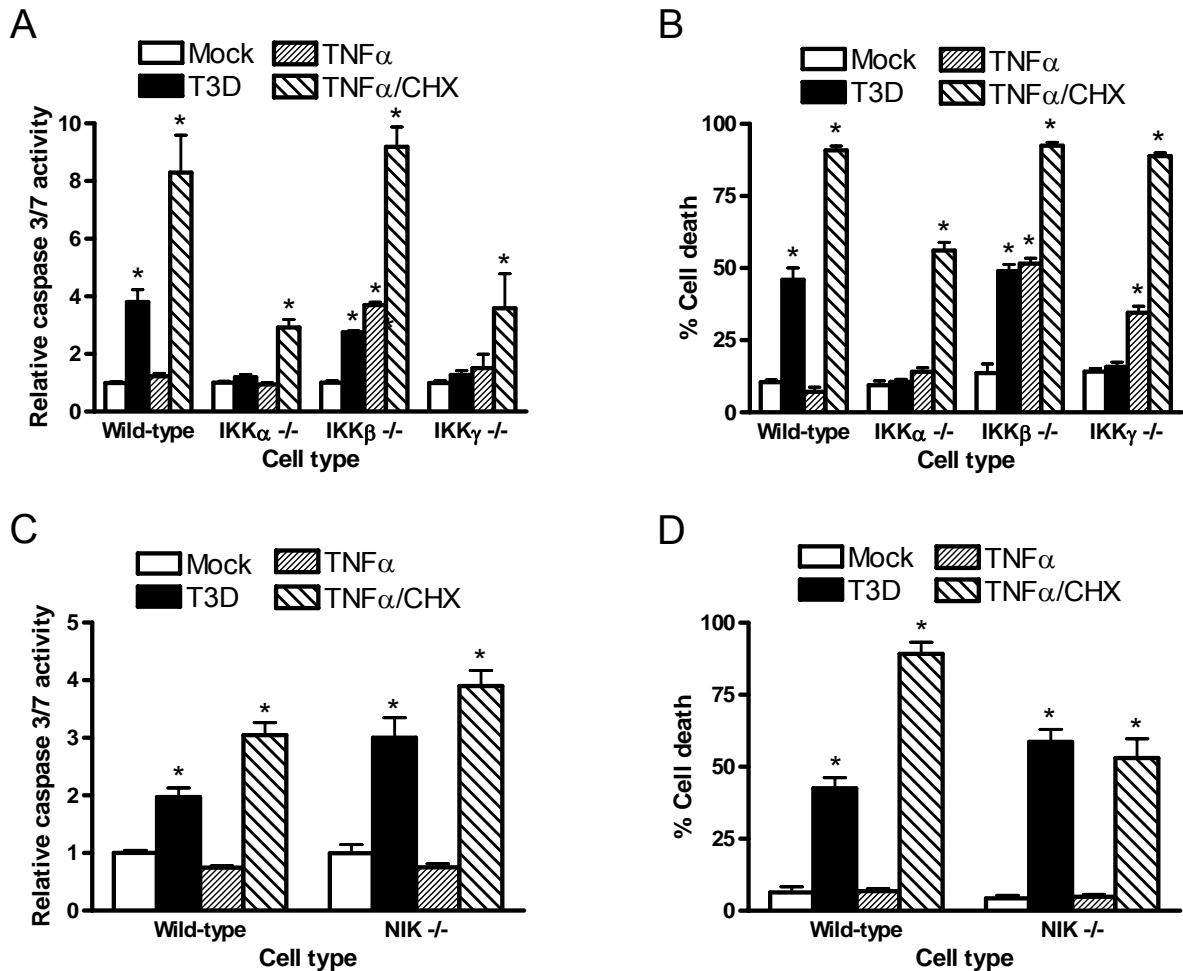


Figure 18. IKK α and IKK γ are required for reovirus-induced apoptosis. Wild-type MEFs or (A) MEFs deficient in IKK α , IKK β , IKK γ , or (C) NIK were mock-infected, infected with reovirus T3D at an MOI of 1000 PFU/cell for 24 h, treated with 10 ng/ml of TNF α for 12 h, or treated with 10 ng/ml of TNF α and 10 μ g/ml of cycloheximide for 12 h. Caspase 3/7 activity was quantified by using a luminescent substrate. The results are expressed as the mean caspase activity relative to mock-infected cells for three independent experiments. Wild-type MEFs or (B) IKK-deficient MEFs or (D) NIK-deficient MEFs were mock-infected, infected with reovirus T3D at an MOI of 1000 PFU/cell for 48 h, treated with 10 ng/ml of TNF α for 24 h, or treated with 10 ng/ml of TNF α and 10 μ g/ml of cycloheximide for 24 h. Cell viability was quantified by trypan blue exclusion. The results are expressed as the mean percentage of cell death for three independent experiments. Error bars indicate standard deviations. *, $P < 0.05$ as determined by Student's t test in comparison to mock-infected cells.

and IKK γ are required for the activation of NF- κ B induction of apoptosis in response to reovirus. In keeping with NF- κ B activation by reovirus, apoptosis is completely independent of the IKK α inducer NIK, indicating a different mechanism of IKK α activation in response to reovirus.

Discussion

Results reported here identify constituents of the NF- κ B signaling apparatus induced by reovirus and provide evidence that NF- κ B activation during reovirus infection requires integral components of both the classical and alternative pathways. Using MEFs deficient in the expression of individual IKK subunits, we demonstrate that reovirus-infected cells lacking IKK α are impaired for NF- κ B activation (Fig. 15) and apoptotic programming (Fig. 18), whereas both of these processes are operative in cells lacking IKK β . Despite its preferential usage of IKK α , reovirus retains the capacity to elicit both NF- κ B activation and apoptosis in the absence of NIK (Fig. 16 and 19), a known activator of IKK α in cytokine-treated cells (95, 163). Furthermore, targeted disruption of the gene encoding IKK γ /Nemo, which is dispensable for cytokine-induced signaling of IKK α (35, 47), significantly attenuates reovirus-induced NF- κ B activation and apoptosis (Fig. 15 and 18). In light of these findings with NIK and IKK γ , the precise mechanism of reovirus action on IKK α remains unclear. The simplest interpretation of these results is that reovirus accesses the cellular NF- κ B machinery by directly interfacing with IKK α /IKK γ complexes, with IKK γ serving as an adaptor that docks one or more reovirus gene products. In keeping with this possibility, IKK γ tethers the HTLV1 Tax protein to IKK complexes, resulting in persistent activation of IKK β and NF- κ B (25, 33). In what may be another related finding, IKK γ also is

required for Tax-induced activation of IKK α (219). Although data emerging from studies of IKK β -deficient mice suggest the presence of functional IKK α /IKK γ complexes (91, 92, 150, 184), direct evidence for the existence of IKK α /IKK γ complexes in wild-type animals has not been reported. Notwithstanding, our results clearly establish that reovirus activates NF- κ B and downstream proapoptotic genes via a mechanism involving IKK α but not IKK β .

The principle in vivo substrate of IKK β is I κ B α (51, 115, 141). This cytoplasmic inhibitor tightly controls the nuclear translocation of p50/RelA dimers (8), effectors of the classical NF- κ B pathway (reviewed in (19, 59, 66)). The principle in vivo substrate of IKK α is p100/NF- κ B2 (163). An integral inhibitor in the alternative NF- κ B pathway, p100 assembles with the transactivator protein RelB (163, 179). Following IKK α -mediated phosphorylation, p100 is processed to p52 via a proteasome-dependent mechanism, permitting the nuclear entry of p52/RelB complexes (163, 179). Given these distinct mechanisms, our findings with reovirus-infected cells suggest an unconventional function for IKK α in substrate targeting. Specifically, we were unable to detect either p52 or RelB DNA-binding activity in nuclear extracts from cells following 4 to 8 h of reovirus infection (Fig. 11B). Instead, at these early timepoints the predominant Rel species detected were p50 and RelA (Fig. 11B), which are primarily under I κ B α control (7, 8). Consistent with this Rel profile, I κ B α protein levels were significantly reduced by 4 h post-infection (Fig. 13). Although p100 processing to p52 was observed at late time points during reovirus infection (16 h), it seems unlikely that this delayed response contributes to the more rapidly evolving signals required for apoptosis (39, 40, 145). Accordingly, we propose that IKK α rather than IKK β targets I κ B α for proteolytic destruction and regulates the nuclear translocation of p50/RelA complexes in reovirus-infected cells. This working model is fully concordant with the phenotype of cell lines deficient for either IKK α , p50, or RelA, all of which are impaired

for reovirus-induced NF- κ B activation and proapoptotic signaling (Figs. 14, 15, and (40)).

In agreement with this model, prior studies with recombinant proteins indicate that IKK α can efficiently phosphorylate NF- κ B-bound forms of I κ B α in vitro (225).

Both IKK α and IKK β contain regulatory serine phosphoacceptors in their so-called "T loop" domains (48, 115). Signal-dependent phosphorylation of the T loop serines in IKK α and IKK β is a prerequisite for their catalytic activation (48). Based on in vitro studies with recombinant proteins, IKK α and IKK β can autophosphorylate at these T loop serines (48, 160, 186). Physiologic agonists of the alternative NF- κ B pathway stimulate T loop phosphorylation and activation of IKK α via the upstream kinase NIK (95, 163, 221). However, NIK is dispensable in the mechanism by which reovirus induces NF- κ B activation and apoptosis (Fig. 16 and 18).

What signal transducers couple reovirus to IKK? Experiments using pharmacological inhibitors suggest that NF- κ B-dependent apoptotic signaling is triggered by viral replication steps that occur after disassembly but prior to RNA synthesis (39). Strain-specific differences in the capacity of reovirus to induce apoptosis segregate with viral genes encoding the σ 1 and μ 1 proteins (38, 145, 199), which play important roles in viral attachment (89, 209) and membrane penetration (26, 27, 101), respectively. Importantly, transient expression of μ 1 is sufficient to induce apoptosis in cell culture (36), implicating this protein in the reovirus/NF- κ B signaling axis. We envision three potential mechanisms by which μ 1, or perhaps another viral gene product, initiates NF- κ B signal transduction during reovirus infection. First, μ 1 may activate viral sensors that mediate the recruitment of the adaptor protein IFN- β promoter stimulator (IPS-1), which leads to the activation of NF- κ B in response to viral infections by recruiting TNF-associated factor 6 to the signaling

complex (84, 116, 164, 222). Second, $\mu 1$ may activate a novel cellular kinase that phosphorylates the T loop of $\text{IKK}\alpha$. Third, $\mu 1$ may interact with IKK complexes directly, leading to conformational changes that stimulate oligomerization and trigger autophosphorylation of the T loop in $\text{IKK}\alpha$ (74, 136). Additional studies will be required to precisely define the mechanism by which reovirus hijacks NF- κ B to mediate apoptotic cell death.

CHAPTER IV

ORGAN-SPECIFIC ROLES FOR TRANSCRIPTION FACTOR NF- κ B IN REOVIRUS-INDUCED APOPTOSIS AND DISEASE

Introduction

Mechanisms of viral disease involve complex interactions of pathogen virulence factors and host responses. Perhaps the best-understood basis of organ-specific viral pathology is the availability of cell-surface molecules required for viral attachment and entry. Rarely, however, is viral disease ascribable solely to receptor recognition. More commonly, additional virus-host interactions determine the outcome of infection (198), and these pivotal steps are of much interest in studies of viral pathogenesis. Factors expected to modulate viral growth and virulence in an organ-dependent manner include the capacity of virus to efficiently utilize the host translational apparatus, including strategies to circumvent antiviral effects of IFN; availability of cellular proteins to facilitate viral replication and gene expression; and changes in the intracellular signaling dynamic induced by viral infection.

The NF- κ B family of transcription factors plays a key role in the regulation of cell growth, activation, differentiation, and survival. Following exposure of cells to a variety of stimuli, NF- κ B is activated and translocates to the nucleus (17), where it serves as a transcriptional regulator (111, 204). In systems in which NF- κ B is activated during apoptosis, NF- κ B can either prevent (15, 97, 111, 202) or potentiate (1, 53, 82, 94) cell death signaling. Following reovirus infection of cultured cells, the heterodimeric NF- κ B complex p50/RelA enters the nucleus and activates proapoptotic gene expression (40). When NF- κ B activation is inhibited using proteasome inhibitors or dominant-negative forms of I κ B α , reovirus-induced apoptosis is blocked (40). Moreover, cell lines deficient in either of the p50

or RelA NF- κ B subunits do not undergo apoptotic cell death following reovirus infection. These findings indicate that activation of NF- κ B in cell culture is required for reovirus-induced apoptosis.

Experiments reported in this chapter demonstrate that the p50 subunit of NF- κ B plays an essential role in the development of encephalitis and myocarditis in reovirus-infected mice. Although reovirus infects the intestine and disseminates systemically following peroral inoculation of mice lacking the NF- κ B p50 subunit, apoptosis is diminished in the brain yet strikingly enhanced in the heart. These findings suggest a novel role for NF- κ B in the pathogenesis of viral infection; it serves a proapoptotic function in the CNS, while mediating a prosurvival function in the myocardium.

Results

Reovirus activates NF- κ B in vivo

To determine whether reovirus is capable of NF- κ B activation in the intact host, we performed in vivo luciferase assays using transgenic mice engineered to express luciferase under control of an HIV long-terminal repeat promoter that contains NF- κ B consensus binding sites (88). These mice were inoculated perorally with either PBS (mock-infected) or 10^4 PFU reovirus strain T3SA+, which was chosen for these studies because of its capacity to activate NF- κ B and induce a potent apoptotic response in cultured cells (38). Seven days after inoculation, the mice were imaged for luciferase activity as a marker for NF- κ B activation (Fig. 19A and B). Little luciferase activity was detected in the mock-infected mice (Fig. 19A). In contrast, reovirus-infected animals exhibited systemic luciferase activity (Fig. 19B), which indicates that reovirus is capable of NF- κ B activation in vivo.

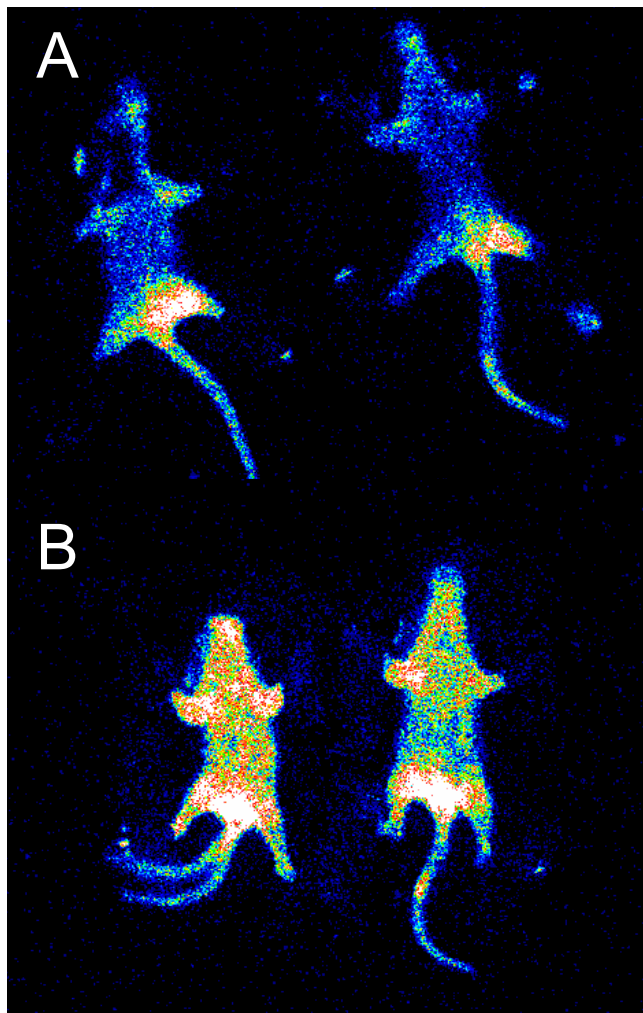


Figure 19. NF- κ B activation following reovirus infection of HLL mice. Newborn HLL mice were inoculated perorally with (A) PBS (mock) or (B) 10^4 PFU of reovirus T3SA+. Mice were inoculated intraperitoneally with luciferin 7 days post-infection and imaged for luciferase activity as a marker for NF- κ B activation. Bioluminescence indicates areas of NF- κ B activation.

Reovirus-induced activation of NF- κ B in the murine CNS and heart is dependent on p50

To determine whether reovirus activates NF- κ B in the murine CNS and heart, we performed EMSAs using brain and heart extracts prepared from reovirus-infected or mock-infected wild-type and p50-null mice. Newborn p50^{+/+} and p50^{-/-} mice were inoculated with either PBS or 10⁴ PFU reovirus T3SA+. Cell extracts were prepared from brain and heart tissue 12 days after inoculation, incubated with a radiolabeled oligonucleotide consisting of the NF- κ B consensus binding sequence, and resolved by PAGE using nondenaturing conditions (Fig. 20A and D). NF- κ B DNA-binding activity was detected in extracts from the brain of reovirus-infected p50^{+/+} but not p50^{-/-} mice (Fig. 20A). Similarly, NF- κ B DNA-binding activity was detected in the heart of p50^{+/+} mice infected with reovirus but not p50^{-/-} animals (Fig. 20D). These findings indicate that reovirus infection in the murine CNS and heart induces nuclear translocation of NF- κ B, which is contingent on the expression of the NF- κ B p50 subunit.

To confirm the specificity of NF- κ B DNA-binding activity in these experiments, we incubated cell extracts from reovirus-infected p50^{+/+} mouse brain and heart with a ³²P-labeled NF- κ B consensus oligonucleotide in the presence of excess unlabeled consensus oligonucleotide (Fig. 20B and E). Binding of the radiolabeled probe was competed with that of unlabeled consensus oligonucleotide, which suggests that the gel-shift activity detected following reovirus infection is specific for sequences bound by NF- κ B.

In cell culture, reovirus infection results in the nuclear translocation of NF- κ B complexes containing subunits p50 and RelA (40). As an additional specificity control in these experiments for the activation of NF- κ B, nuclear extracts were prepared from reovirus-infected p50^{+/+} mouse brain or heart and incubated with an antiserum specific to RelA prior to the addition of the NF- κ B-specific oligonucleotide (Fig. 20C and F). Addition of the

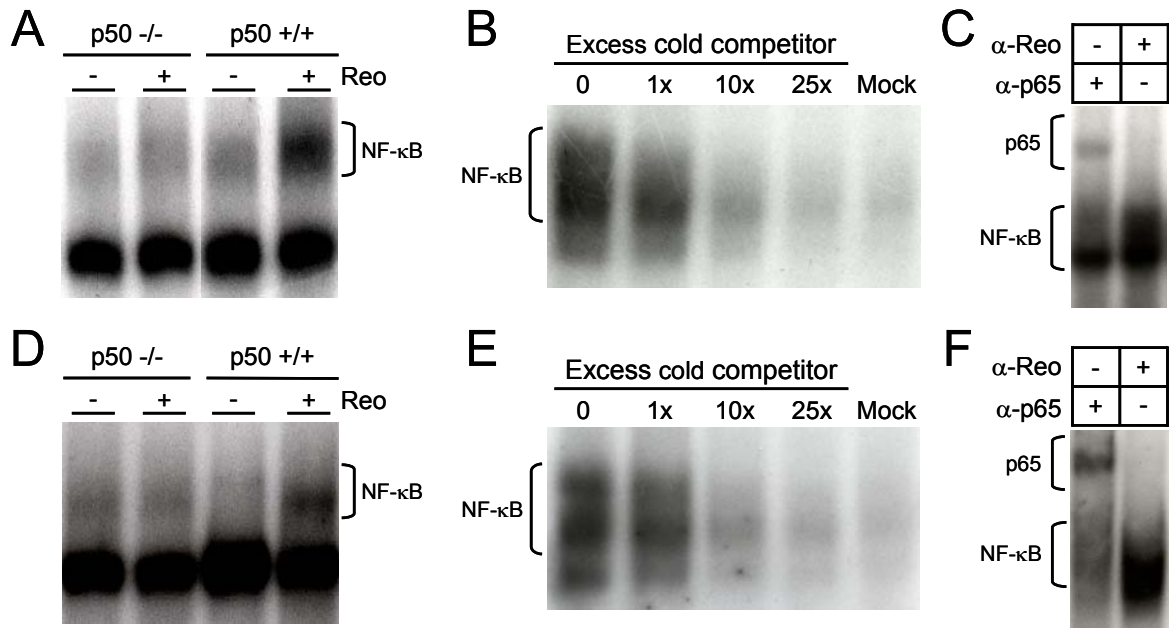


Figure 20. Reovirus-induced NF-κB gel-shift activity following infection of p50 +/+ and p50 -/- mice. (A and C) Newborn p50 +/+ and p50 -/- mice were inoculated perorally with either 10⁴ PFU of reovirus T3SA+ (Reo) or PBS. (A) Brains and (C) hearts were resected 12 days post-inoculation, and cell extracts were prepared. Extracts were incubated with a ³²P-labeled NF-κB consensus oligonucleotide and resolved by nondenaturing polyacrylamide gel electrophoresis. Activated NF-κB complexes are indicated. Shown is a representative experiment of four performed. (B and D) Extracts were prepared from either (B) brains or (D) hearts of p50 +/+ mice 12 days following peroral inoculation with T3SA+. Prior to the addition of the ³²P-labeled oligonucleotide probe, extracts were incubated with either a control antibody specific for reovirus protein σ3 (α-reovirus) or an antibody specific for NF-κB subunit p65 (α-p65). Super-shifted complexes containing p65 are indicated. *, non-specific bands.

RelA-specific antiserum resulted in bands of higher relative molecular mass, which verified that RelA is present in the NF- κ B complexes activated following reovirus infection. These findings provide strong evidence that reovirus infection of the murine CNS and heart induces the nuclear translocation of NF- κ B and this effect is abolished in mice lacking p50.

NF- κ B subunit p50 is not required for efficient reovirus replication or dissemination in the murine host

To determine whether p50 plays a role in reovirus growth in vivo, we inoculated p50^{+/+} and p50^{-/-} mice intracranially or perorally with 10⁴ PFU reovirus T3SA⁺. Viral titers in the brain were determined by plaque assay 2, 4, and 6 days after intracranial inoculation (Fig. 21A) and in the intestine, liver, brain, and heart 4, 6, 8, 10, and 12 days after peroral inoculation (Fig. 21B). Following intracranial inoculation, viral titers in p50^{+/+} and p50^{-/-} mice were equivalent at all time points tested. After peroral inoculation, virus replicated efficiently in the intestines of both p50^{+/+} and p50^{-/-} mice and disseminated to the liver, brain, and heart. Viral titers in the intestine, liver, and brain did not differ between p50^{+/+} and p50^{-/-} mice. In sharp contrast, viral titers in the hearts of p50^{-/-} mice were more than 1,000-fold higher than those in the hearts of p50^{+/+} animals. These findings suggest that p50 is dispensable for reovirus growth in vivo and that the absence of p50 in the heart, but not in other tissues tested, allows for increased reovirus replication.

NF- κ B subunit p50 is required for efficient induction of apoptosis in the CNS following reovirus infection

To assess reovirus-induced pathologic changes in the CNS of p50^{+/+} and p50^{-/-} mice, we prepared brain sections from mice euthanized at 12 days following peroral inoculation with reovirus T3SA⁺ and examined them after staining with H&E (Fig. 22A and B). Brain sections from reovirus-infected p50^{+/+} and p50^{-/-} mice exhibited evidence of

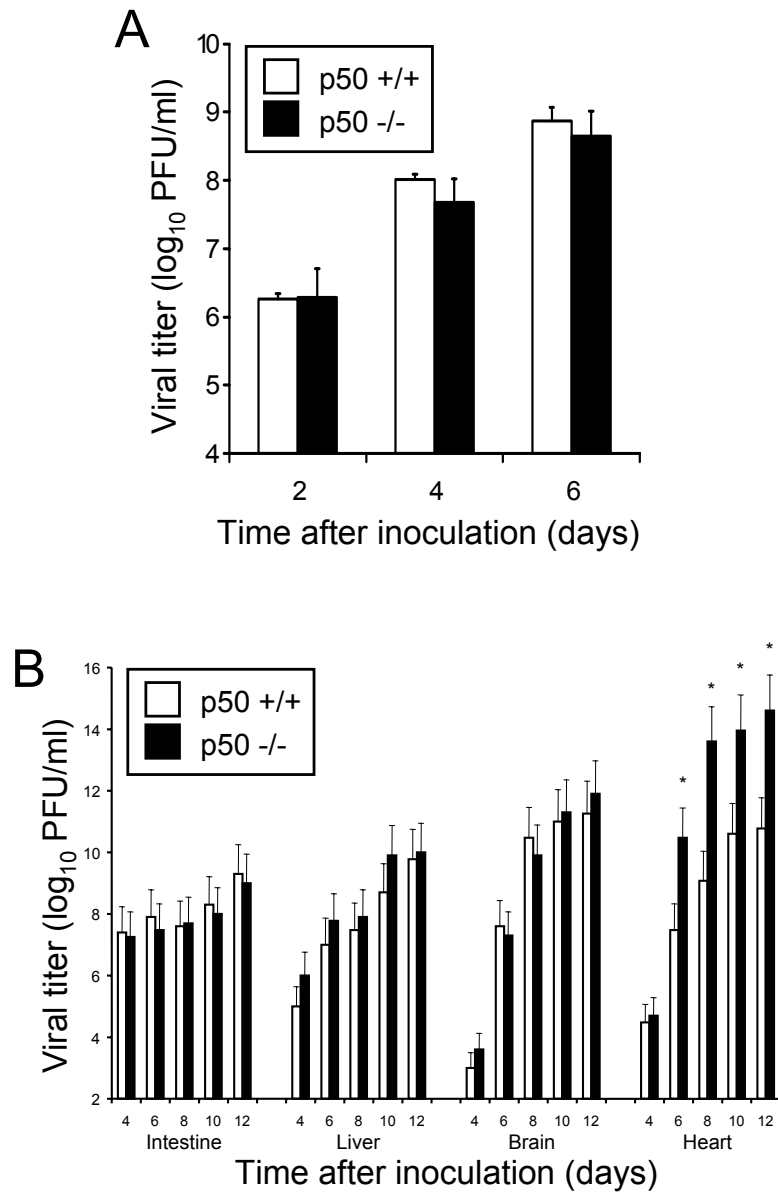


Figure 21. Growth of reovirus in p50 +/+ and p50 -/- mice. (A) Titers of reovirus in brain after intracranial inoculation of p50 +/+ and p50 -/- mice. Newborn mice were inoculated with 10⁴ PFU of reovirus T3SA+. At days 2, 4, and 6 post-inoculation, mice were euthanized, brains were harvested, and viral titers were determined by plaque assay. (B) Titers of reovirus in intestine, liver, brain, and heart after peroral inoculation of p50 +/+ and p50 -/- mice. Newborn mice were inoculated with 10⁴ PFU of T3SA+. At days 4, 6, 8, 10, and 12 post-inoculation, mice were euthanized, organs were harvested, and viral titers were determined by plaque assay. The results are expressed as the mean viral titers for two to four animals for each timepoint. Error bars indicate standard deviations. *, *P* < 0.05 by T test.

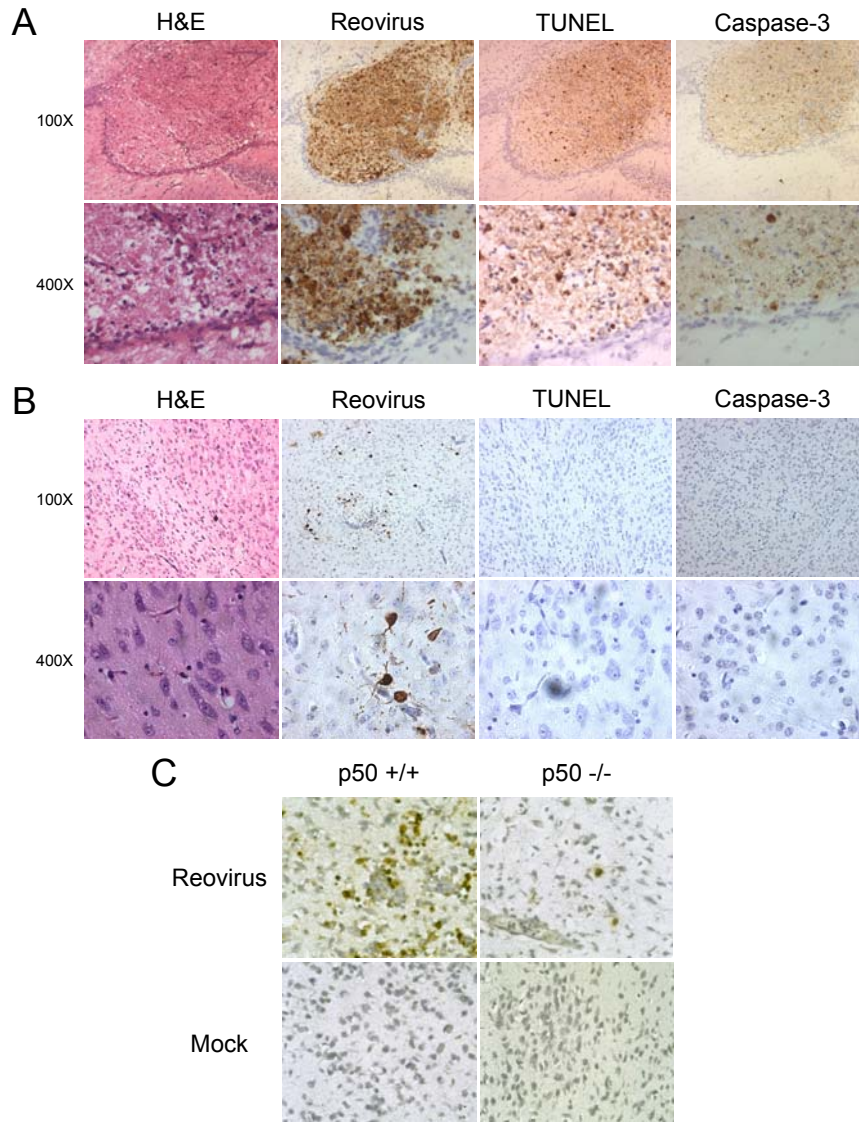


Figure 22. Inflammation, reovirus protein expression, TUNEL staining, and immunohistochemical detection of activated caspase-3 in the brain of reovirus-infected (A) p50 +/+ and (B) p50 -/- mice. Newborn mice were inoculated perorally with 10^4 PFU of reovirus T3SA+. At 12 days post inoculation, brains were harvested, paraffin embedded, sectioned, and stained with hematoxylin and eosin, polyclonal reovirus-specific antiserum, TUNEL, or activated caspase 3-specific antiserum as indicated. Shown are consecutive sections of diencephalon. Original magnifications were 100X (top panels) and 400X (bottom panels). (C) Newborn mice were inoculated intracranially with 10^4 PFU of T3SA+ or gelatin saline (mock). At 6 days post-inoculation, mice were euthanized, and brain sections were stained using a TUNEL assay. Shown are sections of the upper brain stem. Original magnifications were 200X. Brown staining indicates reovirus protein, fragmented DNA, or activated caspase 3.

meningoencephalitis. Inflammatory infiltrates were detected primarily in the cerebral cortex, hippocampus, diencephalon, and brain stem. Morphologically, inflammatory cells were mostly lymphocytes and macrophages/microglia with some plasma cells and neutrophils. Inflammatory changes were more extensive in p50^{+/+} mice (Fig. 22A) than in p50^{-/-} mice (Fig. 22B), which suggests that the neurovirulence of reovirus is attenuated in mice lacking an intact NF- κ B signaling apparatus.

To assess the distribution of reovirus protein expression in the CNS of p50^{+/+} and p50^{-/-} mice, we prepared brain sections from mice euthanized 12 days following peroral inoculation and stained them using a reovirus-specific antiserum (Fig. 22A and B). Immunohistochemical staining for reovirus protein demonstrated the presence of immunoreactive neurons in brains of both p50^{+/+} and p50^{-/-} mice (Fig. 22A and B). Antigen-positive neurons were detected in a pattern recapitulating the inflammatory changes; the cerebral cortex, hippocampus, diencephalon, and brain stem were primarily involved. The number of reovirus-infected cells and their distribution was similar in p50^{+/+} and p50^{-/-} mice (Fig. 22A and B). These results suggest that the lack of p50 does not alter reovirus tropism for specific neural regions.

To determine whether p50 is required for apoptosis in the murine CNS, we prepared brain sections from reovirus-infected p50^{+/+} and p50^{-/-} mice 12 days following peroral inoculation (Fig. 22A and B) or 6 days following intracranial inoculation (Fig. 22C) and assayed them for fragmented DNA using the terminal dUTP nick-end labeling (TUNEL) technique. Apoptotic cells were quantified by counting all TUNEL-positive cells in cortex, hippocampus, basal ganglia, diencephalon, and brain stem of each section obtained from mice inoculated intracranially (Fig. 23). Numbers of TUNEL-positive cells in the brains of infected p50^{+/+} mice were significantly greater than those in the brains of infected p50^{-/-} mice. These findings were the same following both peroral and intracranial inoculation (Fig.

22). Thus, reovirus-induced apoptosis in the murine CNS is dependent on the p50 subunit of NF- κ B.

Activation of caspase 3 is a highly specific biomarker of apoptotic cell death (22). To confirm that DNA fragmentation observed in the brains of reovirus-infected p50^{+/+} mice is due to apoptosis, we stained brain sections with an antiserum specific for the activated form of caspase 3 (Fig. 22A and B). Activated caspase 3 was detected in regions of the brain in which TUNEL-positive staining also was observed. Moreover, cells immunoreactive for caspase 3 were detected at a much higher frequency in the brains of p50^{+/+} mice. Morphologically, cells immunoreactive for caspase 3 were primarily neurons, and most immunoreactive neurons also exhibited morphologic evidence of apoptosis. These results provide additional evidence that expression of NF- κ B subunit p50 is required for efficient induction of apoptosis during reovirus infection in the murine CNS.

Absence of NF- κ B subunit p50 leads to enhanced pathology and massive apoptosis in the murine heart following reovirus infection

Since viral titers in the hearts of p50^{-/-} mice were more than 1,000-fold higher than in those of p50^{+/+} mice (Fig. 21B), we examined heart tissue for evidence of inflammation and tissue injury. Newborn p50^{+/+} and p50^{-/-} mice were inoculated perorally with either 10⁴ PFU reovirus T3SA+ or PBS and weighed daily. Mice were euthanized at various time points after inoculation, and hearts were removed and weighed. There were no significant differences in the heart weights of mock-infected p50^{+/+} and p50^{-/-} mice (Fig. 24A). Surprisingly, heart weights of reovirus-infected p50^{-/-} mice were significantly greater than those of p50^{+/+} mice (Fig. 24B). Differences in the percent heart weight (heart weight relative to total body weight) of infected p50^{+/+} and p50^{-/-} mice became detectable at 8 days after inoculation and continued to increase with time, while there was no significant increase

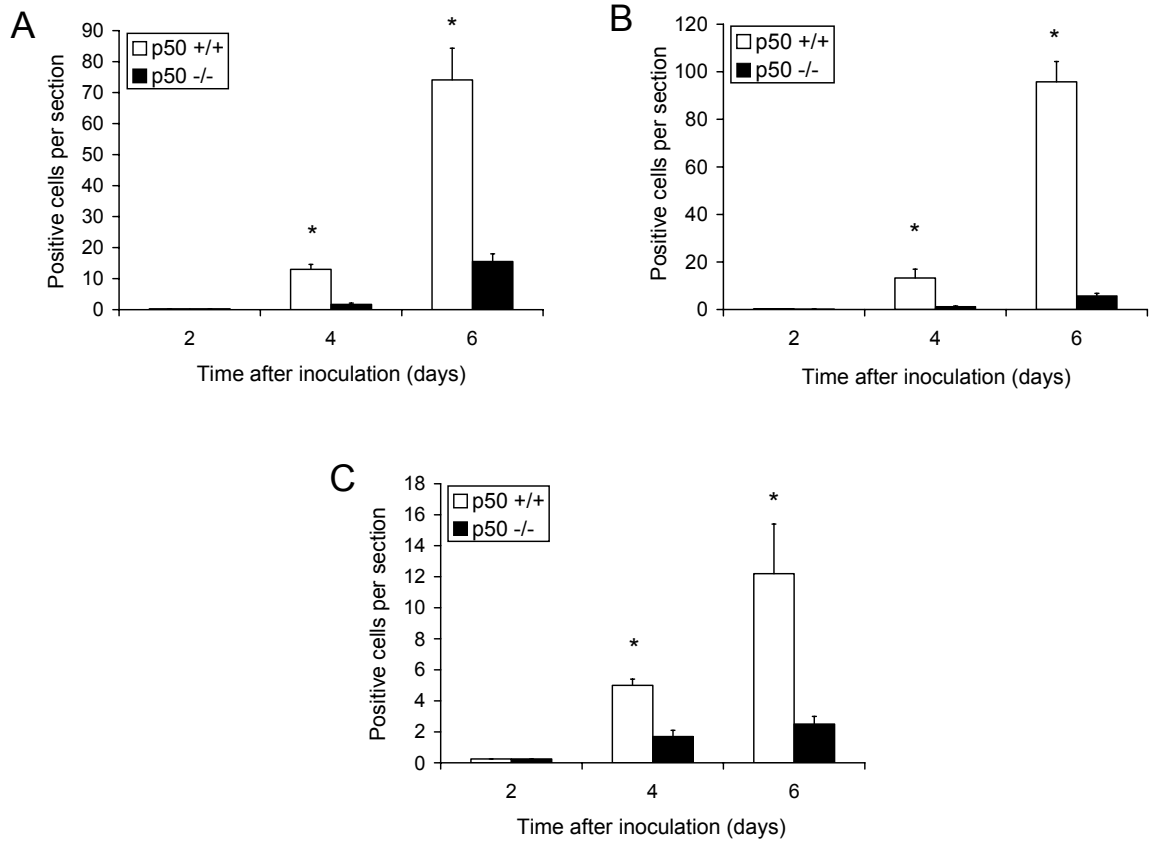


Figure 23. Quantitation of TUNEL staining in (A) cortex and hippocampus, (B) basal ganglia and diencephalon, and (C) brain stem of reovirus-infected p50 +/+ and p50 -/- mice. TUNEL staining was performed using tissue sections prepared 2, 4, and 6 days following intracranial inoculation of p50 +/+ and p50 -/- mice with 10^4 PFU of reovirus T3SA+. For each brain region, all positive cells in a single parasagittal section were counted for four to eight animals. The results are expressed as the mean number of apoptotic cells per region. Error bars indicate standard deviations. *, $P < 0.05$ by T test.

in the percent heart weight of infected p50^{+/+} mice (Fig. 24B). Dramatic differences were observed in the gross appearance of hearts dissected from p50^{+/+} and p50^{-/-} animals following infection with reovirus (Fig. 24C). Hearts from reovirus-infected p50^{-/-} mice had a blanched appearance with diffuse surface irregularities corresponding to confluence of purulent lesions, consistent with overt myocarditis. In contrast, hearts from mock-infected p50^{-/-} or p50^{+/+} mice or reovirus-infected p50^{+/+} mice displayed no overt abnormalities.

To determine whether reovirus-induced myocardial injury in p50^{-/-} mice is associated with contractile dysfunction, we performed echocardiography on 10-day-old mice after peroral inoculation with either reovirus T3SA⁺ or PBS. Fractional shortening, assessed by 2-dimensional, directed M-mode measurements, was substantially decreased in reovirus-infected p50^{-/-} mice (<10%; Fig. 24D), while it was preserved in mock-infected p50^{-/-} mice (>40%; Fig. 24E) and reovirus-infected p50^{+/+} mice (>40%; Fig. 24F). Heart size was also increased in reovirus-infected p50^{-/-} mice compared with mock-infected p50^{-/-} mice and reovirus-infected p50^{+/+} mice. Intact atrioventricular conduction was observed in all mice, which suggests that the pathologic process was not specifically targeted to the conduction system. These results suggest that the myocardial pathology associated with reovirus infection of p50^{-/-} mice is associated with diminished contractility.

On a microscopic level, hearts of p50^{-/-} animals displayed extensive myocyte destruction with features of apoptotic and necrotic cell death. Affected areas were notable for cell fragments, granular debris, and scattered calcifications. Thorough sectioning of the organ block revealed that pathology was not limited to any particular region of the heart. Hearts from reovirus-infected p50^{+/+} mice and mock-infected p50^{-/-} and p50^{+/+} mice demonstrated no significant microscopic pathology. We conclude that reovirus is more pathogenic in the heart in the absence of NF-κB subunit p50.

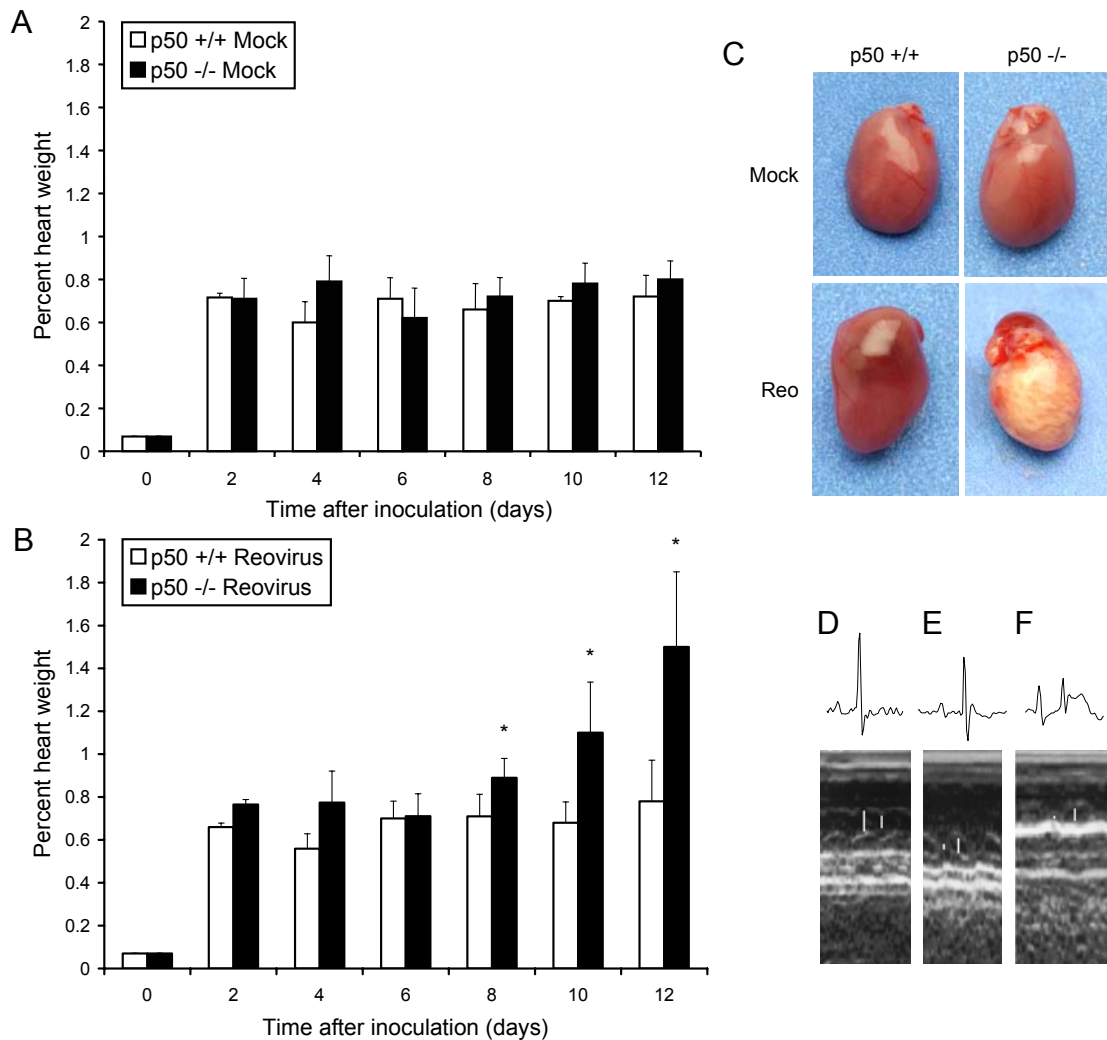


Figure 24. Heart pathology following reovirus infection of p50 +/+ and p50 -/- mice. (A and B) Newborn p50 +/+ and p50 -/- mice were inoculated perorally with either (A) PBS (mock) or (B) 10^4 PFU of reovirus T3SA+, and heart size was monitored at two-day intervals. Percent heart weight was calculated as the ratio of heart weight to body weight. The results are expressed as the mean heart weights of at least four animals for each timepoint. Error bars indicate standard deviations. *, $P < 0.05$ by T test. (C) Hearts from mice euthanized 12 days following peroral inoculation with reovirus T3SA+ or gelatin saline (mock). (D, E, and F) Electrocardiography and echocardiography of (D) reovirus-infected p50 -/-, (E) mock-infected p50 -/-, and (F) reovirus-infected p50 +/+ mice. Newborn mice were inoculated perorally with 10^4 PFU of T3SA+, and tests were performed 10 days post-inoculation. A P-wave/QRS ECG complex is displayed above the corresponding echocardiographic image. Systolic and diastolic LV cavity dimensions are indicated by bars superimposed on the M-mode images.

To assess the extent and location of reovirus infection in the murine myocardium in the presence and absence of p50, we performed reovirus antigen staining on heart sections from p50^{+/+} and p50^{-/-} mice euthanized 12 days following peroral inoculation with reovirus T3SA+ (Fig. 25A and B). Immunohistochemical staining for reovirus protein demonstrated immunoreactive myocytes in heart sections prepared from both p50^{+/+} and p50^{-/-} mice (Fig. 25A and B). However, the number of reovirus-infected cells differed substantially between p50^{+/+} and p50^{-/-} mice, consistent with the significant difference in viral titer in the hearts of these animals.

To determine whether expression of p50 influences apoptosis in the murine heart, we inoculated p50^{+/+} and p50^{-/-} mice perorally with reovirus and assessed them for apoptosis using TUNEL staining (Fig. 25A and B). There were rare TUNEL-positive cells in the hearts of p50^{+/+} mice following reovirus infection (Fig. 25A), whereas numerous foci of apoptosis were present in the hearts of p50^{-/-} mice (Fig. 25B). Interestingly, foci of apoptotic cells in the hearts of p50^{-/-} mice coincided with areas of intense staining for reovirus antigen, which suggests a link between reovirus replication and apoptosis in cardiac myocytes.

To confirm that the absence of p50 leads to enhanced apoptosis in the heart during reovirus infection, we prepared heart sections from p50^{+/+} and p50^{-/-} mice 12 days following peroral inoculation with reovirus and stained them for activated caspase 3 (Fig. 25A and B). Caspase 3 staining revealed numerous positive myocytes in the same areas of the heart that also were positive for reovirus antigen and TUNEL staining. These results suggest that, in contrast to its effects in the murine CNS, the NF- κ B p50 subunit protects against apoptosis induced by reovirus infection in the murine myocardium.

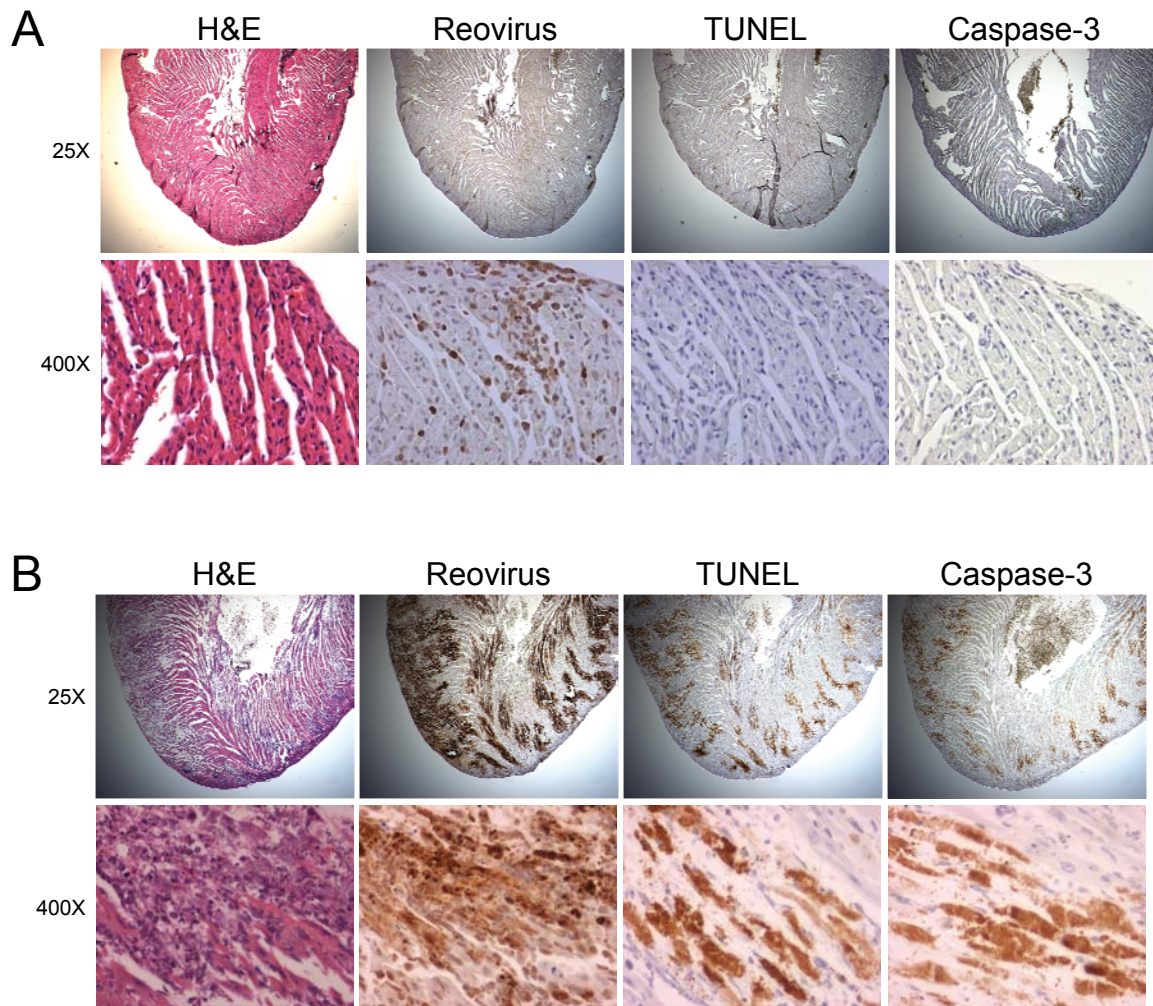


Figure 25. Inflammation, reovirus protein expression, TUNEL staining, and immunohistochemical detection of activated caspase 3 in the heart of reovirus-infected (A) *p50* +/+ and (B) *p50* -/- mice. Newborn mice were inoculated perorally with 10^4 PFU of reovirus T3SA+. At 12 days post inoculation, hearts were harvested, paraffin embedded, sectioned, and stained with hematoxylin and eosin, polyclonal reovirus-specific antiserum, TUNEL, or activated caspase 3-specific antiserum as indicated. Original magnifications were 25X (top panels) and 400X (bottom panels). Brown staining indicates reovirus protein, fragmented DNA, or activated caspase 3.

IFN- β is induced in the heart of wild-type mice following reovirus infection

Results presented thus far demonstrate that enhanced reovirus growth in the heart of p50^{-/-} mice is associated with massive apoptosis. We thought it possible that the absence of NF- κ B-mediated activation of innate immune responses might lead to increased viral replication and resultant pathology in the heart. To test this hypothesis, we inoculated p50^{+/+} and p50^{-/-} mice perorally with reovirus T3SA+ or PBS. Twelve days after inoculation, heart and brain were removed, and levels of IFN- β mRNA were determined using quantitative PCR (Fig. 26). Using GAPDH mRNA as a standardization control, little IFN- β mRNA was induced in the brain of either p50^{-/-} or p50^{+/+} mice in the presence or absence of reovirus infection (Fig. 26). In contrast, IFN- β mRNA levels were substantially increased in the heart of reovirus-infected wild-type mice compared with p50^{-/-} animals (Fig. 26). These results indicate that IFN- β induction by reovirus in the murine heart is dependent on NF- κ B and suggest that IFN- β protects the heart from reovirus-induced apoptosis and disease.

IFN- β treatment of p50-null mice attenuates reovirus-induced myocarditis

To determine whether NF- κ B-mediated expression of IFN- β plays a direct role in protection of the heart against apoptosis and disease caused by reovirus, we tested the effect of IFN- β treatment on reovirus infection of p50^{-/-} mice. Newborn p50^{-/-} mice were inoculated intraperitoneally with either IFN- β or PBS 1 day prior to peroral inoculation with reovirus T3SA+ and treated daily for 9 days thereafter. On day 10, the animals were euthanized, and brain and heart were removed for determination of viral titer and histopathology (Fig. 27). IFN- β treatment significantly decreased viral titer in both brain and heart (Fig. 27A). In p50^{-/-} mice treated with IFN- β , viral titers reached only 10² PFU in the brain and were less than 10² PFU in the heart (Fig. 27A). In parallel with these results,

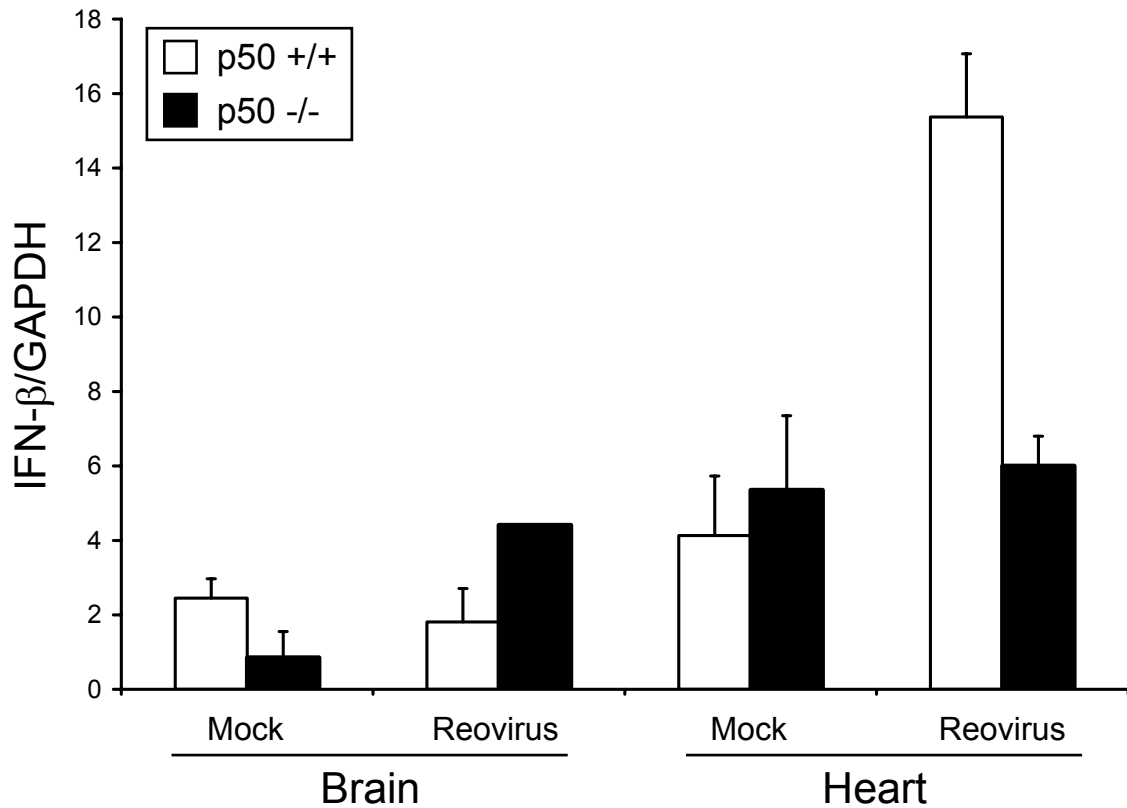


Figure 26. Levels of IFN- β mRNA in brain and heart of p50 +/+ and p50 -/- mice. Newborn mice were inoculated perorally with either PBS (mock) or 10^4 PFU of reovirus T3SA+. At 12 days post-inoculation, brains and hearts were resected, and whole-organ RNA was isolated and used as a template to generate cDNA. Levels of IFN- β and GAPDH cDNA were assessed by real-time PCR. The results are expressed as the mean ratio of IFN- β cDNA to that of GAPDH for two animals. Error bars indicate standard deviations.

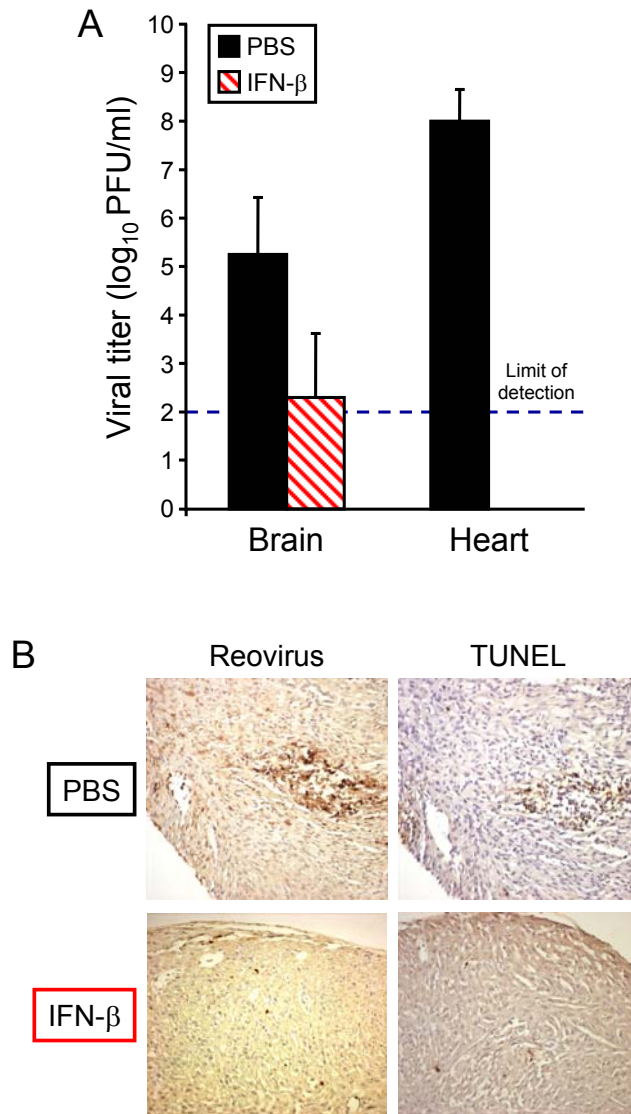


Figure 27. Reovirus replication and apoptosis in infected p50^{-/-} mice following treatment with IFN-β. Newborn mice were inoculated intraperitoneally with either IFN-β or PBS 1 day prior to peroral inoculation with 10⁴ PFU of reovirus T3SA+. Animals were treated with either IFN-β or PBS for an additional 9 days, and brains and hearts were resected. (A) Viral titers in the brain and heart. Organs were homogenized, and viral titers were determined by plaque assay. The results are expressed as the mean viral titers for three animals. Error bars indicate standard deviations. *, *P* < 0.05 by T test. (B) Histopathology of reovirus infection in the heart. Hearts of reovirus-infected p50^{-/-} animals from (A) were paraffin-embedded, sectioned, and stained with polyclonal reovirus-specific antiserum or processed for TUNEL analysis. Original magnifications were 25X (top panels) and 200X (bottom panels). Brown staining indicates reovirus protein or fragmented DNA.

apoptosis in the heart of IFN- β -treated p50^{-/-} mice was substantially diminished (Fig. 27B). Thus, a critical component of the underlying mechanism of NF- κ B-mediated protection against reovirus-induced myocardial injury is contingent on IFN- β .

Discussion

Results reported here indicate organ-specific roles for NF- κ B in the pathogenesis of viral disease, which is a heretofore unknown property of this signaling molecule. The key finding is that marked differences in the pathogenesis of reovirus infection in the CNS and heart are dependent on the action of NF- κ B. Following reovirus infection in the CNS, p50^{+/+} mice exhibited significant neuronal apoptosis, while p50^{-/-} mice displayed a minimal apoptotic response. In sharp contrast, reovirus induced little apoptosis in the heart of p50^{+/+} mice, whereas extensive apoptosis occurred in the heart of p50^{-/-} mice. These findings indicate that NF- κ B subunit p50 plays two distinctly different roles in reovirus pathogenesis, serving a proapoptotic function in the brain, while mediating a prosurvival function in the heart.

Studies using mice with targeted disruptions of specific NF- κ B subunits have shown that NF- κ B serves important functions in the development and function of innate and adaptive immunity (87, 165, 208). Mice lacking p50 have no apparent developmental defects (165), and immune cells mature normally. However, p50^{-/-} mice display defects in B cell activation, isotype switching, and antibody production (165). These defects render p50^{-/-} mice more susceptible to infection by the Gram-positive bacterial pathogen *Streptococcus pneumoniae*, but they remain capable of efficiently clearing infection by the Gram-negative pathogens *Escherichia coli* and *Haemophilus influenzae* (165). When p50^{-/-} mice are infected with encephalomyocarditis virus, they are actually more resistant to infection than controls. This difference is thought to be due to an increase in apoptosis that leads to a

decrease in viral growth (165). These findings stand in stark contrast to what occurs in the CNS and heart of reovirus-infected mice.

In experiments comparing reovirus infection of p50^{+/+} and p50^{-/-} mice, we found that the presence or absence of p50 did not alter primary viral replication in intestinal tissue or dissemination of virus to the liver, brain, or heart. Although viral replication in the brain after intracranial inoculation also was independent of p50, replication in the heart was increased in p50^{-/-} mice by approximately 1,000-fold. What might explain the enhancement of reovirus replication in the heart of p50^{-/-} mice? Reovirus strains have been characterized previously as having the capacity to grow in the murine heart and produce cardiac disease (170, 174). In primary cardiac myocytes, nonmyocarditic reovirus strains induce more IFN- β and are more sensitive to the antiviral effects of this cytokine than myocarditic reovirus strains (175). Furthermore, normally nonmyocarditic strains are capable of producing myocarditis in infected IFN- α/β receptor^{-/-} mice (175). Thus, it appears that type I IFNs restrict viral replication in the heart and attenuate cardiac disease.

NF- κ B is known to induce the expression of several mediators of innate immune responses including type I IFNs (31, 56, 224). Therefore, absence of p50 may allow reovirus to achieve much higher titers and cause myocarditis. We tested this hypothesis by determining brain and heart levels of IFN- β mRNA in response to reovirus infection of p50^{+/+} and p50^{-/-} mice (Fig. 26) and by treating reovirus-infected p50^{-/-} mice with IFN- β (Fig. 27). In these experiments, we found a dramatic increase in IFN- β expression in the hearts of wild-type mice but only a minimal IFN- β response in the hearts of p50-null animals. Moreover, reconstitution of p50^{-/-} mice with IFN- β substantially diminished reovirus replication and apoptosis, which resulted in diminished myocardial injury. These results indicate that IFN- β is a necessary component of the NF- κ B-mediated protective response against reovirus in the heart. However, it is likely that other components of innate immunity

are involved in this effect. Preliminary data from our laboratory suggest that in addition to IFN- β , IL-6, macrophage migration inhibitory factor (MIF), and tumor necrosis factor (TNF) are expressed at higher levels in the heart of p50^{+/+} mice than p50^{-/-} mice (S.M. O'Donnell and T.S. Dermody, unpublished observation). These findings suggest that following reovirus infection of the heart, NF- κ B is activated and leads to induction of potent innate immune responses, which in turn attenuate viral replication at that site, resulting in diminished apoptosis and disease.

The enhanced growth of reovirus in the heart of p50^{-/-} mice compared with p50^{+/+} mice was associated with extensive myocarditis and resultant tissue injury and dysfunction. This result was confirmed by histopathological studies, echocardiography, and physical examination revealing signs of heart failure. The pathology observed in the heart of p50^{-/-} animals was characterized by extensive tissue damage and little inflammatory infiltrate, similar to findings made in previous studies of reovirus myocarditis (174). Therefore, our results suggest that apoptosis is the primary mechanism of cardiac damage in reovirus-induced myocarditis, as reported previously (44). Damage to cardiac myocytes during reovirus infection occurs in the complete absence of adaptive components of host defense (173). It is possible that a similar mechanism occurs in humans, which would explain why some patients with acute myocarditis develop heart failure in the setting of sustained viremia (103).

In contrast to the enhanced growth of reovirus in the heart of p50^{-/-} mice, viral growth in the CNS of p50^{+/+} and p50^{-/-} mice was equivalent. However, we observed dramatic differences in the number of apoptotic cells in the two mouse strains as indicated by TUNEL and caspase 3 staining. Therefore, the efficiency of viral growth is not strictly correlated with the extent of the apoptotic response. Nonetheless, despite these p50-dependent differences in viral growth, our results suggest that apoptosis is an important

mechanism of reovirus-induced disease in both the CNS and heart. In the CNS of p50^{-/-} mice, apoptosis and inflammation following reovirus infection were diminished. However, in the hearts of these animals, apoptosis and tissue injury were enhanced. This correlation between apoptosis and pathology lends support to the hypothesis that therapies directed at blocking programmed cell death might attenuate viral virulence, consistent with results from previous studies of reovirus-induced myocarditis (44). However, our findings suggest that pharmacologic inhibition of NF- κ B activation may reduce pathologic injury at some sites and exacerbate disease at others, depending on the nature of the NF- κ B agonist.

The precise cell types responsible for the p50-dependent effects on apoptosis in response to reovirus infection in mice are not apparent from our study. It is possible that expression of p50 in neurons is required for apoptosis of these cells and expression of p50 in cardiac myocytes mediates protection of these cells against apoptotic injury. However, it is also possible that p50-dependent immune responses contribute to the observed differences in cell fate. For example, NF- κ B-mediated release of cytokines such as TNF- α from immune cells might contribute to the neuronal apoptosis that occurs during reovirus infection of the CNS, whereas NF- κ B-mediated release of type I IFNs from immune cells might mediate a protective effect in the heart. Since adoptive transfer of immune cells is not technically feasible in the newborn mice required for studies of reovirus pathogenesis, discrimination between these possibilities awaits the development of mice with tissue-specific ablation of NF- κ B activity.

The role of NF- κ B in response to a variety of cellular stresses has been studied extensively using cultured cells (60). However, little is known about the contributions of specific NF- κ B subunits *in vivo*. The extensive array of NF- κ B inducers and target genes (130) suggests that numerous mechanisms exist to direct transcription of appropriate NF- κ B-dependent genes in response to specific stimuli. One such regulatory mechanism is likely to

be the activation of specific NF- κ B complexes (e.g., p50/RelA heterodimers) for each inducing signal. Individual homodimeric and heterodimeric NF- κ B complexes exhibit different affinities for target DNA sequences (61), and this provides a potential mechanism by which NF- κ B-inducing stimuli regulate transcriptional activity of specific subsets of cellular genes. We showed previously that reovirus requires p50/RelA for efficient apoptosis in cell culture (40). However, we found in the current study that p50 plays organ-specific roles in disease pathogenesis in vivo. These findings emphasize that NF- κ B subunits can have different functions following activation with the same stimulus depending on the cellular environment. Continuing studies in this area may reveal new layers of control of NF- κ B responses and extend understanding of how viruses cause tissue-specific injury.

CHAPTER V

INTERFERON- β INHIBITS REOVIRUS-INDUCED APOPTOSIS IN CARDIAC MYOCYTES BY BLOCKING VIRAL REPLICATION

Introduction

Viral myocarditis is often fatal in infants and can progress to chronic myocarditis, dilated cardiomyopathy, or cardiac failure in adults (217). Many viruses have been shown to cause myocarditis, but enteroviruses and adenoviruses account for most reported cases (106, 147, 148, 193). Enterovirus-induced myocarditis is immune-mediated (41, 147), while cardiac damage in response to adenovirus is caused by virus-induced cytopathicity (106). Mechanisms used by viruses to directly injure the heart are not well understood.

Certain strains of reovirus cause myocarditis in experimentally infected mice (174). Cardiac damage following reovirus infection is independent of the adaptive immune system (172, 173), which normally plays a protective role in reovirus-infected animals (173). Instead, reovirus directly induces apoptosis in the heart resulting in myocarditis (44). An important determinant of reovirus-induced myocarditis is interferon- β (IFN- β) (128, 175). Strains of reovirus capable of causing myocarditis (i.e., myocarditic strains) induce less IFN- β than nonmyocarditic strains and are not as sensitive to its antiviral effects (175).

IFN- β is secreted from infected cells and binds to the IFN α/β receptor resulting in dimerization and activation of the Janus-associated kinase (JAK) family of kinases. Once activated, JAKs phosphorylate tyrosine residues on the signal transducer and activator of transcription (STAT) molecules STAT 1 and STAT2 (68, 135, 159, 180). The STAT proteins interact with IFN regulatory factor 9 (IRF-9) to form ISGF3, which translocates to the nucleus and enhances the expression of IFN-stimulated genes (ISGs). Classical ISGs

include double-stranded RNA-dependent protein kinase (PKR) and 2'-5' oligoadenylate synthetase, which both function to inhibit translation in infected cells (180).

Reovirus infection leads to NF- κ B activation in numerous cell types (34, 40, 128). However, the outcome of NF- κ B activation varies depending on the infected tissue (128). NF- κ B activation in the CNS leads to high levels of neuronal apoptosis and resultant encephalitis. In contrast, NF- κ B activation in the heart leads to IFN- β production, which limits viral replication and protects against apoptosis. In the absence of NF- κ B signaling, reovirus infection induces widespread apoptotic damage to cardiac myocytes, resulting in myocarditis. Cell types involved in these highly divergent responses to reovirus infection in vivo have not been defined. Moreover, pathways that act upstream and downstream of NF- κ B in reovirus-infected animals are not known.

In the experiments described in this chapter, I used primary cardiac myocyte cultures (PCMCs) to better understand mechanisms of reovirus-induced myocarditis. First, I tested whether PCMCs are permissive for reovirus infection and growth. Second, I assessed PCMCs for apoptosis in response to reovirus. Third, I determined the effect of IFN- β on reovirus infection, growth, and apoptosis. The results suggest that IFN- β mediates an anti-apoptotic role by diminishing viral infection and growth in cardiac myocytes.

Results

Reovirus infection of primary cardiac myocytes

In a previous study, we found that the p50 subunit of NF- κ B is required for induction of IFN- β expression and protection against the apoptotic response elicited by reovirus in the heart (128). To better understand mechanisms of reovirus-induced apoptosis in cardiac

tissue, we generated PCMCs and tested these cultures for the capacity to support reovirus infection. PCMCs were infected with reovirus strain T3SA+, a potent inducer of apoptosis (38), and infectivity was quantified by indirect immunofluorescence (Fig. 28).

Approximately 60 cells per visual field were observed to be infected with reovirus 20 h post-adsorption, suggesting that PCMCs are permissive for reovirus infection.

Since IFN- β serves a protective function in the murine heart (128, 173), we next tested the effect of pretreatment with either IFN- β or IFN- β -specific antiserum on reovirus infection in PCMCs (Fig. 28). Treatment with IFN- β significantly reduced reovirus infection in these cultures in comparison to untreated control cells. Similar results were obtained when myocytes were treated with ribavirin, a viral RNA synthesis inhibitor (139), prior to infection. In contrast, treatment with IFN- β -specific antiserum had little effect on reovirus infection in the myocyte cultures, suggesting that cells present in the intact heart other than myocytes are responsible for secreting cardioprotective IFN- β . Together, these data indicate that reovirus is capable of infecting cardiac myocytes and that infection is potently inhibited by the exogenous administration of IFN- β .

Reovirus growth in primary cardiac myocytes

To determine whether PCMCs are capable of supporting the complete reovirus replication cycle, we measured yields of infectious progeny by plaque assay following a time course of reovirus T3SA+ infection (Fig. 29). Reovirus produced high titers in PCMCs at 24 and 48 h post-infection, reaching yields in excess of 100-fold at the later time point.

However, reovirus growth in cardiac myocytes was virtually abolished by pretreatment with IFN- β . Similarly, treatment with either ribavirin or E64, a protease inhibitor that blocks reovirus disassembly (5), diminished reovirus growth in PCMCs. In keeping with our

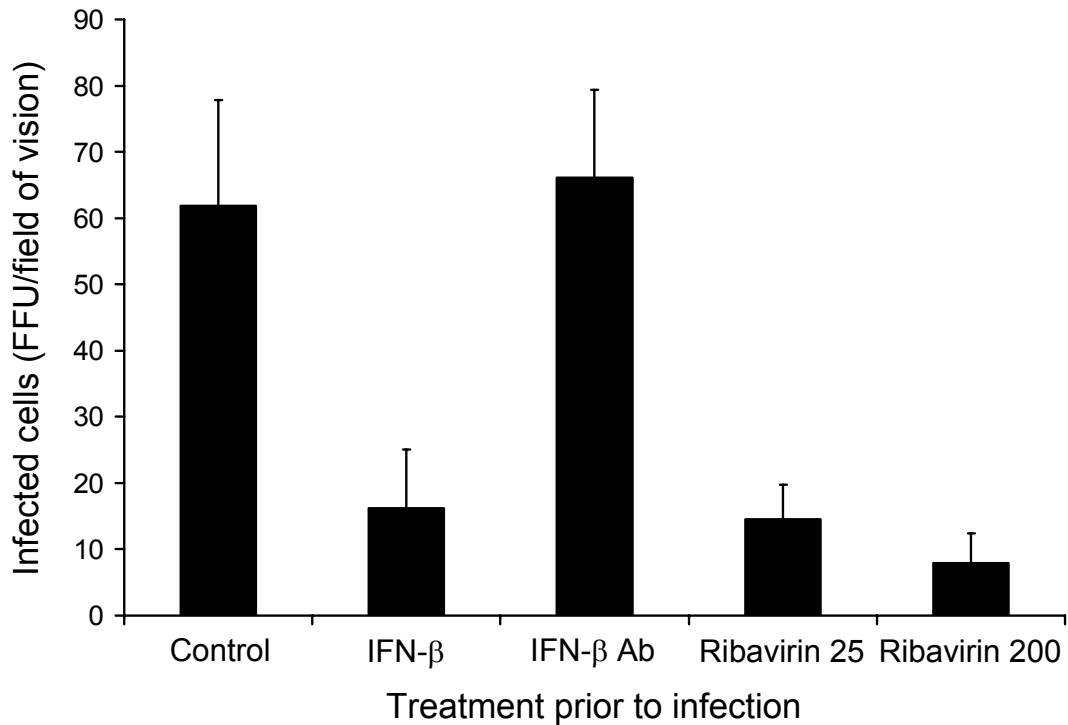


Figure 28. Reovirus infection in PCMCs. PCMCs were pretreated with either fresh medium (control), 1.2×10^4 units of IFN- β , 275 neutralizing units of IFN- β -specific antiserum, or 25 or 200 μ M of ribavirin. Cells were then infected with T3SA+ at an MOI of 10 PFU/cell. After 24 h incubation, cells were fixed and incubated with reovirus-specific antiserum. Infected cells were identified by using indirect immunofluorescence. The results are expressed as the mean fluorescent focus units/field of vision for three independent experiments. Error bars indicate standard deviations.

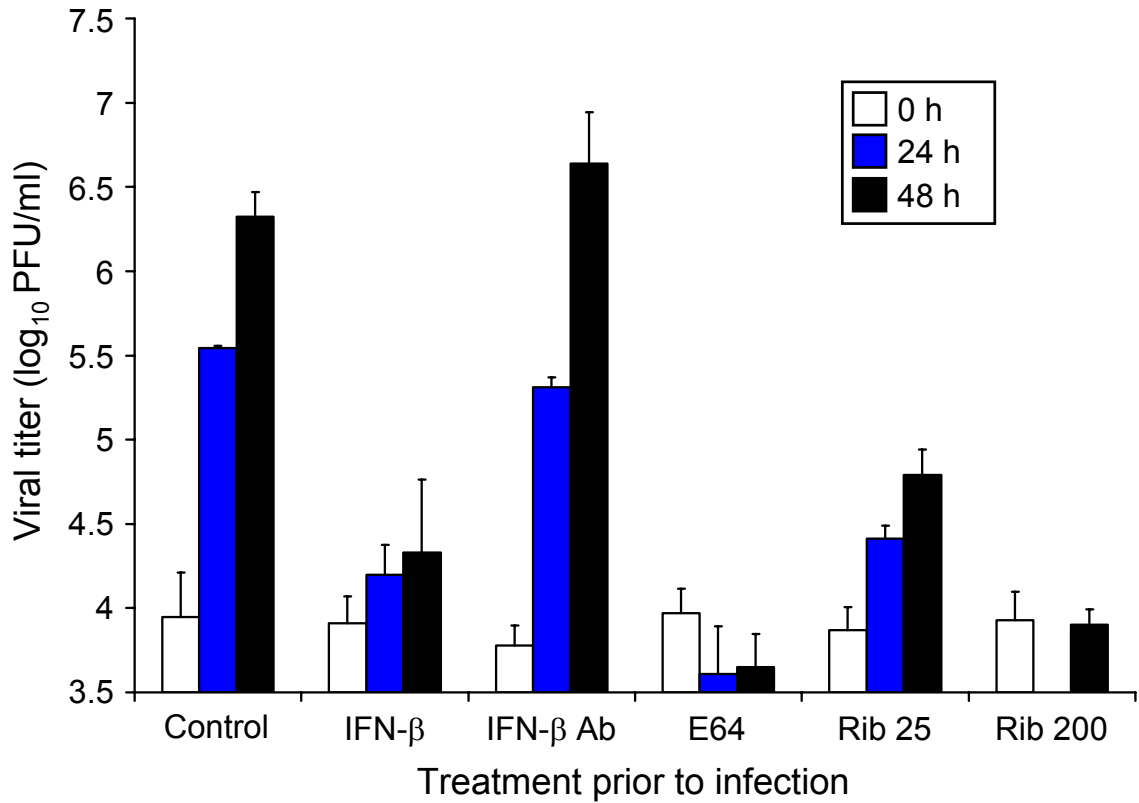


Figure 29. Reovirus growth in PCMCs. PCMCs were pretreated with either fresh medium (control), 1.2×10^4 units of IFN- β , 275 neutralizing units of IFN- β -specific antiserum, 100 μ M E64, or 25 or 200 μ M of ribavirin. Cells were then infected with T3SA+ at an MOI of 10 PFU/cell and incubated for the times shown. Cells and medium were frozen and thawed twice, and viral titers were determined by plaque assay. The results are expressed as the mean viral titers for three independent experiments. Error bars indicate standard deviations.

findings in the immunofluorescence assays of new viral protein synthesis, IFN- β -specific antiserum treatment had little effect on reovirus growth in PCMCs. From these data, we conclude that PCMCs are capable of supporting reovirus growth and that IFN- β reduces the production of viral progeny in these cultures.

Reovirus-induced caspase 3/7 activation in primary cardiac myocytes

To determine whether reovirus is capable of inducing apoptosis in PCMCs, we infected the cultures with reovirus T3SA+ and assessed apoptosis by quantitation of caspase 3/7 activity (Fig. 30). In comparison to mock-infected cells, levels of caspase 3/7 activity were substantially greater in cells infected with T3SA+. Similar to viral growth assays, caspase 3/7 activity was diminished by pretreatment with IFN- β and completely abolished by either E64 or ribavirin. Caspase 3/7 activity in PCMCs treated with IFN- β -specific antiserum prior to reovirus infection was unaffected in comparison to mock-infected PCMCs. These data indicate that inhibition of caspase 3/7 activity by IFN- β correlates with inhibition of viral growth.

Reovirus-induced caspase 3/7 activation in cardiac myocytes lacking the IFN- α/β receptor

To obtain additional evidence for an antiviral function of IFN- β in reovirus infection of PCMCs, we generated cardiac myocytes from mice deficient in the IFN- α/β receptor (119). These cultures were tested for the capacity to support reovirus growth by plaque assay (Fig. 31). Reovirus produced high titers in IFN- α/β receptor-null PCMCs at 24 and 48 h post-infection, reaching yields in excess of 50-fold at the later time point. Viral growth was

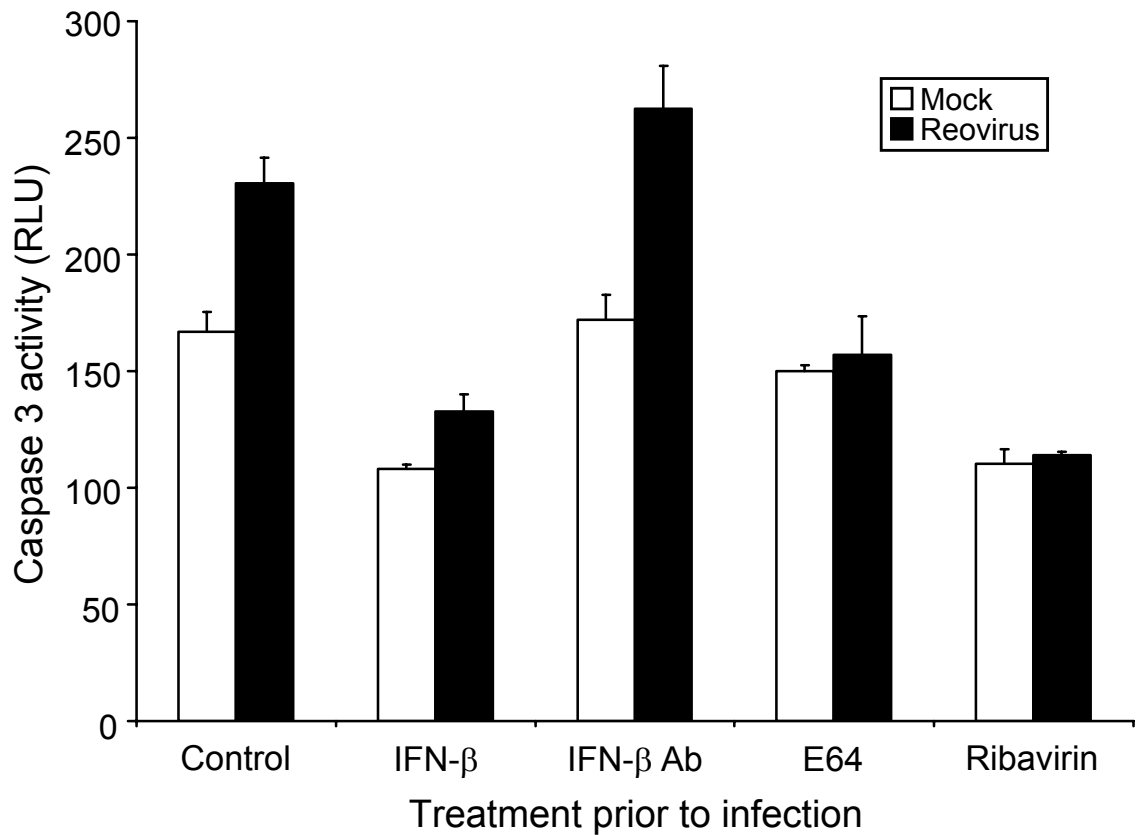


Figure 30. IFN diminishes apoptosis in PCMCs following reovirus infection. PCMCs were pretreated with either fresh medium (control), 1.2×10^4 units of IFN- β , 275 neutralizing units of IFN- β -specific antiserum, 100 μ M E64, or 200 μ M ribavirin. Cells were then either mock-infected or infected with reovirus T3SA+ at an MOI of 100 PFU/cell for 24 h. Caspase 3/7 activity was quantified by using a luminescent substrate. The results are expressed as the mean caspase activity relative to mock-infected cells for three independent experiments. Error bars indicate standard deviations.

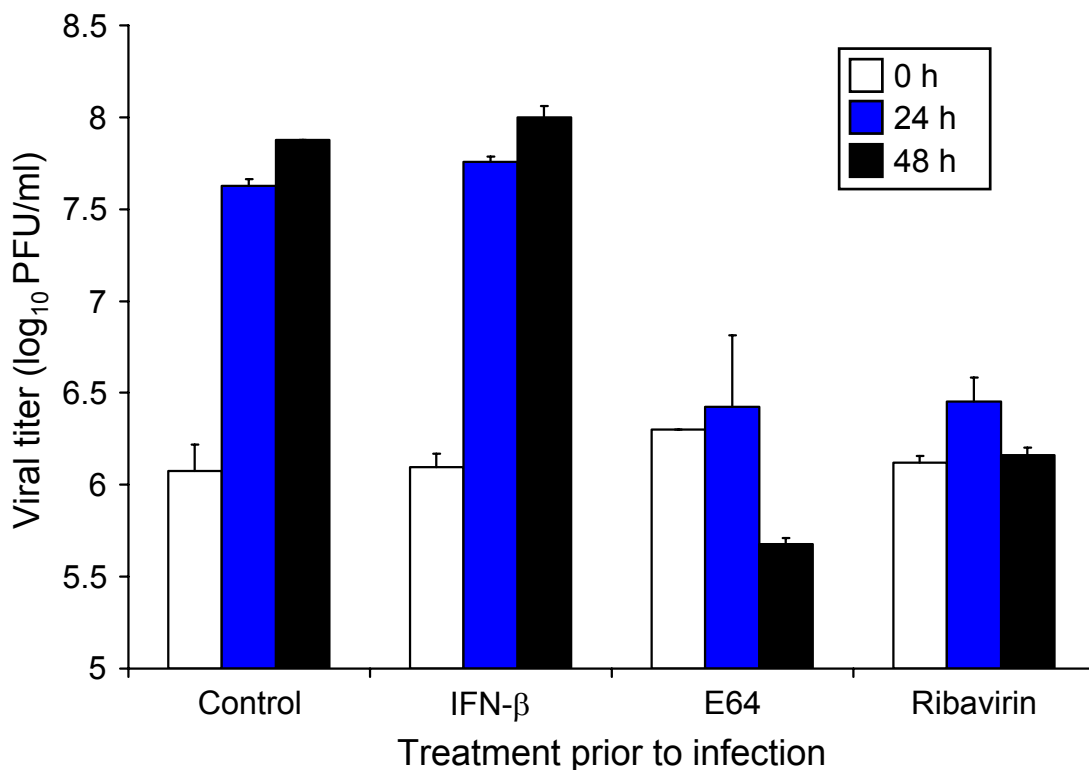


Figure 31. Reovirus growth in PCMCs lacking the IFN- α/β receptor. IFN- α/β receptor-null PCMCs were pretreated with either fresh medium (control), 1.2×10^4 units of IFN- β , $100 \mu\text{M}$ E64, or $200 \mu\text{M}$ ribavirin. Cells were then infected with T3SA+ at an MOI of 10 PFU/cell and incubated for the times shown. Cells and medium were frozen and thawed twice, and viral titers were determined by plaque assay. The results are expressed as the mean viral titers for three independent experiments. Error bars indicate standard deviations.

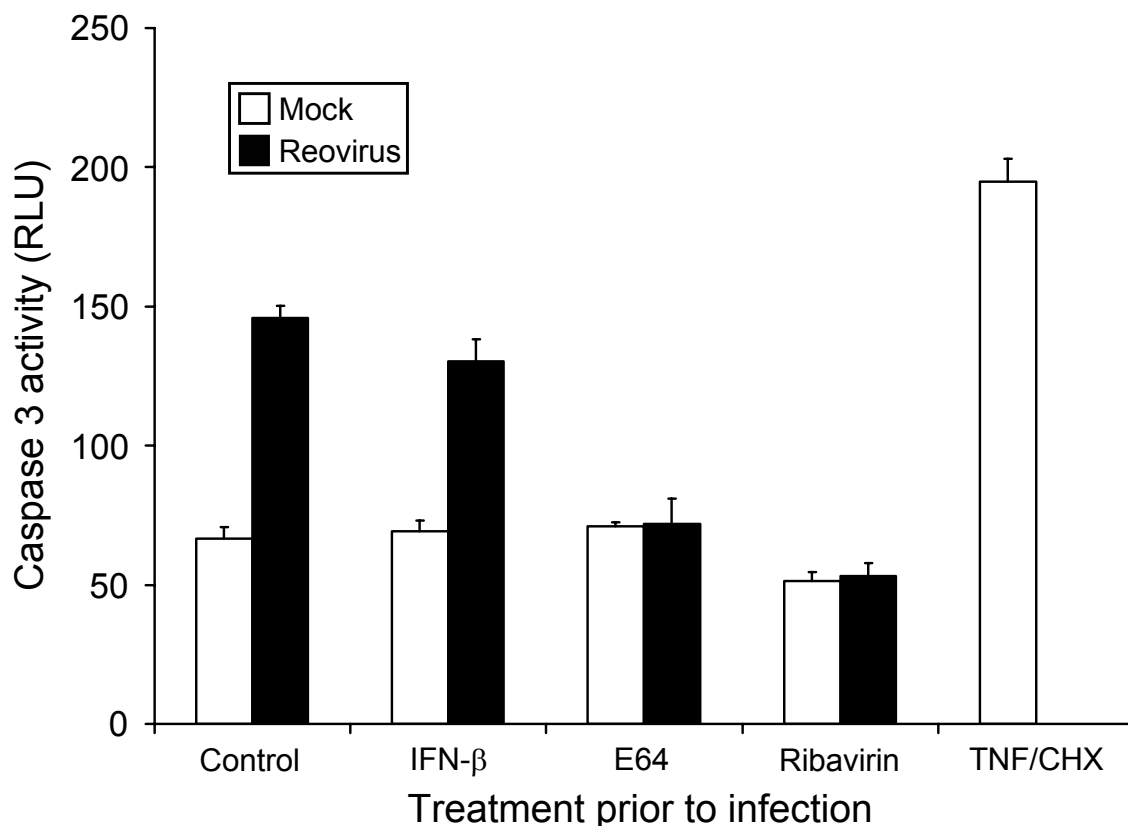


Figure 32. Reovirus induces apoptosis in PCMCs lacking the IFN- α/β receptor. IFN- α/β receptor-null PCMCs were pretreated with either fresh medium (control), 1.2×10^4 units of IFN- β , 100 μ M E64, or 200 μ M ribavirin. Cells were then either mock-infected, infected with reovirus T3SA+ at an MOI of 100 PFU/cell for 24 h, or treated with 10 ng/ml of TNF α and 10 μ g/ml of cycloheximide (CHX) for 12 h. Caspase 3/7 activity was quantified by using a luminescent substrate. The results are expressed as the mean caspase activity relative to mock-infected cells for three independent experiments. Error bars indicate standard deviations.

blocked by treating PCMCs with either E64 or ribavirin prior to infection. As expected, treatment with IFN- β had no effect on PCMCs lacking expression of the relevant receptor.

We next investigated whether reovirus is capable of inducing apoptosis in cardiac myocytes lacking the IFN- α/β receptor. IFN- α/β receptor-null PCMCs were infected with reovirus T3SA+, and apoptosis was assessed by quantitation of caspase 3/7 activity (Fig. 32). Reovirus induced substantial levels of caspase 3/7 activity in the receptor-null PCMCs, and this activity was blocked by treatment of cells with either E64 or ribavirin prior to infection. The increase in caspase 3/7 activity induced by reovirus in IFN- α/β receptor-null PCMCs paralleled that in reovirus-infected wild-type PCMCs (compare Figs. 30 and 31). Therefore, signaling from the IFN- α/β receptor during reovirus infection of these cells does not contribute to apoptosis.

Discussion

This study was designed to determine the relationship of IFN, viral replication, and apoptosis in reovirus-infected cardiac myocytes. Two important conclusions emerge from these experiments. First, reovirus infection of PCMCs leads to increased caspase 3/7 activity, indicative of apoptosis. Second, treatment with IFN- β inhibits reovirus growth and decreases virus-induced apoptosis in PCMCs. Together, these findings suggest that IFN- β -mediated inhibition of reovirus replication in cardiac myocytes diminishes apoptotic cell death.

Myocytes lost or damaged during viral infection are not replenished, which raises the possibility that these cells have a unique response in the presence of virus. Previous reports indicate that basal levels of IFN- β are higher in PCMCs than in primary cardiac fibroblast cultures (PCFCs) (181). Furthermore, PCMCs express more IFN- β than PCFCs when exposed to reovirus (181). This heightened IFN response suggests that these differentiated,

nondividing, essential cells display an enhanced immune response against pathogens such as reovirus. However, we found that the pretreatment of PCMCs with an antiserum specific for IFN- β had no effect on reovirus infection (Fig. 28), growth (Fig. 29), or apoptosis (Fig. 30). Additionally, PCMCs isolated from IFN- α/β receptor-null mice are fully permissive for reovirus growth (Fig. 31) and undergo apoptosis following reovirus infection (Fig. 32). These findings suggest that IFN- β expressed by PCMCs in response to reovirus is not sufficient to inhibit viral replication or apoptosis. Collectively, these results support the hypothesis that the IFN- β responsible for inducing the antiviral response in PCMCs following reovirus infection is produced by another cell type, perhaps in PCFCs.

NF- κ B induces the expression of type I IFNs following stimulation with numerous agonists (31, 56, 224). We and others previously have shown that numerous ISGs are induced in an NF- κ B-dependent manner in reovirus-infected cells (45, 129, 178). Since reovirus-induced apoptosis is also NF- κ B-dependent, it seemed possible that IFN- β expression as a result of NF- κ B activation elicits programmed cell death in infected cells by an autocrine pathway. In support of this possibility, IFN- α/β enhances apoptosis in response to double-stranded RNA and influenza virus (185), suggesting that IFN- α/β release sensitizes cells for apoptosis in response to certain stimuli. This response could aid in viral clearance by earmarking infected cells for elimination by phagocytic cells. However, this mechanism is not involved in the cell death response in PCMCs following reovirus infection. There are three lines of evidence that support this conclusion. First, pretreatment with IFN- β diminishes apoptosis in PCMCs in response to reovirus (Fig. 30). Second, pretreatment with IFN- α/β -specific antiserum had no effect on reovirus-induced apoptosis (Fig. 30). Third, reovirus infection of IFN- α/β receptor-null PCMCs and wild-type PCMCs produced equivalent levels of apoptosis (Fig. 32). It is possible that IFN functions to sensitize some

types of cells to apoptosis following reovirus infection, but this cytokine does not enhance death signaling in cardiac myocytes.

Previous reports indicate that reovirus replication is not required for apoptosis in HeLa cells (39) and L929 cells(199). However, we found that viral replication is required for apoptosis in reovirus-infected PCMCs. Reovirus replication is inhibited in PCMCs following pretreatment with IFN- β , which also diminishes reovirus-induced apoptosis (Figs. 29 and 30). We also observed that pretreatment with RNA synthesis inhibitor ribavirin reduced both viral growth and apoptosis in reovirus-infected PCMCs (Figs. 31 and 32). These data are consistent with data gathered from animals infected with reovirus demonstrating that IFN- β treatment inhibits both viral growth and abolishes apoptosis in the heart (128). Together, these findings suggest that viral replication is required for reovirus-induced apoptosis in cardiac myocytes and that IFN- β functions in blocking apoptosis by reducing reovirus growth.

In this study, we show that reovirus growth in PCMCs is diminished by pretreatment with IFN- β and this blockade of viral replication correlates with inhibition of reovirus-induced apoptosis. We also found that endogenous IFN- β produced by PCMCs is not sufficient to limit reovirus growth, suggesting that PCMCs must be preexposed to IFN- β to inhibit viral infection. Future studies will identify the cell types responsible for producing cardioprotective IFN and elucidate mechanisms of the IFN-mediated antiviral state in cardiac myocytes.

CHAPTER VI

SUMMARY AND FUTURE DIRECTIONS

Processes by which viruses injure and kill their host cells are essential determinants of viral pathogenesis. Although general features of virus-induced cell death are understood, little is known about the cellular sensors of viral infection that trigger cell killing. A thorough understanding of mechanisms of virus-induced apoptosis is essential for uncovering a role for this apoptotic process in viral pathogenesis and designing antiviral therapeutics targeting specific signaling pathways elicited by viruses responsible for cell death and disease. The work described in this thesis uses mammalian reovirus, a highly tractable experimental model, to elucidate intracellular signaling pathways activated by viruses to cause cell death and disease.

The data presented in this thesis support the following conclusions: 1) reovirus-induced apoptosis is independent of viral attachment to cell-surface receptors such as JAM-A and sialic acid (Chapter II); 2) reovirus stimulates IKK complexes consisting of the α and γ subunits to phosphorylate I κ B α leading to NF- κ B activation and apoptosis (Chapter III); 3) NF- κ B activation functions in a proapoptotic manner in the brain and an antiapoptotic manner in the heart of reovirus-infected animals (Chapter IV); and 4) IFN- β mediates an antiviral state by inhibiting viral proliferation and apoptosis in cardiac myocytes (Chapter V). This chapter summarizes the data presented in this dissertation and highlights future directions for this research.

The role of $\mu 1$ in reovirus-induced apoptosis

Results from Chapter II demonstrate that signaling pathways activated by binding of $\sigma 1$ to JAM-A and sialic acid are dispensable for reovirus-mediated apoptosis. Instead, we found that the $\mu 1$ protein plays an essential function in stimulating proapoptotic machinery. Analysis of T1L x T3D reassortant viruses revealed that the $\mu 1$ -encoding M2 gene segment is the only viral determinant of the apoptosis-inducing capacity of reovirus when infection is initiated via Fc receptors. Additionally, a temperature-sensitive, membrane penetration-defective M2 mutant, tsA279.64, is an inefficient inducer of apoptosis. The $\mu 1$ protein contains three putative membrane-interaction motifs, including the N-terminal myristate moiety and two amphipathic α -helices (79, 93, 121, 123), and three known proteolytic cleavage sites. These include an autocatalytic cleavage site at amino acid 42, which separates $\mu 1N$ and $\mu 1C$, and a cleavage site at amino acid 580, which releases the δ and ϕ fragments (27, 121, 127). While cleavage at the autocatalytic site is required for membrane penetration, the physiologic consequences of the δ - ϕ cleavage are unknown (27, 127). This cleavage occurs concomitantly with the formation of ISVPs and allows release of δ into the cytoplasm following endosomal membrane penetration (27). A third, less understood, cleavage leads to release of ~ 10 C-terminal amino acids (114).

Future studies will identify the mechanism of $\mu 1$ -induced apoptosis following reovirus infection. To determine whether $\mu 1$ is sufficient for induction of death signaling, cells will be transfected with plasmids encoding full-length $\mu 1$, $\mu 1$ cleavage fragments, or $\mu 1$ truncation mutants and tested for NF- κ B activation and apoptosis induction. This strategy will allow us to extensively mutagenize regions within $\mu 1$ and rapidly screen for domains that affect its capacity to induce apoptosis.

To define functional domains in $\mu 1$ important for proapoptotic signaling, we will use a reverse genetics approach recently established in our laboratory to test viruses containing of specific point mutations in the $\mu 1$ protein for the capacity to induce apoptosis. The glycine residue at the myristoylation site will be substituted with alanine, and apolar residues within the amphipathic α -helices will be replaced with polar residues to disrupt helix stability. These mutations will likely alter $\mu 1$ -membrane interactions. Cleavage sites in $\mu 1$ will be altered individually and in combination to assess the role of specific $\mu 1$ cleavage events in apoptosis induction. These studies will identify regions in $\mu 1$ required for reovirus-induced apoptosis and may allow $\mu 1$ cleavage events to be disassociated from $\mu 1$ -mediated membrane penetration in proapoptotic signaling.

The role of Rel subunits p52 and c-Rel in reovirus-induced apoptosis

We found in chapter III that both p52 (16 h) and c-Rel (8 h) are activated following the initial induction of NF- κ B complexes containing p50 and RelA. Processing of p100 results in the formation of p52, but it is unclear how c-Rel becomes activated following reovirus infection. Levels of both I κ B β and I κ B ϵ remain unchanged following an 8 h timecourse of reovirus infection, suggesting that c-Rel is not activated via degradation of either of these I κ B isoforms. Reovirus-induced c-Rel activation could result from nuclear translocation of NF- κ B complexes consisting of p50 and RelA at early times of infection and induction of c-Rel expression leading to its subsequent activation in the form of c-Rel homodimers or RelA/c-Rel heterodimers. Interestingly, previous reports indicate that NF- κ B activation is abolished at late times of infection (6-8 h) in both p50-

and RelA-deficient cell lines following reovirus infection (40). These findings suggest that both p50 and RelA are required for c-Rel induction in response to reovirus.

It is possible that initial activation of p50/RelA NF- κ B complexes inhibits apoptosis at early times during infection and complexes containing p52 or c-Rel promote apoptosis at later times of infection. To test the role of p52 and c-Rel in reovirus-induced apoptosis, we will use cells deficient in either p52/NF- κ B2 or c-Rel to determine whether reovirus is capable of inducing apoptosis in the absence of these signaling molecules. Alternatively, overexpression of the Rel subunits p50 and RelA could be used to assess whether these NF- κ B complexes function to inhibit apoptosis when constitutively active during reovirus infection. Results from these experiments will define the role of p52 and c-Rel in reovirus-induced apoptosis.

The mechanism of IKK activation in response to reovirus

Results from chapter III illustrate that reovirus stimulates IKK complexes consisting of the α and γ subunits. Upon activation, IKK phosphorylates I κ B α leading to the nuclear translocation of p50/RelA complexes. This novel NF- κ B pathway activated by reovirus is independent of NIK, which is responsible for phosphorylating IKK α following the induction of the alternative pathway of NF- κ B activation by some agonists(95, 163, 221). The mechanism elicited by reovirus that is responsible for IKK stimulation remains unresolved and is currently being investigated in our laboratory.

Since μ 1 plays an important role in reovirus-induced apoptosis, we envision a mechanism in which this viral protein interacts directly with IKK inducing a conformational change in the complex and subsequent autophosphorylation of the catalytic subunits. We have begun to test this hypothesis by transiently expressing μ 1 in combination with

individual IKK subunits and performing immunoprecipitation assays with antiserum specific for the appropriate IKK molecule followed by immunoblotting using $\mu 1$ -specific antiserum. Additional experiments along this line of inquiry will resolve whether $\mu 1$ can directly activate IKK.

An alternative explanation for the mechanism of IKK activation in response to reovirus is that $\mu 1$, or another viral protein, interacts with a kinase or an adaptor protein upstream of IKK resulting in the phosphorylation of the IKK catalytic subunits. To identify these possible interactions, yeast-two-hybrid experiments could be utilized to determine possible $\mu 1$ -interacting candidates that may potentially function in IKK activation. Mutants of $\mu 1$ will be used to determine the domains that are required for this interaction. These experiments will elucidate the mechanism of IKK activation in response to reovirus and further characterize the function of $\mu 1$ in reovirus-induced apoptosis.

The role of IKK in reovirus pathogenesis

Findings reported in chapter IV indicate that NF- κ B activation in the CNS leads to high levels of neuronal apoptosis and encephalitis. In contrast, NF- κ B activation in the heart leads to IFN- β production, which limits viral replication and protects against apoptosis. In the absence of NF- κ B signaling, reovirus infection induces widespread apoptotic damage to cardiac myocytes, resulting in myocarditis. Mechanisms underlying the divergent cellular fates following NF- κ B activation by reovirus in vivo remain unclear. Data from chapter III suggests that IKK α and IKK γ are required for reovirus-induced NF- κ B activation in cell culture. These findings implicate the alternative pathway of NF- κ B signaling in reovirus-infected cells. However, we also have evidence indicating that p50/RelA heterodimers are the predominant nuclear species following reovirus infection of cultured cells (Chapter III)

and in vivo (Chapter IV), consistent with the classical mode of NF- κ B signaling. In light of these results, we think it possible that the differential effects of NF- κ B signaling in reovirus disease could be attributable to tissue-specific activation of different IKK subunits, which in turn influence the composition of nuclear NF- κ B complexes. Considering the findings presented in chapters III and IV, these mechanisms may involve tissue-specific activation of different IKK subunits, which in turn may influence the composition of nuclear NF- κ B complexes. Experiments using tissue-specific IKK α - or IKK β -deficient mice should clarify the function of IKK in reovirus-induced disease.

Conclusions

With this research, we set out to establish a better understanding of the apoptotic response induced during reovirus infection that culminates in disease. The studies performed in this thesis carefully dissect mechanisms of reovirus-induced NF- κ B activation and apoptosis. The long-term goal of this work is to identify intracellular events elicited by reovirus that activate NF- κ B resulting in apoptosis induction and tissue damage in the host. Knowledge gained from this research could lead to the development of therapeutics designed specifically to inhibit viral replication or block signaling pathways required for virus-induced apoptosis. Identification of a novel NF- κ B activation pathway elicited by reovirus is particularly intriguing due to the potential impact in the field. These findings set the stage for precise biochemical analysis of the mechanisms employed by reovirus to induce apoptosis and cause disease.

CHAPTER VII

DETAILED METHODS OF PROCEDURE

Cells, viruses, and antibodies

Spinner-adapted murine L929 cells were grown in either suspension or monolayer cultures in Joklik's modified Eagle's minimal essential medium (Irvine Scientific, Santa Ana, Calif.) supplemented to contain 5% fetal bovine serum (Gibco-BRL, Gaithersburg, Md.), 2 mM L-glutamine, 100 U of penicillin per ml, 100 mg of streptomycin per ml, and 0.25 mg of amphotericin per ml (Gibco-BRL). HeLa cells and MEFs were maintained in monolayer cultures in Dulbecco's minimal essential medium (Gibco-BRL) supplemented to contain 10% fetal bovine serum, L-glutamine, and antibiotics as described for L cells. CHO cells were maintained in Ham's F12 medium supplemented with fetal bovine serum, L-glutamine, and antibiotics as described for HeLa cells.

The prototype reovirus strain T3D are laboratory stocks. Reovirus strain T3SA+ was generated by reassortment of reovirus strains T1L and type 3 clone 44-MA (12). Viral stocks were prepared by plaque purification and passage in L cells (205). Purified virions were prepared by using second- and third-passage L-cell lysate stocks as previously described (58, 155). Viral particles were freon-extracted from infected-cell lysates, layered onto 1.2 to 1.4 g/cm³ CsCl gradients, and centrifuged at 62,000 x g for 18 h. Bands corresponding to virions (1.36 g/cm³) were collected and dialyzed in virion storage buffer (150 mM NaCl, 15 mM MgCl₂, 10 mM Tris [pH 7.4]). Concentrations of reovirus virions in purified preparations were determined from the equivalence 1 OD₂₆₀ = 2.1 x 10¹² virions. The particle-to-PFU ratio of stocks used for viral infectivity assays was approximately 10-100 to 1.

Generation and characterization of mAbs 5C6, 9BG5, and 7F4, which are specific for the type 1 σ 1, type 3 σ 1, and λ 2 proteins, respectively, have been previously described (23, 195). The immunoglobulin G (IgG) fractions of polyclonal rabbit antisera raised against T1L and T3D (206) were purified by using protein A-sepharose as previously described (10). A mixture of these sera was capable of recognizing all strains of reovirus used in this study. Protein-A purified, JAM-A-specific mAb J10.4 was obtained from Dr. Charles Parkos (Emory University) (99). Anti-Myc mAb 9E10 and anti-Fc rat mAb were purchased from BD Biosciences (San Jose, CA). Fluorescent dye-conjugated secondary antibodies were purchased from Molecular Probes (Eugene, OR). Antisera specific for $\text{I}\kappa\text{B}\alpha$, $\text{I}\kappa\text{B}\beta$, $\text{I}\kappa\text{B}\epsilon$, p50, RelA/RelA, RelB, c-Rel, IKK γ , and β -actin were purchased from Santa Cruz Biotechnology (Santa Cruz, CA). The antibody antiserum for p100/p52 was purchased from Upstate Biotechnology (Lake Placid, NY). The agonistic lymphotoxin- β receptor antiserum was purchased from BD Biosciences (San Jose, CA). The IKK inhibitor BAY 65-1942 was obtained from Dr. K. Ziegelbauer (Bayer Health Care AG, Leverkusen, Germany). Rabbit polyclonal antiserum specific to the activated form of caspase 3 (anti-caspase 3/Asp 175) was purchased from Cell Signaling Technology (Danvers, MA). IFN- β and IFN- α/β -specific antiserum was purchased from Calbiochem (San Diego, CA).

Generation of CHO cells stably expressing JAM-A or JAM-A Δ CT

Human JAM-A was subcloned into expression plasmid pcDNA3.1 (Invitrogen, Carlsbad, CA). Truncation mutant JAM-A Δ CT was generated by PCR using full-length JAM-A cDNA as template. Sequences encoding amino acids 1-260 (Δ 261-299) were cloned and appended with a stop codon using T7 primer and 5'-TACGGGATCCTCAGGCAAACCAGATGCC-3' as forward and reverse primers,

respectively. The PCR product was digested with *Bam*HI and introduced into pcDNA3.1 using complementary restriction sites. Fidelity of cloning was confirmed by automated sequencing. CHO cells stably expressing empty vector alone, JAM-A, and JAM-A Δ CT were generated by transfection of CHO-K1 cells with empty pcDNA3.1 vector, pcDNA3.1 encoding JAM-A, or pcDNA3.1 encoding JAM-A Δ CT. Cells were grown to 50% confluence in 6 cm dishes (Costar, Cambridge, MA) and transfected with 4 μ g of each plasmid by using Lipofectamine Plus reagent (Invitrogen) according to the manufacturer's instructions. Transfected cells were selected by growth in the presence of 1 mg per ml G418. After the tenth passage in the presence of G418, cells expressing high levels of JAM-A as assessed by JAM-A-specific mAb J10.4 staining (mean fluorescence intensity > 5000) were separated using a BD FACsort cell sorter (Becton-Dickinson, Palo Alto, CA).

Immunoblot assays

Following treatment, whole-cell extracts were generated by incubation with lysis buffer (10 mM HEPES [pH7.4], 10 mM KCL, 0.1 mM EDTA, 0.1 mM EGTA, 1 mM DTT, 0.1% Igepal, 1 mM Na₄O₇P₂, 1 mM NaF, 1 mM NaVO₃, and 1 μ M microcystin). Extracts (10-50 μ g total protein) were resolved by electrophoresis in 10% polyacrylamide gels and transferred to nitrocellulose membranes. Membranes were blocked at 4°C overnight in blocking buffer (PBS containing 0.1% Tween-20 and 5% BSA). Immunoblots were performed by incubating the membranes with primary antibodies diluted 1:500 to 1:2000 in blocking buffer at room temperature for 1 h. Membranes were washed three times for 10 min each with washing buffer (PBS containing 0.1 Tween-20) and incubated with horseradish peroxidase-conjugated goat anti-rabbit (Amersham Biosciences, Piscataway, NJ) and bovine anti-goat antibodies (Santa Cruz Biotechnology) diluted 1:2000 and 1:3000, respectively.

Following three washes, membranes were incubated for 1 min with chemiluminescent peroxidase substrate (Amersham Biosciences) and exposed to film. Band intensity was quantified using the Image J program (NIH, Bethesda, MD).

Flow cytometric analysis for JAM-A surface expression

CHO cells stably transfected with empty vector, JAM-A, or JAM-A Δ CT were detached from plates using PBS containing 10 mM EDTA. Cells were washed twice with chilled PBS prior to incubation with 10 μ g per ml of either JAM-A specific mAb J10.4 or an isotype-matched control mAb at 4°C for 1 h. Cells were stained with a 1:1000 dilution of PE-labeled anti-mouse IgG at 4°C for 1 h and analyzed using a FACScan flow cytometer (Becton-Dickinson).

Fluorescent-focus assays of viral infectivity

Monolayers of cells (2×10^5) in 24-well plates (Costar) were adsorbed with various MOIs of reovirus at room temperature for 1 h. Following removal of the inoculum, cells were washed with PBS and incubated in complete medium at 37°C for 18 h to permit completion of a single cycle of viral replication. Monolayers were fixed with 1 ml of methanol at -20°C for a minimum of 30 min, washed twice with PBS, blocked with 2.5% Ig-free bovine serum albumin (Sigma-Aldrich, St. Louis, MO) in PBS, and incubated at room temperature for 1 h with polyclonal rabbit anti-reovirus serum at a 1:1000 dilution in PBS-0.5% Triton X-100. Monolayers were washed twice with PBS-0.5% Triton X-100 and incubated with a 1:1000 dilution of Alexa546-labeled anti-rabbit IgG. Monolayers were washed with PBS, and infected cells were visualized by indirect immunofluorescence using an Axiovert 200 fluorescence microscope (Carl Zeiss, New York, NY). Infected cells were

identified by the presence of intense cytoplasmic fluorescence that was excluded from the nucleus. No background staining of uninfected control monolayers was noted. Reovirus antigen-positive cells were quantified by counting fluorescent cells in at least three random fields of view in duplicate wells at a magnification of 20X.

Antibody-mediated infections

Reovirus virions (1×10^{11}) were incubated at 4°C overnight with various concentrations of mAb in 1 ml PBS. Cells were adsorbed with virus at an MOI of either 100 or 500 PFU per ml at room temperature for 1 h. Following removal of the inoculum, cells were washed with PBS and incubated in complete medium at 37°C for various intervals. For inhibition of viral disassembly and RNA synthesis, cells were maintained in 20 mM AC or 200 µM ribavirin, respectively, throughout the course of infection. For inhibition of disassembly, cells also were pretreated for 1 h with medium containing 20 mM AC.

Quantitation of apoptosis by acridine orange (AO) staining

Cells (2×10^5) grown in 24-well tissue-culture plates were adsorbed with reovirus virions or mAb-virion complexes at various MOIs. Following incubation at 37°C for 48 h, the percentage of apoptotic cells was determined by using AO staining as previously described (199). For each experiment, 200 to 300 cells were counted in three independent wells, and the percentage of cells exhibiting condensed chromatin was determined by epillumination fluorescence microscopy using a fluorescein filter set (Carl Zeiss).

Electrophoretic mobility shift assay (EMSA)

Cells (3×10^6) grown in 100 mm tissue-culture dishes (Costar, Cambridge, MA) were treated with 20 ng/ml of TNF- α (Sigma-Aldrich, St. Louis, MO), adsorbed with T3D at a multiplicity of infection (MOI) of 100 plaque forming units (PFU)/cell, or treated with gel saline (mock-infection). After incubation at 37°C for various intervals, nuclear extracts (10 μ g total protein) were assayed for NF- κ B activation by an EMSA using a 32 P-labeled oligonucleotide consisting of the NF- κ B consensus-binding sequence (Santa Cruz Biotechnology) as previously described (40). For supershift assays, 2 μ g of rabbit polyclonal antiserum specific for p50, p52, RelA, RelB, or c-Rel was added to the binding-reaction mixtures and incubated at 4°C for 30 min prior to the addition of radiolabeled oligonucleotide. Nucleoprotein complexes were subjected to electrophoresis in native 5% polyacrylamide gels at 180 V for 90 min, dried under vacuum, and exposed to Biomax MR film (Kodak, Rochester, NY). Band intensity was quantified by determining photostimulus luminescence (PSL) units using a Fuji2000 phosphor imager and the Multi Gauge software (Fuji Medical Systems, Inc., Stamford, CT).

Kinase assay

Cells (8×10^5) were treated with 20 ng/ml of TNF α , adsorbed with T3D at an MOI of 100 PFU/cell, or mock-infected. Whole-cell extracts were incubated with an IKK γ -specific antiserum in the presence of ELB buffer (50 mM HEPES [pH 7.4], 250 mM NaCl, 5 mM EDTA, 0.1% Igepal). Immunoprecipitates were equilibrated in kinase buffer (10 mM HEPES [pH 7.4], 0.5 mM dithiothreitol, 5 mM MgCl₂, 1 mM MnCl₂, 12.5 mM β -glycerophosphate, 50 μ M Na₃VO₄, 2 mM NaF) and incubated with 10 μ M ATP, 5 μ Ci of [γ - 32 P]ATP (Perkin Elmer), and 1 μ g of recombinant GST protein fused to amino acids 1-54 of

I κ B α (GST-I κ B α) at 30°C for 30 minutes (32). Kinase reactions were terminated by heat denaturation in the presence of 1% SDS. Radiolabeled products were resolved by SDS-PAGE, transferred to nitrocellulose membranes, and visualized by autoradiography.

Caspase 3 activity assay

Cells (3×10^3) grown in clear-bottom, black-walled, 96-well tissue-culture plates (Costar) were inoculated with 10 ng/ml of TNF α , a combination of 10 ng/ml of TNF α and 10 μ g/ml of cycloheximide (Sigma-Aldrich), T3D at an MOI of 1000 PFU/cell, or mock-infected. Following incubation at 37°C for 24 and 12 h with respect to T3D- or TNF α -treatment, caspase 3 activity was quantified by using the Caspase-Glo 3/7 Assay (Promega). Luminescence was detected by using a Topcount NXT luminometer (Packard Biosciences Co., Meriden, CT).

Trypan blue exclusion assay

Cells (4×10^4) grown in 6-well tissue-culture plates were inoculated with 10 ng/ml of TNF α , a combination of 10 ng/ml of TNF α and 10 μ g/ml of cycloheximide, T3D at an MOI of 1000 PFU/cell, or mock-infected. Following incubation at 37°C for 48 and 24 h with respect to T3D- or TNF α -treatment, cells were collected and washed with PBS. The cell pellet was resuspended in 50 ml of PBS and stained using 100 μ l of a solution containing 0.4% trypan blue (Kodak) in PBS. For each experiment, 200 to 300 cells were counted and the percentage of cell death was determined by light microscopy (Axiovert 200; Zeiss, Oberkochen, Germany).

Mice and inoculations

HIV long-terminal repeat luciferase (HLL) mice were generated as described previously (18). Control p50^{+/+} mice (B6129PF1/J-A^{W-J/A^W}) and p50^{-/-} mice (B6129P-Nfkb1^{tm1Bal}) (165) were obtained from the Jackson Laboratory. Newborn mice weighing 2.0-2.5g (2-4 days old) were inoculated either intracranially or perorally with purified T3SA+ diluted in PBS. Intracranial inoculations were delivered to the right and left hemispheres (5 μ l each) using a Hamilton syringe (BD Biosciences) and a 30-gauge needle (196). Peroral inoculations were delivered into the stomach (50 μ l) by passage of a polyethylene catheter 0.61 mm in diameter (BD Biosciences) through the esophagus (154). The inoculum contained 0.5% (vol/vol) green food coloring so that accuracy of delivery could be judged. For determination of NF- κ B activation, viral titer, and immunohistochemical staining, mice were euthanized at various intervals following inoculation and organs were collected.

Assessment of NF- κ B activation by in vivo luciferase activity

Two-day-old HLL mice were inoculated perorally with either 10⁴ PFU T3SA+ or PBS. Mice were anesthetized with isoflurane before imaging and immobilized for the duration of the integration time of photon counting (3 minutes). Luciferin (0.75 g/mouse in 0.2 ml isotonic saline) was inoculated intraperitoneally and mice were imaged using an intensified charge-coupled device camera (C2400-32; Hamamatsu Corp.). For the duration of photon counting, mice were placed inside a light-tight box. Light emission from each mouse was detected as photon counts and a digital false-color photon emission image of the mouse was generated.

In vivo EMSAs

Two-day-old p50^{+/+} and p50^{-/-} mice were inoculated perorally with either 10⁴ PFU T3SA+ or PBS. Mice were euthanized 12 days after inoculation. Brains and hearts were aseptically removed, snap frozen on dry ice, and stored at -70°C. Organs were weighed, placed in a mortar with liquid nitrogen, and ground into a powder. Lysis buffer (20 mM HEPES [pH 7.9], 25% glycerol, 0.42 M NaCl, 1.5 mM MgCl₂, 0.2 mM EDTA, 0.5 mM phenylmethylsulfonyl fluoride, 0.5 mM dithiothreitol) was added in a ratio of 1 ml per 200 mg of tissue. Samples were frozen and thawed 3 times and centrifuged at 12,000 g for 10 minutes. The supernatant was used as the whole-cell extract.

Whole-cell extracts (10 µg total protein) were assayed for NF-κB activation by EMSA using a ³²P-labeled oligonucleotide (1 ng) consisting of the NF-κB consensus binding sequence (Santa Cruz Biotechnology Inc.) as described above and previously (40). For competition experiments, unlabeled consensus oligonucleotide at various concentrations was added to the reaction mixtures along with radiolabeled oligonucleotide. For supershift experiments, 1 µl of a rabbit polyclonal antiserum specific to RelA (250 µg/ml; Santa Cruz Biotechnology Inc.) was added to the binding reaction mixtures and incubated at 4°C for 30 minutes prior to the addition of radiolabeled oligonucleotide. Nucleoprotein complexes were subjected to electrophoresis in native polyacrylamide gels, which were dried and exposed to film.

Determination of viral titer in infected organs.

Organs (intestine, liver, heart, and brain) from infected p50^{+/+} and p50^{-/-} were placed into vials containing 1 ml gelatin saline, frozen (-20°C) and thawed once, and

sonicated for 20 seconds. Titers of virus present in organ homogenates were determined by plaque assay using L cell monolayers (205).

Histology, immunohistochemistry, and TUNEL staining

Litters of newborn p50^{+/+} and p50^{-/-} mice were inoculated intracranially or perorally with either 10⁴ PFU T3SA⁺ or PBS. Mice were euthanized, and brain and heart tissues were fixed in 10% buffered paraformaldehyde. Fixed organs were embedded in paraffin, and 6- μ m histological sections were prepared. Sections were stained with H&E for evaluation of histopathologic changes, processed for immunohistochemical detection of reovirus antigen, assayed for DNA fragmentation using the TUNEL technique (201), or processed for the immunohistochemical detection of activated caspase 3 (12). Cells demonstrating TUNEL staining were quantitated separately in each parasagittal brain section in the following regions: cerebral cortex, hippocampus, basal ganglia, diencephalons, and brain stem. The mean number of positive cells per region was determined for each treatment group and time point. Observers were blinded to the identity of the mouse strain and the nature of the inoculum.

Echocardiography

Echocardiography was performed on conscious 10-day-old pups as previously described for adult mice (152) except that the total field depth was set to 1 cm (minimum possible), and external heating and rapid sample acquisition were used to prevent excessive heat loss. Electrocardiograms were digitally sampled and corresponds to the usual surface lead I.

RNA isolation and real-time PCR

Two-day-old p50^{+/+} and p50^{-/-} mice were inoculated perorally with either 10⁴ PFU T3SA⁺ or PBS. Mice were euthanized, and brain and heart tissues were homogenized using a Dounce homogenizer. RNA was extracted from brain and heart homogenates using the TRIZOL RNA extraction protocol (Invitrogen Corp.). RNA (3 µg) was used in a reverse transcription reaction containing x10 buffer, 25 mM MgCl₂, 100 µM dithiothreitol, 1 U RNasin (Promega), 10 mM dNTPs, 50 µM random hexamers, and 1 U AMV reverse transcriptase (Promega). The reaction was incubated at 43°C for 1 h and then at 95°C for 10 min.

Real-time PCR reactions were carried out using the Bio-Rad iCycler and iQ Supermix buffer containing DNA polymerase and SYBR Green (Bio-Rad Laboratories). Two to 3 replicate amplification reactions were performed in 96-well plates (Bio-Rad Laboratories). Each reaction contained 12.5 µl iQ Supermix buffer, 300 nM forward and reverse primers, and 1 µl cDNA in a final volume of 25 µl. Primers for the reactions were as follows: A) IFN-β forward, 5'-GGAGATGACGGAGAAGATGC-3', B) IFN-β reverse, 5'-CCCAGTGCTGGAGAAATTGT-3', C) GAPDH forward, 5'-CAACTACATGGTCTACATGTTC-3', D) GAPDH reverse, 5'-CTCGCTCCTGGAAGATG-3'. Cycling conditions were as follows: 95°C for 10 min and then 45 cycles at 95°C for 15 sec, 60°C for 30 sec, and 72°C for 15 sec.

Data were analyzed using Bio-Rad iCycler PCR detection and analysis software version 3.0 (Bio-Rad Laboratories). DNA was quantitated using the standard curve method with the background subtracted. Known concentrations of cDNA were used to obtain the standard curve for each gene (concentrations between 0.0228 and 710 ng). A melting curve

was determined for each sample to detect primer dimers, in which case data were not used. Results are expressed as values for IFN- β cDNA divided by those for GAPDH cDNA.

IFN- β treatment of mice

Two-day-old p50^{-/-} mice were inoculated intraperitoneally with either 5×10^4 U IFN- β (Calbiochem) suspended in PBS containing 0.1% BSA or PBS alone in a volume of 25 μ l 1 day prior to peroral inoculation with 10^4 PFU T3SA+. Infected mice were treated daily for 9 days with either IFN- β or PBS. On day 10, following viral inoculation, animals were euthanized and organs were removed. Organs were processed for determination of viral titer and histopathological analysis.

Animal husbandry and experimental procedures were performed in accordance with NIH Public Health Service policy and approved by the Vanderbilt University School of Medicine Institutional Animal Care and Use Committee.

Primary cardiac myocyte generation

To generate primary cardiac myocyte cultures, 2- to 4-day-old neonates were euthanized and the apical two-thirds of the hearts were removed, minced, and trypsinized (13). Cells were plated at a density of 1.25×10^6 per well in six-well plates (Costar) and incubated for 1.5 to 2 h in order to isolate rapidly adhering cardiac fibroblasts. Cardiac myocytes were resuspended in DMEM (Gibco BRL) supplemented with 7% fetal calf serum (Gibco BRL), 0.06% thymidine (Sigma-Aldrich) and plated as indicated for each procedure. Myocyte cultures contained 5 to 20% fibroblasts, consistent with levels reported by others (65, 72, 113), and consistent with cell heterogeneity in the heart.

Statistical analysis

Mean values obtained in infectivity and apoptosis assays were compared using the unpaired Student's *t* test as applied with Microsoft Excel software. *P* values of less than 0.05 were considered to be statistically significant. The contribution of each of the reovirus gene segments to apoptosis induction was assessed by using the non-parametric Mann-Whitney test without adjusting for multiple comparisons and the panel of T1L x T3D reassortant viruses as previously described ((145)).

APPENDIX A

JAM-A-INDEPENDENT, ANTIBODY-MEDIATED UPTAKE OF REOVIRUS INTO
CELLS LEADS TO APOPTOSIS

Pranav Danthi, Mark W. Hansberger, Jacquelyn A. Campbell, J. Craig Forrest,
and Terence S. Dermody

Journal of Virology. 80(3):1261-1270, 2006

JAM-A-Independent, Antibody-Mediated Uptake of Reovirus into Cells Leads to Apoptosis

Pranav Danthi,^{1,2} Mark W. Hansberger,^{2,3} Jacquelyn A. Campbell,^{2,3}
J. Craig Forrest,^{2,3†} and Terence S. Dermody^{1,2,3*}

Departments of Pediatrics¹ and Microbiology and Immunology³ and Elizabeth B. Lamb Center for Pediatric Research,²
Vanderbilt University School of Medicine, Nashville, Tennessee 37232

Received 1 September 2005/Accepted 31 October 2005

Apoptosis plays a major role in the cytopathic effect induced by reovirus following infection of cultured cells and newborn mice. Strain-specific differences in the capacity of reovirus to induce apoptosis segregate with the S1 and M2 gene segments, which encode attachment protein σ 1 and membrane penetration protein μ 1, respectively. Virus strains that bind to both junctional adhesion molecule-A (JAM-A) and sialic acid are the most potent inducers of apoptosis. In addition to receptor binding, events in reovirus replication that occur during or after viral disassembly but prior to initiation of viral RNA synthesis also are required for reovirus-induced apoptosis. To determine whether reovirus infection initiated in the absence of JAM-A and sialic acid results in apoptosis, Chinese hamster ovary (CHO) cells engineered to express Fc receptors were infected with reovirus using antibodies directed against viral outer-capsid proteins. Fc-mediated infection of CHO cells induced apoptosis in a σ 1-independent manner. Apoptosis following this uptake mechanism requires acid-dependent proteolytic disassembly, since treatment of cells with the weak base ammonium chloride diminished the apoptotic response. Analysis of T1L \times T3D reassortant viruses revealed that the μ 1-encoding M2 gene segment is the only viral determinant of the apoptosis-inducing capacity of reovirus when infection is initiated via Fc receptors. Additionally, a temperature-sensitive, membrane penetration-defective M2 mutant, *tsA279.64*, is an inefficient inducer of apoptosis. These data suggest that signaling pathways activated by binding of σ 1 to JAM-A and sialic acid are dispensable for reovirus-mediated apoptosis and that the μ 1 protein plays an essential role in stimulating proapoptotic signaling.

The mammalian reoviruses are prototype members of the *Orthoreovirus* genus within the *Reoviridae* family (70). These viruses are composed of two concentric icosahedral capsids enclosing a segmented, double-stranded RNA genome (46). Reoviruses are highly virulent in newborn mice and injure a variety of organs, including the brain, heart, and liver (70). Apoptosis induced as a consequence of reovirus infection plays an important role in the pathogenesis of both reovirus-induced encephalitis (48, 50, 57) and myocarditis (20, 21, 50). Reoviruses also induce apoptosis of cultured cells (19, 59, 71).

Reovirus infection is initiated by the attachment of virions to cell surface receptors via the σ 1 protein (37, 74). The σ 1 protein of all three reovirus serotypes engages junctional adhesion molecule-A (JAM-A) (5, 11, 27, 53). The σ 1 protein also binds to cell surface carbohydrate; however, the type of carbohydrate bound varies with serotype (1, 23, 51, 52). After receptor binding, virions are internalized into cells by receptor-mediated endocytosis (7, 26). Virions undergo acid-dependent proteolytic disassembly within cellular endosomes, leading to the formation of infectious subviral particles (ISVPs) (2, 8, 15, 24, 63, 66). ISVPs are characterized by the loss of outer-capsid protein σ 3, a conformational change in attachment pro-

tein σ 1, and cleavage of outer-capsid protein μ 1 to form particle-associated fragments δ and ϕ (13, 44, 47). Subsequent to ISVP formation the σ 1 protein is shed, and the μ 1 cleavage fragments undergo conformational rearrangement, yielding ISVP*s (12, 14). ISVP*s are putative entry intermediates that penetrate endosomes and deliver transcriptionally active cores into the cytoplasm (45, 49).

Clues about mechanisms by which reoviruses induce apoptosis first emerged from studies of strain-specific differences in the efficiency of apoptosis induction. Reovirus strain type 3 Dearing (T3D) induces apoptosis in cultured cells more efficiently than strain type 1 Lang (T1L) (17, 59, 71). Studies using T1L \times T3D reassortant viruses demonstrated that these strain-specific effects are determined by the viral S1 and M2 gene segments (59, 71, 72). The S1 gene encodes the attachment protein σ 1 (37, 74), and the M2 gene encodes membrane penetration protein μ 1 (38, 44, 49). Thus, these genetic experiments suggest critical functions for the σ 1 and μ 1 proteins in apoptosis induction by reovirus.

Analysis of reovirus strains T3/C44-SA– (T3SA–) and T3/C44MA-SA+ (T3SA+), which are isogenic at all loci except for a single amino acid polymorphism in σ 1 (4), has pointed to an important role for sialic acid binding in reovirus-induced apoptosis (17). Sialic-acid-binding strain T3SA+ induces apoptosis significantly more efficiently than non-sialic-acid-binding strain T3SA–. Concordantly, removal of cell surface sialic acid with neuraminidase or blockade of virus binding to cell surface sialic acid using a soluble competitor, sialyllactose, abolishes the capacity of T3SA+ to induce apoptosis (17). However, engagement of sialic acid is not sufficient to induce apoptosis.

* Corresponding author. Mailing address: Lamb Center for Pediatric Research, D7235 MCN, Vanderbilt University School of Medicine, Nashville, TN 37232. Phone: (615) 343-9943. Fax: (615) 343-9723. E-mail: terry.dermody@vanderbilt.edu.

† Present address: Department of Microbiology and Immunology, Yerkes National Primate Research Center, Emory University, Atlanta, GA 30329.

Blockade of $\sigma 1$ binding to JAM-A using either $\sigma 1$ - or JAM-A-specific monoclonal antibodies (MAbs) also diminishes the apoptosis-inducing capacity of sialic-acid-binding reoviruses (5, 71). Collectively, these data demonstrate that reovirus strains that bind to both JAM-A and sialic acid are the most potent inducers of apoptosis.

In addition to receptor binding, postattachment events also are required for reovirus-mediated apoptosis induction (18). Inhibition of viral disassembly using ammonium chloride (AC), a weak base that increases vacuolar pH (43), or E64, an inhibitor of cysteine proteases such as those contained in the endocytic compartment (3), abolishes reovirus-induced apoptosis. On the other hand, interference with steps in viral replication subsequent to ISVP formation and membrane penetration using ribavirin, an inhibitor of viral RNA synthesis (55), does not perturb apoptosis induced by reovirus (18). Thus, in addition to sialic acid- and JAM-A-mediated attachment of reovirus to cells, replication steps during or after viral disassembly that occur before the cytoplasmically delivered core becomes transcriptionally active also contribute to reovirus-induced apoptosis. Since the M2-encoded $\mu 1$ protein functions in virus-induced endosomal membrane penetration following disassembly but prior to viral RNA synthesis (38, 44, 49), the deleterious effects of reovirus disassembly inhibitors on apoptosis induction suggest a functional link between the M2 gene segment and differences in the efficiency of apoptosis exhibited by different reovirus strains (59, 71, 72).

In this study, we determined whether reovirus is capable of inducing apoptosis independent of JAM-A and sialic acid binding. We found that antibody-mediated uptake of reovirus into JAM-A-negative, Fc-receptor-expressing cells results in productive infection and leads to apoptosis in a $\sigma 1$ -independent fashion. Moreover, apoptosis induced following this uptake pathway also is dependent on viral disassembly. Analysis of reassortant viruses and an M2 mutant virus demonstrates that the $\mu 1$ protein influences the strength of proapoptotic signaling following reovirus infection. These data suggest that signaling induced as a result of $\sigma 1$ interactions with JAM-A and sialic acid are not necessary for apoptosis induced by reovirus and that the $\mu 1$ protein is the viral factor that stimulates the cellular apoptotic machinery.

MATERIALS AND METHODS

Cells, viruses, and antibodies. HeLa cells were maintained in Dulbecco's modified Eagle medium supplemented to contain 10% fetal bovine serum (FBS), 50 U per ml of penicillin, and 50 μ g per ml streptomycin (Invitrogen, Carlsbad, CA). Chinese hamster ovary (CHO) cells were maintained in HAM's F12 medium supplemented to contain 10% FBS, 50 U per ml of penicillin, and 50 μ g per ml streptomycin. For maintenance of stably transfected CHO cells, the medium was additionally supplemented to contain 1 mg per ml G418 (Invitrogen). CHO-B1 cells, which express the B1 isoform of murine Fc receptor II, were obtained from Ira Mellman (Yale University). Cells were maintained in MEM Alpha supplemented to contain 10% FBS, 50 U per ml of penicillin, 50 μ g per ml streptomycin, and 10 μ M methotrexate (EMD Biosciences, San Diego, CA) as previously described (34).

T1L and T3D are laboratory stocks. Isolation and characterization of T3SA- and T3SA+ have been previously described (4). Reovirus temperature-sensitive mutant *tsA279.64* was obtained from Kevin Coombs (University of Manitoba) (30). Purified reovirus virions were generated by using second- or third-passage L-cell lysate stocks of twice-plaque-purified reovirus as previously described (28). Viral particles were reon-extracted from infected cell lysates, layered onto 1.2- to 1.4-g/cm³ CsCl gradients, and centrifuged at 62,000 $\times g$ for 18 h. Bands corresponding to virions (1.36 g/cm³) were collected and dialyzed in virion

storage buffer (150 mM NaCl, 15 mM MgCl₂, 10 mM Tris-HCl [pH 7.4]). Concentrations of reovirus virions in purified preparations were determined from an equivalence where an optical density at 260 nm of 1 equaled 2.1 $\times 10^{12}$ virions (64).

Reovirus T3D virions were inactivated using a UV cross-linker (Ultra-lum-UVC-508; Marsh Biomedical, Rochester, NY). Virus at a concentration of 10⁹ PFU per ml was irradiated by using short-wave (254 nm) UV on ice at a distance of 10 cm for 5 min at 1,20,000 μ J/cm² in a 6-cm tissue culture dish (Costar, Cambridge, MA). These conditions are sufficient to reduce viral infectivity to levels that are undetectable by fluorescent focus assays using confluent L929 cell monolayers (data not shown).

Generation and characterization of MAbs 5C6, 9BG5, and 7F4, which are specific for the type 1 $\sigma 1$, type 3 $\sigma 1$, and $\lambda 2$ proteins, respectively, have been previously described (10, 73). The immunoglobulin G (IgG) fractions of polyclonal rabbit antisera raised against T1L and T3D (76) were purified by using protein A-Sepharose as previously described (4). A mixture of these sera was capable of recognizing all strains of reovirus used in this study. Protein A-purified, JAM-A-specific MAb J10.4 was obtained from Charles Parkos (Emory University) (40). Human coxsackievirus and adenovirus receptor (hCAR)-specific MAb RmcB was provided by Jeffrey Bergelson (University of Pennsylvania). Anti-Myc MAb 9E10 and rat anti-Fc MAb were obtained from BD Biosciences (San Jose, CA). Fluorescent dye-conjugated secondary antibodies were obtained from Molecular Probes (Invitrogen).

Generation of CHO cells stably expressing JAM-A or JAM- Δ CT. Human JAM-A was subcloned into expression plasmid pcDNA3.1 (Invitrogen). Truncation mutant JAM- Δ CT was generated by PCR using full-length JAM-A cDNA as template. Sequences encoding amino acids 1 to 260 (Δ 261 to 299) were cloned and appended with a stop codon using T7 primer and 5'-TACGGGATCCTCAGGCAAACCAGATGCC-3' as forward and reverse primers, respectively. The gene-specific primer encompasses nucleotides 981 to 995 of the JAM-A cDNA. The PCR product was digested with BamHI and introduced into pcDNA3.1 using complementary restriction sites. Fidelity of cloning was confirmed by automated sequencing. CHO cells stably expressing empty vector alone, JAM-A, and JAM- Δ CT were generated by transfection of CHO-K1 cells with empty pcDNA3.1 vector, pcDNA3.1 encoding JAM-A, or pcDNA3.1 encoding JAM- Δ CT. Cells were grown to 50% confluence in 6-cm dishes and transfected with 4 μ g of each plasmid by using Lipofectamine Plus reagent (Invitrogen) according to the manufacturer's instructions. Transfected cells were selected by growth in the presence of 1 mg per ml G418. After the 10th passage in the presence of G418, cells expressing high levels of JAM-A as assessed by JAM-A-specific MAb J10.4 staining (mean fluorescence intensity, >5,000) were separated using a BD FACSort cell sorter (Becton-Dickinson, Palo Alto, CA).

Immunoblot for JAM-A. Cell extracts were prepared from CHO cells (1 $\times 10^6$) transfected with empty vector, JAM-A, or JAM- Δ CT by sonication in phosphate-buffered saline (PBS) supplemented to contain protease inhibitor cocktail (Roche, Indianapolis, IN). Extracts were resolved by electrophoresis in 10% polyacrylamide gels and transferred to nitrocellulose membranes. Immunoblots were performed by using JAM-A-specific MAb J10.4 followed by horseradish peroxidase-conjugated goat anti-mouse secondary antibody (Amersham Pharmacia Biotech, Piscataway, NJ), each diluted 1:1,000 in PBS containing 0.1% Tween 20 and 5% low-fat dry milk.

Flow cytometric analysis for JAM-A surface expression. CHO cells stably transfected with empty vector, JAM-A, or JAM- Δ CT were detached from plates using PBS containing 10 mM EDTA. Cells were washed twice with chilled PBS prior to incubation with 10 μ g per ml of either JAM-A specific MAb J10.4 or control MAb (hCAR-specific MAb) at 4°C for 1 h. Cells were stained with a 1:1,000 dilution of phycoerythrin (PE)-labeled anti-mouse IgG at 4°C for 1 h and analyzed using a FACScan flow cytometer (Becton-Dickinson).

Assessment of viral infectivity by indirect immunofluorescence. Monolayers of cells (2 $\times 10^5$) in 24-well plates (Costar) were adsorbed with the indicated multiplicity of infection (MOI) of reovirus at room temperature for 1 h. Following removal of the inoculum, cells were washed with PBS and incubated in complete medium at 37°C for 18 h to permit completion of a single cycle of viral replication. Monolayers were fixed with 1 ml of methanol at -20°C for a minimum of 30 min, washed twice with PBS, blocked with 2.5% Ig-free bovine serum albumin (Sigma-Aldrich, St. Louis, MO) in PBS, and incubated at room temperature for 1 h with polyclonal rabbit anti-reovirus serum at a 1:1,000 dilution in PBS-0.5% Triton X-100. Monolayers were washed twice with PBS-0.5% Triton X-100 and incubated with a 1:1,000 dilution of Alexa546-labeled anti-rabbit IgG. Monolayers were washed with PBS, and infected cells were visualized by indirect immunofluorescence using an Axiovert 200 fluorescence microscope (Carl Zeiss, New York, NY). Infected cells were identified by the presence of intense cytoplasmic fluorescence that was excluded from the nucleus. No back-

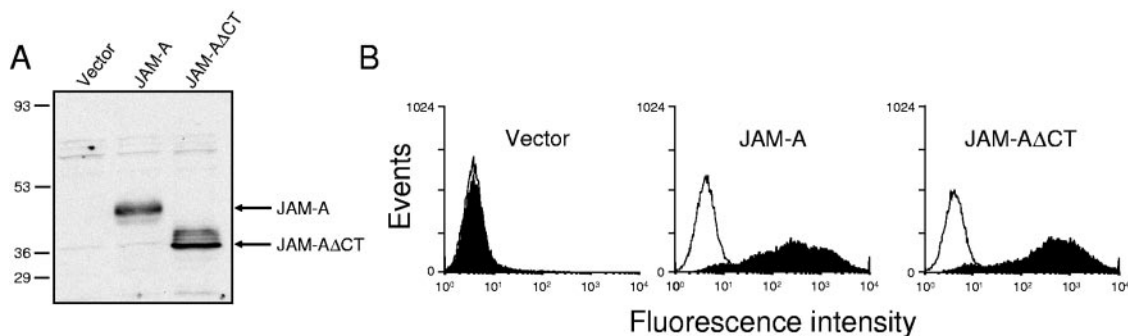


FIG. 1. Stable expression of JAM-A and JAM-A Δ CT in CHO cells. (A) Whole-cell lysates (1×10^5 cell equivalents) were prepared from CHO cells stably transfected with empty vector, JAM-A, or JAM-A Δ CT; resolved by sodium dodecyl sulfate-polyacrylamide gel electrophoresis; transferred to nitrocellulose; and immunoblotted using anti-JAM-A MAb J10.4. The positions of full-length JAM-A and truncated JAM-A Δ CT are shown on the right. The positions of molecular mass standards (in kilodaltons) are shown on the left. (B) Stably transfected CHO cells (1×10^6) were incubated with either anti-JAM MAb J10.4 (filled histograms) or an isotype-matched control (anti-hCAR) MAb (open histograms) at $10 \mu\text{g}$ per ml, followed by incubation with PE-labeled anti-mouse Ig secondary antibody. The results are presented as fluorescence intensity.

ground staining of uninfected control monolayers was noted. Reovirus antigen-positive cells were quantified by counting fluorescent cells in at least three random fields of view in duplicate wells at a primary magnification of $20\times$.

Antibody-mediated infections. Reovirus virions (1×10^{11}) were incubated at 4°C overnight with various concentrations of MAbs in 1 ml PBS. Cells were adsorbed with virus at an MOI of either 100 or 500 PFU per ml at room temperature for 1 h. Following removal of the inoculum, cells were washed with PBS and incubated in complete medium at 37°C for various intervals. For inhibition of viral disassembly and RNA synthesis, cells were maintained in 20 mM AC or 200 μM ribavirin, respectively, throughout the course of infection. For inhibition of disassembly, cells also were pretreated for 1 h with medium containing 20 mM AC.

Quantitation of apoptosis by acridine orange (AO) staining. Cells (2×10^5) grown in 24-well tissue culture plates were adsorbed with reovirus virions or MAb-virion complexes at various MOIs. Following incubation at 37°C for 48 h, the percentage of apoptotic cells was determined by using AO staining as previously described (71). For each experiment, 200 to 300 cells were counted in three independent wells, and the percentage of cells exhibiting condensed chromatin was determined by epi-illumination fluorescence microscopy using a fluorescein filter set (Carl Zeiss).

Antibody-mediated cross-linking of Fc receptors. Cells (2×10^5) were chilled to 4°C and incubated with $1 \mu\text{g}$ per ml of rat anti-Fc MAb 2.4G2 at 4°C for 30 min. Unbound antibody was removed by washing with chilled PBS, and cells were incubated with $5 \mu\text{g}$ per ml of IgM specific for rat IgG at 4°C for 30 min. Following incubation at 37°C for 48 h, cells were scored for apoptosis.

Statistical analysis. Mean values obtained in infectivity and apoptosis assays were compared using the unpaired Student's *t* test as applied with Microsoft Excel software. *P* values of less than 0.05 were considered statistically significant. The contribution of each of the reovirus gene segments to apoptosis induction was assessed by using the nonparametric Mann-Whitney test without adjusting for multiple comparisons and a panel of T1L \times T3D reassortant viruses as previously described (59).

RESULTS

A JAM-A truncation mutant lacking the cytoplasmic tail is expressed at the cell surface. Anti-JAM-A MAb J10.4, which inhibits reovirus binding to JAM-A, also blocks reovirus-induced apoptosis (5). These findings suggest that JAM-A binding is essential for reovirus-induced apoptosis. The JAM-A cytoplasmic tail is approximately 45 amino acids in length, contains 13 potential phosphorylation sites, and interacts with several PDZ domain-containing proteins, suggesting a role in ligand-induced cell signaling (6, 25). To determine whether the cytoplasmic tail of JAM-A contributes to reovirus-induced apoptosis by evoking proapoptotic signaling events, CHO cells were stably transfected with empty vector or vector encoding full-

length JAM-A or a C-terminally truncated form of JAM-A that lacks the cytoplasmic tail (JAM-A Δ CT). CHO cells were selected for these experiments, since they are poorly permissive to reovirus infection (27); yields of reovirus following infection of CHO cells are 100- to 1,000-fold higher following ectopic expression of JAM-A (11, 27). Whole-cell extracts from stably expressing cells were analyzed for expression of JAM-A by immunoblotting (Fig. 1A). While no JAM-A-specific band was detected in the vector-transfected cells, both full-length JAM-A and the faster migrating JAM-A Δ CT proteins were expressed to high levels in the cell lines tested. The surface expression of both JAM-A and JAM-A Δ CT was assessed by flow cytometry using JAM-A-specific MAb J10.4 (Fig. 1B). Both wild-type and mutant JAM-A proteins displayed approximately equivalent surface expression, suggesting that removal of the C-terminal domain of JAM-A does not prevent transport of JAM-A to the cell surface. These stably transfected cells are therefore suitable for analysis of infection and apoptosis induction by reovirus.

Reovirus induces equivalent levels of apoptosis in CHO cells that express JAM-A and JAM-A Δ CT. To determine whether CHO cells stably expressing JAM-A Δ CT can support reovirus infection, cells were adsorbed with reovirus strain T3D at an MOI of 10 PFU per cell, and viral infectivity was assessed by using indirect immunofluorescence (Fig. 2A). CHO cells transfected with either empty vector or those engineered to stably express full-length JAM-A were used as controls. In contrast to vector-transfected cells, cells expressing either JAM-A or JAM-A Δ CT were equivalently capable of supporting infection by T3D. These data indicate that although JAM-A expression is required for efficient infection of CHO cells, the JAM-A cytoplasmic tail is dispensable.

To determine whether the JAM-A cytoplasmic tail is required for apoptosis, stably transfected CHO cell lines were adsorbed with T3D at an MOI of 100 PFU per cell, and apoptosis was assessed by using AO staining (Fig. 2B). None of the cell lines tested showed significant apoptosis following mock infection ($<5\%$). T3D infection of cells transfected with vector alone induced levels of apoptosis equivalent to those following mock infection of cells. In contrast, T3D infection of either the JAM-A- or JAM-A Δ CT-expressing cell lines in-

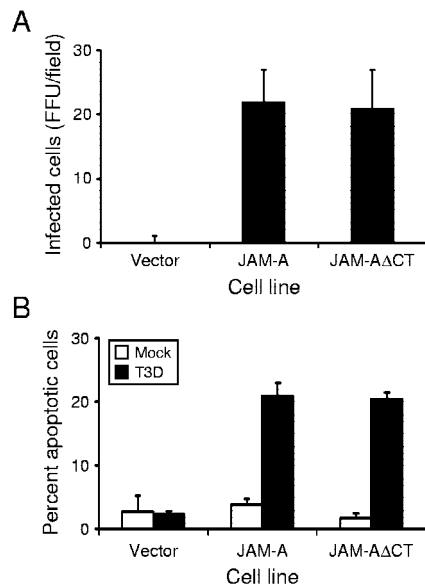


FIG. 2. Infection and apoptosis of JAM-A- and JAM-A Δ CT-expressing CHO cells. (A) Cells were adsorbed with T3D at an MOI of 10 PFU per cell. After incubation at 37°C for 18 h, cells were fixed using methanol. Infected cells were visualized by immunostaining with polyclonal rabbit anti-reovirus sera, followed by incubation with Alexa546-labeled anti-rabbit IgG. Reovirus-infected cells were quantified by counting fluorescent cells. The results are presented as mean fluorescent focus units (FFU) per field. Error bars indicate standard deviations. (B) Cells were adsorbed with either PBS (mock) or T3D at an MOI of 100 PFU per cell. Cells were harvested at 48 h after infection and stained with AO. The results are expressed as the mean percentage of cells undergoing apoptosis for three independent experiments. Error bars indicate standard deviations.

duced an equivalent percentage of cells to undergo apoptosis (~22%). Therefore, analogous to our findings in the infectivity assays, the cytoplasmic tail of JAM-A is not required for reovirus-induced apoptosis.

Antibody-mediated uptake of reovirus into Fc receptor-expressing cells leads to infection and apoptosis. To determine whether the requirement for JAM-A during reovirus infection and apoptosis can be bypassed, we utilized antibody-mediated infection of Fc receptor-expressing CHO (CHO-B1) cells. These cells stably express the B1 isoform of the mouse Fc receptor II (34). Therefore, in the absence of JAM-A, these cells should allow internalization of antibody-reovirus complexes into cells via Fc receptors, resulting in efficient infection of normally nonpermissive cells. For these experiments, T3D virions were incubated with increasing concentrations of σ 1-specific, neutralizing MAb 9BG5 (10) prior to infection of CHO-B1 cells. HeLa cells were used in parallel to confirm the neutralizing efficacy of MAb 9BG5 at the concentrations tested. For each cell line, the number of infected cells was assessed 18 h postinfection by indirect immunofluorescence. As anticipated, the efficiency of reovirus infection of HeLa cells decreased in proportion to antibody concentration, with little infection detected in the presence of 2.5 μ g per ml of 9BG5 (Fig. 3A). We conclude that 9BG5 interferes with σ 1-JAM-A interactions, which are critical for reovirus infection of HeLa cells. In contrast, the efficiency of infection of CHO-B1 cells by T3D increased in proportion to 9BG5 concentration,

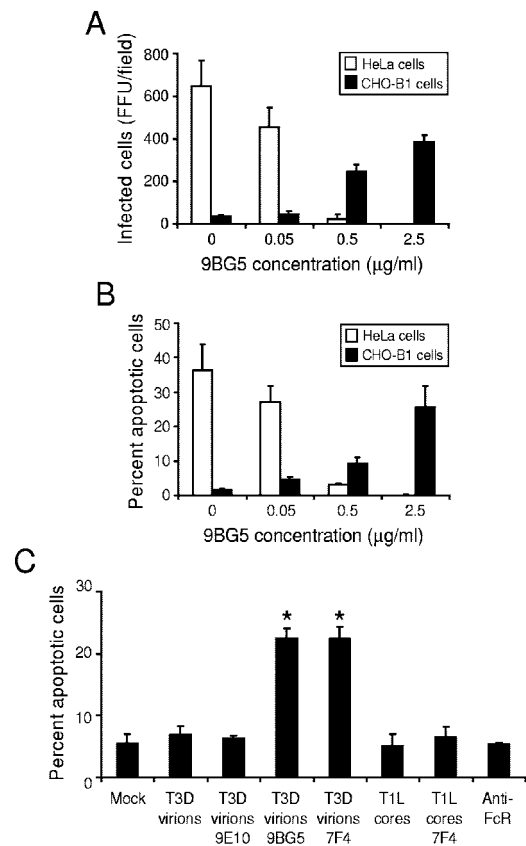


FIG. 3. Infection and apoptosis of HeLa cells and CHO-B1 cells in the presence of MAb 9BG5. (A) Reovirus T3D particles were incubated overnight with the indicated concentration of MAb 9BG5 and adsorbed to either HeLa cells or CHO-B1 cells at an MOI of 100 PFU per cell. After incubation at 37°C for 18 h, cells were fixed using methanol. Infected cells were visualized by immunostaining with polyclonal rabbit anti-reovirus sera, followed by Alexa546-labeled anti-rabbit IgG. Reovirus-infected cells were quantified by counting fluorescent cells. The results are presented as mean fluorescent focus units (FFU) per field. Error bars indicate standard deviations. (B) HeLa cells or CHO-B1 cells were adsorbed with 100 PFU per cell of either virus or virus-antibody complex, harvested at 48 h after infection, and stained with AO. (C) CHO-B1 cells were mock-infected, infected with T3D virions with or without 2.5 μ g per ml of Myc-specific MAb 9E10 (antibody control), σ 1-specific MAb 9BG5, or λ 2-specific MAb 7F4 at an MOI of 100 PFU per cell or were infected with T1L core particles with or without 2.5 μ g per ml of MAb 7F4 at an MOI of 10^4 particles per cell. CHO-B1 cells also were incubated with 1 μ g per ml of anti-Fc receptor rat IgG MAb 2.4G2, followed by incubation with 5 μ g per ml of IgM specific for rat IgG (anti-FcR). Cells were harvested at 48 h after infection and stained with AO. The results are expressed as the mean percentage of cells undergoing apoptosis for three independent experiments. Error bars indicate standard deviations. *, $P < 0.05$ as determined by Student's t test in comparison to T3D incubated with control MAb 9E10.

with maximal infection observed in the presence of a completely neutralizing concentration of 9BG5, 2.5 μ g per ml (Fig. 3A). These findings demonstrate that reovirus infection can be established in a JAM-A-independent manner if an alternative high-affinity binding moiety is provided. These data corroborate a previous report of antibody-mediated enhancement of reovirus infection of a murine macrophage-like cell line (9).

To determine whether infection initiated in a JAM-A-inde-

pendent manner also triggers apoptosis, the capacity of reovirus-9BG5 complexes to induce apoptotic cell death of both HeLa cells and CHO-B1 cells was assessed by using AO staining (Fig. 3B). Approximately 35% of HeLa cells showed apoptotic nuclei at 48 h postinfection in the absence of antibody treatment of virions. Consistent with the decrease in the capacity of reovirus to infect HeLa cells in the presence of 9BG5, the percentage of cells undergoing apoptosis also decreased with increasing 9BG5 concentrations. However, in the absence of 9BG5, T3D induced minimal apoptosis in CHO-B1 cells in comparison to mock-infected cells. In concordance with the infectivity data, the percentage of apoptotic CHO-B1 cells increased with increasing concentrations of 9BG5, with maximal apoptosis seen following pretreatment with 2.5 μ g per ml MAb (~25%). These findings demonstrate that reovirus infection initiated in the absence of JAM-A binding also leads to apoptosis. Therefore, σ 1-JAM-A interactions or signaling pathways induced as a consequence of these interactions are dispensable for apoptosis induction by reovirus.

To exclude the possibility that binding of MAb to the Fc receptor contributes to apoptosis induction, we tested whether incubation of reovirus with irrelevant anti-Myc MAb 9E10 was capable of inducing apoptosis (Fig. 3C). While incubation of T3D with two different MAbs directed against the reovirus outer-capsid, 7F4 (λ 2) and 9BG5 (σ 1), induced 21% and 22% apoptosis, respectively, following infection of CHO-B1 cells, incubation of T3D with MAb 9E10 failed to induce apoptosis at levels higher than those of mock-infected cells. These findings suggest that only antibodies directed against reovirus outer-capsid proteins allow virus attachment to CHO-B1 cells and subsequent induction of apoptosis. To exclude the involvement of signaling induced as a result of Fc receptor cross-linking due to binding of reovirus-antibody complexes, Fc receptors were cross-linked using 2.4G2 (a rat anti-Fc receptor MAb) and an IgM antibody directed against rat IgG. This treatment did not induce apoptosis in CHO-B1 cells in comparison to mock-treated cells. As an additional control for the effect of cross-linking Fc receptors, T1L core particles, which lack outer-capsid proteins σ 1, σ 3, and μ 1, were incubated with MAb 7F4 and added to CHO-B1 cells. Neither untreated cores nor 7F4-core complexes induced apoptosis of these cells. These data suggest that apoptosis does not result from proapoptotic signaling induced as a consequence of Fc-receptor cross-linking but requires binding of reovirus particles containing outer-capsid proteins.

Viral disassembly is required for apoptosis induced by Fc-mediated uptake of reovirus. To determine whether viral disassembly in cellular endosomes is required for apoptosis following Fc-mediated delivery of reovirus, CHO-B1 cells were treated with AC prior to infection by MAb-treated T3D virions. Treatment of cells with 20 mM AC, a concentration sufficient to block reovirus disassembly (66, 77), abolished the capacity of T3D to induce apoptosis (Fig. 4A). Thus, acid-dependent proteolytic disassembly is required for apoptosis induction by this uptake mechanism. To determine whether the apoptosis-inhibitory effect of AC is due to blockade of viral RNA synthesis, we tested ribavirin, an inhibitor of viral RNA synthesis (55), for the capacity to diminish apoptosis. In keeping with our previously published results (18), apoptosis induced by reovirus infection via Fc-mediated uptake was unaf-

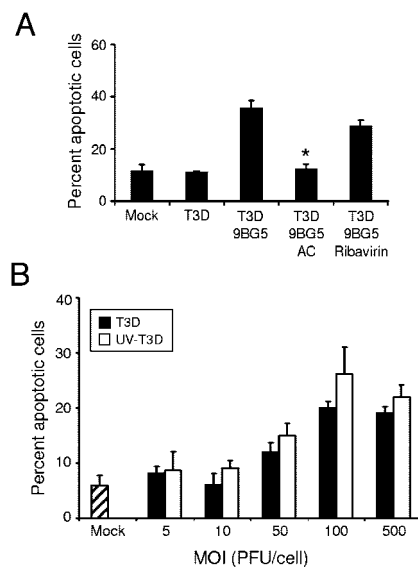


FIG. 4. Apoptosis following Fc receptor-mediated uptake of viable and UV-inactivated reovirus virions. (A) T3D alone or preincubated with 2.5 μ g per ml of MAb 9BG5 was adsorbed to CHO-B1 cells at an MOI of 500 PFU per cell. (B) UV-inactivated T3D preincubated with 2.5 μ g per ml of MAb 9BG5 was adsorbed to CHO-B1 cells at the indicated MOIs. After incubation at 37°C for 48 h in untreated medium or medium containing either 20 mM AC or 200 μ M ribavirin, cells were stained with AO. The results are expressed as the mean percentage of cells undergoing apoptosis for three independent experiments. Error bars indicate standard deviations. *, $P < 0.05$ as determined by Student's *t* test in comparison to T3D incubated with MAb 9BG5.

ected by ribavirin (Fig. 4A). To corroborate these findings, we tested the apoptosis-inducing capacity of UV-inactivated reovirus virions, which are incapable of establishing productive infection (60 and data not shown). We found that UV-inactivated reovirus induced apoptosis following Fc receptor-mediated uptake of a high MOI of virus (Fig. 4B), consistent with our previously published observations (71). Collectively, these results demonstrate that steps in reovirus replication that occur after attachment but before transcription are required for induction of apoptosis, regardless of the type of receptor used to initiate infection (18). In addition, these results suggest that death signaling during reovirus infection may occur independently of receptor engagement.

Fc receptor-dependent infection abolishes σ 1-related differences in the apoptosis-inducing capacity of reovirus. Differences in the capacity of some reovirus strains to induce apoptosis are linked to differences in the affinity for sialic acid (17). To determine whether reovirus strains that are incapable of binding to sialic acid can induce apoptosis when infection is initiated via Fc-dependent uptake, strains T1L and T3SA-, neither of which is capable of binding to sialic acid (4, 16, 23), were incubated with σ 1-specific antibodies and adsorbed to CHO-B1 cells. Incubation of T1L virions with type 1 σ 1-specific MAb 5C6 (73) and incubation of T3SA- virions with type 3 σ 1-specific 9BG5 (10) resulted in significantly higher levels of apoptosis in CHO-B1 cells in comparison to levels observed following infection with untreated T1L and T3SA- virions (Fig. 5). The percentage of cells undergoing apoptosis following antibody-mediated infection of non-sialic-acid-binding

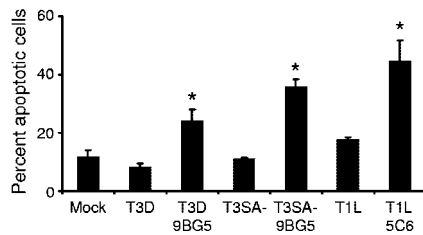


FIG. 5. Apoptosis induction in CHO-B1 cells following Fc-mediated infection by T1L and T3SA-. Cells were adsorbed with T3D, T3SA-, or T1L with or without 2.5 μ g per ml of MAb 9BG5 (for type 3 strains) or MAb 5C6 (for T1L) at an MOI of 100 PFU per cell. After incubation at 37°C for 48 h, cells were harvested and stained with AO. The results are expressed as the mean percentage of cells undergoing apoptosis for three independent experiments. Error bars indicate standard deviations. *, $P < 0.05$ as determined by Student's t test in comparison to the same strain incubated without antibody.

reovirus strains was at least equal to that observed following infection with T3D. Therefore, σ 1-related differences in apoptosis efficiency are overcome when infection is initiated via Fc-mediated uptake. These results make it unlikely that the σ 1 protein is the viral effector of apoptosis induction.

Differences in apoptosis induction following Fc receptor-dependent infection of T1L \times T3D reassortant viruses are linked to the M2 gene segment. We have demonstrated previously that the viral S1 and M2 gene segments segregate with differences in the apoptosis-inducing capacity of T1L and T3D (59, 71). To ascertain whether any strain-specific differences exist when the effect of the S1 gene segment is circumvented by Fc receptor-dependent uptake, CHO-B1 cells were adsorbed with T1L \times T3D reassortant viruses after incubation with σ 1-specific antibodies. Type 1 and type 3 strains were incubated with σ 1-specific MAbs 5C6 and 9BG5, respectively, prior to infection. Each of the reassortant viruses tested produced a similar number of infected cells as assessed by indirect immunofluorescence (data not shown), suggesting equivalent efficiency of antibody-mediated uptake and infection. The percentage of cells undergoing apoptosis as a result of antibody-mediated infection of cells was assessed at 48 h after infection. The reassortant viruses were ranked from highest to lowest by apoptosis-inducing capacity (Table 1). Although the reassortants did not cluster distinctly into two groups with high and low apoptotic potential, six of the seven strains with the highest levels of apoptosis had an M2 gene segment derived from T3D. Conversely, seven of the eight strains with the lowest levels of apoptosis had an M2 gene segment derived from T1L. Analysis of the data using the Mann-Whitney test showed that only the M2 gene segregated at a statistically significant level with the capacity of these strains to induce apoptosis ($P = 0.02$). There was not a statistically significant association between apoptosis and the S1 gene ($P = 0.28$), which is the primary apoptosis determinant following infection of JAM-A-expressing cells (17, 59, 71, 72), when infection was initiated in an Fc-dependent fashion. These data suggest that the M2-encoding μ 1 protein, which functions in penetration of cell membranes (38, 44, 49), is the primary viral determinant of strain-specific differences in apoptosis induction following infection by Fc-mediated uptake.

Reovirus mutant tsA279 is inefficient in apoptosis induction. To determine whether a mutant virus with a defective μ 1

TABLE 1. Apoptosis induction by T1L \times T3D reassortant viruses in CHO-B1 cells

Virus isolate	Origin of gene segments ^a												% Apoptosis ^b	SD
	L1	L2	L3	M1	M2	M3	S1	S2	S3	S4				
Reassortant														
EB138	D	L	L	D	D	L	D	D	L	L	80.5	3.84		
KC150	D	L	L	L	D	L	D	D	L	D	62.8	2.23		
KC9	D	D	L	D	D	D	L	D	D	D	58.6	3.28		
EB97	D	D	L	D	D	D	D	D	D	L	52.3	3.89		
EB68	L	D	L	L	D	L	L	L	D	D	41.2	4.98		
1HA.3	L	L	L	L	L	L	D	L	L	L	40.6	7.15		
EB144	L	L	L	L	D	D	L	L	D	L	38.2	3.99		
EB98	L	D	L	L	L	L	D	L	D	D	32.6	3.17		
EB121	D	D	L	D	L	D	L	D	D	D	28.9	8.13		
EB113	L	L	L	D	L	L	L	L	D	L	26.6	3.85		
G16	L	L	L	D	L	L	L	D	L	L	24.4	3.62		
G2	L	D	L	L	L	L	D	L	L	L	23.1	4.90		
EB143	D	L	L	L	L	L	D	L	L	L	23.0	4.05		
EB145	D	D	D	D	D	L	L	D	D	D	16.2	3.40		
EB120	D	D	D	L	L	D	D	D	L	L	14.5	3.33		
Parental														
T3D	D	D	D	D	D	D	D	D	D	D	23.0	1.81		
T1L	L	L	L	L	L	L	L	L	L	L	33.6	2.34		

^a Parental origin of each gene segment: L, gene segment derived from T1L; D, gene segment derived from T3D.

^b CHO-B1 cells (2×10^5) were adsorbed with virus strains at an MOI of 100 PFU per cell. After 1 h, the inoculum was removed, fresh medium was added, and cells were incubated at 37°C for 48 h and stained with AO to assess apoptosis. Shown are the mean percentage and standard deviations of cells undergoing apoptosis for three independent experiments. The M2 gene was the only gene associated with the efficiency of apoptosis as determined by using the nonparametric Mann-Whitney test, without adjusting for multiple comparisons ($P = 0.02$).

protein is altered in the capacity to trigger apoptosis, we used reovirus strain tsA279.64, which contains a temperature-sensitive mutation that maps to the M2 gene segment (30). This virus was derived from a coinfection of T1L and tsA279, which contains temperature-sensitive mutations in both the M2 and L2 gene segments. The tsA279.64 virus contains the mutant M2 gene segment but not the mutant L2 gene segment, thus facilitating analysis of the contribution of the M2 gene segment to apoptosis induction. When assembled at nonpermissive temperature, virions containing the mutant M2 gene segment cannot penetrate membranes due to a misfolded μ 1 protein (30). To examine whether μ 1-mediated membrane penetration is required for apoptosis induction, HeLa cells were adsorbed with increasing MOIs of tsA279.64 virions assembled under permissive and nonpermissive conditions. The percentage of cells with apoptotic nuclei was assessed by using AO staining 48 h after infection at nonpermissive temperature (Fig. 6). At all MOIs tested, particles assembled at nonpermissive temperature induced less apoptosis than particles assembled at permissive temperature. These data demonstrate that virions containing a μ 1 protein that is inefficient in membrane penetration are less potent inducers of apoptosis, which further highlights a key role for the μ 1 protein in apoptosis induction.

DISCUSSION

We have previously shown that binding of reovirus to JAM-A and sialic acid is required for efficient induction of apoptosis (5, 17). In addition, we have reported that viral disassembly in cel-

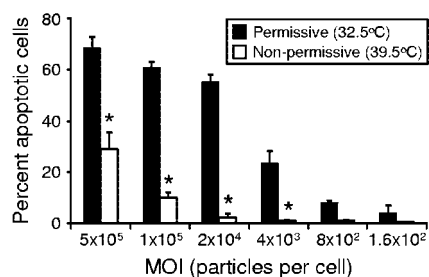


FIG. 6. Apoptosis induced by μ 1 temperature-sensitive mutant *tsA279.64*. HeLa cells were adsorbed with *tsA279.64* grown at permissive or nonpermissive temperatures at the MOIs shown. After incubation at 37°C for 48 h, cells were harvested and stained with AO. The results are expressed as the mean percentage of cells undergoing apoptosis for three independent experiments. Error bars indicate standard deviations. *, $P < 0.05$ as determined by Student's t test in comparison to virions grown at permissive temperature at an equivalent MOI.

lular endosomes is also necessary for apoptosis induction by reovirus (18). However, since receptor binding is a prerequisite for virus disassembly, these findings do not resolve the question of whether reovirus attachment and disassembly provide two distinct signals, both of which are required for apoptosis induction, or whether the viral disassembly events are sufficient for proapoptotic signaling. To address this question, we uncoupled reovirus attachment to JAM-A and sialic acid from viral disassembly by providing an alternative means of viral entry. We report here that antibody-mediated uptake of reovirus into Fc receptor-expressing CHO cells independent of binding to JAM-A and sialic acid leads to productive infection (9) and apoptosis. Furthermore, we demonstrate that antibody-directed binding of reovirus to Fc receptors expressed on CHO cells is not sufficient for reovirus-induced apoptosis. Analogous to JAM-A- and sialic acid-dependent infection, viral replication steps during or after disassembly in endosomes but prior to RNA synthesis also are required for reovirus-induced apoptosis when infection is initiated by Fc-mediated uptake. Analysis of apoptosis induction by T1L \times T3D reassortant viruses following Fc-mediated uptake showed that differences in the efficiency of apoptosis exhibited by type 1 and type 3 strains segregate with the μ 1-encoding M2 gene segment. Neither core particles that lack the μ 1 protein and are therefore incapable of penetrating endosomal membranes nor the thermosensitive M2 mutant virus *tsA279.64*, which contains a misfolded, penetration-defective μ 1 protein, can efficiently induce apoptosis. These findings suggest that reovirus membrane penetration protein μ 1 induces proapoptotic signaling during or after endosomal membrane penetration.

In our reassortant analysis, the viral M2 gene segment was the only viral gene segment that segregated at a statistically significant level with apoptosis-inducing capacity. Although levels of apoptosis induced by reassortant viruses containing a T3D M2 gene segment were generally higher than those induced by reassortant viruses containing a T1L M2 gene segment, the percentage of cells undergoing apoptosis formed a continuum of values rather than two distinct clusters. Since our data suggest that apoptosis is induced during or after endosomal membrane penetration mediated by the μ 1 protein, steps in viral replication preceding membrane penetration, such as

attachment, internalization, and disassembly, also may influence the magnitude of the apoptotic response. Thus, viral gene products that mediate these steps also may contribute to the observed differences in levels of apoptosis. Minor strain-specific effects attributed to other viral gene segments also may explain our finding that antibody-mediated uptake of parental strain T1L into Fc receptor-expressing cells induced higher levels of apoptosis than those induced by T3D (Fig. 5, Table 1). Alternatively, the type 1 and type 3 σ 1-specific MAbs used in our experiments may differ in either affinity for σ 1 or efficiency in internalization via Fc receptors. However, we think that this explanation is unlikely, since no association between the σ 1-encoding S1 gene and apoptosis-inducing potential was observed. Therefore, although it is likely that there are multiple viral genetic determinants of reovirus-induced apoptosis, our statistical analysis of T1L \times T3D reassortant viruses, in addition to our findings using M2 temperature-sensitive mutant *tsA279.64*, lead us to conclude that the M2-encoded μ 1 protein is the primary mediator of proapoptotic signaling.

In addition to the findings here, three independent lines of evidence support a crucial role for μ 1 in reovirus-induced apoptosis. First, differences in apoptosis efficiency displayed by strains T1L and T3D following infection of JAM-A-expressing cells are linked in part to the μ 1-encoding M2 gene (59, 71, 72). Second, studies using pharmacologic inhibitors of reovirus replication place the apoptosis-inducing events subsequent to viral disassembly but prior to RNA synthesis (18), which coincides with μ 1-mediated membrane penetration (12, 38, 44, 49). Third, transient transfection of a plasmid encoding T3D μ 1 is sufficient to induce apoptosis in CHO cells (C. M. Coffey, L. J. Anguish, A. Sheh, I. S. Kim, K. Chandran, M. L. Nibert, and J. S. Parker, Abstr. Am. Soc. Virol. Annu. Meet., abstr. W41-4, 2005). Interestingly, although plasmid-mediated expression of μ 1 neither mimics normal delivery of μ 1 via endosomal rupture during viral membrane penetration nor de novo expression of μ 1 in infected cells (since μ 1 is mostly found associated with its protector protein σ 3 [61, 62, 67]), it leads to the same consequence.

It is not known how the viral disassembly events culminating in μ 1-mediated membrane penetration elicit proapoptotic signaling. We envision two possibilities. First, endosomal disruption by μ 1 may lead to release of hydrolytic enzymes such as cathepsins, which in turn damage mitochondria and stimulate death signaling (22, 29, 58). Interestingly, mitochondrial injury has been reported as early as 4 h following reovirus adsorption (35, 36), suggesting the involvement of an early viral replication event. It is also possible that release of these enzymes causes apoptosis via their action on death regulators such as Bid (65). Of note, Bid cleavage has been observed during reovirus infection and has been hypothesized to play a role in apoptosis induction (35). Second, fragments of μ 1 produced during proteolytic viral disassembly are known to gain access to the cytoplasm (14). These fragments may activate other cellular sensors of viral infection or directly injure mitochondria to induce apoptosis. Concordantly, the μ 1 protein localizes to mitochondria during infection or when expressed from plasmids in transfected cells (C. M. Coffey, L. J. Anguish, A. Sheh, I. S. Kim, K. Chandran, M. L. Nibert, and J. S. Parker, Abstr. Am. Soc. Virol. Annu. Meet., abstr. W41-4, 2005), suggesting a postendosomal site of action. Interestingly, a 30-residue C-termi-

nal fragment of $\mu 1$ is sufficient to localize to mitochondria and induce apoptosis (C. M. Coffey, L. J. Anguish, A. Sheh, I. S. Kim, K. Chandran, M. L. Nibert, and J. S. Parker, Abstr. Am. Soc. Virol. Annu. Meet., abstr. W41-4, 2005).

Although our findings point to $\mu 1$ as a key viral regulator of proapoptotic signaling, this work does not explain the previously established unequivocal association between the S1-encoded $\sigma 1$ protein and the efficiency of apoptosis induction by reovirus (59, 71, 72). Strains encoding a $\sigma 1$ protein capable of binding to JAM-A and sialic acid are the most potent inducers of apoptosis (17). We did not observe efficient infection of CHO-B1 cells in the absence of MAb pretreatment at the MOIs used. Therefore, we think that these cells do not express sufficient quantities of sialic acid or JAM-A on the cell surface to effect productive infection. Thus, infection of these cells appears to be dependent only on the presence of a high-affinity receptor such as the Fc receptor. Since the efficiency of antibody-mediated uptake and delivery of both sialic-acid-binding and non-sialic-acid-binding strains of reovirus via Fc receptors is essentially equivalent in CHO-B1 cells, $\sigma 1$ -related differences are negated. An alternative explanation for our findings is that antibody-mediated attachment of virions to Fc receptors stimulates a signaling cascade in cells that mimics signaling induced as a consequence of $\sigma 1$ binding to JAM-A and sialic acid and that Fc receptor-mediated signaling acts in concert with the viral disassembly events to elicit apoptosis. However, given the marked differences in functional properties displayed by JAM-A and Fc receptors, this explanation seems less likely. Therefore, our current and previous studies suggest that the linkage of $\sigma 1$ to apoptosis efficiency is not related to $\sigma 1$ -mediated stimulation of the cellular proapoptotic machinery but rather the capacity of $\sigma 1$ to efficiently deliver virions into endosomes for disassembly. We hypothesize that, as opposed to viral infection, which requires penetration by just one infectious virion, efficient apoptosis induction by reovirus requires endosomal penetration by multiple virions. Since sialic acid allows more avid binding of virions to cells (4), we think that this entry route may deliver virions more efficiently into endosomal compartments for uncoating and subsequent membrane penetration, leading to higher levels of apoptosis (17).

This study highlights a new role for the viral membrane penetration protein $\mu 1$ in apoptosis induction. Other viruses, such as coronavirus, Sindbis virus, and vaccinia virus, also have been reported to require postattachment cell entry events in endosomes to induce apoptosis (33, 39, 54). However, the viral determinants of apoptosis by these viruses are unknown. Interestingly, entry of Sindbis virus into endosomes induces apoptosis through activation of sphingomyelinases and release of the proapoptotic second messenger, ceramide (32). Although we anticipate that interactions between the enveloped Sindbis virus with endosomes differ from those with $\mu 1$, it is possible that a lipid second messenger also plays a role in reovirus-induced apoptosis. Collectively, these studies point to cellular endosomes as sites from which proapoptotic signaling events are initiated and imply a conserved mechanism by which host cells detect the presence of invading pathogens. Pathogen detection during the entry phase may allow host cells to more efficiently limit the spread of infection by initiating cell death. Alternatively, induction of apoptosis by a virus early in its replication cycle may prevent or attenuate the development of

an inflammatory response, thereby allowing the virus to better evade host defenses. A fascinating similarity exists between the properties of reovirus protein $\mu 1$ and several toxins elaborated by bacteria and viruses. Analogous to the capacity of $\mu 1$ to mediate membrane permeabilization (12, 31, 41, 69), α toxin of *Staphylococcus aureus*, lysteriolysin O of *Listeria monocytogenes*, and killer toxins (K1 and K2) of the yeast L-A virus also can form pores in host cell membranes (42, 68, 75, 78). Interestingly, each of these toxins also has the capacity to induce apoptotic cell death (56, 75). Our ongoing studies are focused on understanding the precise mechanism by which $\mu 1$ induces apoptosis during reovirus infection. Through these studies we hope to gain broader insight into events at the pathogen-host interface that evoke death signaling and cause disease.

ACKNOWLEDGMENTS

We thank John Parker and members of our laboratory for many helpful discussions and Jim Chappell, Geoff Holm, and Denise Wetzel for careful review of the manuscript. We are grateful to the Nashville Veterans Affairs Hospital Flow Cytometry Facility for assistance and data analysis.

This research was supported by Public Health Service awards T32 CA09385 (J.A.C. and J.C.F.) and R01 AI50080 and the Elizabeth B. Lamb Center for Pediatric Research. Additional support was provided by Public Health Service awards CA68485 for the Vanderbilt-Ingram Cancer Center and DK20593 for the Vanderbilt Diabetes Research and Training Center.

REFERENCES

1. Armstrong, G. D., R. W. Paul, and P. W. Lee. 1984. Studies on reovirus receptors of L cells: virus binding characteristics and comparison with reovirus receptors of erythrocytes. *Virology* **138**:37–48.
2. Baer, G. S., D. H. Ebert, C. J. Chung, A. H. Erickson, and T. S. Dermody. 1999. Mutant cells selected during persistent reovirus infection do not express mature cathepsin L and do not support reovirus disassembly. *J. Virol.* **73**:9532–9543.
3. Barrett, A. J., A. A. Kembhavi, M. A. Brown, H. Kirschke, C. G. Knight, M. Tamai, and K. Hanada. 1982. L-trans-epoxysuccinyl-leucylamido(4-guanidino) butane (E-64) and its analogues as inhibitors of cysteine proteinases including cathepsins B, H and L. *Biochem. J.* **201**:189–198.
4. Barton, E. S., J. L. Connolly, J. C. Forrest, J. D. Chappell, and T. S. Dermody. 2001. Utilization of sialic acid as a coreceptor enhances reovirus attachment by multistep adhesion strengthening. *J. Biol. Chem.* **276**:2200–2211.
5. Barton, E. S., J. C. Forrest, J. L. Connolly, J. D. Chappell, Y. Liu, F. Schnell, A. Nusrat, C. A. Parkos, and T. S. Dermody. 2001. Junction adhesion molecule is a receptor for reovirus. *Cell* **104**:441–451.
6. Bazzoni, G., O. M. Martinez-Estrada, F. Orsenigo, M. Cordenonsi, S. Citi, and E. Dejana. 2000. Interaction of junctional adhesion molecule with the tight junction components ZO-1, cingulin, and occludin. *J. Biol. Chem.* **275**:20520–20526.
7. Borsa, J., B. D. Morash, M. D. Sargent, T. P. Copps, P. A. Lievaart, and J. G. Szekely. 1979. Two modes of entry of reovirus particles into L cells. *J. Gen. Virol.* **45**:161–170.
8. Borsa, J., M. D. Sargent, P. A. Lievaart, and T. P. Copps. 1981. Reovirus: evidence for a second step in the intracellular uncoating and transcriptase activation process. *Virology* **111**:191–200.
9. Burstin, S. J., M. W. Brandriss, and J. J. Schlesinger. 1983. Infection of a macrophage-like cell line, P388D1 with reovirus; effects of immune ascitic fluids and monoclonal antibodies on neutralization and on enhancement of viral growth. *J. Immunol.* **130**:2915–2919.
10. Burstin, S. J., D. R. Spriggs, and B. N. Fields. 1982. Evidence for functional domains on the reovirus type 3 hemagglutinin. *Virology* **117**:146–155.
11. Campbell, J. A., P. Schelling, J. D. Wetzel, E. M. Johnson, J. C. Forrest, G. A. Wilson, M. Aurrand-Lions, B. A. Imhof, T. Stehle, and T. S. Dermody. 2005. Junctional adhesion molecule-A serves as a receptor for prototype and field-isolate strains of mammalian reovirus. *J. Virol.* **79**:7967–7978.
12. Chandran, K., D. L. Faretta, and M. L. Nibert. 2002. Strategy for nonenveloped virus entry: a hydrophobic conformer of the reovirus membrane penetration protein $\mu 1$ mediates membrane disruption. *J. Virol.* **76**:9920–9933.
13. Chandran, K., and M. L. Nibert. 2003. Animal cell invasion by a large nonenveloped virus: reovirus delivers the goods. *Trends Microbiol.* **11**:374–382.

14. Chandran, K., J. S. Parker, M. Ehrlich, T. Kirchhausen, and M. L. Nibert. 2003. The delta region of outer-capsid protein μ 1 undergoes conformational change and release from reovirus particles during cell entry. *J. Virol.* **77**:13361–13375.
15. Chang, C. T., and H. J. Zweerink. 1971. Fate of parental reovirus in infected cell. *Virology* **46**:544–555.
16. Chappell, J. D., J. L. Duong, B. W. Wright, and T. S. Dermody. 2000. Identification of carbohydrate-binding domains in the attachment proteins of type 1 and type 3 reoviruses. *J. Virol.* **74**:8472–8479.
17. Connolly, J. L., E. S. Barton, and T. S. Dermody. 2001. Reovirus binding to cell surface sialic acid potentiates virus-induced apoptosis. *J. Virol.* **75**:4029–4039.
18. Connolly, J. L., and T. S. Dermody. 2002. Virion disassembly is required for apoptosis induced by reovirus. *J. Virol.* **76**:1632–1641.
19. Connolly, J. L., S. E. Rodgers, P. Clarke, D. W. Ballard, L. D. Kerr, K. L. Tyler, and T. S. Dermody. 2000. Reovirus-induced apoptosis requires activation of transcription factor NF- κ B. *J. Virol.* **74**:2981–2989.
20. DeBiasi, R., C. Edelstein, B. Sherry, and K. Tyler. 2001. Calpain inhibition protects against virus-induced apoptotic myocardial injury. *J. Virol.* **75**:351–361.
21. DeBiasi, R. L., B. A. Robinson, B. Sherry, R. Bouchard, R. D. Brown, M. Rizeq, C. Long, and K. L. Tyler. 2004. Caspase inhibition protects against reovirus-induced myocardial injury in vitro and in vivo. *J. Virol.* **78**:11040–11050.
22. Deiss, L. P., H. Galinka, H. Berissi, O. Cohen, and A. Kimchi. 1996. Cathepsin D protease mediates programmed cell death induced by interferon-gamma, Fas/APO-1 and TNF-alpha. *EMBO J.* **15**:3861–3870.
23. Dermody, T. S., M. L. Nibert, R. Bassel-Duby, and B. N. Fields. 1990. A σ 1 region important for hemagglutination by serotype 3 reovirus strains. *J. Virol.* **64**:5173–5176.
24. Ebert, D. H., J. Deussing, C. Peters, and T. S. Dermody. 2002. Cathepsin L and cathepsin B mediate reovirus disassembly in murine fibroblast cells. *J. Biol. Chem.* **277**:24609–24617.
25. Ebnat, K., C. U. Schulz, M. K. Meyer Zu Brickwedde, G. G. Pendl, and D. Vestweber. 2000. Junctional adhesion molecule interacts with the PDZ domain-containing proteins AF-6 and ZO-1. *J. Biol. Chem.* **275**:27979–27988.
26. Ehrlich, M., W. Boll, A. Van Oijen, R. Hariharan, K. Chandran, M. L. Nibert, and T. Kirchhausen. 2004. Endocytosis by random initiation and stabilization of clathrin-coated pits. *Cell* **118**:591–605.
27. Forrest, J. C., J. A. Campbell, P. Schelling, T. Stehle, and T. S. Dermody. 2003. Structure-function analysis of reovirus binding to junctional adhesion molecule 1. Implications for the mechanism of reovirus attachment. *J. Biol. Chem.* **278**:48434–48444.
28. Furlong, D. B., M. L. Nibert, and B. N. Fields. 1988. Sigma 1 protein of mammalian reoviruses extends from the surfaces of viral particles. *J. Virol.* **62**:246–256.
29. Guicciardi, M. E., J. Deussing, H. Miyoshi, S. F. Bronk, P. A. Svingen, C. Peters, S. H. Kaufmann, and G. J. Gores. 2000. Cathepsin B contributes to TNF-alpha-mediated hepatocyte apoptosis by promoting mitochondrial release of cytochrome c. *J. Clin. Investig.* **106**:1127–1137.
30. Hazelton, P. R., and K. M. Coombs. 1995. The reovirus mutant tsA279 has temperature-sensitive lesions in the M2 and L2 genes: the M2 gene is associated with decreased viral protein production and blockade in trans-membrane transport. *Virology* **207**:46–58.
31. Hooper, J. W., and B. N. Fields. 1996. Role of the μ 1 protein in reovirus stability and capacity to cause chromium release from host cells. *J. Virol.* **70**:459–467.
32. Jan, J. T., S. Chatterjee, and D. E. Griffin. 2000. Sindbis virus entry into cells triggers apoptosis by activating sphingomyelinase, leading to the release of ceramide. *J. Virol.* **74**:6425–6432.
33. Jan, J. T., and D. E. Griffin. 1999. Induction of apoptosis by Sindbis virus occurs at cell entry and does not require viral replication. *J. Virol.* **73**:10296–10302.
34. Joiner, K. A., S. A. Fuhrman, H. M. Miettinen, L. H. Kasper, and I. Mellman. 1990. Toxoplasma gondii: fusion competence of parasitophorous vacuoles in Fc receptor-transfected fibroblasts. *Science* **249**:641–646.
35. Kominsky, D. J., R. J. Bickel, and K. L. Tyler. 2002. Reovirus-induced apoptosis requires both death receptor- and mitochondrial-mediated caspase-dependent pathways of cell death. *Cell Death Differ.* **9**:926–933.
36. Kominsky, D. J., R. J. Bickel, and K. L. Tyler. 2002. Reovirus-induced apoptosis requires mitochondrial release of Smac/DIABLO and involves reduction of cellular inhibitor of apoptosis protein levels. *J. Virol.* **76**:11414–11424.
37. Lee, P. W., E. C. Hayes, and W. K. Joklik. 1981. Protein σ 1 is the reovirus cell attachment protein. *Virology* **108**:156–163.
38. Liemann, S., K. Chandran, T. S. Baker, M. L. Nibert, and S. C. Harrison. 2002. Structure of the reovirus membrane-penetration protein, μ 1, in a complex with its protector protein, σ 3. *Cell* **108**:283–295.
39. Liu, Y., Y. Cai, and X. Zhang. 2003. Induction of caspase-dependent apoptosis in cultured rat oligodendrocytes by murine coronavirus is mediated during cell entry and does not require virus replication. *J. Virol.* **77**:11952–11963.
40. Liu, Y., A. Nusrat, F. J. Schnell, T. A. Reaves, S. Walsh, M. Ponchet, and C. A. Parkos. 2000. Human junction adhesion molecule regulates tight junction resealing in epithelia. *J. Cell Sci.* **113**:2363–2374.
41. Lucia-Jandris, P., J. W. Hooper, and B. N. Fields. 1993. Reovirus M2 gene is associated with chromium release from mouse L cells. *J. Virol.* **67**:5339–5345.
42. Martinac, B., H. Zhu, A. Kubalski, X. L. Zhou, M. Culbertson, H. Bussey, and C. Kung. 1990. Yeast K1 killer toxin forms ion channels in sensitive yeast spheroplasts and in artificial liposomes. *Proc. Natl. Acad. Sci. USA* **87**:6228–6232.
43. Maxfield, F. R. 1982. Weak bases and ionophores rapidly and reversibly raise the pH in endocytic vesicles in cultured mouse fibroblasts. *J. Cell Biol.* **95**:676–681.
44. Nibert, M. L., and B. N. Fields. 1992. A carboxy-terminal fragment of protein μ 1/ μ 1C is present in infectious subviral particles of mammalian reoviruses and is proposed to have a role in penetration. *J. Virol.* **66**:6408–6418.
45. Nibert, M. L., A. L. Odegard, M. A. Agosto, K. Chandran, and L. A. Schiff. 2005. Putative autocleavage of reovirus μ 1 protein in concert with outer-capsid disassembly and activation for membrane permeabilization. *J. Mol. Biol.* **345**:461–474.
46. Nibert, M. L., and L. A. Schiff. 2001. Reoviruses and their replication, p. 1679–1728. *In* D. M. Knipe and P. M. Howley (ed.), *Fields Virology*, 4th ed. Lippincott Williams & Wilkins, Philadelphia, Pa.
47. Nibert, M. L., L. A. Schiff, and B. N. Fields. 1991. Mammalian reoviruses contain a myristoylated structural protein. *J. Virol.* **65**:1960–1967.
48. Oberhaus, S. M., R. L. Smith, G. H. Clayton, T. S. Dermody, and K. L. Tyler. 1997. Reovirus infection and tissue injury in the mouse central nervous system are associated with apoptosis. *J. Virol.* **71**:2100–2106.
49. Odegard, A. L., K. Chandran, X. Zhang, J. S. Parker, T. S. Baker, and M. L. Nibert. 2004. Putative autocleavage of outer capsid protein μ 1, allowing release of myristoylated peptide μ 1N during particle uncoating, is critical for cell entry by reovirus. *J. Virol.* **78**:8732–8745.
50. O'Donnell, S. M., M. W. Hansberger, J. L. Connolly, J. D. Chappell, M. J. Watson, J. M. Pierce, J. D. Wetzel, W. Han, E. S. Barton, J. C. Forrest, T. Valyi-Nagy, F. E. Yull, T. S. Blackwell, J. N. Rottman, B. Sherry, and T. S. Dermody. 2005. Organ-specific roles for transcription factor NF- κ B in reovirus-induced apoptosis and disease. *J. Clin. Investig.* **115**:2341–2350.
51. Paul, R. W., A. H. Choi, and P. W. K. Lee. 1989. The α -anomeric form of sialic acid is the minimal receptor determinant recognized by reovirus. *Virology* **172**:382–385.
52. Paul, R. W., and P. W. K. Lee. 1987. Glycophorin is the reovirus receptor on human erythrocytes. *Virology* **159**:94–101.
53. Protá, A. E., J. A. Campbell, P. Schelling, J. C. Forrest, T. R. Peters, M. J. Watson, M. Aurrand-Lions, B. Imhof, T. S. Dermody, and T. Stehle. 2003. Crystal structure of human junctional adhesion molecule 1: implications for reovirus binding. *Proc. Natl. Acad. Sci. USA* **100**:5366–5371.
54. Ramsey-Ewing, A., and B. Moss. 1998. Apoptosis induced by a postbinding step of vaccinia virus entry into Chinese hamster ovary cells. *Virology* **242**:138–149.
55. Rankin, U. T., Jr., S. B. Eppes, J. B. Antczak, and W. K. Joklik. 1989. Studies on the mechanism of the antiviral activity of ribavirin against reovirus. *Virology* **168**:147–158.
56. Reiter, J., E. Herker, F. Madeo, and M. J. Schmitt. 2005. Viral killer toxins induce caspase-mediated apoptosis in yeast. *J. Cell Biol.* **168**:353–358.
57. Richardson-Burns, S. M., D. J. Kominsky, and K. L. Tyler. 2002. Reovirus-induced neuronal apoptosis is mediated by caspase 3 and is associated with the activation of death receptors. *J. Neurovirol.* **8**:365–380.
58. Roberg, K. 2001. Relocalization of cathepsin D and cytochrome c early in apoptosis revealed by immunoelectron microscopy. *Lab. Investig.* **81**:149–158.
59. Rodgers, S. E., E. S. Barton, S. M. Oberhaus, B. Pike, C. A. Gibson, K. L. Tyler, and T. S. Dermody. 1997. Reovirus-induced apoptosis of MDCK cells is not linked to viral yield and is blocked by Bcl-2. *J. Virol.* **71**:2540–2546.
60. Shaw, J. E., and D. C. Cox. 1973. Early inhibition of cellular DNA synthesis by high multiplicities of infectious and UV-irradiated reovirus. *J. Virol.* **12**:704–710.
61. Shepard, D. A., J. G. Ehnstrom, and L. A. Schiff. 1995. Association of reovirus outer capsid proteins σ 3 and μ 1 causes a conformational change that renders σ 3 protease sensitive. *J. Virol.* **69**:8180–8184.
62. Shepard, D. A., J. G. Ehnstrom, P. J. Skinner, and L. A. Schiff. 1996. Mutations in the zinc-binding motif of the reovirus capsid protein σ 3 eliminate its ability to associate with capsid protein μ 1. *J. Virol.* **70**:2065–2068.
63. Silverstein, S. C., C. Astell, D. H. Levin, M. Schonberg, and G. Acs. 1972. The mechanism of reovirus uncoating and gene activation *in vivo*. *Virology* **47**:797–806.
64. Smith, R. E., H. J. Zweerink, and W. K. Joklik. 1969. Polypeptide components of virions, top component and cores of reovirus type 3. *Virology* **39**:791–810.
65. Stoka, V., B. Turk, S. L. Schendel, T. H. Kim, T. Cirman, S. J. Snipas, L. M. Ellerby, D. Bredezen, H. Freeze, M. Abrahamson, D. Bromme, S. Krajewski, J. C. Reed, X. M. Yin, V. Turk, and G. S. Salvesen. 2001. Lysosomal protease

- pathways to apoptosis. Cleavage of bid, not pro-caspases, is the most likely route. *J. Biol. Chem.* **276**:3149–3157.
66. **Sturzenbecker, L. J., M. L. Nibert, D. B. Furlong, and B. N. Fields.** 1987. Intracellular digestion of reovirus particles requires a low pH and is an essential step in the viral infectious cycle. *J. Virol.* **61**:2351–2361.
 67. **Tillotson, L., and A. J. Shatkin.** 1992. Reovirus polypeptide $\sigma 3$ and N-terminal myristoylation of polypeptide $\mu 1$ are required for site-specific cleavage to $\mu 1C$ in transfected cells. *J. Virol.* **66**:2180–2186.
 68. **Tipper, D. J., and M. J. Schmitt.** 1991. Yeast dsRNA viruses: replication and killer phenotypes. *Mol. Microbiol.* **5**:2331–2338.
 69. **Tosteson, M. T., M. L. Nibert, and B. N. Fields.** 1993. Ion channels induced in lipid bilayers by subviral particles of the nonenveloped mammalian reoviruses. *Proc. Natl. Acad. Sci. USA* **90**:10549–10552.
 70. **Tyler, K. L.** 2001. Mammalian reoviruses, p. 1729–1745. *In* D. M. Knipe and P. M. Howley (ed.), *Fields Virology*, 4th ed. Lippincott Williams & Wilkins, Philadelphia, Pa.
 71. **Tyler, K. L., M. K. Squier, S. E. Rodgers, S. E. Schneider, S. M. Oberhaus, T. A. Grdina, J. J. Cohen, and T. S. Dermody.** 1995. Differences in the capacity of reovirus strains to induce apoptosis are determined by the viral attachment protein $\sigma 1$. *J. Virol.* **69**:6972–6979.
 72. **Tyler, K. L., M. K. T. Squier, A. L. Brown, B. Pike, D. Willis, S. M. Oberhaus, T. S. Dermody, and J. J. Cohen.** 1996. Linkage between reovirus-induced apoptosis and inhibition of cellular DNA synthesis: role of the S1 and M2 genes. *J. Virol.* **70**:7984–7991.
 73. **Virgin, H. W., IV, M. A. Mann, B. N. Fields, and K. L. Tyler.** 1991. Monoclonal antibodies to reovirus reveal structure/function relationships between capsid proteins and genetics of susceptibility to antibody action. *J. Virol.* **65**:6772–6781.
 74. **Weiner, H. L., K. A. Ault, and B. N. Fields.** 1980. Interaction of reovirus with cell surface receptors. I. Murine and human lymphocytes have a receptor for the hemagglutinin of reovirus type 3. *J. Immunol.* **124**:2143–2148.
 75. **Weinrauch, Y., and A. Zychlinsky.** 1999. The induction of apoptosis by bacterial pathogens. *Annu. Rev. Microbiol.* **53**:155–187.
 76. **Wetzel, J. D., J. D. Chappell, A. B. Fogo, and T. S. Dermody.** 1997. Efficiency of viral entry determines the capacity of murine erythroleukemia cells to support persistent infections by mammalian reoviruses. *J. Virol.* **71**:299–306.
 77. **Wetzel, J. D., G. J. Wilson, G. S. Baer, L. R. Dunnigan, J. P. Wright, D. S. H. Tang, and T. S. Dermody.** 1997. Reovirus variants selected during persistent infections of L cells contain mutations in the viral S1 and S4 genes and are altered in viral disassembly. *J. Virol.* **71**:1362–1369.
 78. **Wickner, R. B.** 1996. Double-stranded RNA viruses of *Saccharomyces cerevisiae*. *Microbiol. Rev.* **60**:250–265.

APPENDIX B

I κ B KINASE SUBUNITS α AND γ ARE REQUIRED FOR ACTIVATION OF NF- κ B
AND INDUCTION OF APOPTOSIS BY MAMMALIAN REOVIRUS

Mark W. Hansberger, Jacquelyn A. Campbell, Pranav Danthi, Pia Arrate, Kevin N.
Pennington, Kenneth B. Marcu, Dean W. Ballard, and Terence S. Dermody

Journal of Virology. Accepted with revisions.

I κ B Kinase Subunits α and γ Are Required for Activation of NF- κ B and Induction of Apoptosis by Mammalian Reovirus

5

Mark W. Hansberger,^{1,2} Jacquelyn A. Campbell,^{1,2} Pranav Danthi,^{2,3} Pia Arrate,¹ Kevin N. Pennington,¹ Kenneth B. Marcu,^{4,5,6} Dean W. Ballard,¹ and Terence S. Dermody^{1,2,3*}

10

Departments of Microbiology and Immunology¹ and Pediatrics³ and Elizabeth B Lamb Center for Pediatric Research,² Vanderbilt University School of Medicine, Nashville, Tennessee 37232 and Departments of Biochemistry and Cell Biology⁴ and Microbiology⁵ and Institute for Cell and Developmental Biology,⁶ State University of New York at Stony Brook, Stony Brook, New York 11794

15

*Corresponding author. Mailing address: Lamb Center for Pediatric Research, D7235 MCN, Vanderbilt University School of Medicine, Nashville, TN 37232. Phone: (615) 343-9943. Fax: (615) 343-9723. E-mail: terry.dermody@vanderbilt.edu.

20

Running title: IKK activation and reovirus apoptosis

25

30

35

40

45

ABSTRACT

Reoviruses induce apoptosis both in cultured cells and in vivo. Apoptosis plays a major role in the pathogenesis of reovirus encephalitis and myocarditis in infected animals. Reovirus-induced apoptosis is dependent on activation of transcription factor NF- κ B and downstream cellular genes. To better understand the mechanism of NF- κ B activation by reovirus, NF- κ B signaling intermediates under reovirus control were investigated at the level of Rel, I κ B, and I κ B kinase (IKK) proteins. We found that reovirus infection leads initially to nuclear translocation of p50 and RelA, followed by delayed mobilization of c-Rel and p52. This biphasic pattern of Rel protein activation is associated with degradation of the NF- κ B inhibitor I κ B α , but not the structurally-related inhibitors I κ B β or I κ B ϵ . Using cells deficient in individual IKK subunits, we demonstrate that IKK α but not IKK β is required for reovirus-induced NF- κ B activation and apoptosis. Despite the preferential usage of IKK α , both NF- κ B activation and apoptosis were attenuated in cells lacking IKK γ /Nemo, an essential regulatory subunit of IKK β . Moreover, deletion of the gene encoding NF- κ B-inducing kinase (NIK), which is known to modulate IKK α function, had no inhibitory effect on either response in reovirus-infected cells. Collectively, these findings indicate a novel pathway of NF- κ B/Rel activation involving IKK α and IKK γ /Nemo, which together mediate the expression of downstream proapoptotic genes in reovirus-infected cells.

70

75

80

85

90

INTRODUCTION

95 Mammalian reoviruses are nonenveloped viruses that contain a genome of 10
segments of double-stranded RNA (43). Following infection of newborn mice, reovirus
disseminates systemically, causing injury to the central nervous system (CNS), heart, and
liver (65). Apoptosis induced by reovirus appears to be the primary mechanism for virus-
induced encephalitis (44, 45, 48) and myocarditis (19, 20, 45). Disassembly of
100 internalized virus in the endocytic pathway provides the viral trigger for stimulating the
signaling pathways that elicit an apoptotic response (16, 18).

Transcription factor NF- κ B plays an important regulatory role in apoptosis
evoked by reovirus in cultured cells (17) and in vivo (45). Inducible members of the NF-
 κ B family are sequestered in the cytoplasm by inhibitory I κ B proteins, including I κ B α ,
105 I κ B β , I κ B ϵ , and p100 (2, 28, 57, 68, 71). In response to a wide variety of NF- κ B
inducers, I κ B proteins are phosphorylated at specific serine residues, earmarking these
molecules for destruction by the ubiquitin-proteasome pathway (6, 10, 28, 46, 64, 71).
Phosphorylation of I κ B proteins is mediated by cytokine-inducible I κ B kinases (IKKs)
IKK α and IKK β (39, 67), which can form higher order complexes containing a
110 regulatory subunit called IKK γ /Nemo (23, 41, 51, 75, 78). A primary function of IKK β is
to modulate the inhibitory interaction of I κ B α with the prototypical form of NF- κ B
containing p50/RelA dimers (22, 23, 41, 47, 58). This regulatory circuit, termed the
classical pathway of NF- κ B activation, is strictly dependent on the presence of
IKK γ /Nemo (53, 54, 75). In sharp contrast, IKK α functions in an alternative IKK γ -
115 independent pathway of NF- κ B activation that leads to proteolytic processing of
p100/NF- κ B2 and production of a fully functional p52 Rel subunit (13, 55, 60). Unlike
the classical, IKK β -directed pathway of NF- κ B activation, the alternative pathway
involving IKK α is dependent on prior phosphorylation of this IKK by NF- κ B-inducing
kinase (NIK) (36, 55, 73).

120 To better understand the mechanism of NF- κ B activation by reovirus, we
conducted experiments to define the NF- κ B/Rel, I κ B, and IKK proteins that are under
reovirus control. These studies revealed that NF- κ B/Rel proteins are mobilized to the
nuclear compartment with biphasic kinetics following reovirus infection. Reovirus-
125 induced activation of NF- κ B/Rel proteins is accompanied by selective degradation of
I κ B α , suggesting a role for IKK β . However, subsequent studies with IKK subunit-
deficient cells clearly demonstrate that IKK α rather than IKK β plays an essential role in
the mechanism by which reovirus activates NF- κ B and downstream apoptotic genes. We
also assembled evidence indicating that the reovirus/IKK α axis is intact in cells lacking
130 NIK, an upstream activator of IKK α , but not in cells lacking the IKK β regulatory subunit
IKK γ /Nemo. Taken together, these data suggest that reovirus activates the IKK α pathway
of the NF- κ B signaling apparatus downstream of NIK, perhaps via direct interactions
with the regulatory subunit IKK γ /Nemo.

135

MATERIALS AND METHODS

140

Cells, viruses, and reagents. HeLa cells, 293T cells, and murine embryo fibroblasts (MEFs) were maintained in DMEM containing 10% fetal bovine serum (FBS), 2 mM L-glutamine, 100 U/ml of penicillin, 100 µg/ml streptomycin, and 25 ng/ml of amphotericin B (Invitrogen, Carlsbad, CA). MEFs deficient in IKK α (29, 33), IKK β (34, 61), IKK γ (53), and NIK (76) have been described previously.

145

Reovirus type 3 Dearing (T3D) is a laboratory stock. Purified reovirus virions were generated by using second- or third-passage L-cell lysate stocks of twice-plaque-purified reovirus as described previously (24). Viral particles were Freon-extracted from infected cell lysates, layered onto 1.2- to 1.4-g/cm³ CsCl gradients, and centrifuged at 62,000 x g for 18 h. Bands corresponding to virions (1.36 g/cm³) were collected and dialyzed in virion storage buffer (150 mM NaCl, 15 mM MgCl₂, 10 mM Tris-HCl [pH 7.4]). Concentrations of reovirus virions in purified preparations were determined from an equivalence of one optical density unit at 260 nm equals 2.1 x 10¹² virions (59). Viral titer was determined by plaque assay using L cells (69).

150

155

Antisera specific for I κ B α , I κ B β , I κ B ϵ , p50, p65/RelA, RelB, c-Rel, IKK γ , and β -actin were purchased from Santa Cruz Biotechnology (Santa Cruz, CA). The antibody antiserum for p100/p52 was purchased from Upstate Biotechnology (Lake Placid, NY). The agonistic lymphotoxin- β receptor antiserum was purchased from BD Biosciences (San Jose, CA). The IKK inhibitor BAY 65-1942 was obtained from Dr. K. Ziegelbauer (Bayer Health Care AG, Leverkusen, Germany).

160

Electrophoretic mobility shift assay (EMSA). Cells (3 x 10⁶) grown in 100 mm tissue-culture dishes (Costar, Cambridge, MA) were treated with 20 ng/ml of TNF- α (Sigma-Aldrich, St. Louis, MO), adsorbed with T3D at a multiplicity of infection (MOI) of 100 plaque forming units (PFU)/cell, or treated with gel saline (mock-infection). After incubation at 37°C for various intervals, nuclear extracts (10 µg total protein) were assayed for NF- κ B activation by an EMSA using a ³²P-labeled oligonucleotide consisting of the NF- κ B consensus-binding sequence (Santa Cruz Biotechnology) as previously described (17). For supershift assays, 2 µg of rabbit polyclonal antiserum specific for p50, p52, RelA, RelB, or c-Rel was added to the binding-reaction mixtures and incubated at 4°C for 30 min prior to the addition of radiolabeled oligonucleotide. Nucleoprotein complexes were subjected to electrophoresis in native 5% polyacrylamide gels at 180 V for 90 min, dried under vacuum, and exposed to Biomax MR film (Kodak, Rochester, NY). Band intensity was quantified by determining photostimulus luminescence (PSL) units using a Fuji2000 phosphor imager and the Multi Gauge software (Fuji Medical Systems, Inc., Stamford, CT).

170

175

180

Immunoblot assay. Cells (8 x 10⁵) were treated with 20 ng/ml of TNF- α , adsorbed with T3D at an MOI of 100 PFU/cell, or mock-infected. Whole-cell extracts

were generated by incubation with lysis buffer (10 mM HEPES [pH7.4], 10 mM KCL, 0.1 mM EDTA, 0.1 mM EGTA, 1 mM DTT, 0.1% Igepal, 1 mM Na₄O₇P₂, 1 mM NaF, 1 mM NaVO₃, and 1 μM microcystin). Extracts (10-50 μg total protein) were resolved by electrophoresis in 10% polyacrylamide gels and transferred to nitrocellulose membranes. Membranes were blocked at 4°C overnight in blocking buffer (PBS containing 0.1% Tween-20 and 5% BSA). Immunoblots were performed by incubating the membranes with primary antibodies diluted 1:500 to 1:2000 in blocking buffer at room temperature for 1 h. Membranes were washed three times for 10 min each with washing buffer (PBS containing 0.1 Tween-20) and incubated with horseradish peroxidase-conjugated goat anti-rabbit (Amersham Biosciences, Piscataway, NJ) and bovine anti-goat antibodies (Santa Cruz Biotechnology) diluted 1:2000 and 1:3000, respectively. Following three washes, membranes were incubated for 1 min with chemiluminescent peroxidase substrate (Amersham Biosciences) and exposed to film. Band intensity was quantified using the Image J program (NIH, Bethesda, MD).

Kinase assay. Cells (8×10^5) were treated with 20 ng/ml of TNF α , adsorbed with T3D at an MOI of 100 PFU/cell, or mock-infected. Whole-cell extracts were incubated with an IKK γ -specific antiserum in the presence of ELB buffer (50 mM HEPES [pH 7.4], 250 mM NaCl, 5 mM EDTA, 0.1% Igepal). Immunoprecipitates were equilibrated in kinase buffer (10 mM HEPES [pH 7.4], 0.5 mM dithiothreitol, 5 mM MgCl₂, 1 mM MnCl₂, 12.5 mM β -glycerophosphate, 50 μM Na₃VO₄, 2 mM NaF) and incubated with 10 μM ATP, 5 μCi of [γ -³²P]ATP (Perkin Elmer), and 1 μg of recombinant GST protein fused to amino acids 1-54 of I κ B α (GST-I κ B α) at 30°C for 30 minutes (11). Kinase reactions were terminated by heat denaturation in the presence of 1% SDS. Radiolabeled products were resolved by SDS-PAGE, transferred to nitrocellulose membranes, and visualized by autoradiography.

Caspase 3 activity assay. Cells (3×10^3) grown in clear-bottom, black-walled, 96-well tissue-culture plates (Costar) were inoculated with 10 ng/ml of TNF α , a combination of 10 ng/ml of TNF α and 10 μg/ml of cycloheximide (Sigma-Aldrich), T3D at an MOI or 1000 PFU/cell, or mock-infected. Following incubation at 37°C for 24 and 12 h with respect to T3D- or TNF α -treatment, caspase 3 activity was quantified by using the Caspase-Glo 3/7 Assay (Promega). Luminescence was detected by using a Topcount NXT luminometer (Packard Biosciences Co., Meriden, CT).

Trypan blue exclusion assay. Cells (4×10^4) grown in 6-well tissue-culture plates were inoculated with 10 ng/ml of TNF α , a combination of 10 ng/ml of TNF α and 10 μg/ml of cycloheximide, T3D at an MOI of 1000 PFU/cell, or mock-infected. Following incubation at 37°C for 48 and 24 h with respect to T3D- or TNF α -treatment, cells were collected and washed with PBS. The cell pellet was resuspended in 50 ml of PBS and stained using 100 ml of a solution containing 0.4% trypan blue (Kodak) in PBS. For each experiment, 200 to 300 cells were counted and the percentage of cell death was determined by light microscopy (Axiovert 200; Zeiss, Oberkochen, Germany).

Statistical analysis. Mean values obtained in EMSA, immunoblot, and apoptosis assays were compared using the unpaired Student's *t* test as applied with Microsoft Excel software (Microsoft, Redmond, WA). *P* values of less than 0.05 were considered to be statistically significant.

235

240

245

250

255

260

265

270

RESULTS

275

Reovirus infection results in the biphasic activation of NF- κ B/Rel DNA-binding proteins. In prior studies, we found that reovirus activates the functional expression of p50/RelA complexes, suggesting the involvement of classical NF- κ B signaling (17). However, it remained unclear whether NF- κ B/Rel proteins linked to the alternative pathway of the NF- κ B pathway are activated during reovirus infection. To more completely define the composition of NF- κ B complexes activated by reovirus, we used nuclear extracts from reovirus-infected HeLa cells and Rel-specific antibodies to monitor the composition of DNA-binding complexes formed in EMSAs. NF- κ B/Rel DNA-binding activity was readily detected over background levels (mock treatment) within 2 hours after infection with reovirus strain T3D (Fig. 1A), which potently induces apoptosis in cultured cells (17, 49, 66) and the murine CNS (44). Peak levels of NF- κ B/Rel DNA-binding activity were observed at 4-8 h post-infection. Supershift analysis of extracts obtained at 4, 6, and 8 h post-infection revealed the presence of DNA/protein complexes containing p50 and RelA, but neither p52 nor RelB (Fig. 1B), suggesting preferential usage of the classical versus alternative NF- κ B pathway by reovirus. Complexes containing c-Rel were apparent in supershift assays only after 8 h of infection (Fig. 1B). Thus, reovirus induces a biphasic pattern of NF- κ B/Rel activation featuring the initial nuclear translocation of complexes consisting of p50 and RelA, followed by those containing p50, RelA, and c-Rel. Given that the cellular gene encoding c-Rel contains functional NF- κ B binding sites (26), this expression pattern may reflect de novo synthesis of c-Rel rather than its mobilization from a latent cytoplasmic pool.

These initial experiments conducted over an 8 h timecourse provided no evidence for the capacity of reovirus to stimulate the nuclear expression of p52, a signature Rel protein involved in the alternative pathway of NF- κ B signaling. To further investigate whether reovirus interfaces with the alternative NF- κ B pathway, we extended the timecourse of T3D infection to 24 h and monitored extracts for processing of p100 to p52 (55). Levels of p100 were significantly reduced between 16 and 24 h post-infection (Fig. 2). Consistent with a precursor/product relationship, diminution in p100 protein levels were accompanied by a significant increase in the steady-state levels of p52 (Fig. 2, panels A and C). Taken together with the NF- κ B/Rel profiling data shown in Fig. 1B, this finding suggests that reovirus engages not only the classical pathway of NF- κ B signaling but also the alternative pathway, albeit at much later times of infection.

Reovirus infection leads to the selective degradation of I κ B α . Activation of the classical NF- κ B pathway by physiologic agonists is primarily dependent on degradation of I κ B α (reviewed in (3, 25, 27)), an inhibitor that sequesters p50/RelA complexes in the cytoplasmic compartment (2). We have previously shown that degradation-resistant forms of I κ B α attenuate reovirus-induced apoptosis, which is critically dependent on NF- κ B activation (17). However, mammalian cells express other labile inhibitors that are structurally similar to I κ B α , such as I κ B β (37) and I κ B ϵ (71). Indeed, prior studies suggest a potential role for signal-dependent degradation of I κ B β (63) and I κ B ϵ (71) in the inducible nuclear entry of c-Rel. To determine whether any of these inhibitors is

under reovirus control, we monitored their levels in T3D-infected cells in
320 immunoblotting studies using I κ B-specific antibodies. The cellular pool of I κ B α was
significantly reduced within 4 h after infection with T3D (Fig. 3, A and B). In contrast,
levels of I κ B β and I κ B ϵ were maintained under the same stimulatory conditions over the
entire 8 h timecourse (Fig. 2, C-F). We conclude that I κ B α is a primary cellular target of
325 reovirus, which is fully consistent with its capacity to stimulate nuclear translocation of
NF- κ B p50/RelA.

IKK α and IKK γ are required for reovirus-induced NF- κ B activation. We
next investigated the mechanism by which reovirus destabilizes I κ B proteins. Cytokine-
induced degradation of NF- κ B inhibitors is dependent on their phosphorylation at
330 specific serine residues by IKKs such as IKK α and IKK β (6, 23, 78). These structurally-
related enzymes can interact and form higher order complexes with other cellular proteins
(reviewed in (25, 27)). Integration of the regulatory protein IKK γ /Nemo into such
complexes is required for activation of IKK β (53, 54, 75) but not IKK α (13, 21, 55). The
most well-characterized substrate of IKK β is I κ B α (30, 41), whereas IKK α catalyzes
335 phosphorylation of p100/NF- κ B2 (55, 73).

To determine whether either IKK α or IKK β is required for reovirus-induced
activation of NF- κ B, cellular IKK complexes were immunopurified from HeLa cells
either before or after infection with T3D and monitored for their capacity to
340 phosphorylate I κ B α in vitro. In keeping with the kinetics of I κ B α degradation (Fig. 3A)
and NF- κ B (Fig. 1A) activation, I κ B kinase activity exceeding basal levels in uninfected
cells was readily detected within 4 h after exposure to T3D and sustained for at least an
additional 4 h (Fig. 4A). These data suggest that IKKs are critically involved in the
mechanism by which reovirus diminishes the cellular pool of I κ B α (Fig. 3A).

To determine whether IKK activation is required for the nuclear translocation of
NF- κ B by reovirus, cells were treated with escalating doses of the IKK inhibitor BAY
65-1942 prior to infection with T3D. Importantly, BAY 65-1942 inhibits IKK β more
efficiently than IKK α (79). As demonstrated in EMSAs, treatment of cells with BAY 65-
350 1942 suppressed NF- κ B signaling induced by reovirus (Fig. 4, B and C), although
incompletely, perhaps reflecting incomplete blockade of IKK α . Immunoblotting studies
of nuclear extracts from the same panel of infected cells indicated that BAY 65-1942 had
a profound inhibitory effect on reovirus-induced nuclear translocation of p65/RelA (Figs.
4, D and E), which is primarily under the control of IKK β . These pharmacological data
355 suggest that reovirus activates NF- κ B via a mechanism involving either IKK α , IKK β , or
both of these IKKs.

To identify the IKK subunits responsible for NF- κ B activation by reovirus, NF-
 κ B DNA-binding activity was assessed in MEFs deficient for IKK α , IKK β , or the IKK β
360 regulatory subunit IKK γ /Nemo. In initial experiments, EMSAs were conducted with
nuclear extracts from wild-type MEFs following infection with T3D for 8 h, which
corresponds to peak levels of NF- κ B DNA-binding activity (Fig. 1A). Reovirus induced
NF- κ B DNA binding activity to levels comparable to or exceeding those observed in

control experiments with wild-type MEFs treated with the cytokine TNF α (Fig. 5A), a
365 potent agonist of IKK. Similar results were obtained with nuclear extracts from reovirus-
infected MEFs lacking IKK β (Fig. 5A). However, the capacity of reovirus to activate NF-
 κ B was completely disrupted in MEFs lacking IKK α (Fig. 5A), indicating preferential
usage of this IKK relative to IKK β . MEFs lacking the regulatory subunit IKK γ /Nemo
(Fig. 5A) also were incapable of reovirus-mediated NF- κ B signaling. Immunoblotting
370 studies of nuclear extracts from the same panel of infected cells confirmed these results
(Fig. 5C). Nuclear translocation of p65/RelA was detected in wild-type MEFs and IKK β -
deficient MEFs, but not in MEFs lacking IKK α or IKK γ . Differences in reovirus-
mediated signal transduction in IKK-deficient MEFs could not be attributed to
differences in viral infection or growth (data not shown). Thus, these findings suggest
375 that IKK α and IKK γ are required for reovirus-induced NF- κ B activation.

NIK is capable of phosphorylating and activating IKK α in response to some
agonists of the alternative NF- κ B pathway, such as lymphotoxin β (36, 40). To determine
whether NIK is required for NF- κ B activation in response to reovirus, NIK-deficient
380 MEFs were used to probe for NF- κ B induction by EMSA and immunoblotting in
response to reovirus T3D infection (Fig. 6). Reovirus infection resulted in NF- κ B
activation in both wild-type and NIK-deficient MEFs, indicating that NIK is dispensable
for reovirus-induced NF- κ B activation. Taken together, these data confirm a requirement
for endogenous IKK in the mechanism by which reovirus activates NF- κ B and strongly
385 suggest that this virus selectively utilizes the IKK α arm of the NF- κ B signaling pathway.
Surprisingly, IKK γ /Nemo, which is known to regulate IKK β rather than IKK α , is also
required for NF- κ B activation by reovirus, but NIK is dispensable.

IKK α and IKK γ are required for reovirus-induced apoptosis. Since IKK α
390 and IKK γ are required for NF- κ B activation following reovirus infection (Fig. 5), we
examined whether IKK stimulation by reovirus leads to apoptotic cell death. IKK-
deficient MEFs were infected with reovirus T3D, and apoptosis was assessed by
quantitation of caspase 3 activity (Fig. 7A). Levels of activated caspase 3 following
infection of wild-type and IKK β -deficient MEFs were substantially greater than those
395 following infection of MEFs deficient in either IKK α or IKK γ . To corroborate these
results, we tested wild-type and IKK-null MEFs for viability following infection with
T3D (Fig. 7B). In comparison to wild-type and IKK β -deficient MEFs, a significantly
greater percentage of IKK α - and IKK γ -deficient MEFs remained viable during a time
course of reovirus infection.
400

To determine whether NIK is required for apoptosis induction following reovirus
infection, NIK-deficient MEFs were infected with reovirus T3D, and apoptosis was
assessed by quantification of caspase 3 activity (Fig. 7C). Levels of caspase 3 activity in
MEFs deficient in NIK were equivalent to those in wild-type cells following infection
405 with T3D. In parallel with these results, we observed no significant difference in the
viability of wild-type and NIK-deficient MEFs following T3D infection (Fig. 7D).
Together, these functional data with IKK- and NIK-deficient MEFs strongly correlate
with the capacity of reovirus to modulate I κ B α and NF- κ B during infection (Figs. 1-6).

410 Our findings suggest that IKK α and IKK γ are required for the induction of NF- κ B
activation leading to apoptosis in response to reovirus. In keeping with the activation of
NF- κ B by reovirus, apoptosis is completely independent of the IKK α inducer NIK,
415 indicating a different mechanism of IKK α activation in response to reovirus.

415

420

425

430

435

440

445

450

DISCUSSION

Apoptosis is a genetically programmed form of cell death that plays an important regulatory role in many biological processes. Many viruses are capable of inducing apoptosis of infected cells (52). In some cases, apoptosis triggered by viral infection may serve as a component of host defense to limit viral replication or spread. In other instances, apoptosis may enhance viral infection by facilitating viral dissemination or allowing virus to evade host inflammatory responses (4, 5, 52). Apoptosis has been shown to play an important role in reovirus-induced disease (19, 20, 44, 45). Although we previously uncovered an essential function for NF- κ B activation in reovirus-induced apoptosis (17), it was not known how reovirus activates this signal-transduction mechanism. Results reported here identify constituents of the NF- κ B signaling apparatus induced by reovirus and provide evidence that NF- κ B activation during reovirus infection requires integral components of both the classical and alternative pathways.

Using MEFs deficient in the expression of individual IKK subunits, we demonstrate that reovirus-infected cells lacking IKK α are impaired for NF- κ B activation (Fig. 5) and apoptotic programming (Fig. 7), whereas both of these processes are operative in cells lacking IKK β . Despite its preferential usage of IKK α , reovirus retains the capacity to elicit both NF- κ B activation and apoptosis in the absence of NIK (Fig. 6 and 7), a known activator of IKK α in cytokine-treated cells (36, 55). Furthermore, targeted disruption of the gene encoding IKK γ /Nemo, which is dispensable for cytokine-induced signaling of IKK α (13, 21), significantly attenuates reovirus-induced NF- κ B activation and apoptosis (Fig. 5 and 7). In light of these findings with NIK and IKK γ , the precise mechanism of reovirus action on IKK α remains unclear. The simplest interpretation of these results is that reovirus accesses the cellular NF- κ B machinery by directly interfacing with IKK α /IKK γ complexes, with IKK γ serving as an adaptor that docks one or more reovirus gene products. In keeping with this possibility, IKK γ tethers the HTLV1 Tax protein to IKK complexes, resulting in persistent activation of IKK β and NF- κ B (7, 12). In what may be another related finding, IKK γ also is required for Tax-induced activation of IKK α (72). Although data emerging from studies of IKK β -deficient mice suggest the presence of functional IKK α /IKK γ complexes (34, 35, 50, 61), direct evidence for the existence of IKK α /IKK γ complexes in wild-type animals has not been reported. Notwithstanding, our results clearly establish that reovirus activates NF- κ B and downstream proapoptotic genes via a mechanism involving IKK α but not IKK β .

490

The principle *in vivo* substrate of IKK β is I κ B α (23, 41, 47). This cytoplasmic inhibitor tightly controls the nuclear translocation of p50/RelA dimers (2), effectors of the classical NF- κ B pathway (reviewed in (3, 25, 27)). The principle *in vivo* substrate of IKK α is p100/NF- κ B2 (55). An integral inhibitor in the alternative NF- κ B pathway, p100 assembles with the transactivator protein RelB (55, 60). Following IKK α -mediated phosphorylation, p100 is processed to p52 via a proteasome-dependent mechanism, permitting the nuclear entry of p52/RelB complexes (55, 60). Given these distinct mechanisms, our findings with reovirus-infected cells suggest an unconventional function for IKK α in substrate targeting. Specifically, we were unable to detect either p52 or RelB

500 DNA-binding activity in nuclear extracts from cells following 4 to 8 h of reovirus
infection (Fig. 1B). Instead, at these early timepoints the predominant Rel species
detected were p50 and RelA (Fig. 1B), which are primarily under I κ B α control (1, 2).
Consistent with this Rel profile, I κ B α protein levels were significantly reduced by 4 h
505 post-infection (Fig. 3). Although p100 processing to p52 was observed at late time points
during reovirus infection (16 h), it seems unlikely that this delayed response contributes
to the more rapidly evolving signals required for apoptosis (16, 17, 49). Accordingly, we
propose that IKK α rather than IKK β targets I κ B α for proteolytic destruction and
regulates the nuclear translocation of p50/RelA complexes in reovirus-infected cells. This
510 working model is fully concordant with the phenotype of cell lines deficient for either
IKK α , p50, or p65/RelA, all of which are impaired for reovirus-induced NF- κ B
activation and proapoptotic signaling (Figs. 4, 5, and (17)). In agreement with this model,
prior studies with recombinant proteins indicate that IKK α can efficiently phosphorylate
NF- κ B-bound forms of I κ B α in vitro (77).

515 Both IKK α and IKK β contain regulatory serine phosphoacceptors in their so-
called "T loop" domains (22, 41). Signal-dependent phosphorylation of the T loop serines
in IKK α and IKK β is a prerequisite for their catalytic activation (22). Based on in vitro
studies with recombinant proteins, IKK α and IKK β can autophosphorylate at these T
520 loop serines (22, 54, 62). Physiologic agonists of the alternative NF- κ B pathway
stimulate T loop phosphorylation and activation of IKK α via the upstream kinase NIK
(36, 55, 73). However, NIK is dispensable in the mechanism by which reovirus induces
NF- κ B activation and apoptosis (Fig. 6 and 7). What signal transducers couple reovirus
to IKK? Experiments using pharmacological inhibitors suggest that NF- κ B-dependent
525 apoptotic signaling is triggered by viral replication steps that occur after disassembly but
prior to RNA synthesis (16). Strain-specific differences in the capacity of reovirus to
induce apoptosis segregate with viral genes encoding the σ 1 and μ 1 proteins (15, 49, 66),
which play important roles in viral attachment (32, 70) and membrane penetration (8, 9,
38), respectively. Importantly, transient expression of μ 1 is sufficient to induce apoptosis
in cell culture (14), implicating this protein in the reovirus/NF- κ B signaling axis. We
530 envision three potential mechanisms by which μ 1, or perhaps another viral gene product,
initiates NF- κ B signal transduction during reovirus infection. First, μ 1 may activate viral
sensors that mediate the recruitment of the adaptor protein interferon- β promoter
stimulator (IPS-1), which mediates the activation of NF- κ B in response to viral infections
by recruiting TNF-associated factor 6 to the signaling complex (31, 42, 56, 74). Second,
535 μ 1 may activate a novel cellular kinase that phosphorylates the T loop of IKK α . Third,
 μ 1 may interact with IKK complexes directly, leading to conformational changes that
stimulate oligomerization and trigger autophosphorylation of the T loop in IKK α {Poyet,
2000 #5490; Inohara, 2000 #4965; . Studies to test these models for reovirus-induced
activation of IKK α are currently underway.

540

Reovirus infection leads to NF- κ B activation in numerous cell types {Connolly,
2000 #2472; Clarke, 2003 #5019; O'Donnell, 2005 #5195}. However, the functional
consequences of NF- κ B activation in vivo differ depending on the infected tissue. NF- κ B
activation in the CNS leads to high levels of neuronal apoptosis and encephalitis (45). In

545 contrast, NF- κ B activation in the heart leads to interferon- β production, which limits viral
replication and protects against apoptosis (45). In the absence of NF- κ B signaling,
reovirus infection induces widespread apoptotic damage to cardiac myocytes, resulting in
myocarditis. Mechanisms underlying the divergent cellular fates following NF- κ B
550 activation by reovirus in vivo remain unclear. Considering the results presented in this
study, these mechanisms may involve tissue-specific activation of different IKK subunits,
which in turn may influence the composition of nuclear NF- κ B complexes. Experiments
using tissue-specific IKK α - or IKK β -deficient mice should clarify the function of IKK in
reovirus-induced disease.

555

560

565

570

575

580

585

590

ACKNOWLEDGEMENTS

We thank members of our laboratory for many helpful discussions and Jim Chappell, Geoff Holm, and Denise Wetzel for careful review of the manuscript. We
595 thank Amgen for providing NIK-deficient cells. We thank Dr. Robert D. Schreiber for providing NIK wild-type cells. We thank Dr. Karl Ziegelbauer and Bayer Health Care AG for providing BAY 65-1942.

This research was supported by Public Health Service awards T32 CA09385 (J.A.C.), R01 AI52379 and CA82556 (D.W.B.), and R01 AI50080 (T.S.D.) and the
600 Elizabeth B. Lamb Center for Pediatric Research. Additional support was provided by Public Health Service awards CA68485 for the Vanderbilt-Ingram Cancer Center and DK20593 for the Vanderbilt Diabetes Research and Training Center.

605

610

615

620

625

630

635

REFERENCES

- 640 1. **Baeuerle, P., and D. Baltimore.** 1989. A 65-kD subunit of active NF- κ B is required for inhibition of NF- κ B by I κ B. *Genes & Development* **3**:1689-1698.
2. **Baeuerle, P., and D. Baltimore.** 1988. I κ B: a specific inhibitor of the NF- κ B transcription factor. *Science* **242**:540-546.
3. **Bonizzi, G., and M. Karin.** 2004. The two NF-kappaB activation pathways and their role in innate and adaptive immunity. *Trends Immunol* **25**:280-288.
- 645 4. **Bowie, A. G., J. Zhan, and W. L. Marshall.** 2004. Viral appropriation of apoptotic and NF-kappaB signaling pathways. *J. Cell. Biochem.* **91**:1099-1108.
5. **Boya, P., A. L. Pauleau, D. Poncet, R. A. Gonzalez-Polo, N. Zamzami, and G. Kroemer.** 2004. Viral proteins targeting mitochondria: controlling cell death. *Biochemical & Biophysical Acta* **1659**:178-189.
- 650 6. **Brown, K., S. Gerstberger, L. Carlson, G. Franzoso, and U. Siebenlist.** 1995. Control of I kappa B-alpha proteolysis by site-specific, signal-induced phosphorylation. *Science* **267**:1485-1488.
7. **Carter, R. S., B. C. Geyer, M. Xie, C. A. Acevedo-Suarez, and D. W. Ballard.** 655 2001. Persistent activation of NF-kappa B by the tax transforming protein involves chronic phosphorylation of IkappaB kinase subunits IKKbeta and IKKgamma. *Journal of Biological Chemistry* **276**:24445-24448.
8. **Chandran, K., D. L. Farsetta, and M. L. Nibert.** 2002. Strategy for nonenveloped virus entry: a hydrophobic conformer of the reovirus membrane penetration protein μ 1 mediates membrane disruption. *Journal of Virology* 660 **76**:9920-9933.
9. **Chandran, K., J. S. Parker, M. Ehrlich, T. Kirchhausen, and M. L. Nibert.** 2003. The delta region of outer-capsid protein μ 1 undergoes conformational change and release from reovirus particles during cell entry. *Journal of Virology* 665 **77**:13361-13375.
10. **Chen, Z., J. Hagler, V. J. Palombella, F. Melandri, D. Scherer, D. Ballard, and T. Maniatis.** 1995. Signal-induced site-specific phosphorylation targets I kappa B alpha to the ubiquitin-proteasome pathway. *Genes & Development* **9**:1585-1597.
- 670 11. **Chu, Z. L., J. A. DiDonato, J. Hawiger, and D. W. Ballard.** 1998. The tax oncoprotein of human T-cell leukemia virus type 1 associates with and persistently activates IkappaB kinases containing IKKalpha and IKKbeta. *Journal of Biological Chemistry* **273**:15891-4.
12. **Chu, Z. L., Y. A. Shin, J. M. Yang, J. A. DiDonato, and D. W. Ballard.** 1999. 675 IKKgamma mediates the interaction of cellular IkappaB kinases with the tax transforming protein of human T cell leukemia virus type 1. *Journal of Biological Chemistry* **274**:15297-300.
13. **Claudio, E., K. Brown, S. Park, H. Wang, and U. Siebenlist.** 2002. BAFF-induced NEMO-independent processing of NF-kappa B2 in maturing B cells. *Nat. Immunol.* **3**:958-965.
- 680 14. **Coffey, C. M., A. Sheh, I. S. Kim, K. Chandran, M. L. Nibert, and J. S. Parker.** 2006. Reovirus Outer Capsid Protein {micro}1 Induces Apoptosis and

- Associates with Lipid Droplets, Endoplasmic Reticulum, and Mitochondria.
Journal of Virology **80**:8422-8438.
- 685 15. **Connolly, J. L., E. S. Barton, and T. S. Dermody.** 2001. Reovirus binding to cell surface sialic acid potentiates virus-induced apoptosis. Journal of Virology **75**:4029-4039.
16. **Connolly, J. L., and T. S. Dermody.** 2002. Virion disassembly is required for apoptosis induced by reovirus. Journal of Virology **76**:1632-1641.
- 690 17. **Connolly, J. L., S. E. Rodgers, P. Clarke, D. W. Ballard, L. D. Kerr, K. L. Tyler, and T. S. Dermody.** 2000. Reovirus-induced apoptosis requires activation of transcription factor NF- κ B. Journal of Virology **74**:2981-2989.
18. **Danthi, P., M. W. Hansberger, J. A. Campbell, J. C. Forrest, and T. S. Dermody.** 2006. JAM-A-independent, antibody-mediated uptake of reovirus into cells leads to apoptosis. Journal of Virology **80**:1261-1270.
- 695 19. **DeBiasi, R., C. Edelstein, B. Sherry, and K. Tyler.** 2001. Calpain inhibition protects against virus-induced apoptotic myocardial injury. Journal of Virology **75**:351-361.
20. **DeBiasi, R. L., B. A. Robinson, B. Sherry, R. Bouchard, R. D. Brown, M. Rizeq, C. Long, and K. L. Tyler.** 2004. Caspase inhibition protects against reovirus-induced myocardial injury in vitro and in vivo. Journal of Virology **78**:11040-11050.
- 700 21. **Dejardin, E., N. M. Droin, M. Delhase, E. Haas, Y. Cao, C. Makris, Z. W. Li, M. Karin, C. F. Ware, and D. R. Green.** 2002. The lymphotoxin-beta receptor induces different patterns of gene expression via two NF-kappaB pathways. Immunity **17**:525-535.
- 705 22. **Delhase, M., M. Hayakawa, Y. Chen, and M. Karin.** 1999. Positive and negative regulation of IkappaB kinase activity through IKKbeta subunit phosphorylation. Science **284**:309-313.
- 710 23. **DiDonato, J. A., M. Hayakawa, D. M. Rothwarf, E. Zandi, and M. Karin.** 1997. A cytokine-responsive IkappaB kinase that activates the transcription factor NF-kappaB. Nature **388**:548-554.
24. **Furlong, D. B., M. L. Nibert, and B. N. Fields.** 1988. Sigma 1 protein of mammalian reoviruses extends from the surfaces of viral particles. Journal of Virology **62**:246-256.
- 715 25. **Ghosh, S., and M. Karin.** 2002. Missing pieces in the NF-kappaB puzzle. Cell **109 Suppl**:S81-S96.
26. **Grumont, R. J., I. B. Richardson, C. Gaff, and S. Gerondakis.** 1993. rel/NF-kappa B nuclear complexes that bind kB sites in the murine c-rel promoter are required for constitutive c-rel transcription in B-cells. Cell Growth Differ **4**:731-743.
- 720 27. **Hayden, M. S., and S. Ghosh.** 2004. Signaling to NF- κ B. Genes Dev **18**:2195-2224.
28. **Heusch, M., L. Lin, R. Geleziunas, and W. C. Greene.** 1999. The generation of nfkb2 p52: mechanism and efficiency. Oncogene **18**:6201-6208.
- 725 29. **Hu, Y., V. Baud, M. Delhase, P. Zhang, T. Deerinck, M. Ellisman, R. Johnson, and M. Karin.** 1999. Abnormal morphogenesis but intact IKK

- activation in mice lacking the IKK α subunit of IkappaB kinase. *Science* **284**:316-320.
- 730 30. **Huynh, Q. K., H. Boddupalli, S. A. Rouw, C. M. Koboldt, T. Hall, C. Sommers, S. D. Hauser, J. L. Pierce, R. G. Combs, B. A. Reitz, J. A. Diaz-Collier, R. A. Weinberg, B. L. Hood, B. F. Kilpatrick, and C. S. Tripp.** 2000. Characterization of the recombinant IKK1/IKK2 heterodimer. Mechanisms regulating kinase activity. *Journal of Biological Chemistry* **275**:25883-25891.
- 735 31. **Kawai, T., K. Takahashi, S. Sato, C. Coban, H. Kumar, H. Kato, K. J. Ishii, O. Takeuchi, and S. Akira.** 2005. IPS-1, an adaptor triggering RIG-I- and Mda5-mediated type I interferon induction. *Nat. Immunol.* **6**:981-988.
32. **Lee, P. W., E. C. Hayes, and W. K. Joklik.** 1981. Protein σ 1 is the reovirus cell attachment protein. *Virology* **108**:156-163.
- 740 33. **Li, Q., Q. Lu, J. Y. Hwang, D. Buscher, K. F. Lee, J. C. Izpisua-Belmonte, and I. M. Verma.** 1999. IKK1-deficient mice exhibit abnormal development of skin and skeleton. *Genes & Development* **13**:1322-1328.
34. **Li, Q., D. Van Antwerp, F. Mercurio, K. F. Lee, and I. M. Verma.** 1999. Severe liver degeneration in mice lacking the IkappaB kinase 2 gene. *Science* **284**:321-325.
- 745 35. **Li, Z. W., W. Chu, Y. Hu, M. Delhase, T. Deerinck, M. Ellisman, R. Johnson, and M. Karin.** 1999. The IKK β subunit of IkappaB kinase (IKK) is essential for nuclear factor kappaB activation and prevention of apoptosis. *Journal of Experimental Medicine* **189**:1839-1845.
- 750 36. **Ling, L., Z. Cao, and D. V. Goeddel.** 1998. NF-kappaB-inducing kinase activates IKK- α by phosphorylation of Ser-176. *Proc Natl Acad Sci U S A* **95**:3792-7.
37. **Link, E., L. D. Kerr, R. Schreck, U. Zabel, I. Verma, and P. A. Baeuerle.** 1992. Purified I kappa B- β is inactivated upon dephosphorylation. *Journal of Biological Chemistry* **267**:239-246.
- 755 38. **Lucia-Jandris, P., J. W. Hooper, and B. N. Fields.** 1993. Reovirus M2 gene is associated with chromium release from mouse L cells. *Journal of Virology* **67**:5339-5345.
39. **Maniatis, T.** 1997. Catalysis by a multiprotein IkappaB kinase complex. *Science* **278**:818-819.
- 760 40. **Matsushima, A., T. Kaisho, P. D. Rennert, H. Nakano, K. Kurosawa, D. Uchida, K. Takeda, S. Akira, and M. Matsumoto.** 2001. Essential role of nuclear factor (NF)-kappaB-inducing kinase and inhibitor of kappaB (IkappaB) kinase alpha in NF-kappaB activation through lymphotoxin beta receptor, but not through tumor necrosis factor receptor I. *Journal of Experimental Medicine* **193**:631-636.
- 765 41. **Mercurio, F., H. Zhu, B. W. Murray, A. Shevchenko, B. L. Bennett, J. Li, D. B. Young, M. Barbosa, M. Mann, A. Manning, and A. Rao.** 1997. IKK-1 and IKK-2: cytokine-activated IkappaB kinases essential for NF-kappaB activation. *Science* **278**:860-866.
- 770 42. **Meylan, E., J. Curran, K. Hofmann, D. Moradpour, M. Binder, R. Bartenschlager, and J. Tschopp.** 2005. Cardif is an adaptor protein in the RIG-I antiviral pathway and is targeted by hepatitis C virus. *Nature* **437**:1167-1172.

43. **Nibert, M. L., and L. A. Schiff.** 2001. Reoviruses and their replication, p. 1679-
775 1728. *In* D. M. Knipe and P. M. Howley (ed.), *Fields Virology*, Fourth ed.
Lippincott Williams & Wilkins, Philadelphia.
44. **Oberhaus, S. M., R. L. Smith, G. H. Clayton, T. S. Dermody, and K. L. Tyler.**
1997. Reovirus infection and tissue injury in the mouse central nervous system
are associated with apoptosis. *Journal of Virology* **71**:2100-2106.
- 780 45. **O'Donnell, S. M., M. W. Hansberger, J. L. Connolly, J. D. Chappell, M. J.
Watson, J. M. Pierce, J. D. Wetzel, W. Han, E. S. Barton, J. C. Forrest, T.
Valyi-Nagy, F. E. Yull, T. S. Blackwell, J. N. Rottman, B. Sherry, and T. S.
Dermody.** 2005. Organ-specific roles for transcription factor NF- κ B in reovirus-
induced apoptosis and disease. *J Clin Invest* **115**:2341-2350.
- 785 46. **Palombella, V., O. Rando, A. Goldberg, and T. Maniatis.** 1994. The ubiquitin-
proteasome pathway is required for processing the NF-kappa B1 precursor protein
and the activation of NF-kappa B. *Cell* **78**:773-785.
47. **Regnier, C. H., H. Y. Song, X. Gao, D. V. Goeddel, Z. Cao, and M. Rothe.**
1997. Identification and characterization of an IkappaB kinase. *Cell* **90**:373-83.
- 790 48. **Richardson-Burns, S. M., D. J. Kominsky, and K. L. Tyler.** 2002. Reovirus-
induced neuronal apoptosis is mediated by caspase 3 and is associated with the
activation of death receptors. *J Neurovirol* **8**:365-380.
49. **Rodgers, S. E., E. S. Barton, S. M. Oberhaus, B. Pike, C. A. Gibson, K. L.
Tyler, and T. S. Dermody.** 1997. Reovirus-induced apoptosis of MDCK cells is
795 not linked to viral yield and is blocked by Bcl-2. *Journal of Virology* **71**:2540-
2546.
50. **Rothwarf, D. M., and M. Karin.** 1999. e NF-kappa B activation pathway: a
paradigm in information transfer from membrane to nucleus. *Sci STKE*
1999:RE1.
- 800 51. **Rothwarf, D. M., E. Zandi, G. Natoli, and M. Karin.** 1998. IKK-gamma is an
essential regulatory subunit of the IkappaB kinase complex. *Nature* **395**:297-300.
52. **Roulston, A., R. C. Marcellus, and P. E. Branton.** 1999. Viruses and apoptosis.
Annual Review of Microbiology **53**:577-628.
53. **Rudolph, D., W. C. Yeh, A. Wakeham, B. Rudolph, D. Nallainathan, J.
Potter, A. J. Elia, and T. W. Mak.** 2000. Severe liver degeneration and lack of
805 NF-kappaB activation in NEMO/IKKgamma-deficient mice. *Genes Dev* **14**:854-
62.
54. **Schomer-Miller, B., T. Higashimoto, Y. K. Lee, and E. Zandi.** 2006.
Regulation of IkappaB kinase (IKK) complex by IKKgamma-dependent
810 phosphorylation of the T-loop and C terminus of IKKbeta. *Journal of Biological
Chemistry* **281**:15268-15276.
55. **Senftleben, U., Y. Cao, G. Xiao, F. R. Greten, G. Krahn, G. Bonizzi, Y. Chen,
Y. Hu, A. Fong, S. C. Sun, and M. Karin.** 2001. Activation by IKKalpha of a
second, evolutionary conserved, NF-kappa B signaling pathway. *Science*
815 **293**:1495-1499.
56. **Seth, R. B., L. Sun, C. K. Ea, and Z. J. Chen.** 2005. Identification and
characterization of MAVS, a mitochondrial antiviral signaling protein that
activates NF-kappaB and IRF 3. *Cell* **122**:669-682.

57. **Simeonidis, S., S. Liang, G. Chen, and D. Thanos.** 1997. Cloning and functional characterization of mouse IkappaBepsilon. *Proc Natl Acad Sci U S A* **94**:14372-14377.
58. **Sizemore, N., N. Lerner, N. Dombrowski, H. Sakurai, and G. R. Stark.** 2002. Distinct roles of the Ikappa B kinase alpha and beta subunits in liberating nuclear factor kappa B (NF-kappa B) from Ikappa B and in phosphorylating the p65 subunit of NF-kappa B. *Journal of Biological Chemistry* **277**:3863-3869.
59. **Smith, R. E., H. J. Zweerink, and W. K. Joklik.** 1969. Polypeptide components of virions, top component and cores of reovirus type 3. *Virology* **39**:791-810.
60. **Solan, N. J., H. Miyoshi, E. M. Carmona, G. D. Bren, and C. V. Paya.** 2002. RelB cellular regulation and transcriptional activity are regulated by p100. *J Biol Chem* **277**:1405-1418.
61. **Tanaka, M., M. E. Fuentes, K. Yamaguchi, M. H. Durnin, S. A. Dalrymple, K. L. Hardy, and G. DV.** 1999. Embryonic lethality, liver degeneration, and impaired NF-kappa B activation in IKK-beta-deficient mice. *Immunity* **10**:421-429.
62. **Tang, E. D., N. Inohara, C. Y. Wang, G. Nunez, and K. L. Guan.** 2003. Roles for homotypic interactions and transautophosphorylation in IkappaB kinase beta (IKKbeta) activation. *J. Biol. Chem.* **278**:38566-38570.
63. **Thompson, J. E., R. J. Phillips, H. Erdjument-Bromage, P. Tempst, and S. Ghosh.** 1995. I kappa B-beta regulates the persistent response in a biphasic activation of NF-kappa B. *Cell* **80**:573-582.
64. **Traenckner, E. B., H. L. Pahl, T. Henkel, K. N. Schmidt, S. Wilk, and P. A. Baeuerle.** 1995. Phosphorylation of human I kappa B-alpha on serines 32 and 36 controls I kappa B-alpha proteolysis and NF-kappa B activation in response to diverse stimuli. *EMBO Journal* **14**:2876-2883.
65. **Tyler, K. L.** 2001. Mammalian reoviruses, p. 1729-1745. *In* D. M. Knipe and P. M. Howley (ed.), *Fields Virology*, Fourth ed. Lippincott Williams & Wilkins, Philadelphia.
66. **Tyler, K. L., M. K. Squier, S. E. Rodgers, S. E. Schneider, S. M. Oberhaus, T. A. Grdina, J. J. Cohen, and T. S. Dermody.** 1995. Differences in the capacity of reovirus strains to induce apoptosis are determined by the viral attachment protein $\sigma 1$. *Journal of Virology* **69**:6972-6979.
67. **Verma, I. M., and J. Stevenson.** 1997. IkappaB kinase: beginning, not the end. *Proceedings of the National Academy of Sciences USA* **94**:11758-11760.
68. **Verma, I. M., J. K. Stevenson, E. M. Schwarz, D. Van Antwerp, and S. Miyamoto.** 1995. Rel/NF-kappa B/I kappa B family: intimate tales of association and disassociation. *Genes & Development* **9**:2723-2735.
69. **Virgin, H. W., IV, R. Bassel-Duby, B. N. Fields, and K. L. Tyler.** 1988. Antibody protects against lethal infection with the neurally spreading reovirus type 3 (Dearing). *Journal of Virology* **62**:4594-4604.
70. **Weiner, H. L., K. A. Ault, and B. N. Fields.** 1980. Interaction of reovirus with cell surface receptors. I. Murine and human lymphocytes have a receptor for the hemagglutinin of reovirus type 3. *Journal of Immunology* **124**:2143-2148.

71. **Whiteside, S. T., J. C. Epinat, N. R. Rice, and A. Israel.** 1997. I kappa B
epsilon, a novel member of the I kappa B family, controls RelA and cRel NF-
kappa B activity. *EMBO Journal* **16**:1413-1426.
72. **Xiao, G., M. E. Cvijic, A. Fong, E. W. Harhaj, M. T. Uhlik, M. Waterfield,
and S. C. Sun.** 2001. Retroviral oncoprotein Tax induces processing of NF-
kappaB2/p100 in T cells: evidence for the involvement of IKKalpha. *EMBO
Journal* **20**:6805-6815.
73. **Xiao, G., E. W. Harhaj, and S. C. Sun.** 2001. NF-kappaB-inducing kinase
regulates the processing of NF-kappaB2 p100. *Molecular & Cellular Biology*
7:401-409.
74. **Xu, L. G., Y. Y. Wang, K. J. Han, L. Y. Li, Z. Zhai, and H. B. Shu.** 2005.
VISA is an adapter protein required for virus-triggered IFN-beta signaling.
Molecular Cell **19**:727-740.
75. **Yamaoka, S., G. Courtois, C. Bessia, S. T. Whiteside, R. Weil, F. Agou, H. E.
Kirk, R. J. Kay, and A. Israel.** 1998. Complementation cloning of NEMO, a
component of the IkappaB kinase complex essential for NF-kappaB activation.
Cell **93**:1231-1240.
76. **Yin, L., L. Wu, H. Wesche, C. D. Arthur, J. M. White, D. V. Goeddel, and R.
D. Schreiber.** 2001. Defective lymphotoxin-beta receptor-induced NF-kappaB
transcriptional activity in NIK-deficient mice. *Science* **291**:2162-2165.
77. **Zandi, E., Y. Chen, and M. Karin.** 1998. Direct phosphorylation of IkappaB by
IKKalpha and IKKbeta: discrimination between free and NF-kappaB-bound
substrate. *Science* **281**:1360-1363.
78. **Zandi, E., D. M. Rothwarf, M. Delhase, M. Hayakawa, and M. Karin.** 1997.
The IkappaB kinase complex (IKK) contains two kinase subunits, IKKalpha and
IKKbeta, necessary for IkappaB phosphorylation and NF-kappaB activation. *Cell*
91:243-252.
79. **Ziegelbauer, K., F. Gantner, N. W. Lukacs, A. Berlin, K. Fuchikami, T. Niki,
K. Sakai, H. Inbe, K. Takeshita, M. Ishimori, H. Komura, T. Murata, T.
Lowinger, and K. B. Bacon.** 2005. A selective novel low-molecular-weight
inhibitor of IkappaB kinase-beta (IKK-beta) prevents pulmonary inflammation
and shows broad anti-inflammatory activity. *Br J Pharmacol* **145**:178-192.

FIGURE LEGENDS

910

FIG. 1. Biphasic activation of NF- κ B/Rel proteins in reovirus-infected cells. (A) Nuclear extracts were prepared from uninfected HeLa cells (0 h), mock-infected cells (Mock), or cells infected with T3D at an MOI of 100 PFU/cell for the times shown. Cells also were treated with 20 ng/ml of TNF α for 30 min as a positive control. Extracts were incubated with a radiolabeled NF- κ B consensus oligonucleotide, and resulting protein-oligonucleotide complexes were resolved by acrylamide gel electrophoresis, dried, and exposed to film. (B) Nuclear extracts prepared at 4, 6, and 8 h post infection were incubated with antisera specific for p50, p52, RelA, RelB, or c-Rel prior to the addition of a radiolabeled NF- κ B consensus oligonucleotide. NF- κ B-containing complexes are indicated.

920

FIG. 2. Processing of p100 to p52 during reovirus infection. (A) Whole-cell extracts were prepared from uninfected HeLa cells (0 h), mock-infected cells (Mock), or cells infected with reovirus T3D at an MOI of 100 PFU/cell for the times shown. Cells also were treated with 2 μ g/ml of an agonistic lymphotoxin- β receptor antiserum for 8 h as a positive control. Extracts were resolved by SDS-PAGE, transferred to nitrocellulose membranes, and immunoblotted by using an antiserum specific for p100/p52. Band intensity was quantified by using the Image J program. The results are presented as the mean ratio of (B) p100/actin or (C) p52/p100 for three independent experiments. Error bars indicate standard deviations. *, $P < 0.05$ as determined by Student's t test in comparison to untreated cells (0 h).

930

FIG. 3. Reovirus infection leads to degradation of I κ B α but not I κ B β or I κ B ϵ . Cytoplasmic extracts were prepared from uninfected HeLa cells (0 h), mock-infected cells (Mock), or cells infected with reovirus T3D at an MOI of 100 PFU/cell for the times shown. Cells also were treated with 20 ng/ml of TNF α for 10 min as a positive control. Extracts were resolved by SDS-PAGE, transferred to nitrocellulose membranes, and immunoblotted by using antisera specific for (A) I κ B α , (C) I κ B β , or (E) I κ B ϵ . An actin-specific antiserum was used to detect levels of actin as a loading control. Band intensity corresponding to levels of (B) I κ B α , (D) I κ B β , and (F) I κ B ϵ was quantified by using the Image J program. The results are presented as the mean ratio of I κ B/actin for three independent experiments. Error bars indicate standard deviations. *, $P < 0.05$ as determined by Student's t test in comparison to untreated cells (0 h).

935

940

FIG. 4. Involvement of IKKs in reovirus-induced NF- κ B activation. (A) Whole-cell extracts were prepared from uninfected HeLa cells (0 h), mock-infected cells (Mock), or cells infected with reovirus T3D at an MOI of 100 PFU/cell for the times shown. Cells also were treated with 20 ng/ml of TNF α for the times shown as a positive control. The IKK complex was immunoprecipitated by using an IKK γ -specific antiserum prior to incubation with a GST-I κ B α substrate in the presence of [γ - 32 P]ATP. Kinase reactions were resolved by SDS-PAGE, transferred to nitrocellulose, and visualized by autoradiography. (B) HeLa cells were pretreated with IKK inhibitor BAY 65-1942 for 1 h at the concentrations shown and uninfected (Untreated), mock-infected (Mock), or infected with reovirus T3D at an MOI of 100 PFU/cell for the times shown. Nuclear

945

950

955 extracts were incubated with a radiolabeled NF- κ B consensus oligonucleotide, and
resulting protein-oligonucleotide complexes were resolved by acrylamide gel
electrophoresis, dried, and exposed to film. (C) Band intensity was quantified by
determining PSL units relative to uninfected cells for four independent experiments.
Error bars indicate standard deviations. *, $P < 0.05$ as determined by Student's t test in
960 comparison to untreated cells (0 μ M). (D) Nuclear extracts from the experiment shown in
panel B were resolved by SDS-PAGE, transferred to nitrocellulose, and immunoblotted
by using a RelA-specific antiserum. (E) Band intensity was quantified relative to
uninfected cells by using the Image J program. The results are presented as the mean
RelA band intensity for three independent experiments. Error bars indicate standard
965 deviations. *, $P < 0.05$ as determined by Student's t test in comparison to untreated cells
(0 μ M).

Fig. 5. IKK α and IKK γ are required for reovirus-induced activation of NF- κ B.
(A) Wild-type MEFs or MEFs deficient in IKK α , IKK β , or IKK γ were uninfected (0 h),
970 mock-infected (Mock), infected with reovirus T3D at an MOI of 100 PFU/cell for 8 h, or
treated with 20 ng/ml of TNF α for 1 h. Nuclear extracts were incubated with a
radiolabeled NF- κ B consensus oligonucleotide. Resulting protein-oligonucleotide
complexes were resolved by acrylamide gel electrophoresis, dried, and exposed to film.
NF- κ B-containing complexes are indicated. (B) Band intensity was quantified by
975 determining PSL units relative to uninfected cells for three independent experiments.
Error bars indicate standard deviations. *, $P < 0.05$ as determined by Student's t test in
comparison to mock-treated cells (0 h). (C) Nuclear extracts from the experiment shown
in panel A were resolved by SDS-PAGE, transferred to nitrocellulose, and
immunoblotted by using a RelA-specific antiserum.

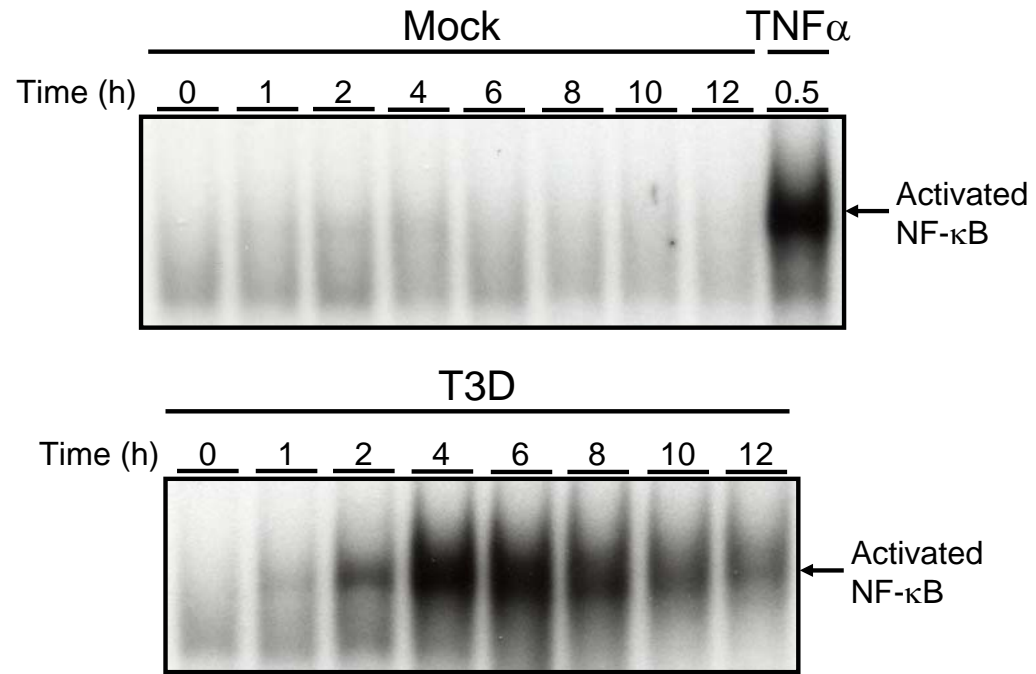
980
FIG. 6. Reovirus-induced activation of NF- κ B in NIK-deficient cells. (A) Wild-
type MEFs or NIK-deficient MEFs were uninfected (0 h), mock-infected (Mock),
infected with reovirus T3D at an MOI of 1000 PFU/cell for 8 h, or treated with 20 ng/ml
of TNF α for 30 min. Nuclear extracts were incubated with a radiolabeled NF- κ B
985 consensus oligonucleotide. Resulting protein-oligonucleotide complexes were resolved
by acrylamide gel electrophoresis, dried, and exposed to film. NF- κ B-containing
complexes are indicated. (B) Nuclear extracts from the experiment shown in panel A
were resolved by SDS-PAGE, transferred to nitrocellulose, and immunoblotted by using
a RelA-specific antiserum.

990
FIG. 7. IKK α and IKK γ are required for reovirus-induced apoptosis. Wild-type
MEFs or (A) MEFs deficient in IKK α , IKK β , IKK γ , or (C) NIK were mock-infected,
infected with reovirus T3D at an MOI of 1000 PFU/cell for 24 h, treated with 10 ng/ml of
TNF α for 12 h, or treated with 10 ng/ml of TNF α and 10 μ g/ml of cycloheximide for 12
995 h. Caspase 3/7 activity was quantified by using a luminescent substrate. The results are
expressed as the mean caspase activity relative to mock-infected cells for three
independent experiments. Wild-type MEFs or (B) IKK-deficient MEFs or (D) NIK-
deficient MEFs were mock-infected, infected with reovirus T3D at an MOI of 1000
PFU/cell for 48 h, treated with 10 ng/ml of TNF α for 24 h, or treated with 10 ng/ml of

1000 TNF α and 10 μ g/ml of cycloheximide for 24 h. Cell viability was quantified by trypan blue exclusion. The results are expressed as the mean percentage of cell death for three independent experiments. Error bars indicate standard deviations. *, $P < 0.05$ as determined by Student's t test in comparison to mock-infected cells.

Figure 1

A



B

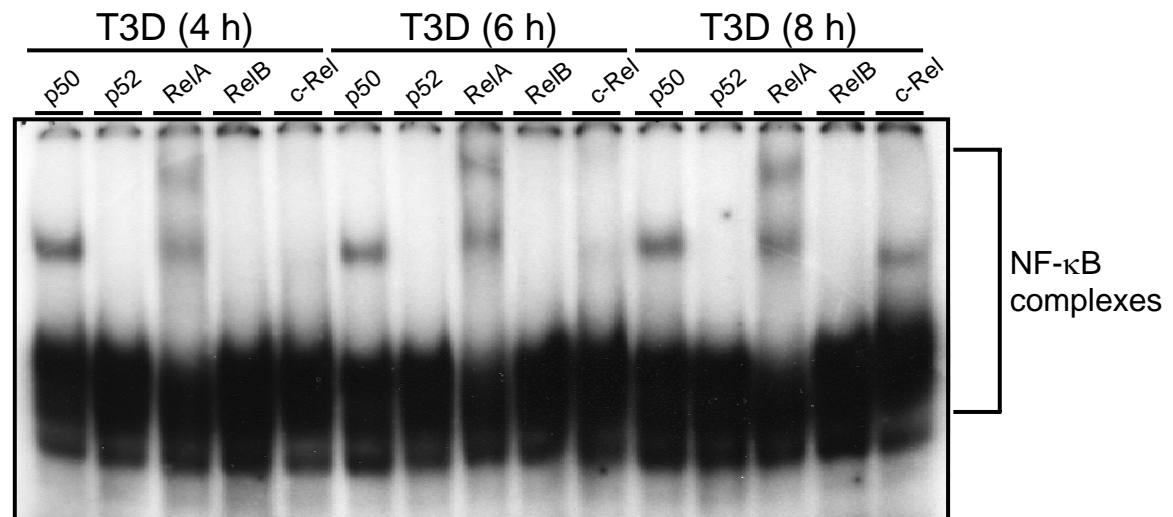
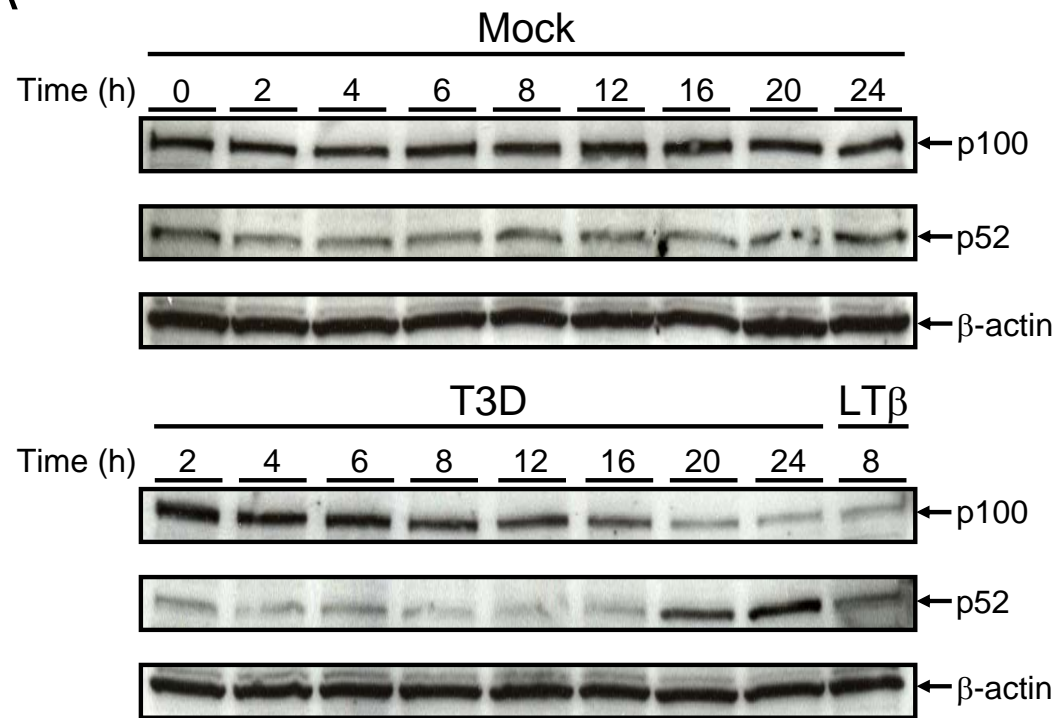
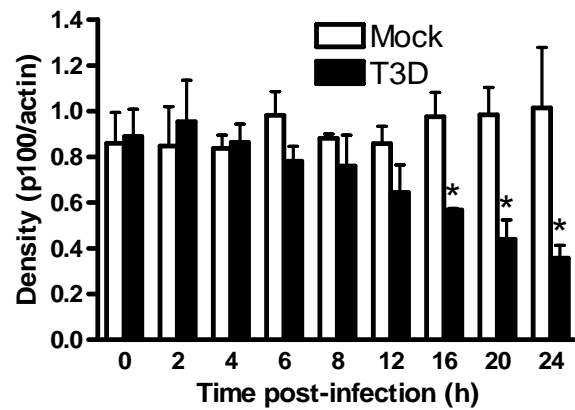


Figure 2

A



B



C

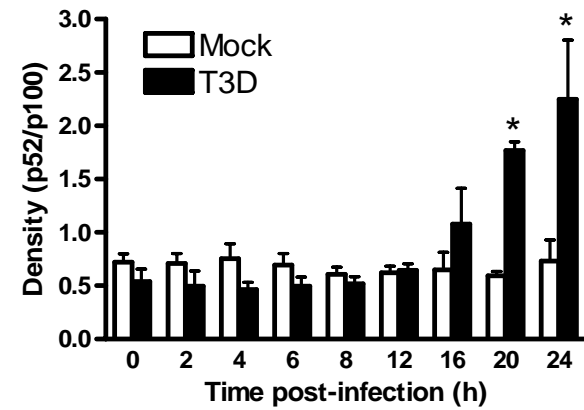


Figure 3

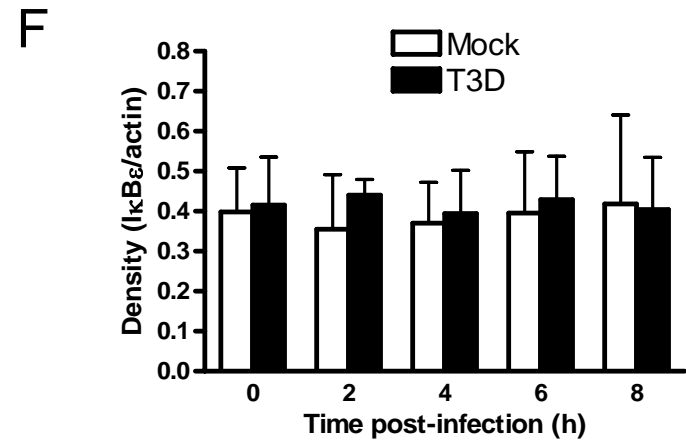
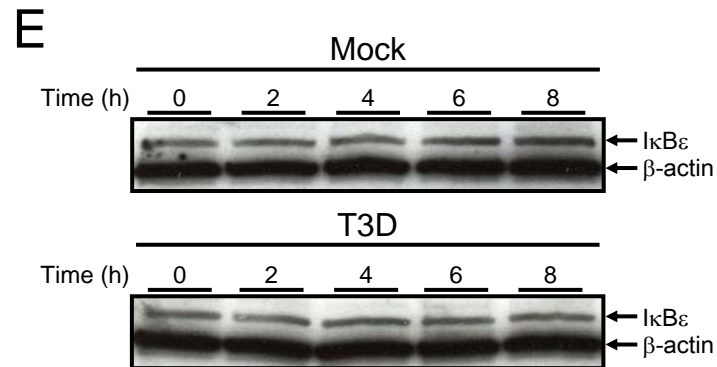
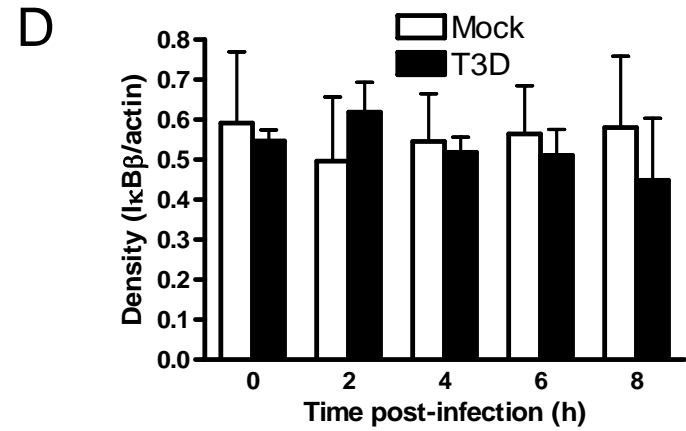
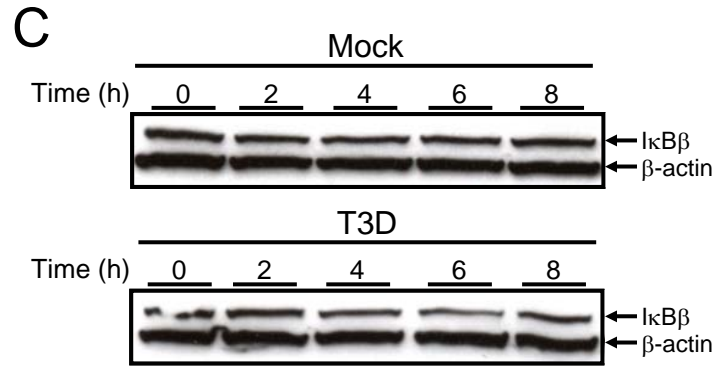
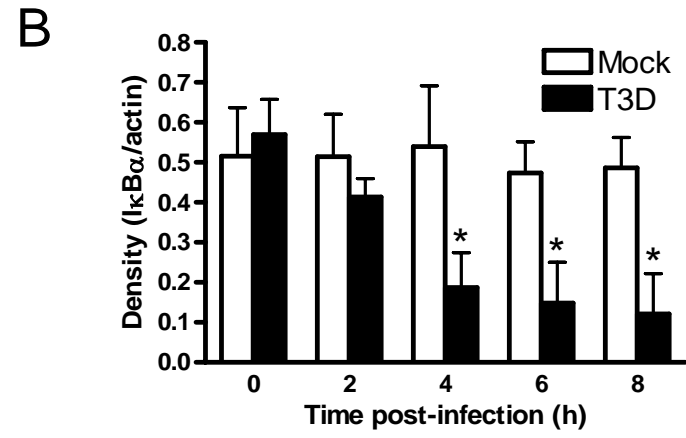
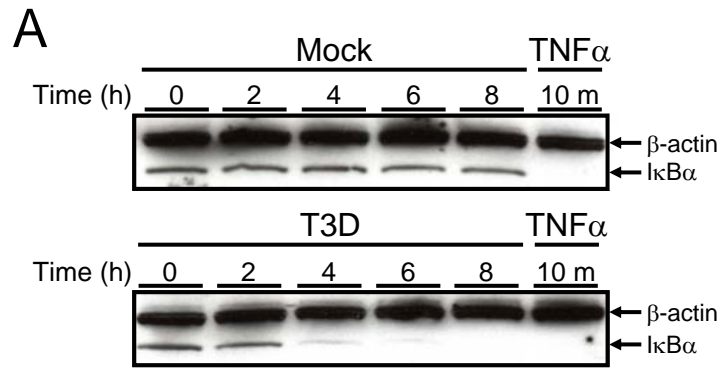


Figure 4

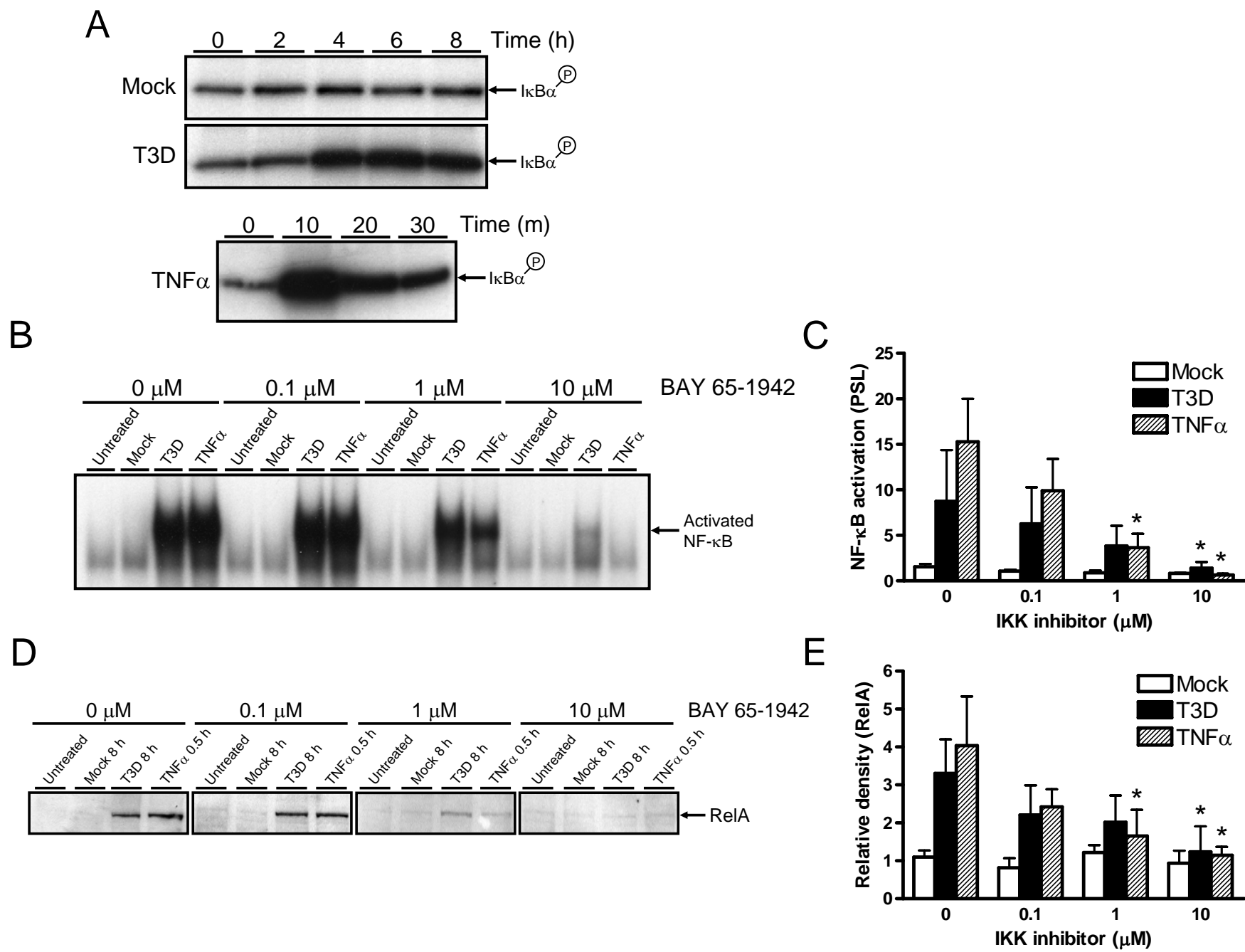


Figure 5

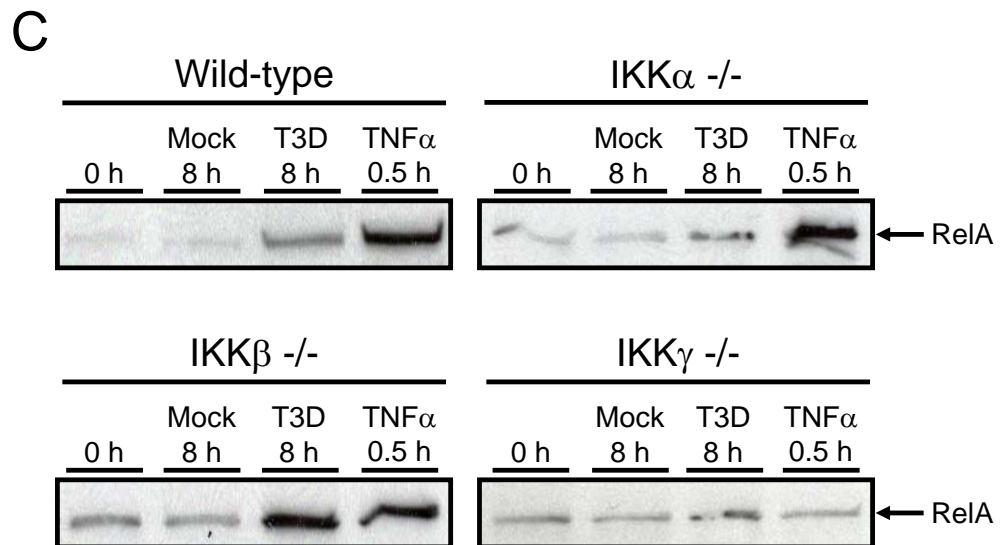
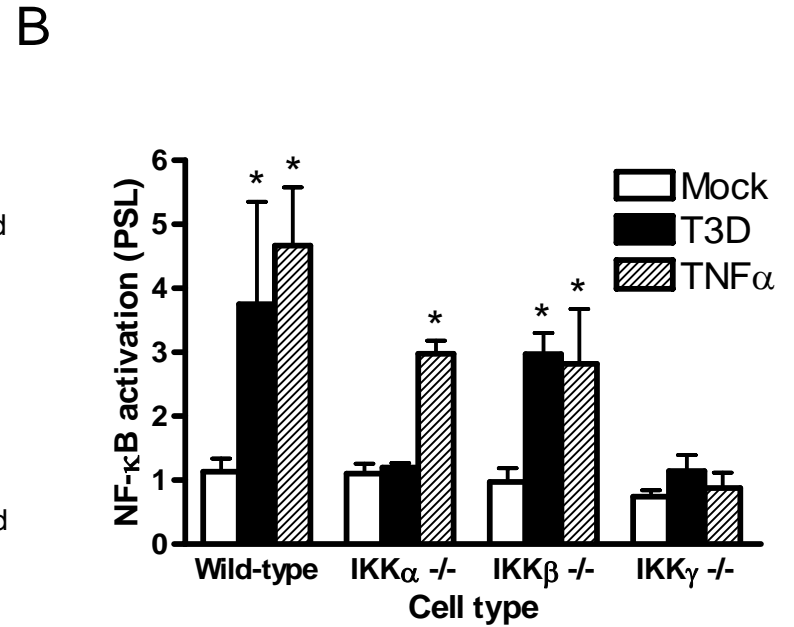
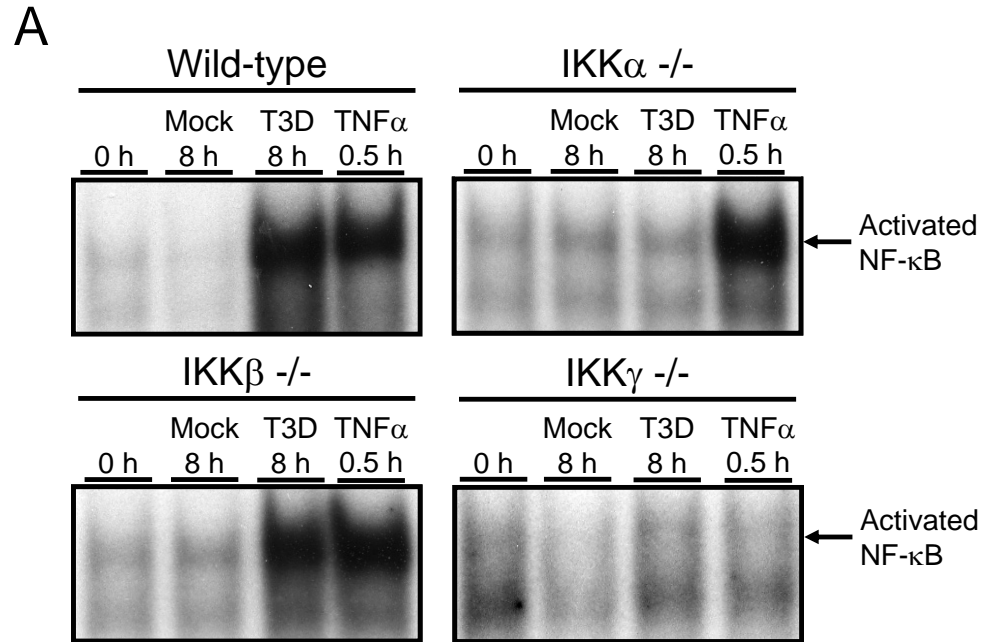
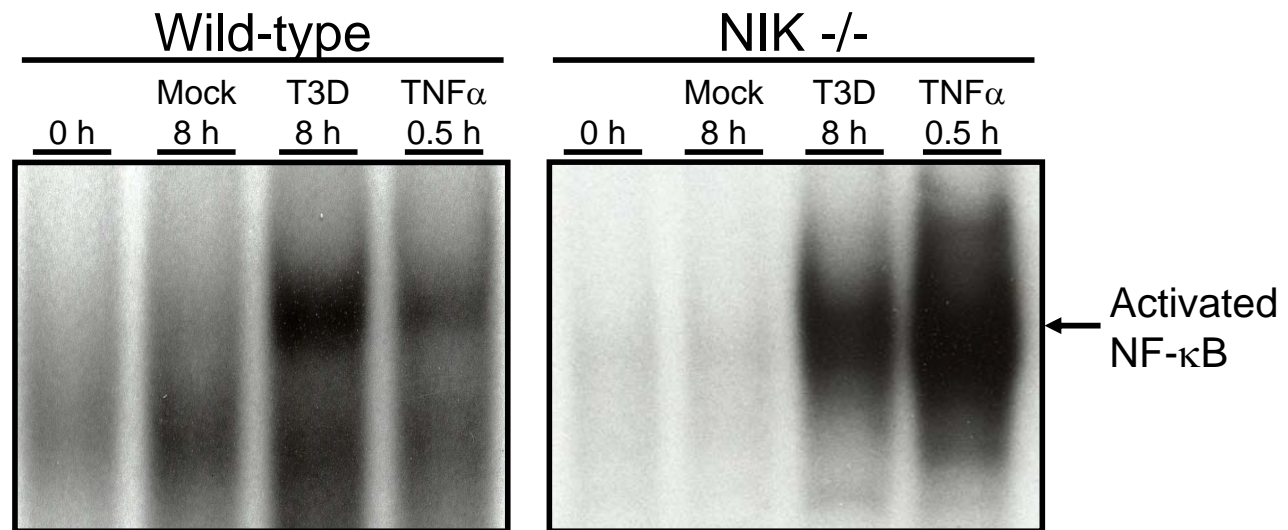


Figure 6

A



B

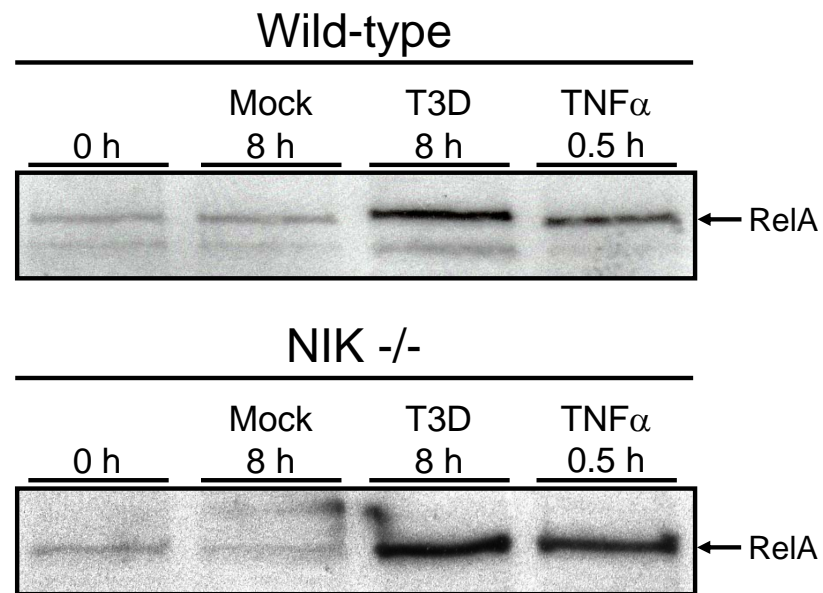
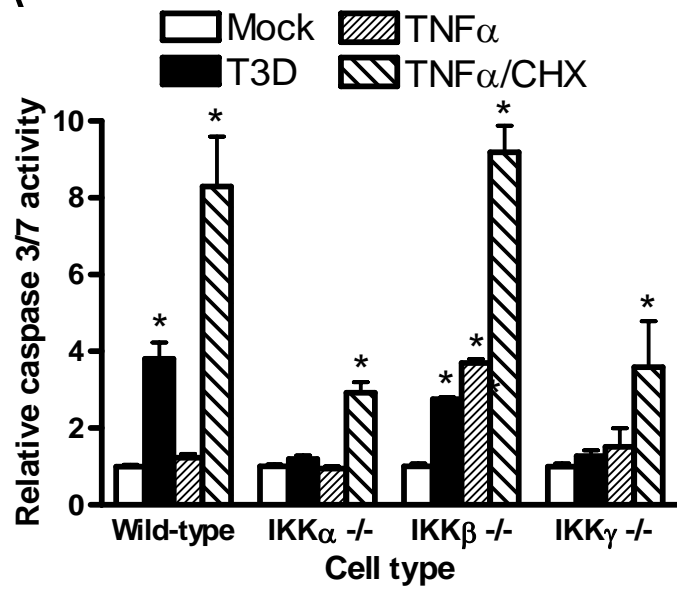
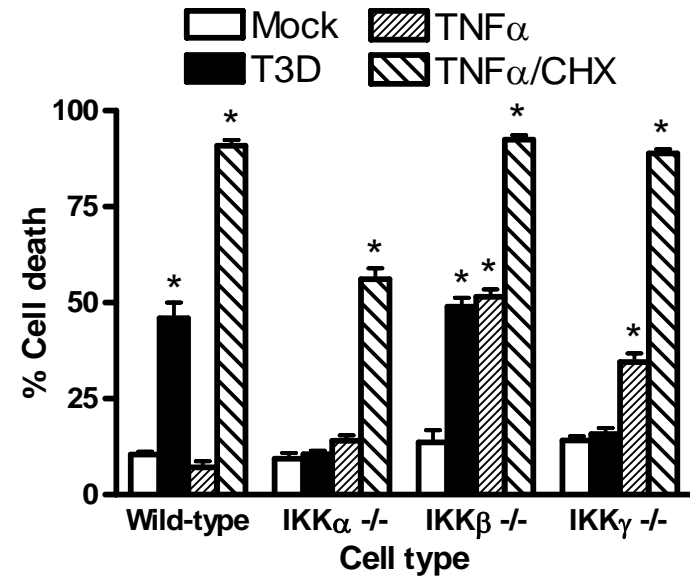


Figure 7

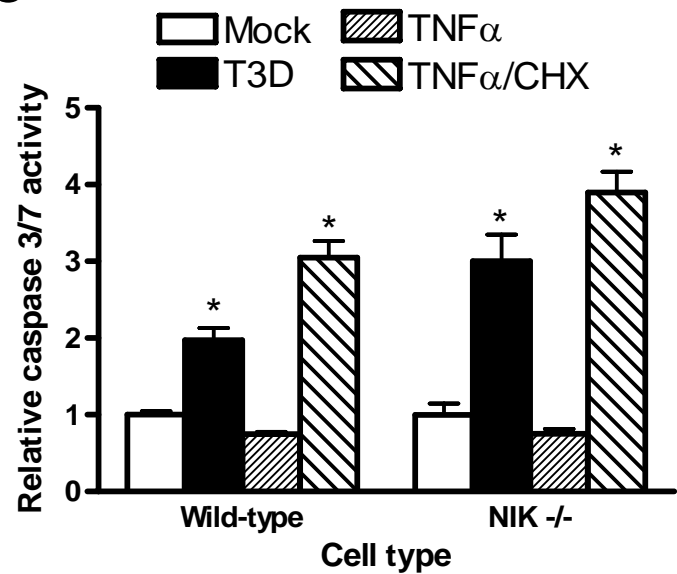
A



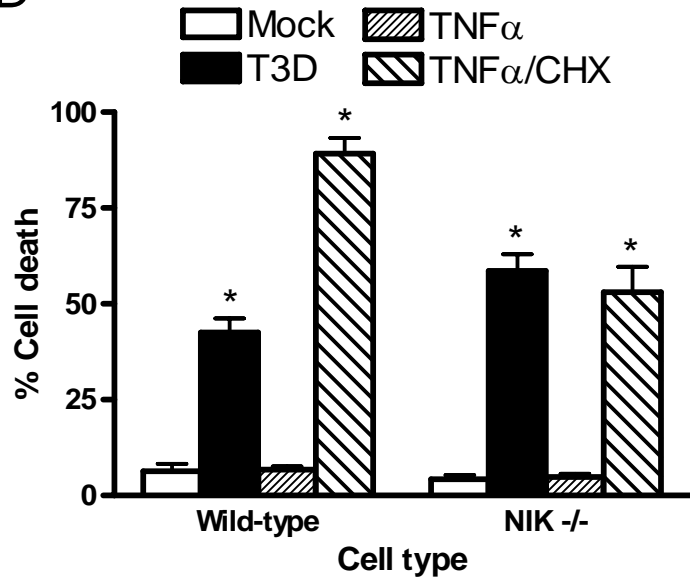
B



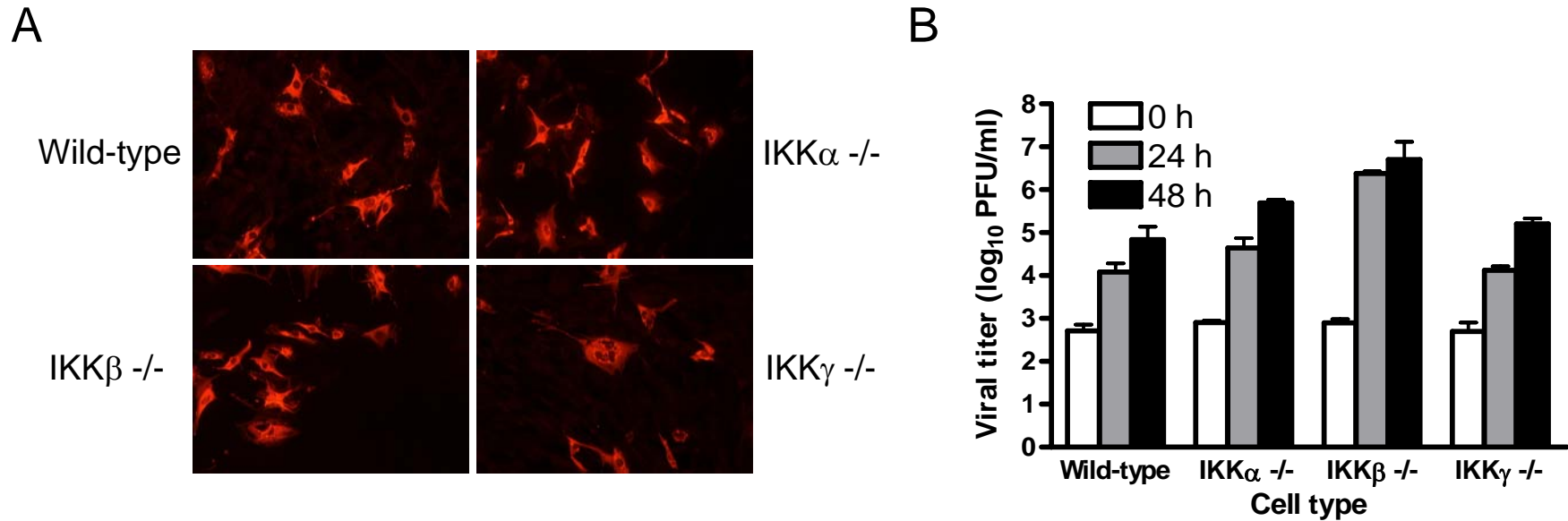
C



D



Data not shown



Data not shown. Cells deficient in IKK subunits are permissive for reovirus infection and growth. (A) Wild-type MEFs or MEFs deficient in IKK α , IKK β , or IKK γ were infected with T3D at an MOI of 1000 PFU/cell. After 24 h incubation, cells were fixed and incubated with reovirus-specific antiserum. Infected cells were identified by using indirect immunofluorescence. (B) Cells and medium were infected with reovirus T3D at an MOI of 1 PFU/cell and incubated for the times shown. Cells and medium were frozen and thawed twice, and viral titers were determined by plaque assay. The results are expressed as the mean viral titers for three independent experiments. Error bars indicate standard deviations.

APPENDIX C

ORGAN-SPECIFIC ROLES FOR TRANSCRIPTION FACTOR NF- κ B IN REOVIRUS-
INDUCED APOPTOSIS AND DISEASE

Sean M. O'Donnell, Mark W. Hansberger, Jodi L. Connolly, James D. Chappell, Melissa J. Watson, Janene M. Pierce, J. Denise Wetzel, Wei Han, Erik S. Barton, J. Craig Forrest, Tibor Valyi-Nagy, Fiona E. Yull, Timothy S. Blackwell, Jeffrey N. Rottman, Barbara Sherry, and Terence S. Dermody

Journal of Clinical Investigation. 115(9): 2341-2350, 2005



Organ-specific roles for transcription factor NF- κ B in reovirus-induced apoptosis and disease

Sean M. O'Donnell,^{1,2} Mark W. Hansberger,^{2,3} Jodi L. Connolly,^{2,3} James D. Chappell,^{2,4} Melissa J. Watson,^{1,2} Janene M. Pierce,⁵ J. Denise Wetzel,^{1,2} Wei Han,⁶ Erik S. Barton,^{2,3} J. Craig Forrest,^{2,3} Tibor Valyi-Nagy,^{2,4} Fiona E. Yull,⁶ Timothy S. Blackwell,⁶ Jeffrey N. Rottman,⁶ Barbara Sherry,⁷ and Terence S. Dermody^{1,2,3}

¹Department of Pediatrics, ²Elizabeth B. Lamb Center for Pediatric Research, ³Department of Microbiology and Immunology, ⁴Department of Pathology, ⁵Department of Surgery, and ⁶Department of Medicine, Vanderbilt University School of Medicine, Nashville, Tennessee, USA. ⁷Department of Molecular Biomedical Sciences, North Carolina State University, Raleigh, North Carolina, USA.

Reovirus induces apoptosis in cultured cells and in vivo. In cell culture models, apoptosis is contingent upon a mechanism involving reovirus-induced activation of transcription factor NF- κ B complexes containing p50 and p65/RelA subunits. To explore the in vivo role of NF- κ B in this process, we tested the capacity of reovirus to induce apoptosis in mice lacking a functional *nfk1/p50* gene. The genetic defect had no apparent effect on reovirus replication in the intestine or dissemination to secondary sites of infection. In comparison to what was observed in wild-type controls, apoptosis was significantly diminished in the CNS of p50-null mice following reovirus infection. In sharp contrast, the loss of p50 was associated with massive reovirus-induced apoptosis and uncontrolled reovirus replication in the heart. Levels of IFN- β mRNA were markedly increased in the hearts of wild-type animals but not p50-null animals infected with reovirus. Treatment of p50-null mice with IFN- β substantially diminished reovirus replication and apoptosis, which suggests that IFN- β induction by NF- κ B protects against reovirus-induced myocarditis. These findings reveal an organ-specific role for NF- κ B in the regulation of reovirus-induced apoptosis, which modulates encephalitis and myocarditis associated with reovirus infection.

Introduction

Mechanisms of viral disease involve complex interactions of pathogen virulence factors and host responses. Perhaps the best-understood basis of organ-specific viral pathology is the availability of cell-surface molecules required for viral attachment and entry. Rarely, however, is viral disease ascribable solely to receptor recognition. More commonly, additional virus-host interactions determine the outcome of infection (1), and these pivotal steps are of much interest in studies of viral pathogenesis. Factors expected to modulate viral growth and virulence in an organ-dependent manner include the capacity of virus to efficiently utilize the host translational apparatus, including strategies to circumvent antiviral effects of IFN; availability of cellular proteins to facilitate viral replication and gene expression; and changes in the intracellular signaling dynamic induced by viral infection.

Mammalian orthoreoviruses (simply called reoviruses here) have served as highly tractable models for studies of viral pathogenesis. Reoviruses are nonenveloped, icosahedral viruses with a genome consisting of 10 double-stranded RNA segments (2). After infection of newborn mice, reoviruses disseminate systemically, producing injury to a variety of organs, including the CNS, heart, and liver (3). Strain-specific differences in receptor utilization influence some types of reovirus disease (4, 5); however, disease pathogenesis at other sites is more complex (6, 7).

The NF- κ B family of transcription factors plays a key role in the regulation of cell growth, activation, differentiation, and survival. Following exposure of cells to a variety of stimuli, NF- κ B is activated and translocated to the nucleus (8), where it serves as a transcriptional regulator (9, 10). In systems in which NF- κ B is activated during apoptosis, NF- κ B can either prevent (10–13) or potentiate (14–17) cell death signaling. Following reovirus infection of cultured cells, the heterodimeric NF- κ B complex p50/p65 translocates to the nucleus and activates proapoptotic gene expression (18). When NF- κ B activation is inhibited using proteasome inhibitors or dominant-negative forms of I κ B α , reovirus-induced apoptosis is blocked (18). Moreover, cell lines deficient in either of the p50 or p65 NF- κ B subunits do not undergo apoptotic cell death following reovirus infection. These findings indicate that activation of NF- κ B in cell culture is required for reovirus-induced apoptosis.

In the CNS (19) and heart (20) of newborn mice, reovirus induces the morphological and biochemical features of apoptosis. This cell-death response in brain and heart tissue is associated with reovirus-induced disease. Inhibitors of apoptosis ameliorate heart disease (20), which indicates a causal relationship between programmed cell death and reovirus-induced myocarditis. However, the molecular basis of CNS and cardiac pathology during reovirus infection has not been fully elucidated.

We now demonstrate that the p50 subunit of NF- κ B plays an essential role in the development of encephalitis and myocarditis in reovirus-infected mice. Although reovirus infects the intestine and disseminates systemically following peroral inoculation of mice lacking the NF- κ B p50 subunit, apoptosis is diminished in the brain yet strikingly enhanced in the heart. These findings sug-

Nonstandard abbreviations used: EMSA, electrophoretic mobility shift assay; HLL, HIV long-terminal repeat luciferase; L cell, L929 cell.

Conflict of interest: The authors have declared that no conflict of interest exists.

Citation for this article: *J. Clin. Invest.* 115:2341–2350 (2005). doi:10.1172/JCI22428.

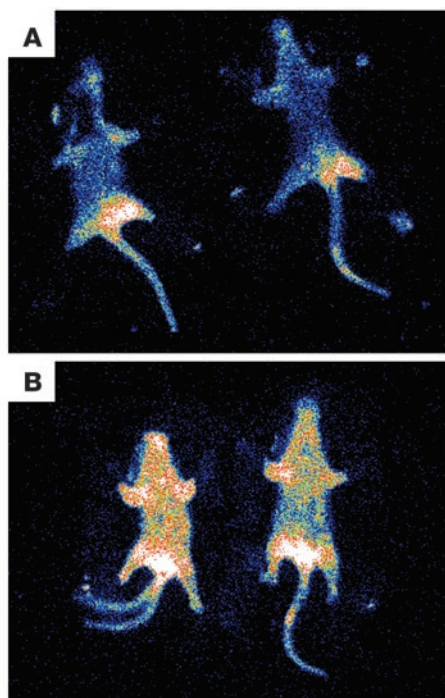


Figure 1

NF- κ B activation following reovirus infection of HLL mice. Newborn HLL mice were inoculated perorally with PBS (**A**) or 10^4 PFU reovirus T3SA+ (**B**). Mice were inoculated intraperitoneally with luciferin 7 days after infection and imaged for luciferase activity as a marker for NF- κ B activation. Bioluminescence indicates areas of NF- κ B activation.

gest a novel role for NF- κ B in the pathogenesis of viral infection; it serves a proapoptotic function in the CNS, while mediating a prosurvival function in the myocardium.

Results

Reovirus activates NF- κ B in vivo. To determine whether reovirus is capable of NF- κ B activation in the intact host, we performed in vivo luciferase assays using transgenic mice engineered to express luciferase under control of an HIV long-terminal repeat promoter that contains NF- κ B consensus binding sites (21). These mice were inoculated perorally with either PBS (mock-infected) or 10^4 PFU reovirus strain T3SA+, which was chosen for these studies because of its capacity to activate NF- κ B and induce a potent apoptotic response in cultured cells (22). Seven days after inoculation, the mice were imaged for luciferase activity as a marker for NF- κ B activation (Figure 1, A and B). Little luciferase activity was detected in the mock-infected mice (Figure 1A). In contrast, reovirus-infected animals exhibited systemic luciferase activity (Figure 1B), which indicated that reovirus is capable of NF- κ B activation in vivo.

Reovirus-induced activation of NF- κ B in the murine CNS and heart is dependent on p50. To determine whether reovirus activates NF- κ B in the murine CNS and heart, we performed electrophoretic mobility shift assays (EMSA) using brain and heart extracts prepared from reovirus-infected or mock-infected wild-type and p50-null mice. Newborn p50^{+/+} and p50^{-/-} mice were inoculated with either PBS or 10^4 PFU reovirus T3SA+. Cell extracts were prepared from brain and heart tissue 12 days after inoculation, incubated with a radiolabeled oligonucleotide consisting of the NF- κ B consensus binding sequence, and resolved by PAGE using nondenaturing conditions (Figure 2, A and D). NF- κ B DNA-binding activity was detected in extracts from the brain of reovirus-infected p50^{+/+} but not p50^{-/-} mice (Figure 2A). Similarly, NF- κ B DNA-binding activity was detected in the heart of p50^{+/+} mice infected with reovirus but not p50^{-/-} animals (Figure 2D). These findings indicate that reovirus infection in

the murine CNS and heart induces nuclear translocation of NF- κ B, which is contingent on the expression of the NF- κ B p50 subunit.

To confirm the specificity of NF- κ B DNA-binding activity in these experiments, we incubated cell extracts from reovirus-infected p50^{+/+} mouse brain and heart with a ³²P-labeled NF- κ B consensus oligonucleotide in the presence of excess unlabeled consensus oligonucleotide (Figure 2, B and E). Binding of the radiolabeled probe was competed with that of unlabeled consensus oligonucleotide, which suggests that the gel-shift activity detected following reovirus infection is specific for sequences that are bound by NF- κ B.

In cell culture, reovirus infection results in the nuclear translocation of NF- κ B complexes containing subunits p50 and p65 (18). As an additional specificity control in these experiments for the activation of NF- κ B, nuclear extracts were prepared from reovirus-infected p50^{+/+} mouse brain or heart and incubated with an antiserum specific to p65 prior to the addition of the NF- κ B-specific oligonucleotide (Figure 2, C and F). Addition of the p65-specific antiserum resulted in bands of higher relative molecular mass, which verified that p65 is present in the NF- κ B complexes activated following reovirus infection. These findings provide strong evidence that reovirus infection of the murine CNS induces the nuclear translocation of NF- κ B and this effect is abolished in mice lacking p50.

NF- κ B subunit p50 is not required for efficient reovirus replication or dissemination in the murine host. To determine whether p50 plays a role in reovirus growth in vivo, we inoculated p50^{+/+} and p50^{-/-} mice intracranially or perorally with 10^4 PFU reovirus T3SA+. Viral titers in the brain were determined by plaque assay 2, 4, and 6 days after intracranial inoculation (Figure 3A) and in the intestine, liver, brain, and heart 4, 6, 8, 10, and 12 days after peroral inoculation (Figure 3B). Following intracranial inoculation, viral titers in p50^{+/+} and p50^{-/-} mice were equivalent at all time points tested. After peroral inoculation, virus replicated efficiently in the intestines of both p50^{+/+} and p50^{-/-} mice and disseminated to the liver, brain, and heart. Viral titers in the intestine, liver, and brain did not differ between p50^{+/+} and p50^{-/-} mice. In sharp contrast, viral titers in the hearts of p50^{-/-} mice were more than 1,000-fold higher than those in the hearts of p50^{+/+} animals. These findings suggest that p50 is dispensable for reovirus growth in vivo and that the absence of p50 in the heart, but not in other tissues tested, allows for increased reovirus replication.

NF- κ B subunit p50 is required for efficient induction of apoptosis in the CNS following reovirus infection. To assess reovirus-induced pathologic changes in the CNS of p50^{+/+} and p50^{-/-} mice, we prepared brain sections from mice euthanized at 12 days following peroral inoculation with reovirus T3SA+ and examined them after staining with H&E (Figure 4, A and B and data not shown). Brain sections from reovirus-infected p50^{+/+} and p50^{-/-} mice exhibited evidence of meningoencephalitis. Inflammatory infiltrates were detected primarily in the cerebral cortex, hippocampus, diencephalon, and brain stem. Morphologically, inflammatory cells were mostly lymphocytes and macrophages/microglia with some plasma cells and neutrophils. Inflammatory changes were more extensive in p50^{+/+} mice (Figure 4A) than in p50^{-/-} mice (Figure 4B),

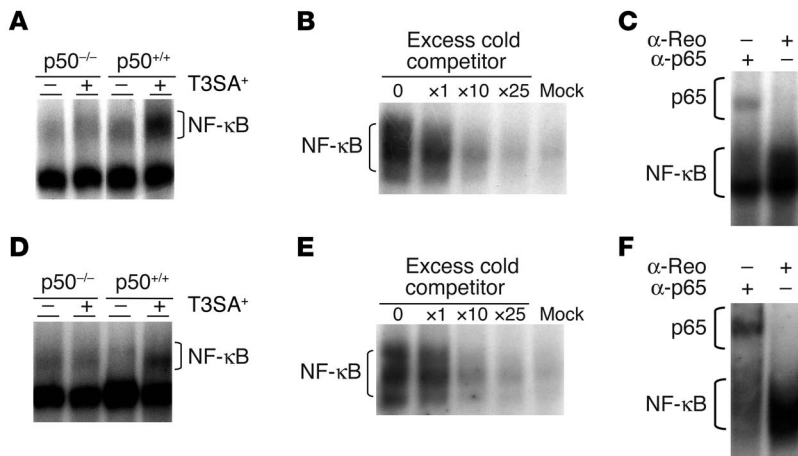


Figure 2 Reovirus-induced NF-κB gel-shift activity following infection of p50^{+/+} and p50^{-/-} mice. (A and D) Newborn p50^{+/+} and p50^{-/-} mice were inoculated perorally with either 10⁴ PFU reovirus T3SA⁺ or PBS. Brains (A) and hearts (D) were resected 12 days after inoculation, and cell extracts were prepared. Extracts were incubated with a ³²P-labeled NF-κB consensus oligonucleotide and resolved by nondenaturing PAGE. Activated NF-κB complexes are indicated. Shown is a representative experiment of 4 performed. (B and E) Extracts were prepared from either brains (B) or hearts (E) of reovirus-infected p50^{+/+} mice and incubated with ³²P-labeled NF-κB consensus oligonucleotide in the presence of unlabeled NF-κB consensus probe (cold competitor) at the molar concentrations shown. Extracts prepared from either brains or hearts of uninfected p50^{+/+} mice were incubated with ³²P-labeled NF-κB consensus oligonucleotide and electrophoresed in the lane labeled “Mock.” NF-κB complexes are indicated. (C and F) Extracts were prepared from either brains (C) or hearts (F) of reovirus-infected p50^{+/+} mice, and prior to the addition of the ³²P-labeled oligonucleotide probe, extracts were incubated with either a control antibody specific to reovirus protein σ3 (α-Reo) or an antibody specific to NF-κB subunit p65 (α-p65). Supershifted complexes containing p65 are indicated.

which suggests that the neurovirulence of reovirus is attenuated in mice lacking an intact NF-κB signaling apparatus.

To assess the distribution of reovirus protein expression in the CNS of p50^{+/+} and p50^{-/-} mice, we prepared brain sections from mice euthanized 12 days following peroral inoculation and stained them using a reovirus-specific antiserum (Figure 4, A and B and data not shown). Immunohistochemical staining for reovirus protein demonstrated the presence of immunoreactive neurons in brains of both p50^{+/+} and p50^{-/-} mice (Figure 4, A and B). Antigen-positive neurons were detected in a pattern recapitulating the inflammatory changes; the cerebral cortex, hippocampus, diencephalon, and brain stem were primarily involved. The number of reovirus-infected cells and their distribution was similar in p50^{+/+} and p50^{-/-} mice (Figure 4, A and B). These results suggest that the lack of p50 does not alter reovirus tropism for specific neural regions.

To determine whether p50 is required for apoptosis in the murine CNS, we prepared brain sections from reovirus-infected p50^{+/+} and p50^{-/-} mice 12 days following peroral inoculation (Figure 4, A and B) or 6 days following intracranial inoculation (Figure 4C) and assayed them for fragmented DNA using the TUNEL technique. Apoptotic cells were quantitated by counting all TUNEL-positive cells in cortex, hippocampus, basal ganglia, diencephalon, and brain stem of each section obtained from mice inoculated intracranially (Figure 5). Numbers of TUNEL-positive cells in the brains of infected p50^{+/+} mice were significantly greater than those in the brains of infected p50^{-/-} mice. These findings were the same following both peroral

and intracranial inoculation (Figure 4). Thus, reovirus-induced apoptosis in the murine CNS is dependent on the p50 subunit of NF-κB.

Activation of caspase-3 is a highly specific biomarker of apoptotic cell death (23). To confirm that DNA fragmentation observed in the brains of reovirus-infected p50^{+/+} mice is due to apoptosis, we stained brain sections with an antiserum specific to the activated form of caspase-3 (Figure 4, A and B). Activated caspase-3 was detected in regions of the brain in which TUNEL-positive staining also was observed. Moreover, cells immunoreactive for caspase-3 were detected at a much higher frequency in the brains of p50^{+/+} mice. Morphologically, cells immunoreactive for caspase-3 were primarily neurons, and most immunoreactive neurons also exhibited morphologic evidence of apoptosis. These results provide additional evidence that expression of NF-κB subunit p50 is required for efficient induction of apoptosis during reovirus infection in the murine CNS.

Absence of NF-κB subunit p50 leads to enhanced pathology and massive apoptosis in the murine heart following reovirus infection. Since viral titers in the hearts of p50^{-/-} mice were more than 1,000-fold higher than in those of p50^{+/+} mice (Figure 3B), we examined heart tissue for evidence of inflammation and tissue injury. Newborn p50^{+/+} and p50^{-/-} mice were inoculated perorally with either 10⁴ PFU reovirus T3SA⁺ or PBS and weighed daily. Mice were euthanized at various time points following inoculation, and hearts were removed and weighed. There were no significant differences in the heart weights of mock-infected p50^{+/+} and p50^{-/-} mice

(Figure 6A). Surprisingly, heart weights of reovirus-infected p50^{-/-} mice were significantly greater than those of p50^{+/+} mice (Figure 6B). Differences in the percent heart weight (heart weight relative to total body weight) of infected p50^{+/+} and p50^{-/-} mice became detectable at 8 days after inoculation and continued to increase with time, while there was no significant increase in the percent heart weight of infected p50^{+/+} mice (Figure 6B). Dramatic differences were observed in the gross appearance of hearts dissected from p50^{+/+} and p50^{-/-} animals following infection with reovirus (Figure 6C). Hearts from reovirus-infected p50^{-/-} mice had a blanched appearance with diffuse surface irregularities corresponding to confluence of purulent lesions, consistent with overt myocarditis. In contrast, hearts from mock-infected p50^{-/-} or p50^{+/+} mice or reovirus-infected p50^{+/+} mice displayed no overt abnormalities.

To determine whether reovirus-induced myocardial injury in p50^{-/-} mice is associated with contractile dysfunction, we performed echocardiography on 10-day-old mice after peroral inoculation with either reovirus T3SA⁺ or PBS. Fractional shortening, assessed by 2-dimensional, directed M-mode measurements, was substantially decreased in reovirus-infected p50^{-/-} mice (~10%; Figure 6D), while it was preserved in mock-infected p50^{-/-} mice (>40%; Figure 6E) and reovirus-infected p50^{+/+} mice (>40%; Figure 6F). Heart size was also increased in reovirus-infected p50^{-/-} mice compared with mock-infected p50^{-/-} mice and reovirus-infected p50^{+/+} mice. Intact atrioventricular conduction was observed in all mice, which suggests that the pathologic process was not specifically

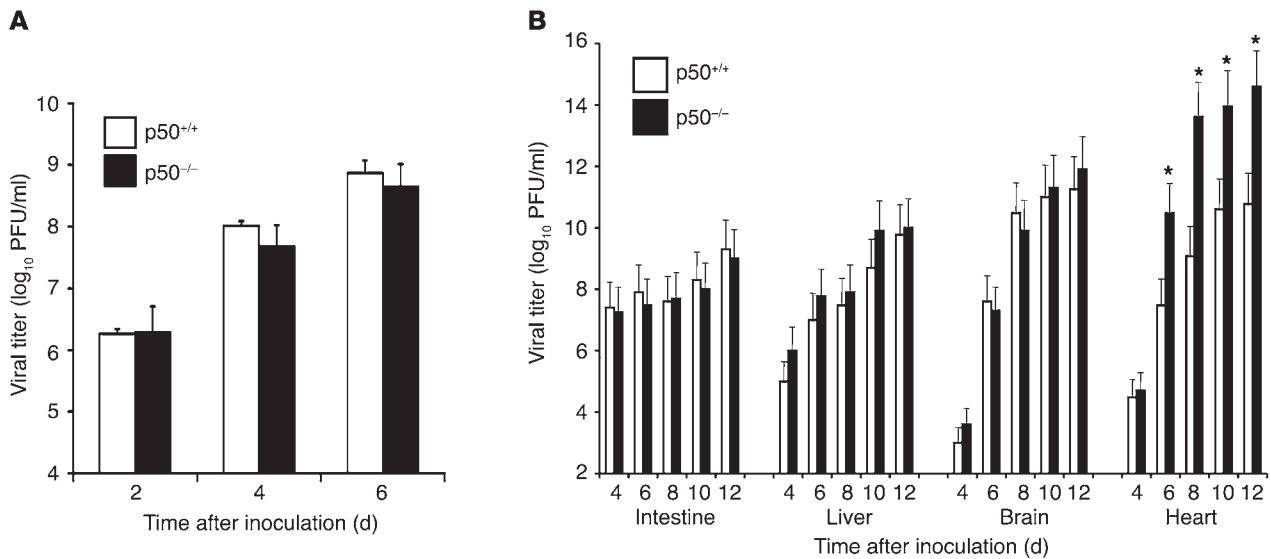


Figure 3 Growth of reovirus in p50^{+/+} and p50^{-/-} mice. **(A)** Titers of reovirus in brain after intracranial inoculation of p50^{+/+} and p50^{-/-} mice. Newborn mice were inoculated with 10⁴ PFU reovirus T3SA⁺. At days 2, 4, and 6 after inoculation, mice were euthanized, brains were harvested, and viral titers were determined by plaque assay. **(B)** Titers of reovirus in intestine, liver, brain, and heart after peroral inoculation of p50^{+/+} and p50^{-/-} mice. Newborn mice were inoculated with 10⁴ PFU T3SA⁺. At days 4, 6, 8, 10, and 12 after inoculation, mice were euthanized, organs were harvested, and viral titers were determined by plaque assay. The results are expressed as the mean viral titers for 2–4 **(A)** or 4–8 **(B)** animals for each time point. Error bars indicate SDs. *P < 0.05 by Student's t test.

targeted to the conduction system. These results suggest that the myocardial pathology associated with reovirus infection of p50^{-/-} mice is associated with diminished contractility.

On a microscopic level, hearts of p50^{-/-} animals displayed extensive myocyte destruction with features of apoptotic and necrotic cell death. Affected areas were notable for cell fragments, granular debris, and scattered calcifications. Thorough sectioning of the organ block revealed that pathology was not limited to any particular region of the heart. Hearts from reovirus-infected p50^{+/+} mice and mock-infected p50^{-/-} and p50^{+/+} mice demonstrated no significant microscopic pathology. We conclude that reovirus is more pathogenic in the heart in the absence of NF-κB subunit p50.

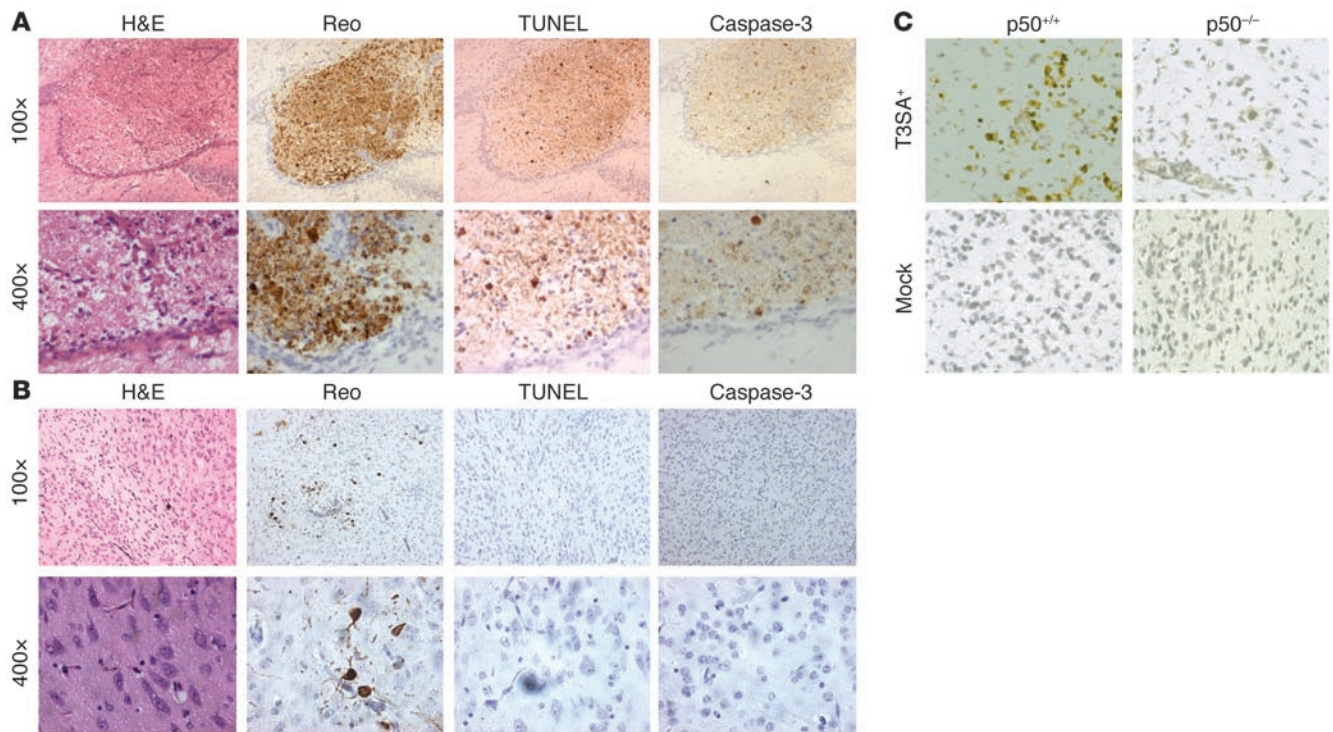
To assess the extent and location of reovirus infection in the murine myocardium in the presence and absence of p50, we performed reovirus antigen staining on heart sections from p50^{+/+} and p50^{-/-} mice euthanized 12 days following peroral inoculation with reovirus T3SA⁺ (Figure 7, A and B). Immunohistochemical staining for reovirus protein demonstrated immunoreactive myocytes in heart sections prepared from both p50^{+/+} and p50^{-/-} mice (Figure 7, A and B). However, the number of reovirus-infected cells differed substantially between p50^{+/+} and p50^{-/-} mice, consistent with the significant difference in viral titer in the hearts of these animals.

To determine whether expression of p50 influences apoptosis in the murine heart, we inoculated p50^{+/+} and p50^{-/-} mice perorally with reovirus and assessed them for apoptosis using TUNEL staining (Figure 7, A and B). There were rare TUNEL-positive cells in the hearts of p50^{+/+} mice following reovirus infection (Figure 7A), whereas numerous foci of apoptosis were present in the hearts of p50^{-/-} mice (Figure 7B). Interestingly, foci of apoptotic cells in the hearts of p50^{-/-} mice coincided with areas of intense staining for reovirus antigen, which suggests a link between reovirus replication and apoptosis in cardiomyocytes.

To confirm that the absence of p50 leads to enhanced apoptosis in the heart during reovirus infection, we prepared heart sections from p50^{+/+} and p50^{-/-} mice 12 days following peroral inoculation with reovirus and stained them for activated caspase-3 (Figure 7, A and B). Caspase-3 staining revealed numerous positive myocytes in the same areas of the heart that also were positive for reovirus antigen and TUNEL staining. These results suggest that, in contrast to its effects in the murine CNS, the NF-κB p50 subunit protects against apoptosis induced by reovirus infection in the murine myocardium.

IFN-β is induced in the heart of wild-type mice following reovirus infection. Results presented thus far demonstrate that enhanced reovirus growth in the heart of p50^{-/-} mice is associated with massive apoptosis. We thought it possible that the absence of NF-κB-mediated activation of innate immune responses might lead to increased viral replication and resultant pathology in the heart. To test this hypothesis, we inoculated p50^{+/+} and p50^{-/-} mice perorally with reovirus T3SA⁺ or PBS. Twelve days after inoculation, heart and brain were removed, and levels of IFN-β mRNA were determined using real-time PCR (Figure 8). Using GAPDH mRNA as a standardization control, little IFN-β mRNA was induced in the brain of either p50^{-/-} or p50^{+/+} mice in the presence or absence of reovirus infection (Figure 8). In contrast, IFN-β mRNA levels were substantially increased in the heart of reovirus-infected wild-type mice compared with p50^{-/-} animals (Figure 8). These results indicate that IFN-β induction by reovirus in the murine heart is dependent on NF-κB and suggest that IFN-β protects the heart from reovirus-induced apoptosis and disease.

IFN-β treatment of p50-null mice attenuates reovirus-induced myocarditis. To determine whether NF-κB-mediated expression of IFN-β plays a direct role in protection of the heart against apoptosis and disease caused by reovirus, we tested the effect of IFN-β treatment on reovirus infection of p50^{-/-} mice. Newborn p50^{-/-} mice were inoculated intraperitoneally with either IFN-β or PBS 1 day prior

**Figure 4**

Inflammation, reovirus protein expression, TUNEL staining, and immunohistochemical detection of activated caspase-3 in the brain of reovirus-infected p50^{+/+} (A) and p50^{-/-} (B) mice. Newborn mice were inoculated perorally with 10⁴ PFU reovirus T3SA⁺. At 12 days after inoculation, brains were harvested, paraffin embedded, sectioned, and stained with H&E, polyclonal reovirus-specific antiserum (Reo), TUNEL, or activated caspase-3-specific antiserum as indicated. Shown are consecutive sections of diencephalon. Original magnification, ×100 (top panels) and ×400 (bottom panels). (C) Newborn mice were inoculated intracranially with 10⁴ PFU T3SA⁺ or gelatin saline (Mock). At 6 days after inoculation, mice were euthanized, and brain sections were stained using a TUNEL assay. Shown are sections of the upper brain stem. Original magnification, ×200. Brown staining indicates reovirus protein, fragmented DNA, or activated caspase-3.

to peroral inoculation with reovirus T3SA⁺ and treated daily for 9 days thereafter. On day 10, the animals were euthanized, and brain and heart were removed for determination of viral titer and histopathology (Figure 9). IFN-β treatment significantly decreased viral titer in both brain and heart (Figure 9A). In p50^{-/-} mice treated with IFN-β, viral titers reached only 10² PFU in the brain and were less than 10² PFU in the heart (Figure 9A). In parallel with these results, apoptosis in the heart of IFN-β-treated p50^{-/-} mice was substantially diminished (Figure 9B). Thus, a critical component of the underlying mechanism of NF-κB-mediated protection against reovirus-induced myocardial injury is contingent on IFN-β.

Discussion

Here we report organ-specific roles for NF-κB in the pathogenesis of viral disease, which is a heretofore unknown property of this signaling molecule. The key finding is that marked differences in the pathogenesis of reovirus infection in the CNS and heart are dependent on the action of NF-κB. Following reovirus infection in the CNS, p50^{+/+} mice exhibited significant neuronal apoptosis, while p50^{-/-} mice displayed a minimal apoptotic response. In sharp contrast, reovirus induced little apoptosis in the heart of p50^{+/+} mice, whereas extensive apoptosis occurred in the heart of p50^{-/-} mice. These findings indicate that NF-κB subunit p50 plays 2 distinctly different roles in reovirus pathogenesis, serving a proapoptotic function in the brain, while mediating a prosurvival function in the heart.

The NF-κB family of transcription factors is composed of p50/p105, p52/p100, p65 (RelA), c-Rel, and RelB. Studies using mice with targeted disruptions of specific NF-κB subunits have shown that NF-κB serves important functions in the development and function of innate and adaptive immunity (24–26). Mice lacking p50 have no apparent developmental defects (24), and immune cells mature normally. However, p50^{-/-} mice display defects in B cell activation, isotype switching, and antibody production (24). These defects render p50^{-/-} mice more susceptible to infection by the Gram-positive bacterial pathogen *Streptococcus pneumoniae*, but they remain capable of efficiently clearing infection by the Gram-negative pathogens *Escherichia coli* and *Haemophilus influenzae* (24). When p50^{-/-} mice are infected with encephalomyocarditis virus, they are actually more resistant to infection than controls. This difference is thought to be due to an increase in apoptosis that leads to a decrease in viral growth (24). These findings stand in stark contrast to what occurs in the CNS and heart of reovirus-infected mice.

In experiments comparing reovirus infection of p50^{+/+} and p50^{-/-} mice, we found that the presence or absence of p50 did not alter primary viral replication in intestinal tissue or dissemination of virus to the liver, brain, or heart. Although viral replication in the brain after intracranial inoculation also was independent of p50, replication in the heart was increased in p50^{-/-} mice by approximately 1,000-fold. What might explain the enhancement of reovirus replication in the heart of p50^{-/-} mice? Reovirus strains have

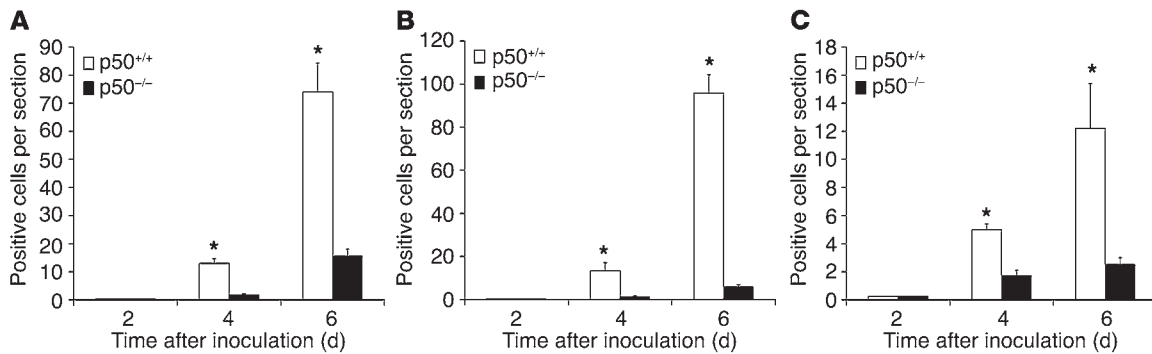


Figure 5 Quantitation of TUNEL staining in cortex and hippocampus (A), basal ganglia and diencephalon (B), and brain stem (C) of reovirus-infected p50^{+/+} and p50^{-/-} mice. TUNEL staining was performed using tissue sections prepared 2, 4, and 6 days following intracranial inoculation of p50^{+/+} and p50^{-/-} mice with 10⁴ PFU reovirus T3SA⁺. For each brain region, all positive cells in a single parasagittal section were counted for 4–8 animals. The results are expressed as the mean number of apoptotic cells per region. Error bars indicate SDs. **P* < 0.05 by Student's *t* test.

been characterized previously as having the capacity to grow in the murine heart and produce cardiac disease (27, 28). In primary cardiomyocytes, nonmyocarditic reovirus strains induce more IFN- β and are more sensitive to the antiviral effects of this cytokine than myocarditic reovirus strains (29). Furthermore, normally nonmyocarditic strains are capable of producing myocarditis in infected IFN- α/β mice (29). Thus, it appears that type I IFNs restrict viral replication in the heart and attenuate cardiac disease.

NF- κ B is known to induce the expression of several mediators of innate immune responses including type I IFNs (30–32). Therefore, absence of p50 may allow reovirus to achieve much higher titers and cause myocarditis. We tested this hypothesis by determining brain and heart levels of IFN- β mRNA in response to reovirus infection of p50^{+/+} and p50^{-/-} mice (Figure 8) and by treating reovirus-infected p50^{-/-} mice with IFN- β (Figure 9). In these experiments, we found a dramatic increase in IFN- β expression in the hearts of wild-type mice but only a minimal IFN- β response in the hearts of p50-null animals. Moreover, reconstitution of p50^{-/-} mice with IFN- β substantially diminished reovirus replication and apoptosis, which resulted in diminished myocardial injury. These results indicate that IFN- β is a necessary component of the NF- κ B-mediated protective response against reovirus in the heart. However, it is likely that other components of innate immunity are involved in this effect. Preliminary data from our laboratory suggest that in addition to IFN- β , IL-6, MIF, and TNF are expressed at higher levels in the heart of p50^{+/+} mice than p50^{-/-} mice (S.M. O'Donnell and T.S. Dermody, unpublished observation). These findings suggest that following reovirus infection of the heart, NF- κ B is activated and leads to induction of potent innate immune responses, which in turn attenuate viral replication at that site, resulting in diminished apoptosis and disease.

The enhanced growth of reovirus in the heart of p50^{-/-} mice compared with p50^{+/+} mice was associated with extensive myocarditis and resultant tissue injury and dysfunction. This result was confirmed by histopathological studies, echocardiography, and physical examination revealing signs of heart failure. The pathology observed in the heart of p50^{-/-} animals was characterized by extensive tissue damage and little inflammatory infiltrate, similar to findings made in previous studies of reovirus myocarditis (27). Therefore, our results suggest that apoptosis is the primary mechanism of cardiac damage in reovirus-induced myocarditis, as reported previously (20). Damage to cardiomyocytes during reovirus infection occurs in

the complete absence of adaptive components of host defense (33). It is possible that a similar mechanism occurs in humans, which would explain why some patients with acute myocarditis develop heart failure in the setting of sustained viremia (34).

In contrast to the enhanced growth of reovirus in the heart of p50^{-/-} mice, viral growth in the CNS of p50^{+/+} and p50^{-/-} mice was equivalent. However, we observed dramatic differences in the number of apoptotic cells in the 2 mouse strains as indicated by TUNEL and caspase-3 staining. Therefore, the efficiency of viral growth is not strictly correlated with the extent of the apoptotic response. Nonetheless, despite these p50-dependent differences in viral growth, our results suggest that apoptosis is an important mechanism of reovirus-induced disease in both the CNS and heart. In the CNS of p50^{-/-} mice, apoptosis and inflammation following reovirus infection were diminished. However, in the hearts of these animals, apoptosis and tissue injury were enhanced. This correlation between apoptosis and pathology lends support to the hypothesis that therapies directed at blocking programmed cell death might attenuate viral virulence, consistent with results from previous studies of reovirus-induced myocarditis (20). However, our findings suggest that pharmacologic inhibition of NF- κ B activation may reduce pathologic injury at some sites and exacerbate disease at others, depending on the nature of the NF- κ B agonist.

The precise cell types responsible for the p50-dependent effects on apoptosis in response to reovirus infection in mice are not apparent from our study. It is possible that expression of p50 in neurons is required for apoptosis of these cells and expression of p50 in cardiomyocytes mediates protection of these cells against apoptotic injury. However, it is also possible that p50-dependent immune responses contribute to the observed differences in cell fate. For example, NF- κ B-mediated release of cytokines such as TNF- α from immune cells might contribute to the neuronal apoptosis that occurs during reovirus infection of the CNS, whereas NF- κ B-mediated release of type I IFNs from immune cells might mediate a protective effect in the heart. Since adoptive transfer of immune cells is not technically feasible in the newborn mice required for studies of reovirus pathogenesis, discrimination between these possibilities awaits the development of mice with tissue-specific ablation of NF- κ B activity.

The role of NF- κ B in response to a variety of cellular stresses has been studied extensively using cultured cells (35). However, little is known about the contributions of specific NF- κ B subunits in vivo.

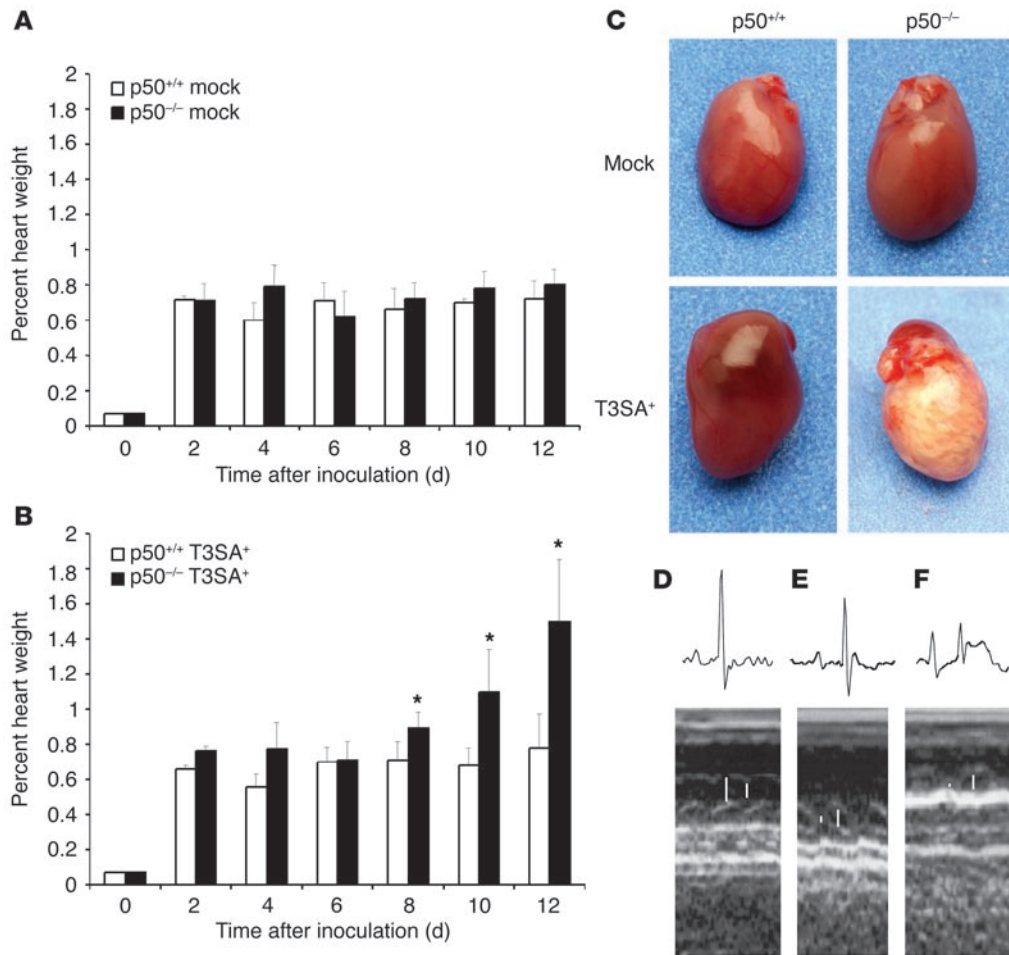


Figure 6 Heart pathology following reovirus infection of p50^{+/+} and p50^{-/-} mice. **(A and B)** Newborn p50^{+/+} and p50^{-/-} mice were inoculated perorally with either PBS (mock) **(A)** or 10⁴ PFU reovirus T3SA⁺ **(B)**, and heart size was monitored at 2-day intervals. Percent heart weight was calculated as heart weight divided by body weight. The results are expressed as the mean heart weights of at least 4 animals for each time point. Error bars indicate SDs. *P < 0.05 by Student's *t* test. **(C)** Hearts from mice euthanized 12 days following peroral inoculation with reovirus T3SA⁺ or gelatin saline (Mock). **(D, E, and F)** Electrocardiography and echocardiography of reovirus-infected p50^{-/-} **(D)**, mock-infected p50^{-/-} **(E)**, and reovirus-infected **(F)** p50^{+/+} mice. Newborn mice were inoculated perorally with 10⁴ PFU T3SA⁺, and tests were performed 10 days after inoculation. A P-wave/QRS ECG complex is displayed above the corresponding echocardiographic image. Systolic and diastolic LV cavity dimensions are indicated by bars superimposed on the M-mode images.

The extensive array of NF-κB inducers and target genes (36) suggests that numerous mechanisms exist to direct transcription of appropriate NF-κB-dependent genes in response to specific stimuli. One such regulatory mechanism is likely to be the activation of specific NF-κB complexes (e.g., p50/p65 heterodimers) for each inducing signal. Individual homodimeric and heterodimeric NF-κB complexes exhibit different affinities for target DNA sequences (37), and this provides a potential mechanism by which NF-κB-inducing stimuli regulate transcriptional activity of specific subsets of cellular genes. We showed previously that reovirus requires p50/p65 for efficient apoptosis in cell culture (18). However, we found in the current study that p50 plays organ-specific roles in disease pathogenesis *in vivo*. These findings emphasize that NF-κB subunits can have different functions following activation with the same stimulus depending on the cellular environment. Continuing studies in this area may

reveal new layers of control of NF-κB responses and extend understanding of how viruses cause tissue-specific injury.

Methods

Cells, virus, and antibodies. Spinner-adapted murine L929 cells (L cells) were grown in suspension or monolayer culture and maintained as described previously (18). Reovirus strain T3SA⁺ was generated by reassortment of reovirus strains type 1 Lang (T1L) and type 3 clone 44-MA (5). Virus was purified after growth in L cells by cesium chloride gradient centrifugation (38). Rabbit polyclonal anti-reovirus serum raised against strain T1L was obtained as described previously (22). Rabbit polyclonal antiserum specific to the activated form of caspase-3 (anti-caspase-3/Asp 175) was obtained from Cell Signaling Technology.

Mice and inoculations. HIV long-terminal repeat luciferase (HLL) mice were generated as described previously (39). Control p50^{+/+} mice (B6129PF1/J-A^W/A^W) and p50^{-/-} mice (B6129P-Nfkb1^{tm1Bal}) (24) were obtained from The Jackson Laboratory. Newborn mice weighing 2.0–2.5 g (2–4 days old) were inoculated either intracranially or perorally with purified T3SA⁺ diluted in PBS. Intracranial inoculations were delivered to the right and left cerebral hemispheres (5 μl each) using a Hamilton syringe (BD Bio-

sciences) and a 30-gauge needle (40). Peroral inoculations were delivered into the stomach (50 μl) by passage of a polyethylene catheter 0.61 mm in diameter (BD) through the esophagus (41). The inoculum contained 0.5% (vol/vol) green food coloring so that accuracy of delivery could be judged. For determination of NF-κB activation, viral titer, and immunohistochemical staining, mice were euthanized at various intervals following inoculation, and organs were collected.

Assessment of NF-κB activation by *in vivo* luciferase activity. Two-day-old HLL mice were inoculated perorally with either 10⁴ PFU T3SA⁺ or PBS. Mice were anesthetized with isoflurane before imaging and immobilized for the duration of the integration time of photon counting (3 minutes). Luciferin (0.75 g/mouse in 0.2 ml isotonic saline) was inoculated intraperitoneally, and mice were imaged using an intensified charge-coupled device camera (C2400-32; Hamamatsu Corp.). For the duration of photon counting, mice were placed inside a light-tight box. Light

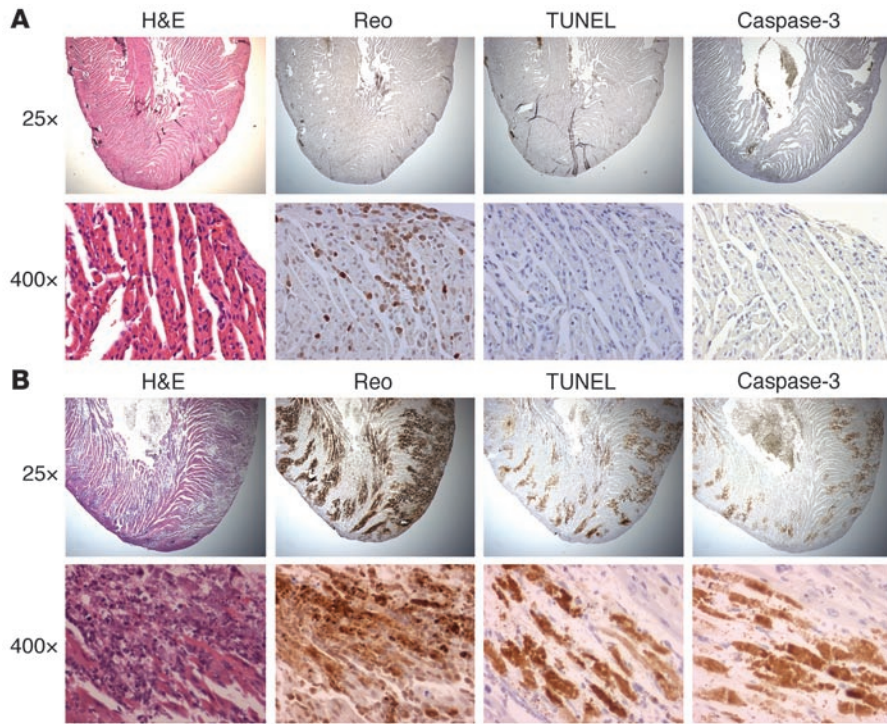


Figure 7
Inflammation, reovirus protein expression, TUNEL staining, and immunohistochemical detection of activated caspase-3 in the heart of reovirus-infected p50^{+/+} (A) and p50^{-/-} mice (B). Newborn mice were inoculated perorally with 10⁴ PFU reovirus T3SA⁺. At 12 days after inoculation, hearts were harvested, paraffin embedded, sectioned, and stained with H&E, polyclonal reovirus-specific antiserum, TUNEL, or activated caspase-3-specific antiserum as indicated. Original magnification, ×25 (top panels) and ×400 (bottom panels). Brown staining indicates reovirus protein, fragmented DNA, or activated caspase-3.

emission from each mouse was detected as photon counts, and a digital false-color photon emission image of the mouse was generated.

EMSA. Two-day-old p50^{+/+} and p50^{-/-} mice were inoculated perorally with either 10⁴ PFU T3SA⁺ or PBS. Mice were euthanized 12 days after inoculation. Brains and hearts were aseptically removed, snap frozen on dry ice, and stored at -70°C. Organs were weighed, placed in a mortar with liquid nitrogen, and ground into a powder. Lysis buffer (20 mM HEPES [pH 7.9], 25% glycerol, 0.42 M NaCl, 1.5 mM MgCl₂, 0.2 mM EDTA, 0.5 mM phenylmethylsulfonyl fluoride, 0.5 mM dithiothreitol) was added in a ratio of 1 ml per 200 mg of tissue. Samples were frozen and thawed 3 times and centrifuged at 12,000 g for 10 minutes. The supernatant was used as the whole-cell extract.

Whole-cell extracts (10 µg total protein) were assayed for NF-κB activation by EMSA using a ³²P-labeled oligonucleotide (1.0 ng) consisting of the NF-κB consensus binding sequence (Santa Cruz Biotechnology Inc.) as described previously (18). For competition experiments, unlabeled consensus oligonucleotide at various concentrations was added to the reaction mixtures along with radiolabeled oligonucleotide. For supershift experiments, 1 µl of a rabbit polyclonal antiserum specific to p65 (250 µg/ml; Santa Cruz Biotechnology Inc.) was added to the binding reaction mixtures and incubated at 4°C for 30 minutes prior to the addition of radiolabeled oligonucleotide. Nucleoprotein complexes were subjected to electrophoresis in native polyacrylamide gels, which were dried and exposed to film.

Determination of viral titer in infected organs. Organs (intestine, liver, heart, and brain) from infected p50^{+/+} and p50^{-/-} mice were placed into vials containing 1 ml gelatin saline, frozen (-20°C) and thawed once, and sonicated for 20 seconds. Titers of virus present in organ homogenates were determined by plaque assay using L cell monolayers (42).

Histology, immunohistochemistry, and TUNEL staining. Litters of newborn p50^{+/+} and p50^{-/-} mice were inoculated intracranially or perorally with either 10⁴ PFU T3SA⁺ or PBS. Mice were euthanized, and brain and heart tissues were fixed in 10% buffered paraformaldehyde. Fixed organs were embedded in paraffin, and 6-µm histological sections were prepared. Sections were stained with H&E for evaluation of histopathologic changes, processed for immunohistochemical

detection of reovirus protein, assayed for DNA fragmentation using the TUNEL technique (43), or processed for the immunohistochemical detection of activated caspase-3 (5). Cells demonstrating TUNEL staining were quantitated separately in each parasagittal brain section in the following regions: cerebral cortex, hippocampus, basal ganglia, diencephalon, and brain stem. The mean number of positive cells per region was determined for each treatment group and time point. Observers were blinded to the identity of the mouse strain and the nature of the inoculum.

Echocardiography. Echocardiography was performed on conscious 10-day-old pups as previously described for adult mice (44) except that the total field depth was set to 1 cm (minimum possible), and external heating and rapid

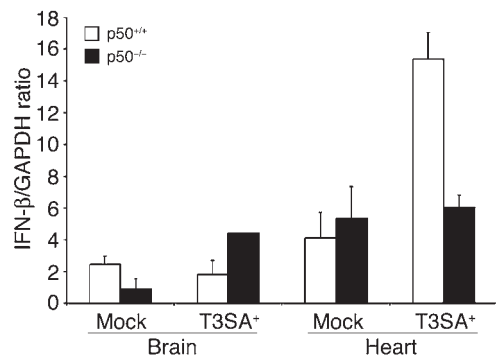
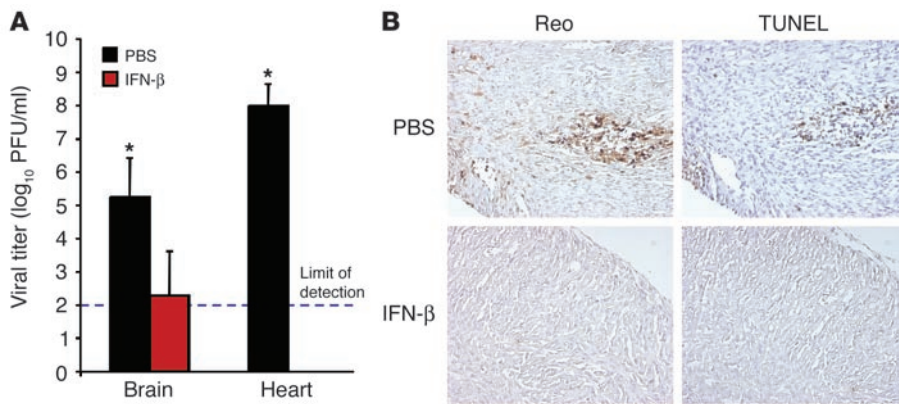


Figure 8
Levels of IFN-β mRNA in brain and heart of p50^{+/+} and p50^{-/-} mice. Newborn mice were inoculated perorally with either PBS (Mock) or 10⁴ PFU reovirus T3SA⁺. At 12 days after inoculation, brains and hearts were resected, and whole-organ RNA was isolated and used as a template to generate cDNA. Levels of IFN-β and GAPDH cDNA were assessed by real-time PCR. The results are expressed as the mean ratio of IFN-β cDNA to that of GAPDH for 2 animals. Error bars indicate SDs.

**Figure 9**

Reovirus replication and apoptosis in infected $p50^{-/-}$ mice following treatment with IFN- β . Newborn mice were inoculated intraperitoneally with either IFN- β or PBS 1 day prior to peroral inoculation with 10^4 PFU reovirus T3SA⁺. Animals were treated with either IFN- β or PBS for an additional 9 days, and brains and hearts were resected. (A) Viral titers in the brain and heart. Organs were homogenized, and viral titers were determined by plaque assay. The results are expressed as the mean viral titers for 3 animals. Error bars indicate SDs. * $P < 0.05$ by Student's t test. (B) Histopathology of reovirus infection in the heart. Hearts of the reovirus-infected $p50^{-/-}$ animals represented in A were paraffin embedded, sectioned, and stained with polyclonal reovirus-specific antiserum or processed for TUNEL analysis. Original magnification, $\times 100$. Brown staining indicates reovirus protein or fragmented DNA.

sample acquisition were used to prevent excessive heat loss. Electrocardiograms were digitally sampled and correspond to the usual surface lead I.

RNA isolation and real-time PCR. Two-day-old $p50^{+/+}$ and $p50^{-/-}$ mice were inoculated perorally with either 10^4 PFU T3SA⁺ or PBS. Mice were euthanized, and brain and heart tissues were homogenized using a Dounce homogenizer. RNA was extracted from brain and heart homogenates using the TRIZOL RNA extraction protocol (Invitrogen Corp.). Three micrograms of RNA was used in a reverse-transcription reaction containing $\times 10$ buffer, 25 mM MgCl₂, 100 μ M dithiothreitol, and 1 U RNasin (Promega), 10 mM dNTPs, 50 μ M random hexamers, and 1 U AMV reverse transcriptase (Promega). The reaction was incubated at 43°C for 1 hour and then at 95°C for 10 minutes.

Real-time PCR reactions were carried out using the Bio-Rad iCycler and iQ Supermix buffer containing DNA polymerase and SYBR Green (Bio-Rad Laboratories). Two to 3 replicate amplification reactions were performed in 96-well plates (Bio-Rad Laboratories). Each reaction contained 12.5 μ l iQ Supermix buffer, 300 nM forward and reverse primers, and 1 μ l cDNA in a final volume of 25 μ l. Primers for the reactions were as follows: (a) IFN- β forward, 5'-GGAGATGACGGAGAAGATGC-3', (b) IFN- β reverse, 5'-CCCAGT-GCTGGAGAAATTGT-3', (c) GAPDH forward, 5'-CAACTACATGGTCTA-CATGTTTC-3', and (d) GAPDH reverse, 5'-CTCGCTCCTGGAAGATG-3'. Cycling conditions were as follows: 95°C for 10 minutes and then 45 cycles at 95°C for 15 seconds, 60°C for 30 seconds, and 72°C for 15 seconds.

Data were analyzed using Bio-Rad iCycler PCR detection and analysis software version 3.0 (Bio-Rad Laboratories). DNA was quantitated using the standard curve method with the background subtracted. Known concentrations of cDNA were used to obtain the standard curve for each gene (concentrations between 0.0228 and 710 ng). A melting curve was determined for each sample to detect primer dimers, in which case data were not used. Results are expressed as values for IFN- β cDNA divided by those for GAPDH cDNA.

IFN- β treatment of mice. Two-day-old $p50^{-/-}$ mice were inoculated intraperitoneally with either 5×10^4 U IFN- β (Calbiochem) suspended in PBS containing 0.1% BSA or PBS alone in a volume of 25 μ l 1 day prior to peroral inoculation with 10^4 PFU T3SA⁺. Infected mice were treated daily for 9 days with either IFN- β or PBS. On day 10 following viral inoculation, animals

were euthanized, and organs were removed. Organs were processed for determination of viral titer and histopathological analysis.

Animal husbandry and experimental procedures were performed in accordance with NIH Public Health Service policy and approved by the Vanderbilt University School of Medicine Institutional Animal Care and Use Committee.

Data analysis. Results are expressed as the mean \pm SD. Differences between mean values were compared using unpaired Student's t tests as applied with Microsoft Excel software. P values less than 0.05 were considered statistically significant.

Acknowledgments

We thank Kelly Parman at the Vanderbilt Mouse Pathology Core Lab for tissue sectioning and Greg Hanley and Joan Richerson for expert veterinary care. We are grateful to Dean Ballard for review of the manuscript and Scott Baldwin and Luc Van Kaer for essential discussions. This research was supported by NIH Public Health Service awards T32 AI07474 (to S.M. O'Donnell and T. Valyi-Nagy), T32 HL07751 (to J.D. Chappell), T32 CA09385 (to J.C. Forrest), and R01 AI50080, and grants from the National Science Foundation (to E.S. Barton), the Vanderbilt University Medical Scholars Program (to M.J. Watson), the Vanderbilt University Research Council (to E.S. Barton and J.C. Forrest), and the Elizabeth B. Lamb Center for Pediatric Research. Additional support was provided by NIH Public Health Service awards CA68485 to the Vanderbilt-Ingram Cancer Center and DK20593 to the Vanderbilt Diabetes Research and Training Center.

Received for publication June 14, 2004, and accepted in revised form May 31, 2005.

Address correspondence to: Terence S. Dermody, Elizabeth B. Lamb Center for Pediatric Research, D7235 Medical Center North, Vanderbilt University School of Medicine, 1161 21st Avenue South, Nashville, Tennessee 37232, USA. Phone: (615) 343-9943; Fax: (615) 343-9723; E-mail: terry.dermody@vanderbilt.edu.

Jodi L. Connolly's present address is: Isis Pharmaceuticals, Carlsbad, California, USA.

Melissa J. Watson's present address is: Department of Surgery, UCLA Medical Center, Los Angeles, California, USA.

Erik S. Barton's present address is: Department of Pathology, Washington University School of Medicine, St. Louis, Missouri, USA.

J. Craig Forrest's present address is: Department of Microbiology and Immunology, Emory University School of Medicine, Atlanta, Georgia, USA.

Tibor Valyi-Nagy's present address is: Department of Pathology, University of Illinois-Chicago, Chicago, Illinois, USA.



1. Tyler, K.L., and Nathanson, N. 2001. Pathogenesis of viral infections. In *Fields virology*. D.M. Knipe and P.M. Howley, editors. Lippincott-Raven. Philadelphia, Pennsylvania, USA. 199–243.

2. Tyler, K.L. 2001. Mammalian reoviruses. In *Fields virology*. D.M. Knipe and P.M. Howley, editors. Lippincott-Raven. Philadelphia, Pennsylvania, USA. 1729–1945.

3. Virgin, H.W., Tyler, K.L., and Dermody, T.S. 1997. Reovirus. In *Viral pathogenesis*. N. Nathanson, editor. Lippincott-Raven. New York, New York, USA. 669–699.

4. Weiner, H.L., Powers, M.L., and Fields, B.N. 1980. Absolute linkage of virulence and central nervous system tropism of reoviruses to viral hemagglutinin. *J. Infect. Dis.* **141**:609–616.

5. Barton, E.S., et al. 2003. Utilization of sialic acid as a coreceptor is required for reovirus-induced biliary disease. *J. Clin. Invest.* **111**:1823–1833. doi:10.1172/JCI200316303.

6. Sherry, B., and Fields, B.N. 1989. The reovirus M1 gene, encoding a viral core protein, is associated with the myocarditic phenotype of a reovirus variant. *J. Virol.* **63**:4850–4856.

7. Sherry, B., and Blum, M.A. 1994. Multiple viral core proteins are determinants of reovirus-induced acute myocarditis. *J. Virol.* **68**:8461–8465.

8. Beg, A.A., et al. 1992. I kappa B interacts with the nuclear localization sequences of the subunits of NF-kappa B: a mechanism for cytoplasmic retention. *Genes Dev.* **6**:1899–1913.

9. Verma, I.M., Stevenson, J.K., Schwarz, E.M., Van Antwerp, D., and Miyamoto, S. 1995. Rel/NF-kappa B/I kappa B family: intimate tales of association and disassociation [review]. *Genes Dev.* **9**:2723–2735.

10. May, M.J., and Ghosh, S. 1997. Rel/NF-kappa B and I kappa B proteins: an overview [review]. *Semin. Cancer Biol.* **8**:63–73.

11. Beg, A., and Baltimore, D. 1996. An essential role for NF-kB in preventing TNF- α -induced cell death. *Science.* **274**:782–784.

12. Liu, T., Tang, Q., and Hendricks, R.L. 1996. Inflammatory infiltration of the trigeminal ganglion after herpes simplex virus type 1 corneal infection. *J. Virol.* **70**:264–271.

13. Van Antwerp, D., Martin, S., Kafri, T., Green, D., and Verma, I. 1996. Suppression of TNF- α -induced apoptosis by NF-kappaB. *Science.* **274**:787–789.

14. Abbadie, C., Kabrun, N., Bouali, F., Vandenbunder, B., and Enrietto, P. 1993. High levels of *c-rel* expression are associated with programmed cell death in the developing avian embryo and in bone marrow cells *in vitro*. *Cell.* **75**:899–912.

15. Jung, M., Zhang, Y., Lee, S., and Dritschilo, A. 1995. Correction of radiation sensitivity in ataxia telangiectasia cells by a truncated I κ B- α . *Science.* **268**:1619–1621.

16. Lin, K.I., et al. 1995. Thiol agents and Bel-2 identify an alphavirus-induced apoptotic pathway that requires activation of the transcription factor NF-kappa B. *J. Cell Biol.* **131**:1149–1161.

17. Dumont, A., et al. 1999. Hydrogen peroxide-induced apoptosis is CD95-independent, requires the release of mitochondria-derived reactive oxygen species and the activation of NF-kappaB. *Oncogene.* **18**:747–757.

18. Connolly, J.L., et al. 2000. Reovirus-induced apoptosis requires activation of transcription factor NF-kB. *J. Virol.* **74**:2981–2989.

19. Oberhaus, S.M., Smith, R.L., Clayton, G.H., Dermody, T.S., and Tyler, K.L. 1997. Reovirus infection and tissue injury in the mouse central nervous system are associated with apoptosis. *J. Virol.* **71**:2100–2106.

20. DeBiasi, R., Edelstein, C., Sherry, B., and Tyler, K. 2001. Calpain inhibition protects against virus-induced apoptotic myocardial injury. *J. Virol.* **75**:351–361.

21. Kretzschmar, M., Meisterernst, M., Scheiderei, C., Li, G., and Roeder, R.G. 1992. Transcriptional regulation of the HIV-1 promoter by NF-kappa B *in vitro*. *Genes Dev.* **6**:761–774.

22. Connolly, J.L., Barton, E.S., and Dermody, T.S. 2001. Reovirus binding to cell surface sialic acid potentiates virus-induced apoptosis. *J. Virol.* **75**:4029–4039.

23. Blatt, N.B., and Glick, G.D. 2001. Signaling pathways and effector mechanisms pre-programmed cell death. *Bioorg. Med. Chem.* **9**:1371–1384.

24. Sha, W.C., Liou, H.C., Tuomanen, E.I., and Baltimore, D. 1995. Targeted disruption of the p50 subunit of NF-kappa B leads to multifocal defects in immune responses. *Cell.* **80**:321–330.

25. Kontgen, F., et al. 1995. Mice lacking the *c-rel* proto-oncogene exhibit defects in lymphocyte proliferation, humoral immunity, and interleukin-2 expression. *Genes Dev.* **9**:1965–1967.

26. Weih, F., et al. 1995. Multiorgan inflammation and hematopoietic abnormalities in mice with a targeted disruption of RelB, a member of the NF-kB/Rel family. *Cell.* **80**:331–340.

27. Sherry, B., Schoen, F.J., Wenske, E., and Fields, B.N. 1989. Derivation and characterization of an efficiently myocarditic reovirus variant. *J. Virol.* **63**:4840–4849.

28. Sherry, B., Baty, C.J., and Blum, M.A. 1996. Reovirus-induced acute myocarditis in mice correlates with viral RNA synthesis rather than generation of infectious virus in cardiac myocytes. *J. Virol.* **70**:6709–6715.

29. Sherry, B., Torres, J., and Blum, M.A. 1998. Reovirus induction of and sensitivity to beta interferon in cardiac myocyte cultures correlate with induction of myocarditis and are determined by viral core proteins. *J. Virol.* **72**:1314–1323.

30. Chu, W.M., et al. 1999. JNK2 and IKKbeta are required for activating the innate response to viral infection. *Immunity.* **11**:721–731.

31. Zamanian-Daryoush, M., Mogensen, T.H., DiDonato, J.A., and Williams, B.R. 2000. NF-kappaB activation by double-stranded-RNA-activated protein kinase (PKR) is mediated through NF-kappaB-inducing kinase and IkappaB kinase. *Mol. Cell. Biol.* **20**:1278–1290.

32. Fitzgerald, K.A., et al. 2003. IKKepsilon and TBK1 are essential components of the IRF3 signaling pathway. *Nat. Immunol.* **4**:491–496.

33. Sherry, B., Li, X.Y., Tyler, K.L., Cullen, J.M., and Virgin, H.W. 1993. Lymphocytes protect against and are not required for reovirus-induced myocarditis. *J. Virol.* **67**:6119–6124.

34. Maisch, B., Ristic, A.D., Hufnagel, G., and Pankuweit, S. 2002. Pathophysiology of viral myocarditis: the role of humoral immune response [review]. *Cardiovasc. Pathol.* **11**:112–122.

35. Gilmore, T.D. 1999. The Rel/NF-kB signal transduction pathway: introduction [review]. *Oncogene.* **18**:6842–6844.

36. Pahl, H.L. 1999. Activators and target genes of Rel/NF-kappaB transcription factors. *Oncogene.* **18**:6853–6866.

37. Govind, S. 1999. Control of development and immunity by Rel transcription factors in Drosophila [review]. *Oncogene.* **18**:6875–6887.

38. Furlong, D.B., Nibert, M.L., and Fields, B.N. 1988. Sigma 1 protein of mammalian reoviruses extends from the surfaces of viral particles. *J. Virol.* **62**:246–256.

39. Blackwell, T.S., et al. 2000. Multiorgan nuclear factor kappa B activation in a transgenic mouse model of systemic inflammation. *Am. J. Respir. Crit. Care Med.* **162**:1095–1101.

40. Tyler, K.L., Bronson, R.T., Byers, K.B., and Fields, B.N. 1985. Molecular basis of viral neurotropism: experimental reovirus infection. *Neurology.* **35**:88–92.

41. Rubin, D.H., and Fields, B.N. 1980. Molecular basis of reovirus virulence. Role of the M2 gene. *J. Exp. Med.* **152**:853–868.

42. Virgin, H.W., IV, Bassel-Duby, R., Fields, B.N., and Tyler, K.L. 1988. Antibody protects against lethal infection with the neurally spreading reovirus type 3 (Dearing). *J. Virol.* **62**:4594–4604.

43. Valyi-Nagy, T., Olson, S.J., Valyi-Nagy, K., Montine, T.J., and Dermody, T.S. 2000. Herpes simplex virus type 1 latency in the murine nervous system is associated with oxidative damage to neurons. *Virology.* **278**:309–321.

44. Rottman, J.N., et al. 2003. Temporal changes in ventricular function assessed echocardiographically in conscious and anesthetized mice. *J. Am. Soc. Echocardiogr.* **16**:1150–1157.

REFERENCES

1. **Abbadie, C., N. Kabrun, F. Bouali, B. Vandebunder, and P. Enrietto.** 1993. High levels of *c-rel* expression are associated with programmed cell death in the developing avian embryo and in bone marrow cells *in vitro*. *Cell* **75**:899-912.
2. **Armstrong, G. D., R. W. Paul, and P. W. Lee.** 1984. Studies on reovirus receptors of L cells: virus binding characteristics and comparison with reovirus receptors of erythrocytes. *Virology* **138**:37-48.
3. **Ashkenazi, A., and V. M. Dixit.** 1998. Death receptors: signaling and modulation. *Science* **281**:1305-1308.
4. **Azzam-Smoak, K., D. L. Noah, M. J. Stewart, M. A. Blum, and B. Sherry.** 2002. Interferon regulatory factor-1, interferon-beta, and reovirus-induced myocarditis. *Virology* **298**:20-29.
5. **Baer, G. S., and T. S. Dermody.** 1997. Mutations in reovirus outer-capsid protein $\sigma 3$ selected during persistent infections of L cells confer resistance to protease inhibitor E64. *Journal of Virology* **71**:4921-4928.
6. **Baer, G. S., D. H. Ebert, C. J. Chung, A. H. Erickson, and T. S. Dermody.** 1999. Mutant cells selected during persistent reovirus infection do not express mature cathepsin L and do not support reovirus disassembly. *Journal of Virology* **73**:9532-9543.
7. **Baeuerle, P., and D. Baltimore.** 1989. A 65-kD subunit of active NF- κ B is required for inhibition of NF- κ B by I κ B. *Genes & Development* **3**:1689-1698.
8. **Baeuerle, P., and D. Baltimore.** 1988. I κ B: a specific inhibitor of the NF- κ B transcription factor. *Science* **242**:540-546.
9. **Barrett, A. J., A. A. Kembhavi, M. A. Brown, H. Kirschke, C. G. Knight, M. Tamai, and K. Hanada.** 1982. *L-trans*-Epoxy succinyl-leucylamido(4-guanidino)butane (E-64) and its analogues as inhibitors of cysteine proteinases including cathepsins B, H and L. *Biochemical Journal* **201**:189-198.
10. **Barton, E. S., J. L. Connolly, J. C. Forrest, J. D. Chappell, and T. S. Dermody.** 2001. Utilization of sialic acid as a coreceptor enhances reovirus attachment by multistep adhesion strengthening. *Journal of Biological Chemistry* **276**:2200-2211.

11. **Barton, E. S., J. C. Forrest, J. L. Connolly, J. D. Chappell, Y. Liu, F. Schnell, A. Nusrat, C. A. Parkos, and T. S. Dermody.** 2001. Junction adhesion molecule is a receptor for reovirus. *Cell* **104**:441-451.
12. **Barton, E. S., B. E. Youree, D. H. Ebert, J. C. Forrest, J. L. Connolly, T. Valyi-Nagy, K. Washington, J. D. Wetzel, and T. S. Dermody.** 2003. Utilization of sialic acid as a coreceptor is required for reovirus-induced biliary disease. *Journal of Clinical Investigation* **111**:1823-1833.
13. **Baty, C. J., and B. Sherry.** 1993. Cytopathogenic effect in cardiac myocytes but not in cardiac fibroblasts is correlated with reovirus-induced acute myocarditis. *Journal of Virology* **67**:6295-6298.
14. **Bazzoni, G., O. M. Martinez-Estrada, F. Orsenigo, M. Cordenonsi, S. Citi, and E. Dejana.** 2000. Interaction of junctional adhesion molecule with the tight junction components ZO-1, cingulin, and occludin. *Journal of Biological Chemistry* **275**:20520-20526.
15. **Beg, A., and D. Baltimore.** 1996. An essential role for NF- κ B in preventing TNF- α -induced cell death. *Science* **274**:782-784.
16. **Beg, A., T. Finco, P. Nantermet, and A. Baldwin.** 1993. Tumor necrosis factor and interleukin-1 lead to phosphorylation and loss of I κ B α : a mechanism for NF- κ B activation. *Mol Cell Biol* **13**:3301-3310.
17. **Beg, A. A., S. M. Ruben, R. I. Scheinman, S. Haskill, C. A. Rosen, and A. J. Baldwin.** 1992. I κ B interacts with the nuclear localization sequences of the subunits of NF- κ B: a mechanism for cytoplasmic retention. *Genes & Development* **6**:1899-1913.
18. **Blackwell, T. S., F. E. Yull, C. L. Chen, A. Venkatakrishnan, T. R. Blackwell, D. J. Hicks, L. H. Lancaster, J. W. Christman, and L. D. Kerr.** 2000. Multiorgan nuclear factor kappa B activation in a transgenic mouse model of systemic inflammation. *Am J Respir Crit Care Med* **162**:1095-101.
19. **Bonizzi, G., and M. Karin.** 2004. The two NF-kappaB activation pathways and their role in innate and adaptive immunity. *Trends Immunol* **25**:280-288.
20. **Borsa, J., M. D. Sargent, P. A. Lievaart, and T. P. Copps.** 1981. Reovirus: evidence for a second step in the intracellular uncoating and transcriptase activation process. *Virology* **111**:191-200.
21. **Brown, K., S. Gerstberger, L. Carlson, G. Franzoso, and U. Siebenlist.** 1995. Control of I kappa B-alpha proteolysis by site-specific, signal-induced phosphorylation. *Science* **267**:1485-1488.

22. **Burstin, S. J., M. W. Brandriss, and J. J. Schlesinger.** 1983. Infection of a macrophage-like cell line, P388D1 with reovirus; effects of immune ascitic fluids and monoclonal antibodies on neutralization and on enhancement of viral growth. *J Immunol* **130**:2915-2919.
23. **Burstin, S. J., D. R. Spriggs, and B. N. Fields.** 1982. Evidence for functional domains on the reovirus type 3 hemagglutinin. *Virology* **117**:146-155.
24. **Campbell, J. A., P. Shelling, J. D. Wetzel, E. M. Johnson, G. A. R. Wilson, J. C. Forrest, M. Aurrand-Lions, B. Imhof, T. Stehle, and T. S. Dermody.** 2005. Junctional adhesion molecule-A serves as a receptor for prototype and field-isolate strains of mammalian reovirus. *Journal of Virology* **79**:7967-7978.
25. **Carter, R. S., B. C. Geyer, M. Xie, C. A. Acevedo-Suarez, and D. W. Ballard.** 2001. Persistent activation of NF-kappa B by the tax transforming protein involves chronic phosphorylation of IkappaB kinase subunits IKKbeta and IKKgamma. *Journal of Biological Chemistry* **276**:24445-24448.
26. **Chandran, K., D. L. Farsetta, and M. L. Nibert.** 2002. Strategy for nonenveloped virus entry: a hydrophobic conformer of the reovirus membrane penetration protein $\mu 1$ mediates membrane disruption. *Journal of Virology* **76**:9920-9933.
27. **Chandran, K., J. S. Parker, M. Ehrlich, T. Kirchhausen, and M. L. Nibert.** 2003. The delta region of outer-capsid protein $\mu 1$ undergoes conformational change and release from reovirus particles during cell entry. *Journal of Virology* **77**:13361-13375.
28. **Chappell, J. D., J. L. Duong, B. W. Wright, and T. S. Dermody.** 2000. Identification of carbohydrate-binding domains in the attachment proteins of type 1 and type 3 reoviruses. *Journal of Virology* **74**:8472-8479.
29. **Chappell, J. D., A. Prota, T. S. Dermody, and T. Stehle.** 2002. Crystal structure of reovirus attachment protein $\sigma 1$ reveals evolutionary relationship to adenovirus fiber. *EMBO Journal* **21**:1-11.
30. **Chen, Z., J. Hagler, V. J. Palombella, F. Melandri, D. Scherer, D. Ballard, and T. Maniatis.** 1995. Signal-induced site-specific phosphorylation targets I kappa B alpha to the ubiquitin-proteasome pathway. *Genes & Development* **9**:1585-1597.
31. **Chu, W. M., D. Ostertag, Z. W. Li, L. Chang, Y. Chen, Y. Hu, B. Williams, J. Perrault, and M. Karin.** 1999. JNK2 and IKKbeta are required for activating the innate response to viral infection. *Immunity* **11**:721-31.

32. **Chu, Z. L., J. A. DiDonato, J. Hawiger, and D. W. Ballard.** 1998. The tax oncoprotein of human T-cell leukemia virus type 1 associates with and persistently activates IkappaB kinases containing IKKalpha and IKKbeta. *Journal of Biological Chemistry* **273**:15891-4.
33. **Chu, Z. L., Y. A. Shin, J. M. Yang, J. A. DiDonato, and D. W. Ballard.** 1999. IKKgamma mediates the interaction of cellular IkappaB kinases with the tax transforming protein of human T cell leukemia virus type 1. *Journal of Biological Chemistry* **274**:15297-300.
34. **Clarke, P., S. M. Meintzer, L. A. Moffitt, and K. L. Tyler.** 2003. Two distinct phases of virus-induced nuclear factor kappa B regulation enhance tumor necrosis factor-related apoptosis-inducing ligand-mediated apoptosis in virus-infected cells. *Journal of Biological Chemistry* **278**:18092-18100.
35. **Claudio, E., K. Brown, S. Park, H. Wang, and U. Siebenlist.** 2002. BAFF-induced NEMO-independent processing of NF-kappa B2 in maturing B cells. *Nat. Immunol.* **3**:958-965.
36. **Coffey, C. M., A. Sheh, I. S. Kim, K. Chandran, M. L. Nibert, and J. S. Parker.** 2006. Reovirus Outer Capsid Protein {micro}1 Induces Apoptosis and Associates with Lipid Droplets, Endoplasmic Reticulum, and Mitochondria. *Journal of Virology* **80**:8422-8438.
37. **Cohen, J. J.** 1991. Programmed cell death in the immune system. *Advances in Immunology* **50**:55-85.
38. **Connolly, J. L., E. S. Barton, and T. S. Dermody.** 2001. Reovirus binding to cell surface sialic acid potentiates virus-induced apoptosis. *Journal of Virology* **75**:4029-4039.
39. **Connolly, J. L., and T. S. Dermody.** 2002. Virion disassembly is required for apoptosis induced by reovirus. *Journal of Virology* **76**:1632-1641.
40. **Connolly, J. L., S. E. Rodgers, P. Clarke, D. W. Ballard, L. D. Kerr, K. L. Tyler, and T. S. Dermody.** 2000. Reovirus-induced apoptosis requires activation of transcription factor NF-kB. *Journal of Virology* **74**:2981-2989.
41. **Cook, D. N., M. A. Beck, T. M. Coffman, S. L. Kirby, J. F. Sheridan, I. B. Pragnell, and O. Smithies.** 1995. Requirement of MIP-1 alpha for an inflammatory response to viral infection. *Science* **269**:1583-1585.
42. **Coombs, K. M.** 1998. Stoichiometry of reovirus structural proteins in virus, ISVP, and core particles. *Virology* **243**:218-228.

43. **Coombs, K. M.** 1998. Temperature-sensitive mutants of reovirus. *Current Topics in Microbiology and Immunology* **233**:69-107.
44. **DeBiasi, R., C. Edelstein, B. Sherry, and K. Tyler.** 2001. Calpain inhibition protects against virus-induced apoptotic myocardial injury. *Journal of Virology* **75**:351-361.
45. **DeBiasi, R. L., P. Clarke, S. M. Meintzer, R. M. Jotte, B. K. Kleinschmidt-Demasters, G. L. Johnson, and K. L. Tyler.** 2003. Reovirus-induced alteration in expression of apoptosis and DNA repair genes with potential roles in viral pathogenesis. *J Virol* **77**:8934-8947.
46. **Deiss, L. P., H. Galinka, H. Berissi, O. Cohen, and A. Kimchi.** 1996. Cathepsin D protease mediates programmed cell death induced by interferon-gamma, Fas/APO-1 and TNF-alpha. *Embo J* **15**:3861-3870.
47. **Dejardin, E., N. M. Droin, M. Delhase, E. Haas, Y. Cao, C. Makris, Z. W. Li, M. Karin, C. F. Ware, and D. R. Green.** 2002. The lymphotoxin-beta receptor induces different patterns of gene expression via two NF-kappaB pathways. *Immunity* **17**:525-535.
48. **Delhase, M., M. Hayakawa, Y. Chen, and M. Karin.** 1999. Positive and negative regulation of IkappaB kinase activity through IKKbeta subunit phosphorylation. *Science* **284**:309-313.
49. **Dermody, T. S., M. L. Nibert, R. Bassel-Duby, and B. N. Fields.** 1990. A sigma 1 region important for hemagglutination by serotype 3 reovirus strains. *Journal of Virology* **64**:5173-5176.
50. **Dichter, M. A., and H. L. Weiner.** 1984. Infection of neuronal cell cultures with reovirus mimics in vitro patterns of neurotropism. *Annals of Neurology* **16**:603-610.
51. **DiDonato, J. A., M. Hayakawa, D. M. Rothwarf, E. Zandi, and M. Karin.** 1997. A cytokine-responsive IkappaB kinase that activates the transcription factor NF-kappaB. *Nature* **388**:548-554.
52. **Dryden, K. A., G. Wang, M. Yeager, M. L. Nibert, K. M. Coombs, D. B. Furlong, B. N. Fields, and T. S. Baker.** 1993. Early steps in reovirus infection are associated with dramatic changes in supramolecular structure and protein conformation: analysis of virions and subviral particles by cryoelectron microscopy and image reconstruction. *Journal of Cell Biology* **122**:1023-1041.
53. **Dumont, A., S. P. Hehner, T. G. Hofmann, M. Ueffing, W. Droge, and M. L. Schmitz.** 1999. Hydrogen peroxide-induced apoptosis is CD95-independent,

- requires the release of mitochondria-derived reactive oxygen species and the activation of NF-kappaB. *Oncogene* **18**:747-757.
54. **Ebnet, K., C. U. Schulz, M. K. Meyer Zu Brickwedde, G. G. Pendl, and D. Vestweber.** 2000. Junctional adhesion molecule interacts with the PDZ domain-containing proteins AF-6 and ZO-1. *Journal of Biological Chemistry* **275**:27979-27988.
 55. **Ernst, H., and A. J. Shatkin.** 1985. Reovirus hemagglutinin mRNA codes for two polypeptides in overlapping reading frames. *Proceedings of the National Academy of Sciences USA* **82**:48-52.
 56. **Fitzgerald, K. A., S. M. McWhirter, K. L. Faia, D. C. Rowe, E. Latz, D. T. Golenbock, A. J. Coyle, S. M. Liao, and T. Maniatis.** 2003. IKKepsilon and TBK1 are essential components of the IRF3 signaling pathway. *Nat. Immunol.* **4**:491-496.
 57. **Forrest, J. C., J. A. Campbell, P. Schelling, T. Stehle, and T. S. Dermody.** 2003. Structure-function analysis of reovirus binding to junctional adhesion molecule 1. Implications for the mechanism of reovirus attachment. *The Journal of Biological Chemistry* **278**:48434-48444.
 58. **Furlong, D. B., M. L. Nibert, and B. N. Fields.** 1988. Sigma 1 protein of mammalian reoviruses extends from the surfaces of viral particles. *Journal of Virology* **62**:246-256.
 59. **Ghosh, S., and M. Karin.** 2002. Missing pieces in the NF-kappaB puzzle. *Cell* **109 Suppl**:S81-S96.
 60. **Gilmore, T. D.** 1999. The Rel/NF-κB signal transduction pathway: Introduction. *Oncogene* **18**:6842-6844.
 61. **Govind, S.** 1999. Control of development and immunity by Rel transcription factors in *Drosophila*. *Oncogene* **18**:6875-6887.
 62. **Grimm, S., M. K. A. Bauer, P. A. Baeuerle, and K. Schulze-Osthoff.** 1996. Bcl-2 down-regulates the activity of transcription factor NF-κB induced upon apoptosis. *Journal of Cell Biology* **134**:13-23.
 63. **Grumont, R. J., I. B. Richardson, C. Gaff, and S. Gerondakis.** 1993. rel/NF-kappa B nuclear complexes that bind kB sites in the murine c-rel promoter are required for constitutive c-rel transcription in B-cells. *Cell Growth Differ* **4**:731-743.
 64. **Guicciardi, M. E., J. Deussing, H. Miyoshi, S. F. Bronk, P. A. Svingen, C. Peters, S. H. Kaufmann, and G. J. Gores.** 2000. Cathepsin B contributes to

TNF-alpha-mediated hepatocyte apoptosis by promoting mitochondrial release of cytochrome c. *J Clin Invest* **106**:1127-1137.

65. **Hamamori, Y., M. Yokoyama, M. Yamada, H. Akita, K. Goshima, and H. Fukuzaki.** 1990. 5-Hydroxytryptamine induces phospholipase C-mediated hydrolysis of phosphoinositides through 5-hydroxytryptamine-2 receptors in cultured fetal mouse ventricular myocytes. *Circ Res* **66**:1474-1483.
66. **Hayden, M. S., and S. Ghosh.** 2004. Signaling to NF- κ B. *Genes Dev* **18**:2195-2224.
67. **Hazelton, P. R., and K. M. Coombs.** 1995. The reovirus mutant tsA279 has temperature-sensitive lesions in the M2 and L2 genes: the M2 gene is associated with decreased viral protein production and blockade in transmembrane transport. *Virology* **207**:46-58.
68. **Heim, J. M.** 1999. The Jak-STAT pathway: cytokine signalling from the receptor to the nucleus. *J Recept Signal Transduct Res* **19**:75-120.
69. **Heusch, M., L. Lin, R. Geleziunas, and W. C. Greene.** 1999. The generation of nfkb2 p52: mechanism and efficiency. *Oncogene* **18**:6201-6208.
70. **Hooper, J. W., and B. N. Fields.** 1996. Monoclonal antibodies to reovirus σ 1 and μ 1 proteins inhibit chromium release from mouse L cells. *Journal of Virology* **70**:672-677.
71. **Hooper, J. W., and B. N. Fields.** 1996. Role of the μ 1 protein in reovirus stability and capacity to cause chromium release from host cells. *Journal of Virology* **70**:459-467.
72. **Huber, S. A., and P. A. Lodge.** 1984. Coxsackievirus B-3 myocarditis in Balb/c mice. Evidence for autoimmunity to myocyte antigens. *Am J Pathol* **116**:21-29.
73. **Huynh, Q. K., H. Boddupalli, S. A. Rouw, C. M. Koboldt, T. Hall, C. Sommers, S. D. Hauser, J. L. Pierce, R. G. Combs, B. A. Reitz, J. A. Diaz-Collier, R. A. Weinberg, B. L. Hood, B. F. Kilpatrick, and C. S. Tripp.** 2000. Characterization of the recombinant IKK1/IKK2 heterodimer. Mechanisms regulating kinase activity. *Journal of Biological Chemistry* **275**:25883-25891.
74. **Inohara, N., T. Koseki, J. Lin, L. del Peso, P. C. Lucas, F. F. Chen, Y. Ogura, and G. Nunez.** 2000. An induced proximity model for NF-kappa B activation in the Nod1/RICK and RIP signaling pathways. *Journal of Biological Chemistry* **275**:27823-27831.
75. **Jacobs, B. L., J. A. Atwater, S. M. Munemitsu, and C. E. Samuel.** 1985. Biosynthesis of reovirus-specified polypeptides. The S1 mRNA synthesized in

vivo is structurally and functionally indistinguishable from in vitro-synthesized S1 mRNA and encodes two polypeptides, σ 1a and σ 1bNS. *Virology* **147**:9-18.

76. **Jan, J. T., S. Chatterjee, and D. E. Griffin.** 2000. Sindbis virus entry into cells triggers apoptosis by activating sphingomyelinase, leading to the release of ceramide. *Journal of Virology* **74**:6425-6432.
77. **Jan, J. T., B. H. Chen, S. H. Ma, C. I. Liu, H. P. Tsai, H. C. Wu, S. Y. Jiang, K. D. Yang, and M. F. Shaio.** 2000. Potential dengue virus-triggered apoptotic pathway in human neuroblastoma cells: arachidonic acid, superoxide anion, and NF-kappaB are sequentially involved. *J Virol* **74**:8680-91.
78. **Jan, J. T., and D. E. Griffin.** 1999. Induction of apoptosis by Sindbis virus occurs at cell entry and does not require viral replication. *Journal of Virology* **73**:10296-10302.
79. **Jayasuriya, A. K., M. L. Nibert, and B. N. Fields.** 1988. Complete nucleotide sequence of the M2 gene segment of reovirus type 3 dearing and analysis of its protein product μ 1. *Virology* **163**:591-602.
80. **Joiner, K. A., S. A. Fuhrman, H. M. Miettinen, L. H. Kasper, and I. Mellman.** 1990. *Toxoplasma gondii*: fusion competence of parasitophorous vacuoles in Fc receptor-transfected fibroblasts. *Science* **249**:641-646.
81. **Joklik, W. K.** 1981. Structure and function of the reovirus genome. *Microbiological Reviews* **45**:483-501.
82. **Jung, M., Y. Zhang, S. Lee, and A. Dritschilo.** 1995. Correction of radiation sensitivity in ataxia telangiectasia cells by a truncated I κ B- α . *Science* **268**:1619-1621.
83. **Kauffman, R. S., J. L. Wolf, R. Finberg, J. S. Trier, and B. N. Fields.** 1983. The sigma 1 protein determines the extent of spread of reovirus from the gastrointestinal tract of mice. *Virology* **124**:403-410.
84. **Kawai, T., K. Takahashi, S. Sato, C. Coban, H. Kumar, H. Kato, K. J. Ishii, O. Takeuchi, and S. Akira.** 2005. IPS-1, an adaptor triggering RIG-I- and Mda5-mediated type I interferon induction. *Nat. Immunol.* **6**:981-988.
85. **Kominsky, D. J., R. J. Bickel, and K. L. Tyler.** 2002. Reovirus-induced apoptosis requires both death receptor- and mitochondrial-mediated caspase-dependent pathways of cell death. *Cell Death Differ.* **9**:926-933.
86. **Kominsky, D. J., R. J. Bickel, and K. L. Tyler.** 2002. Reovirus-induced apoptosis requires mitochondrial release of Smac/DIABLO and involves reduction of cellular inhibitor of apoptosis protein levels. *J Virol* **76**:11414-11424.

87. **Kontgen, F., R. J. Grumont, A. Strasser, D. Metcalf, R. Li, D. Tarlington, and S. Gerondakis.** 1995. Mice lacking the *c-rel* proto-oncogene exhibit defects in lymphocyte proliferation, humoral immunity, and interleukin-2 expression. *Genes and Development* **9**:1965-1967.
88. **Kretzschmar, M., M. Meisterernst, C. Scheidereit, G. Li, and R. G. Roeder.** 1992. Transcriptional regulation of the HIV-1 promoter by NF-kappa B in vitro. *Genes Dev* **6**:761-74.
89. **Lee, P. W., E. C. Hayes, and W. K. Joklik.** 1981. Protein σ 1 is the reovirus cell attachment protein. *Virology* **108**:156-163.
90. **Li, J. K.-K., J. D. Keene, P. P. Scheible, and W. K. Joklik.** 1980. Nature of the 3'-terminal sequence of the plus and minus strands of the S1 gene of reovirus serotypes 1, 2, and 3. *Virology* **105**:41-51.
91. **Li, Q., D. Van Antwerp, F. Mercurio, K. F. Lee, and I. M. Verma.** 1999. Severe liver degeneration in mice lacking the IkappaB kinase 2 gene. *Science* **284**:321-325.
92. **Li, Z. W., W. Chu, Y. Hu, M. Delhase, T. Deerinck, M. Ellisman, R. Johnson, and M. Karin.** 1999. The IKKbeta subunit of IkappaB kinase (IKK) is essential for nuclear factor kappaB activation and prevention of apoptosis. *Journal of Experimental Medicine* **189**:1839-1845.
93. **Liemann, S., K. Chandran, T. S. Baker, M. L. Nibert, and S. C. Harrison.** 2002. Structure of the reovirus membrane-penetration protein, μ 1, in a complex with its protector protein, σ 3. *Cell* **108**:283-295.
94. **Lin, K. I., S. H. Lee, R. Narayanan, J. Baraban, J. Hardwick, and R. Ratan.** 1995. Thiol agents and Bcl-2 identify an alphavirus-induced apoptotic pathway that requires activation of the transcription factor NF-kappa B. *Journal of Cell Biology* **131**:1149-1161.
95. **Ling, L., Z. Cao, and D. V. Goeddel.** 1998. NF-kappaB-inducing kinase activates IKK-alpha by phosphorylation of Ser-176. *Proc Natl Acad Sci U S A* **95**:3792-7.
96. **Link, E., L. D. Kerr, R. Schreck, U. Zabel, I. Verma, and P. A. Baeuerle.** 1992. Purified I kappa B-beta is inactivated upon dephosphorylation. *Journal of Biological Chemistry* **267**:239-246.
97. **Liu, T., Q. Tang, and R. L. Hendricks.** 1996. Inflammatory infiltration of the trigeminal ganglion after herpes simplex virus type 1 corneal infection. *Journal of Virology* **70**:264-271.

98. **Liu, Y., Y. Cai, and X. Zhang.** 2003. Induction of caspase-dependent apoptosis in cultured rat oligodendrocytes by murine coronavirus is mediated during cell entry and does not require virus replication. *J Virol* **77**:11952-11963.
99. **Liu, Y., A. Nusrat, F. J. Schnell, T. A. Reaves, S. Walsh, M. Ponchet, and C. A. Parkos.** 2000. Human junction adhesion molecule regulates tight junction resealing in epithelia. *Journal of Cell Science* **113**:2363-2374.
100. **Liu, Z.-G., H. Hsu, D. Goeddel, and M. Karin.** 1996. Dissection of TNF receptor 1 effector functions: JNK activation is not linked to apoptosis while NF- κ B activation prevents cell death. *Cell* **87**:565-576.
101. **Lucia-Jandris, P., J. W. Hooper, and B. N. Fields.** 1993. Reovirus M2 gene is associated with chromium release from mouse L cells. *Journal of Virology* **67**:5339-5345.
102. **Maginnis, M. S., J. C. Forrest, S. A. Kopecky-Bromberg, S. K. Dickeson, S. A. Santoro, M. M. Zutter, G. R. Nemerow, J. M. Bergelson, and T. S. Dermody.** 2006. β 1 integrin mediates internalization of mammalian reovirus. *Journal of Virology* **80**:2760-2770.
103. **Maisch, B., A. D. Ristic, G. Hufnagel, and S. Pankuweit.** 2002. Pathophysiology of viral myocarditis: the role of humoral immune response. *Cardiovasc Pathol* **11**:112-22.
104. **Maniatis, T.** 1997. Catalysis by a multiprotein IkappaB kinase complex. *Science* **278**:818-819.
105. **Marianneau, P., A. Cardona, L. Edelman, V. Deubel, and P. Despres.** 1997. Dengue virus replication in human hepatoma cells activates NF-kappaB which in turn induces apoptotic cell death. *Journal of Virology* **71**:3244-3249.
106. **Martin, A. B., S. Webber, F. J. Fricker, R. Jaffe, G. Demmler, D. Kearney, Y. H. Zhang, J. Bodurtha, B. Gelb, J. Ni, and e. al.** 1994. Acute myocarditis. Rapid diagnosis by PCR in children. *Circulation* **90**:330-339.
107. **Martinac, B., H. Zhu, A. Kubalski, X. L. Zhou, M. Culbertson, H. Bussey, and C. Kung.** 1990. Yeast K1 killer toxin forms ion channels in sensitive yeast spheroplasts and in artificial liposomes. *Proc. Natl. Acad. Sci. U.S.A.* **87**:6228-6232.
108. **Mastrorarde, J. G., B. He, M. M. Monick, N. Mukaida, K. Matsushima, and G. W. Hunninghake.** 1996. Induction of interleukin (IL)-8 gene expression by respiratory syncytial virus involves activation of nuclear factor (NF)-kappa B and NF-IL-6. *J Infect Dis* **174**:262-7.

109. **Matsushima, A., T. Kaisho, P. D. Rennert, H. Nakano, K. Kurosawa, D. Uchida, K. Takeda, S. Akira, and M. Matsumoto.** 2001. Essential role of nuclear factor (NF)-kappaB-inducing kinase and inhibitor of kappaB (IkappaB) kinase alpha in NF-kappaB activation through lymphotoxin beta receptor, but not through tumor necrosis factor receptor I. *Journal of Experimental Medicine* **193**:631-636.
110. **Maxfield, F. R.** 1982. Weak bases and ionophores rapidly and reversibly raise the pH in endocytic vesicles in cultured mouse fibroblasts. *Journal of Cell Biology* **95**:676-681.
111. **May, M. J., and S. Ghosh.** 1997. Rel/NF-kappa B and I kappa B proteins: an overview. *Seminars in Cancer Biology* **8**:63-73.
112. **McCrae, M. A., and W. K. Joklik.** 1978. The nature of the polypeptide encoded by each of the ten double-stranded RNA segments of reovirus type 3. *Virology* **89**:578-593.
113. **McDermott, P., M. Daood, and I. Klein.** 1985. Measurement of myosin adenosinetriphosphatase and myosin content in cultured heart cells. *Archives of Biochemistry & Biophysics* **240**:312-318.
114. **Mendez, II, Y. M. She, W. Ens, and K. M. Coombs.** 2003. Digestion pattern of reovirus outer capsid protein sigma3 determined by mass spectrometry. *Virology* **311**:289-304.
115. **Mercurio, F., H. Zhu, B. W. Murray, A. Shevchenko, B. L. Bennett, J. Li, D. B. Young, M. Barbosa, M. Mann, A. Manning, and A. Rao.** 1997. IKK-1 and IKK-2: cytokine-activated IkappaB kinases essential for NF-kappaB activation. *Science* **278**:860-866.
116. **Meylan, E., J. Curran, K. Hofmann, D. Moradpour, M. Binder, R. Bartenschlager, and J. Tschoop.** 2005. Cardif is an adaptor protein in the RIG-I antiviral pathway and is targeted by hepatitis C virus. *Nature* **437**:1167-1172.
117. **Morgan, E. M., and H. J. Zweerink.** 1975. Characterization of transcriptase and replicase particles isolated from reovirus infected cells. *Virology* **68**:455-466.
118. **Morrison, L. A., R. L. Sidman, and B. N. Fields.** 1991. Direct spread of reovirus from the intestinal lumen to the central nervous system through vagal autonomic nerve fibers. *Proc Natl Acad Sci USA* **88**:3852-3856.
119. **Muller, U., U. Steinhoff, L. F. Reis, S. Hemmi, J. Pavlovic, R. M. Zinkernagel, and M. Aguet.** 1994. Functional role of type I and type II interferons in antiviral defense. *Science* **264**:1918-1921.

120. **Mustoe, T. A., R. F. Ramig, A. H. Sharpe, and B. N. Fields.** 1978. Genetics of reovirus: identification of the dsRNA segments encoding the polypeptides of the μ and σ size classes. *Virology* **89**:594-604.
121. **Nibert, M. L., and B. N. Fields.** 1992. A carboxy-terminal fragment of protein $\mu 1/\mu 1C$ is present in infectious subvirion particles of mammalian reoviruses and is proposed to have a role in penetration. *Journal of Virology* **66**:6408-6418.
122. **Nibert, M. L., and L. A. Schiff.** 2001. Reoviruses and their replication, p. 1679-1728. *In* D. M. Knipe and P. M. Howley (ed.), *Fields Virology*, Fourth ed. Lippincott Williams & Wilkins, Philadelphia.
123. **Nibert, M. L., L. A. Schiff, and B. N. Fields.** 1991. Mammalian reoviruses contain a myristoylated structural protein. *Journal of Virology* **65**:1960-1967.
124. **Noah, D. L., M. A. Blum, and B. Sherry.** 1999. Interferon regulatory factor 3 is required for viral induction of beta interferon in primary cardiac myocyte cultures. *J Virol* **73**:10208-10213.
125. **Oberhaus, S. M., R. L. Smith, G. H. Clayton, T. S. Dermody, and K. L. Tyler.** 1997. Reovirus infection and tissue injury in the mouse central nervous system are associated with apoptosis. *Journal of Virology* **71**:2100-2106.
126. **O'Brien, V.** 1998. Viruses and apoptosis. *Journal of General Virology* **79**:1833-1845.
127. **Odegard, A. L., K. Chandran, X. Zhang, J. S. Parker, T. S. Baker, and M. L. Nibert.** 2004. Putative autocleavage of outer capsid protein $\mu 1$, allowing release of myristoylated peptide $\mu 1N$ during particle uncoating, is critical for cell entry by reovirus. *Journal of Virology* **78**:8732-8745.
128. **O'Donnell, S. M., M. W. Hansberger, J. L. Connolly, J. D. Chappell, M. J. Watson, J. M. Pierce, J. D. Wetzel, W. Han, E. S. Barton, J. C. Forrest, T. Valyi-Nagy, F. E. Yull, T. S. Blackwell, J. N. Rottman, B. Sherry, and T. S. Dermody.** 2005. Organ-specific roles for transcription factor NF- κ B in reovirus-induced apoptosis and disease. *J Clin Invest* **115**:2341-2350.
129. **O'Donnell, S. M., G. H. Holm, J. M. Pierce, B. Tian, M. J. Watson, R. S. Chari, D. W. Ballard, A. R. Brasier, and T. S. Dermody.** 2006. Identification of an NF- κ B-dependent gene network in cells infected by mammalian reovirus. *Journal of Virology* **80**:1077-1086.
130. **Pahl, H. L.** 1999. Activators and target genes of Rel/NF- κ B transcription factors. *Oncogene* **18**:6853-6866.

131. **Pahl, H. L., and P. A. Baeuerle.** 1995. Expression of influenza virus hemagglutinin activates transcription factor NF-kappa B. *J Virol* **69**:1480-4.
132. **Palombella, V., O. Rando, A. Goldberg, and T. Maniatis.** 1994. The ubiquitin-proteasome pathway is required for processing the NF-kappa B1 precursor protein and the activation of NF-kappa B. *Cell* **78**:773-785.
133. **Paul, R. W., A. H. Choi, and P. W. K. Lee.** 1989. The α -anomeric form of sialic acid is the minimal receptor determinant recognized by reovirus. *Virology* **172**:382-385.
134. **Paul, R. W., and P. W. K. Lee.** 1987. Glycophorin is the reovirus receptor on human erythrocytes. *Virology* **159**:94-101.
135. **Pellegrini, S., and I. Dusanter-Fourt.** 1997. The structure, regulation and function of the Janus kinases (JAKs) and the signal transducers and activators of transcription (STATs). *Eur J Biochem* **248**:615-633.
136. **Poyet, J. L., S. M. Srinivasula, J. H. Lin, T. Fernandes-Alnemri, S. Yamaoka, P. N. Tsichlis, and E. S. Alnemri.** 2000. Activation of the Ikappa B kinases by RIP via IKKgamma /NEMO-mediated oligomerization. *Journal of Biological Chemistry* **275**:37966-37977.
137. **Prota, A. E., J. A. Campbell, P. Schelling, J. C. Forrest, T. R. Peters, M. J. Watson, M. Aurrand-Lions, B. Imhof, T. S. Dermody, and T. Stehle.** 2003. Crystal structure of human junctional adhesion molecule 1: implications for reovirus binding. *Proceedings of the National Academy of Sciences USA* **100**:5366-5371.
138. **Ramsey-Ewing, A., and B. Moss.** 1998. Apoptosis induced by a postbinding step of vaccinia virus entry into Chinese hamster ovary cells. *Virology* **242**:138-149.
139. **Rankin, U. T., Jr., S. B. Eppes, J. B. Antczak, and W. K. Joklik.** 1989. Studies on the mechanism of the antiviral activity of ribavirin against reovirus. *Virology* **168**:147-158.
140. **Razvi, E. S., and R. M. Welsh.** 1995. Apoptosis in viral infections. *Advances in Virus Research* **45**:1-60.
141. **Regnier, C. H., H. Y. Song, X. Gao, D. V. Goeddel, Z. Cao, and M. Rothe.** 1997. Identification and characterization of an IkappaB kinase. *Cell* **90**:373-83.
142. **Reinisch, K. M., M. L. Nibert, and S. C. Harrison.** 2000. Structure of the reovirus core at 3.6 Å resolution. *Nature* **404**:960-967.

143. **Reiter, J., E. Herker, F. Madeo, and M. J. Schmitt.** 2005. Viral killer toxins induce caspase-mediated apoptosis in yeast. *J Cell Biol* **168**:353-358.
144. **Roberg, K.** 2001. Relocalization of cathepsin D and cytochrome c early in apoptosis revealed by immunoelectron microscopy. *Lab Invest* **81**:149-158.
145. **Rodgers, S. E., E. S. Barton, S. M. Oberhaus, B. Pike, C. A. Gibson, K. L. Tyler, and T. S. Dermody.** 1997. Reovirus-induced apoptosis of MDCK cells is not linked to viral yield and is blocked by Bcl-2. *Journal of Virology* **71**:2540-2546.
146. **Rodgers, S. E., J. L. Connolly, J. D. Chappell, and T. S. Dermody.** 1998. Reovirus growth in cell culture does not require the full complement of viral proteins: Identification of a σ 1s-null mutant. *Journal of Virology* **72**:8597-8604.
147. **Rose, N. R., and S. L. Hill.** 1996. The pathogenesis of postinfectious myocarditis. *Clinical Immunology and Immunopathology* **80**:S92-S99.
148. **Rose, N. R., D. A. Neumann, and A. Herskowitz.** 1992. Coxsackievirus myocarditis. *Adv Intern Med* **37**:411-429.
149. **Rosen, L.** 1979. Reoviruses, p. 577-584. *In* E. H. Lennette and N. J. Schmidt (ed.), *Diagnostic Procedures for Viral and Rickettsial Infections*. American Public Health Association, New York.
150. **Rothwarf, D. M., and M. Karin.** 1999. The NF-kappa B activation pathway: a paradigm in information transfer from membrane to nucleus. *Sci STKE* **1999**:RE1.
151. **Rothwarf, D. M., E. Zandi, G. Natoli, and M. Karin.** 1998. IKK-gamma is an essential regulatory subunit of the I-kappaB kinase complex. *Nature* **395**:297-300.
152. **Rottman, J. N., G. Ni, M. Khoo, Z. Wang, W. Zhang, M. E. Anderson, and E. C. Madu.** 2003. Temporal changes in ventricular function assessed echocardiographically in conscious and anesthetized mice. *J Am Soc Echocardiogr* **16**:1150-7.
153. **Roulston, A., R. C. Marcellus, and P. E. Branton.** 1999. Viruses and apoptosis. *Annual Review of Microbiology* **53**:577-628.
154. **Rubin, D. H., and B. N. Fields.** 1980. Molecular basis of reovirus virulence: role of the M2 gene. *Journal of Experimental Medicine* **152**:853-868.
155. **Rubin, D. H., D. B. Weiner, C. Dworkin, M. I. Greene, G. G. Maul, and W. V. Williams.** 1992. Receptor utilization by reovirus type 3: distinct binding sites

on thymoma and fibroblast cell lines result in differential compartmentalization of virions. *Microbial Pathogenesis* **12**:351-365.

156. **Rudolph, D., W. C. Yeh, A. Wakeham, B. Rudolph, D. Nallainathan, J. Potter, A. J. Elia, and T. W. Mak.** 2000. Severe liver degeneration and lack of NF-kappaB activation in NEMO/IKKgamma-deficient mice. *Genes Dev* **14**:854-62.
157. **Sabin, A. B.** 1959. Reoviruses: a new group of respiratory and enteric viruses formerly classified as ECHO type 10 is described. *Science* **130**:1387-1389.
158. **Sarkar, G., J. Pelletier, R. Bassel-Duby, A. Jayasuriya, B. N. Fields, and N. Sonenberg.** 1985. Identification of a new polypeptide coded by reovirus gene S1. *Journal of Virology* **54**:720-725.
159. **Schindler, C., and J. E. Darnell, Jr.** 1995. Transcriptional responses to polypeptide ligands: the JAK-STAT pathway. *Annu Rev Biochem* **64**:621-651.
160. **Schomer-Miller, B., T. Higashimoto, Y. K. Lee, and E. Zandi.** 2006. Regulation of IkappaB kinase (IKK) complex by IKKgamma-dependent phosphorylation of the T-loop and C terminus of IKKbeta. *Journal of Biological Chemistry* **281**:15268-15276.
161. **Schonberg, M., S. C. Silverstein, D. H. Levin, and G. Acs.** 1971. Asynchronous synthesis of the complementary strands of the reovirus genome. *Proceedings of the National Academy of Sciences USA* **68**:505-508.
162. **Schwarz, E. M., C. Badorff, T. S. Hiura, R. Wessely, B. Badorff, I. M. Verma, and K. U. Knowlton.** 1998. NF-kappaB-mediated inhibition of apoptosis is required for encephalomyocarditis virus virulence: a mechanism of resistance in p50 knockout mice. *Journal of Virology* **72**:5654-5660.
163. **Senftleben, U., Y. Cao, G. Xiao, F. R. Greten, G. Krahn, G. Bonizzi, Y. Chen, Y. Hu, A. Fong, S. C. Sun, and M. Karin.** 2001. Activation by IKKalpha of a second, evolutionary conserved, NF-kappa B signaling pathway. *Science* **293**:1495-1499.
164. **Seth, R. B., L. Sun, C. K. Ea, and Z. J. Chen.** 2005. Identification and characterization of MAVS, a mitochondrial antiviral signaling protein that activates NF-kappaB and IRF 3. *Cell* **122**:669-682.
165. **Sha, W. C., H. C. Liou, E. I. Tuomanen, and D. Baltimore.** 1995. Targeted disruption of the p50 subunit of NF-kappa B leads to multifocal defects in immune responses. *Cell* **80**:321-330.

166. **Shaw, J. E., and D. C. Cox.** 1973. Early inhibition of cellular DNA synthesis by high multiplicities of infectious and UV-irradiated reovirus. *Journal of Virology* **12**:704-710.
167. **Shen, Y., and T. E. Shenk.** 1995. Viruses and apoptosis. *Current Opinions in Genetics and Development* **5**:105-111.
168. **Shepard, D. A., J. G. Ehnstrom, and L. A. Schiff.** 1995. Association of reovirus outer capsid proteins $\sigma 3$ and $\mu 1$ causes a conformational change that renders $\sigma 3$ protease sensitive. *Journal of Virology* **69**:8180-8184.
169. **Shepard, D. A., J. G. Ehnstrom, P. J. Skinner, and L. A. Schiff.** 1996. Mutations in the zinc-binding motif of the reovirus capsid protein $\sigma 3$ eliminate its ability to associate with capsid protein $\mu 1$. *Journal of Virology* **70**:2065-2068.
170. **Sherry, B., C. J. Baty, and M. A. Blum.** 1996. Reovirus-induced acute myocarditis in mice correlates with viral RNA synthesis rather than generation of infectious virus in cardiac myocytes. *J Virol* **70**:6709-6715.
171. **Sherry, B., and M. A. Blum.** 1994. Multiple viral core proteins are determinants of reovirus-induced acute myocarditis. *Journal of Virology* **68**:8461-8465.
172. **Sherry, B., and B. N. Fields.** 1989. The reovirus M1 gene, encoding a viral core protein, is associated with the myocarditic phenotype of a reovirus variant. *Journal of Virology* **63**:4850-4856.
173. **Sherry, B., X. Y. Li, K. L. Tyler, J. M. Cullen, and H. W. Virgin.** 1993. Lymphocytes protect against and are not required for reovirus-induced myocarditis. *Journal of Virology* **67**:6119-6124.
174. **Sherry, B., F. J. Schoen, E. Wenske, and B. N. Fields.** 1989. Derivation and characterization of an efficiently myocarditic reovirus variant. *Journal of Virology* **63**:4840-4849.
175. **Sherry, B., J. Torres, and M. A. Blum.** 1998. Reovirus induction of and sensitivity to beta interferon in cardiac myocyte cultures correlate with induction of myocarditis and are determined by viral core proteins. *Journal of Virology* **72**:1314-1323.
176. **Simeonidis, S., S. Liang, G. Chen, and D. Thanos.** 1997. Cloning and functional characterization of mouse IkappaBepsilon. *Proc Natl Acad Sci U S A* **94**:14372-14377.
177. **Sizemore, N., N. Lerner, N. Dombrowski, H. Sakurai, and G. R. Stark.** 2002. Distinct roles of the Ikappa B kinase alpha and beta subunits in liberating nuclear

factor kappa B (NF-kappa B) from Ikappa B and in phosphorylating the p65 subunit of NF-kappa B. *Journal of Biological Chemistry* **277**:3863-3869.

178. **Smith, J. A., S. C. Schmechel, B. R. Williams, R. H. Silverman, and L. A. Schiff.** 2005. Involvement of the interferon-regulated antiviral proteins PKR and RNase L in reovirus-induced shutoff of cellular translation. *Journal of Virology* **79**:2240-2250.
179. **Solan, N. J., H. Miyoshi, E. M. Carmona, G. D. Bren, and C. V. Paya.** 2002. RelB cellular regulation and transcriptional activity are regulated by p100. *J Biol Chem* **277**:1405-1418.
180. **Stark, G. R., I. M. Kerr, B. R. Williams, R. H. Silverman, and R. D. Schreiber.** 1998. How cells respond to interferons. *Annu Rev Biochem* **67**:227-264.
181. **Stewart, M. J., K. Smoak, M. A. Blum, and B. Sherry.** 2005. Basal and reovirus-induced beta interferon (IFN-beta) and IFN-beta-stimulated gene expression are cell type specific in the cardiac protective response. *Journal of Virology* **79**:2979-2987.
182. **Stoka, V., B. Turk, S. L. Schendel, T. H. Kim, T. Cirman, S. J. Snipas, L. M. Ellerby, D. Bredesen, H. Freeze, M. Abrahamson, D. Bromme, S. Krajewski, J. C. Reed, X. M. Yin, V. Turk, and G. S. Salvesen.** 2001. Lysosomal protease pathways to apoptosis. Cleavage of bid, not pro-caspases, is the most likely route. *J Biol Chem* **276**:3149-3157.
183. **Sturzenbecker, L. J., M. L. Nibert, D. B. Furlong, and B. N. Fields.** 1987. Intracellular digestion of reovirus particles requires a low pH and is an essential step in the viral infectious cycle. *Journal of Virology* **61**:2351-2361.
184. **Tanaka, M., M. E. Fuentes, K. Yamaguchi, M. H. Durnin, S. A. Dalrymple, K. L. Hardy, and G. DV.** 1999. Embryonic lethality, liver degeneration, and impaired NF-kappa B activation in IKK-beta-deficient mice. *Immunity* **10**:421-429.
185. **Tanaka, N., M. Sato, M. S. Lamphier, H. Nozawa, E. Oda, S. Noguchi, R. D. Schreiber, Y. Tsujimoto, and T. Taniguchi.** 1998. Type I interferons are essential mediators of apoptotic death in virally infected cells. *Genes Cells* **3**:29-37.
186. **Tang, E. D., N. Inohara, C. Y. Wang, G. Nunez, and K. L. Guan.** 2003. Roles for homotypic interactions and transautophosphorylation in IkappaB kinase beta (IKKbeta) activation. *J. Biol. Chem.* **278**:38566-38570.

187. **Tardieu, M., M. L. Powers, and H. L. Weiner.** 1983. Age-dependent susceptibility to reovirus type 3 encephalitis: role of viral and host factors. *Annals of Neurology* **13**:602-607.
188. **Teodoro, J. G., and P. E. Branton.** 1997. Regulation of apoptosis by viral gene products. *Journal of Virology* **71**:1739-1746.
189. **Thompson, J. E., R. J. Phillips, H. Erdjument-Bromage, P. Tempst, and S. Ghosh.** 1995. I kappa B-beta regulates the persistent response in a biphasic activation of NF-kappa B. *Cell* **80**:573-582.
190. **Tillotson, L., and A. J. Shatkin.** 1992. Reovirus polypeptide $\sigma 3$ and N-terminal myristoylation of polypeptide $\mu 1$ are required for site-specific cleavage to $\mu 1C$ in transfected cells. *Journal of Virology* **66**:2180-2186.
191. **Tipper, D. J., and M. J. Schmitt.** 1991. Yeast dsRNA viruses: replication and killer phenotypes. *Mol Microbiol* **5**:2331-2338.
192. **Tosteson, M. T., M. L. Nibert, and B. N. Fields.** 1993. Ion channels induced in lipid bilayers by subviral particles of the nonenveloped mammalian reoviruses. *Proceedings of the National Academy of Sciences USA* **90**:10549-10552.
193. **Tracy, S., V. Wiegand, B. McManus, C. Gauntt, M. Pallansch, M. Beck, and N. Chapman.** 1990. Molecular approaches to enteroviral diagnosis in idiopathic cardiomyopathy and myocarditis. *J Am Coll Cardiol* **15**:1688-1694.
194. **Traenckner, E. B., H. L. Pahl, T. Henkel, K. N. Schmidt, S. Wilk, and P. A. Baeuerle.** 1995. Phosphorylation of human I kappa B-alpha on serines 32 and 36 controls I kappa B-alpha proteolysis and NF-kappa B activation in response to diverse stimuli. *EMBO Journal* **14**:2876-2883.
195. **Tyler, K. L.** 2001. Mammalian reoviruses, p. 1729-1745. *In* D. M. Knipe and P. M. Howley (ed.), *Fields Virology*, Fourth ed. Lippincott Williams & Wilkins, Philadelphia.
196. **Tyler, K. L., R. T. Bronson, K. B. Byers, and B. N. Fields.** 1985. Molecular basis of viral neurotropism: experimental reovirus infection. *Neurology* **35**:88-92.
197. **Tyler, K. L., D. A. McPhee, and B. N. Fields.** 1986. Distinct pathways of viral spread in the host determined by reovirus S1 gene segment. *Science* **233**:770-774.
198. **Tyler, K. L., and N. Nathanson.** 2001. Pathogenesis of viral infections, p. 199-243. *In* D. M. Knipe and P. M. Howley (ed.), *Fields Virology*, Fourth ed. Lippincott-Raven Press, Philadelphia.

199. **Tyler, K. L., M. K. Squier, S. E. Rodgers, S. E. Schneider, S. M. Oberhaus, T. A. Grdina, J. J. Cohen, and T. S. Dermody.** 1995. Differences in the capacity of reovirus strains to induce apoptosis are determined by the viral attachment protein $\sigma 1$. *Journal of Virology* **69**:6972-6979.
200. **Tyler, K. L., M. K. T. Squier, A. L. Brown, B. Pike, D. Willis, S. M. Oberhaus, T. S. Dermody, and J. J. Cohen.** 1996. Linkage between reovirus-induced apoptosis and inhibition of cellular DNA synthesis: role of the S1 and M2 genes. *Journal of Virology* **70**:7984-7991.
201. **Valyi-Nagy, T., S. J. Olson, K. Valyi-Nagy, T. J. Montine, and T. S. Dermody.** 2000. Herpes simplex virus type 1 latency in the murine nervous system is associated with oxidative damage to neurons. *Virology* **278**:309-321.
202. **Van Antwerp, D., S. Martin, T. Kafri, D. Green, and I. Verma.** 1996. Suppression of TNF- α -induced apoptosis by NF- κ B. *Science* **274**:787-789.
203. **Verma, I. M., and J. Stevenson.** 1997. IkappaB kinase: beginning, not the end. *Proceedings of the National Academy of Sciences USA* **94**:11758-11760.
204. **Verma, I. M., J. K. Stevenson, E. M. Schwarz, D. Van Antwerp, and S. Miyamoto.** 1995. Rel/NF-kappa B/I kappa B family: intimate tales of association and disassociation. *Genes & Development* **9**:2723-2735.
205. **Virgin, H. W., IV, R. Bassel-Duby, B. N. Fields, and K. L. Tyler.** 1988. Antibody protects against lethal infection with the neurally spreading reovirus type 3 (Dearing). *Journal of Virology* **62**:4594-4604.
206. **Virgin, H. W., IV, M. A. Mann, B. N. Fields, and K. L. Tyler.** 1991. Monoclonal antibodies to reovirus reveal structure/function relationships between capsid proteins and genetics of susceptibility to antibody action. *Journal of Virology* **65**:6772-6781.
207. **Virgin, H. W., K. L. Tyler, and T. S. Dermody.** 1997. Reovirus, p. 669-699. *In* N. Nathanson (ed.), *Viral Pathogenesis*. Lippincott-Raven, New York.
208. **Weih, F., D. Carrasco, S. K. Durham, D. S. Barton, C. A. Rizzo, R.-P. Ryseck, S. A. Lira, and R. Bravo.** 1995. Multiorgan inflammation and hematopoietic abnormalities in mice with a targeted disruption of RelB, a member of the Nf- κ B/Rel family. *Cell* **80**:331-340.
209. **Weiner, H. L., K. A. Ault, and B. N. Fields.** 1980. Interaction of reovirus with cell surface receptors. I. Murine and human lymphocytes have a receptor for the hemagglutinin of reovirus type 3. *Journal of Immunology* **124**:2143-2148.

210. **Weiner, H. L., D. Drayna, D. R. Averill, Jr, and B. N. Fields.** 1977. Molecular basis of reovirus virulence: role of the S1 gene. *Proceedings of the National Academy of Sciences USA* **74**:5744-5748.
211. **Weiner, H. L., M. L. Powers, and B. N. Fields.** 1980. Absolute linkage of virulence and central nervous system tropism of reoviruses to viral hemagglutinin. *Journal of Infectious Diseases* **141**:609-616.
212. **Weinrauch, Y., and A. Zychlinsky.** 1999. The induction of apoptosis by bacterial pathogens. *Annu. Rev. Microbiol.* **53**:155-187.
213. **Wetzel, J. D., G. J. Wilson, G. S. Baer, L. R. Dunnigan, J. P. Wright, D. S. H. Tang, and T. S. Dermody.** 1997. Reovirus variants selected during persistent infections of L cells contain mutations in the viral S1 and S4 genes and are altered in viral disassembly. *Journal of Virology* **71**:1362-1369.
214. **Whiteside, S. T., J. C. Epinat, N. R. Rice, and A. Israel.** 1997. I kappa B epsilon, a novel member of the I kappa B family, controls RelA and cRel NF-kappa B activity. *EMBO Journal* **16**:1413-1426.
215. **Wickner, R. B.** 1996. Double-stranded RNA viruses of *Saccharomyces cerevisiae*. *Microbiol Rev* **60**:250-265.
216. **Wolf, J. L., D. H. Rubin, R. Finberg, R. S. Kaufman, A. H. Sharpe, J. S. Trier, and B. N. Fields.** 1981. Intestinal M cells: a pathway of entry of reovirus into the host. *Science* **212**:471-472.
217. **Woodruff, J. F.** 1980. Viral myocarditis. A review. *American Journal of Pathology* **101**:425-484.
218. **Wyllie, A. H.** 1997. Apoptosis: an overview. *British Medical Bulletin* **53**:451-465.
219. **Xiao, G., M. E. Cvijic, A. Fong, E. W. Harhaj, M. T. Uhlik, M. Waterfield, and S. C. Sun.** 2001. Retroviral oncoprotein Tax induces processing of NF-kappaB2/p100 in T cells: evidence for the involvement of IKKalpha. *EMBO Journal* **20**:6805-6815.
220. **Xiao, G., A. Fong, and S. C. Sun.** 2004. Induction of p100 processing by NF-KappaB-inducing kinase involves docking IkappaB kinase alpha (IKKalpha) to p100 and IKKalpha-mediated phosphorylation. *Journal of Biological Chemistry* **279**:30099-30105.
221. **Xiao, G., E. W. Harhaj, and S. C. Sun.** 2001. NF-kappaB-inducing kinase regulates the processing of NF-kappaB2 p100. *Molecular & Cellular Biology* **7**:401-409.

222. **Xu, L. G., Y. Y. Wang, K. J. Han, L. Y. Li, Z. Zhai, and H. B. Shu.** 2005. VISA is an adapter protein required for virus-triggered IFN-beta signaling. *Molecular Cell* **19**:727-740.
223. **Yamaoka, S., G. Courtois, C. Bessia, S. T. Whiteside, R. Weil, F. Agou, H. E. Kirk, R. J. Kay, and A. Israel.** 1998. Complementation cloning of NEMO, a component of the IkappaB kinase complex essential for NF-kappaB activation. *Cell* **93**:1231-1240.
224. **Zamanian-Daryoush, M., T. H. Mogensen, J. A. DiDonato, and B. R. Williams.** 2000. NF-kappaB activation by double-stranded-RNA-activated protein kinase (PKR) is mediated through NF-kappaB-inducing kinase and IkappaB kinase. *Mol Cell Biol* **20**:1278-90.
225. **Zandi, E., Y. Chen, and M. Karin.** 1998. Direct phosphorylation of IkappaB by IKKalpha and IKKbeta: discrimination between free and NF-kappaB-bound substrate. *Science* **281**:1360-1363.
226. **Zandi, E., D. M. Rothwarf, M. Delhase, M. Hayakawa, and M. Karin.** 1997. The IkappaB kinase complex (IKK) contains two kinase subunits, IKKalpha and IKKbeta, necessary for IkappaB phosphorylation and NF-kappaB activation. *Cell* **91**:243-252.
227. **Ziegelbauer, K., F. Gantner, N. W. Lukacs, A. Berlin, K. Fuchikami, T. Niki, K. Sakai, H. Inbe, K. Takeshita, M. Ishimori, H. Komura, T. Murata, T. Lowinger, and K. B. Bacon.** 2005. A selective novel low-molecular-weight inhibitor of IkappaB kinase-beta (IKK-beta) prevents pulmonary inflammation and shows broad anti-inflammatory activity. *Br J Pharmacol* **145**:178-192.